

INVESTIGATION OF TRAFFIC DYNAMICS BY AERIAL
PHOTOGRAMMETRY TECHNIQUES

by the
Research Staff
Transportation Research Center
Department of Civil Engineering

FINAL REPORT
EES 278

Prepared in cooperation with the
U.S. Department of Transportation, Federal
Highway Administration and the
Ohio Department of Transportation

Engineering Experiment Station
The Ohio State University
Columbus, Ohio 43210

February 1975

Errata

Some of the pages have been assembled incorrectly and are out of sequence with the text.

Figures 2.3 , 2.4 and 2.5 relate to text on page 14.

Table 3.1 relates to text on page 34.

Figure 3.1 relates to text on page 34.

Figure 3.6 relates to text on page 43.

Figure 3.11 relates to text on page 51.

Figures 3.14 , 3.15 , 3.16 , 3.17 , 3.18 , 3.19 and 3.20 relate to text on page 60.

Figure 3.21 relates to text on page 63.

Figures 3.21 and 3.24 relate to text on page 66.

Figure 3.27 relates to text on page 71.

Figures 4.2 , 4.3 , 4.4 relate to text on page 79.

Figures 4.7 , 4.8 , 4.9 relate to text on page 87.

Page 93, Line 20 `whil` = `while`.

Figures 5.1 and 5.2 relate to text on page 100.

Page 106, Line 2 $C_L = C_1$.

Page 107, Line 17 `turning` = `tuning`.

Figure 5.7 relates to text on page 112.

Figure 5.11 relates to text on page 120.

Page 120, Line 9 `WD 14` = `WG 14`.

Figure 5.14 relates to text on page 126.

Page 145, Line 17 `fourescent` = `fluorescent`.

Figure 7.2 relates to text on page 154.

Figures 7.29 and 7.30 relate to text on page 189.

Figures 3.32 , 7.33 , and 7.35 relate to text on page 194.

Figure 7.36 relates to text on page 196.

1. Report No. OHIO-DOT-09-75		2. Government Accession No.		3. Recipient's Catalog No.	
4. Title and Subtitle Investigation of Traffic Dynamics by Aerial Photogrammetry Techniques				5. Report Date February 1975	
				6. Performing Organization Code EES-278	
7. Author(s) Joseph Treiterer				8. Performing Organization Report No.	
9. Performing Organization Name and Address Ohio State University Engineering Experiment Station 2070 Neil Avenue Columbus, Ohio 43210				10. Work Unit No. (TRAIS)	
				11. Contract or Grant No. Job No. 14162(0)	
12. Sponsoring Agency Name and Address Ohio Department of Transportation Box 899 Columbus, Ohio 43216				13. Type of Report and Period Covered Final Report	
				14. Sponsoring Agency Code	
15. Supplementary Notes Study conducted in cooperation with the U. S. Department of Transportation, Federal Highway Administration					
16. Abstract An aerial traffic survey and data reduction system was developed for the purpose to obtain continuous traffic data on the spacing of vehicles, speed, density, volume, acceleration and deceleration, lane changes and the general behavior of vehicles on two urban freeways in Columbus, Ohio. These data were evaluated with regard to real world safety conditions in the car following, the propagation of disturbances, the stability and the quality of traffic flow. The most important discoveries made were the multilinear speed-density relationships and the hysteresis phenomenon of traffic flow which shows the changing characteristics of traffic flow during the build up phase and the recovery phase of a kinematic disturbance. The new knowledge derived from aerial surveys and the research on traffic dynamics was applied to a ramp metering system for southbound morning peak traffic on I71 and to the development of a loop detector for density and speed measurements. Finally a cost analysis of the aerial survey method was carried out to explore practical applications for freeway operation and control.					
17. Key Words Aerial Survey, Cost of Traffic Survey, Loop Detector, Theory of Traffic Flow, Traffic Control, Traffic Flow, Traffic Safety.			18. Distribution Statement		
19. Security Classif. (of this report) Unclassified		20. Security Classif. (of this page) Unclassified		21. No. of Pages 201	22. Price

PREFACE

This report summarizes the work performed on Research Project EES 278, "Investigations of Traffic Dynamics by Aerial Photogrammetry Techniques".

Research on this project was started in January, 1966 and completed on January 1975, under the sponsorship of the Ohio Department of Transportation in cooperation with the Federal Highway Administration. The work was conducted by the Research Staff of the Transportation Research Center of the Ohio State University under the direction of Dr. Joseph Treiterer, Professor of Civil Engineering.

Recognition is given to the following persons for their contribution to the research project and their effort and assistance in the preparation of this report.

- ✓ Roberto Duarte, Research Associate
- ✓ Prapon Vongvichien, Research Associate
- ✓ Hector Rozas, Research Assistant
- ✓ Kristine Rebholz, Research Assistant, and
- ✓ Rabha A Fadel, Research Assistant

The opinions, findings and conclusions expressed in this publication are those of the authors and not necessarily those of the Ohio Department of Transportation or the Federal Highway Administration. This report does not constitute a standard, specification, or regulation.

TABLE OF CONTENTS

	<u>PAGE</u>
List of Tables	v
List of Figures	vi
CHAPTER 1 INTRODUCTION TO RESEARCH PROJECT	1
CHAPTER 2 DATA ACQUISITION BY AERIAL PHOTOGRAPHY	6
CHAPTER 3 INDIVIDUAL STUDIES OF TRAFFIC DYNAMICS BY AERIAL PHOTO- GRAMMETRY TECHNIQUES	27
CHAPTER 4 APPLICATION	73
CHAPTER 5 LOOP DETECTOR FOR DENSITY AND SPEED MEASUREMENTS	96
CHAPTER 6 COST ANALYSIS OF AERIAL SURVEY DATA	141
CHAPTER 7 STUDY OF TRAFFIC DYNAMICS ON I-70	150

LIST OF TABLES

- Table 3.1 Observed unsafe driving time in freeway traffic for different safety criteria.
- Table 5.1 Different traffic conditions in actuating the loop detector.

Chapter 2: Figures

- 2.1 Vehicle trajectories
- 2.2 Northern corridor of I-71 to Worthington, Ohio
- 2.3 A typical photograph of I-71 taken with the KA-62A aerial camera
- 2.4 The KA-62A aerial camera and bell helicopter
- 2.5 The KA-62A aerial camera and bell helicopter
- 2.6 Vehicle trajectories photos 218-297, lane 1
- 2.7 Basic data reduction equipment
- 2.8 Phase 4 output for lane 1 of photograph 61, flight number 4, film section 1

Chapter 3: Figures

- 3.1 Time-distance diagram for marginally safe spacing for vehicles traveling in a platoon, if the response time t is kept constant
- 3.2 Safe separation concepts applied to speed-density data of platoon 142
- 3.3 Volume-density relationships
- 3.4 Areas investigated to determine volume density relationships
- 3.5 Location of overpasses, exit and entrance ramps, lane 1
- 3.6 Location of data points
- 3.7 Distribution of λ -values
- 3.8 Distribution of $2\lambda\tau$ -values
- 3.9 Identification of group A vehicles (shaded area)
- 3.10 Identification of group B vehicles (shaded area)
- 3.11 Coefficient of variation of speed versus density for group A vehicles
- 3.12 Coefficient of variation of speed versus density for group B vehicles
- 3.13 Energy system proposed by Drew, assuming a linear speed-density relationship
- 3.14 Proposed speed-density hypotheses
- 3.15 Identification of group A vehicles (shaded area)
- 3.16 Identification of group B vehicles (shaded area)
- 3.17 Hand fitted multilinear curve for velocity versus density relationships for group A vehicles

- 3.18 Hand fitted multilinear curve for velocity versus density relationships for group B vehicles
- 3.19 Variation of speed distribution in different density regions for group A vehicles
- 3.20 Variation of speed distribution in different density regions for group B vehicles
- 3.21 Suggested operational regions
- 3.22 Suggested operational standards
- 3.23 Identification of group A vehicles (shaded area)
- 3.24 Identification of group B vehicles (shaded area)
- 3.25 Observed hysteresis loop before and after a jam condition (group A vehicles)
- 3.26 Observed hysteresis loop before and after a jam condition (group B vehicles)
- 3.27 Variation of speed dispersion before and after a jam condition (group A vehicles)
- 3.28 Variation of speed dispersion before and after a jam condition (group B vehicles)

Chapter 4: Figures

- 4.1 Region of concentrated data collection (southbound morning peak)
- 4.2 Velocity-distance profiles for data of Thursday, February 5, 1970
- 4.3 Velocity-distance profiles for data of Tuesday, March 24, 1970
- 4.4 Velocity-distance profiles for data of Thursday, June 18, 1970
- 4.5 Pattern of traveltime with time of day for traveltime runs of February 5 and March 24, 1970
- 4.6 Summary of day to day volume variation at various counting stations for period June 15 to June 19, 1970 (Study interval - 6:30 to 8:30 a.m.)
- 4.7 Schematic for merge area capacity study
- 4.8 Merge area capacity plot for East North Broadway
- 4.9 Merge area capacity plot for Weber Road merge area
- 4.10 Merge area capacity plot for Hudson Street merge area
- 4.11 Typical ramp control installation: freeway terminal
- 4.12 Composite speed-distance profiles for "before" and "after" traveltime data

Chapter 5: Figures

- 5.1 General Form of Speed-Volume Relationship (3)
- 5.2 General Form of Speed-Density Relationship (5)
- 5.3 Representation of a loop tuned circuit (7)
- 5.4 A typical loop detector circuit diagram (7)
- 5.5 Plots of detection versus lateral placement
- 5.6 Plot of detection versus longitudinal placement
- 5.7 Comparison of outputs for varying vehicle sizes
- 5.8 Density measurement with rectangular loop showing pickup-discharge variations
- 5.9 Density measurement with Figure "8" loop (18 ft. section length) showing consistent pickup-discharge variations
- 5.10 Traffic density on I-70 at the test site of loop detector
- 5.11 Location of loop detector on the freeway
- 5.12 Control box connections for field tests of loop detector
- 5.13 Dimensions of the loop detector installed on I-70
- 5.14 Traffic volume and throughput, a comparison of operation conditions.
- 5.15 Loop detector observed from the 18th street overpass
- 5.16 The 8 mm time lapse camera used to collect the film data
- 5.17 The LD-1 tuner and the brush pen recorder during tests

- 5.18 Situation number 1
- 5.19 Situation number 2
- 5.20 Situation number 3
- 5.21 Situation number 4
- 5.22 Situation number 5
- 5.23 Situation number 6
- 5.24 Situation number 7
- 5.25 Situation number 8
- 5.26 Situation number 9

Chapter 7: Figures

- 7.1 Traffic Density Versus Distance
- 7.2 Traffic Density Versus Distance
- 7.3 Traffic Density Versus Time of Day for US 33 EBR - James Rd. Overpass Subsection.
- 7.4 Traffic Density versus time of day for Sign (WB - LA/mi) - US 33 EBR Subsection.
- 7.5 Traffic Density versus time of day for sign (LA/AL) - sign (WB - LA/mi) subsection.
- 7.6 Traffic density versus time of day for sign (MS - Bex) - sign (LA/AL) subsection.
- 7.7 Traffic density versus time of day for sign (MS-Bex)-Kelton overpass subsection.
- 7.8 Traffic density versus time of day for Kelton Overpass - Linwood overpass subsection.
- 7.9 Traffic density versus time of day for Linwood overpass - 18th St. overpass subsection.
- 7.10 Traffic density versus time of day for 18th St. overpass - Linwood overpass subsection.
- 7.11 Traffic density versus time of day for Linwood overpass - Kelton overpass subsection.
- 7.12 Traffic density versus time of day for Kelton overpass - Sign (MS - Bex) subsection.
- 7.13 Traffic density versus time of day for Sign (MS - Bex) - Sign (LA/AL) subsection.

- 7.14 Traffic density versus time of day for Sign (LA/AL) -
Sign (WB - LA/mi) subsection.
- 7.15 Traffic density versus time of day for Sign (WB - LA/mi) -
US 33 EBR subsection.
- 7.16 Traffic density versus time of day for US 33 EBR - James Rd.
overpass subsection.
- 7.17 Velocity - Distance profiles for data of Monday, May 7, 1973.
- 7.18 Velocity - Distance profiles for data of Tuesday, April 24, 1973.
- 7.19 Velocity - Distance profiles for data of Wednesday, May 9, 1973.
- 7.20 Velocity - Distance profiles for data of Thursday, April 26, 1973.
- 7.21 Velocity - Distance profiles for data of Friday, May 4, 1973.
- 7.22 Velocity - Distance profiles for data of Monday, June 18, 1973.
- 7.23 Velocity - Distance profiles for data of Tuesday, May 15, 1973.
- 7.24 Velocity - Distance profiles for data of Wednesday, January 24, 1974.
- 7.25 Velocity - Distance profiles for data of Thursday, April 5, 1973.
- 7.26 Velocity - Distance profiles for data of Friday, June 22, 1973.
- 7.27 Vehicle trajectories of a kinematic disturbance between Nelson and
18th Street. (Lane 3)
- 7.28 Vehicle trajectories of a kinematic disturbance between Nelson and
18th Street. (Lane 4)
- 7.29 Continuous record of the speed density relationship of a platoon of
cars going through a kinematic disturbance.
(Aerial survey data, morning peak hour, I - 71)
- 7.30 Continuous record of the volume-density relationship of a platoon
of cars going through a kinematic disturbance.
(Aerial survey data, morning peak hour, I - 71)

- 7.31 Continuous record of the speed density relationship of a platoon of 8 vehicles going through a kinematic disturbance.
- 7.32 Continuous record of the volume density relationship of a platoon of 8 vehicles going through a kinematic disturbance.
- 7.33 Continuous record of the speed- density relationship of a platoon of 8 vehicles going through a kinematic disturbance.
- 7.34 Continuous record of the volume-density relationship of a platoon of 8 vehicles going through a kinematic disturbance.
- 7.35 Continuous record of the speed-density relationship of a platoon of 7 vehicles going through a kinematic disturbance.
- 7.36 Summary of studied platoon parameters and defined operating regions for platoon B.
- 7.37 Standard deviation of speed (acceleration noise) of a platoon of cars going through a disturbance.
- 7.38 Continuous record of the speed-density relationship of a platoon of 11 vehicles going through a kinematic disturbance.
- 7.39 Continuous record of the volume-density relationship of a platoon of 11 vehicles going through a kinematic disturbance.

CHAPTER 1

INTRODUCTION TO RESEARCH PROJECT

1.1 DESCRIPTION OF RESEARCH PROBLEM

Continued improvement of the design and operation of the highway system depends on the understanding of the dynamics of traffic using the system. This understanding can only be gained once the critical parameters of traffic flow have been identified and measured. A technique for the collection of such data through the utilization of aerial survey methods has been developed by the Transportation Research Center of The Ohio State University. Application of this technique provides continuous data for measuring such attributes of the traffic stream as traffic density, acceleration and deceleration, velocity weaving movements, headways, and spacings.

The aerial photogrammetry technique has been shown to be a most promising method of data collection, permitting sampling of traffic parameters on a continuing, macroscopic basis. The flexibility of this method allows for the study of a section of the traffic stream continuously, registering its behavior and propagation of disturbances. The research program described in this report was undertaken with the purpose of

refining the aerial survey technique and applying it to treat both theoretical and practical problems of highway design and operation.

1.2 RESEARCH OBJECTIVES

The research program focused on four specific objectives:

- 1) The exploration of practical applications of the aerial photogrammetry technique and the conduct of pilot studies in cooperation with the Ohio Department of Transportation.
- 2) The study of traffic dynamics utilizing aerial photography with emphasis on research in the theory of traffic flow.
- 3) The development of methods for the reduction and analysis of aerial photography data.
- 4) The application of the research results towards improved traffic flow and increased safety.

1.3 BACKGROUND

Research on this project was begun in July, 1967. This report concludes the work performed on Research Project EES 278, "Investigation of Traffic Dynamics by Aerial Photogrammetry Techniques". The project was sponsored by the Ohio Department of Transportation, in cooperation with the U. S. Department of Transportation, Federal Highway Administration. Work was conducted by the Research Staff of the O. S. U. Transportation Engineering Center under the direction of Dr. Joseph Treiterer,

Professor of Civil Engineering.

Extensive investigation into the existing principles and techniques used in photogrammetric science was conducted within EES 278 1 and 2 to determine means by which data could be extracted automatically from aerial photographs. Automatic scanning and digitizing devices were evaluated and comprehensive literature surveys were begun in an attempt to improve and simplify the practical applications of aerial traffic surveys. Special camera mounts for helicopters and the necessary control equipment were developed and built while tests were carried out with several cameras and different types of photographic film to determine the limitations of the aerial method.

Computer programs for data processing and data presentation in the form of graphical vehicle trajectories were developed with Interim Report EES 278-2. Research on data presentation was aimed at providing the necessary software for computer compatible automatic data reduction from the aerial photographs.

Report EES 278-3 documented research on two specific studies of traffic dynamics; the potential of traffic energy as a parameter of traffic flow and the characteristics of the traffic stream in the vicinity of a traffic bottleneck. Preliminary findings of a pilot study of urban freeways were included along with the description of a new data reduction system for removing data from photographs with automatic transfer to a punched card output.

1.4 SCOPE

The scope of this study can be described in terms of the phases of research which were pursued. The project objectives were accomplished by structuring the research efforts around six principal phases.

A review of the literature was the first phase of the research; the Lighthill-Whitham Theory of Traffic Flow and its practical application for traffic control were the principal areas of investigation. The literature review provided the basis for identifying the major areas of work and already developed methods and techniques for the study of traffic flow parameters.

The second phase consisted of the testing and selection of the basic methods of investigation. The whole program of research depended very much on an efficient and accurate data reduction system, furthermore, the practical application of aerial traffic survey methods directly depends on the data manipulation. Computer programs were developed during phase two for this purpose.

Phase three consisted of the actual data collection and reduction. With the methods and techniques developed under phase two, traffic behavior was recorded through the use of aerial photography. With the assistance of the Mann Type 829 D 282 Comparator and Type 1945 Data Logger, the data were efficiently and semi automatically reduced.

The fourth phase of research consisted of identification of individual characteristics in traffic; disturbance generation and propagation

(kinematic waves), the hysteresis phenomenon of traffic flow, energy change, stability criteria, and the multilinear speed-density relationships.

These characteristics were used as input to the fifth phase of research.

The model development, testing and further validation were the objectives of phase five. The actual methods of testing the data consist of graphical methods and statistical methods of testing for "goodness of fit" In phase six the implementation and practical application of the research findings was conducted.

CHAPTER 2

DATA ACQUISITION BY AERIAL PHOTOGRAPHY

2.1 INTRODUCTION

The information which can be obtained on traffic flow by photogrammetric techniques is illustrated by the vehicle trajectories shown in Figure 2.1. This represents a continuous record of the movement of each vehicle, with the band width being a function of focal length, camera format, and altitude. The following can readily be obtained by investigation of the vehicle trajectories:

- 1) The number of vehicles crossing a given point during a given time interval. This is represented by the number of trajectories intersecting line A, Figure 2.1.
- 2) The headway distributions in time at certain cross sections of the traffic lane studied (line A, Figure 2.1).
- 3) The traffic density over a certain length of the roadway at a given instant. This is determined by counting the number of trajectories intersecting line B, Figure 2.1.
- 4) The spacing of vehicles at a given instant in time, also obtained from line B of Figure 2.1.

- 5) A continuous record of velocity, acceleration, and deceleration of each vehicle which is obtained from the tangent and changes in the tangent to the vehicle trajectory at any given time.
- 6) The generation, magnitude, propagation, and causes of disturbances which may become obvious from the visual inspection of the vehicle trajectories.
- 7) A visual study of gap acceptance in weaving maneuvers may be made and their frequency and influence on traffic flow can be evaluated.

2.2 STUDY SITE

The area investigated consists of Interstate 71 from the downtown area of Columbus, Ohio, north to Route 161 in Worthington, Ohio, and Interstate 70 from downtown to James Road. These corridors are illustrated by the shaded areas in Figure 2.2. The Northbound portion of I-71 changed from three lanes to two lanes near East North Broadway when the aerial survey was initiated. This reduction in the number of lanes led to disturbances in the traffic flow and generated kinematic and shock waves moving in the southerly direction. On I-70 geometric design features, the curve between Nelson Road and Livingston Avenue, the curve close to the interchange with Route 33 and the downtown interchange with Interstate 71 appear to have a marked effect on traffic flow.

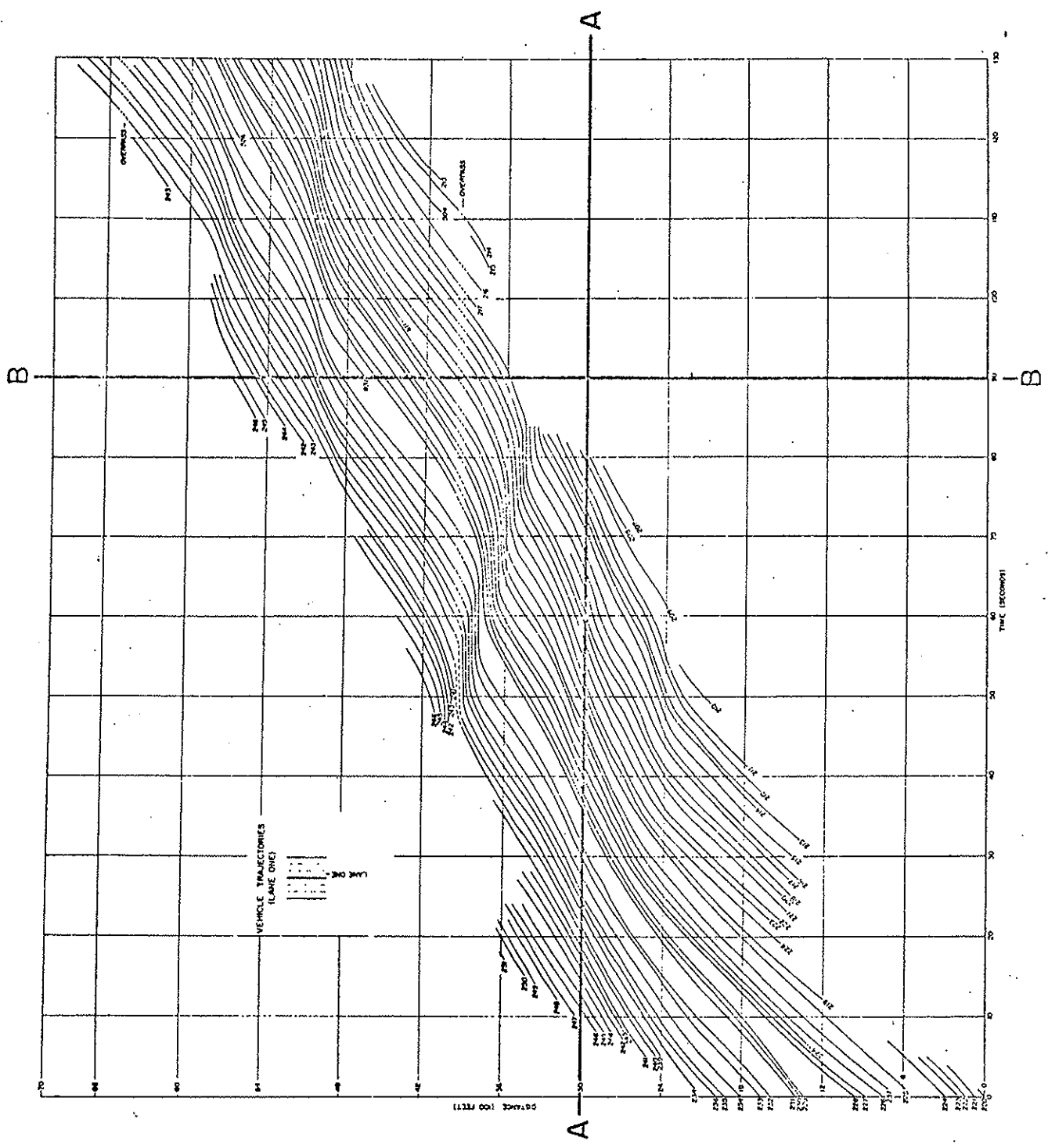


Figure 2.1 Vehicle Trajectories

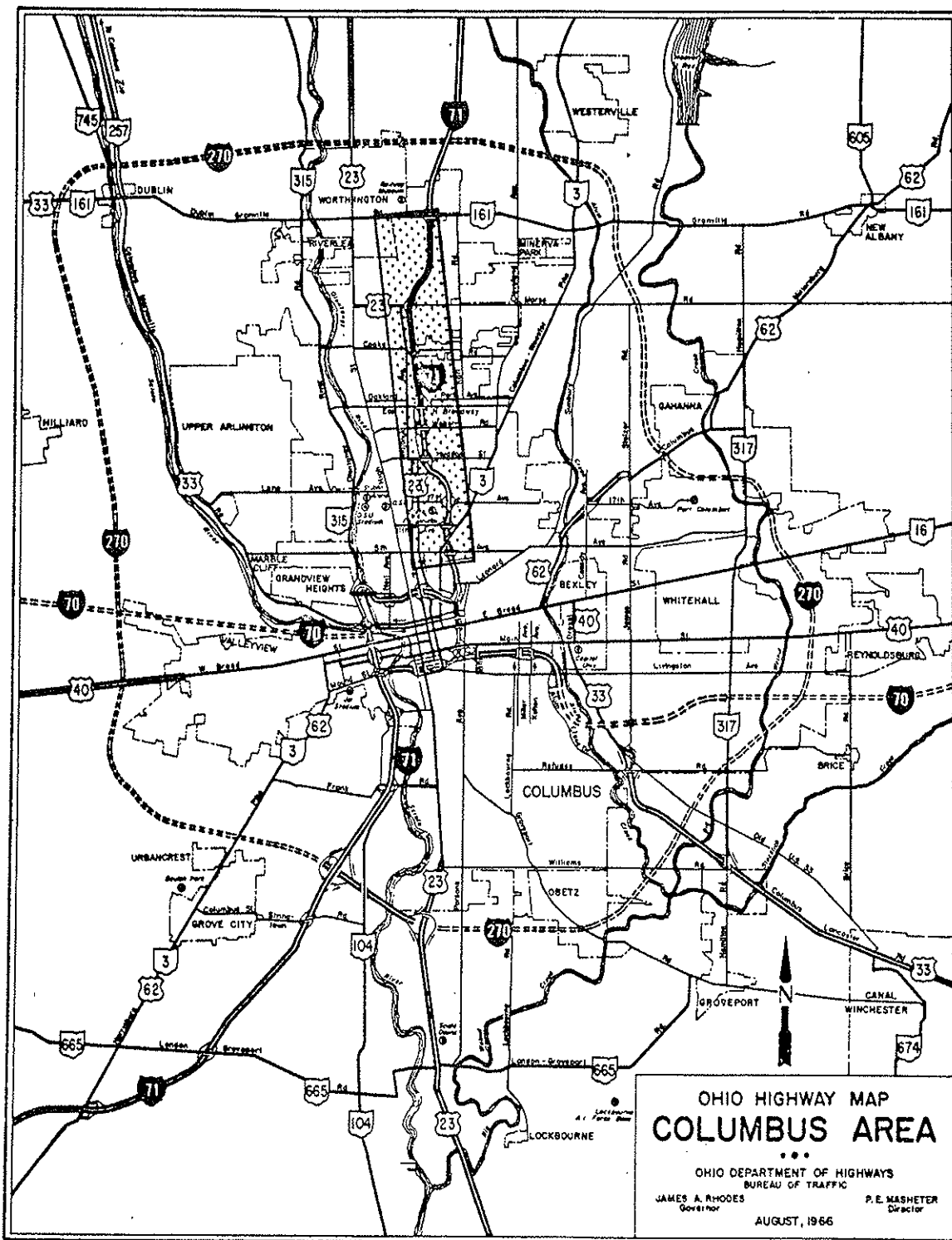


Figure 2.2 Northern Corridor of I-71 to Worthington, Ohio

2.3 DATA COLLECTION

The degree to which data can be provided by aerial traffic surveys depends mainly on three factors:

- 1) Coverage and Obstructions -- The area which can be covered by aerial photographs is basically controlled by altitude, film format, and focal length of the lens. The overlap of successive photographs is controlled by the ground velocity of the aircraft and the time interval between photographs. However, since traffic surveys are normally restricted to a certain area or traffic facility and to measurement of the travel pattern of a group of vehicles, a variable ground velocity ranging from zero to the velocity of the vehicles under consideration is required for the aircraft which carries the camera equipment. Additional factors limiting the coverage by aerial traffic survey are weather conditions, time of day, and the camouflaging effect of shadows and other characteristic elements of the study area such as tunnels, bridges, and trees.
- 2) Time Interval Between Exposures -- The interval between photographs is of great importance for traffic surveys since all calculations on speed, acceleration, and delay are based on the time interval between individual photographs. Furthermore, the degree of detailed description of traffic movement depends solely



Figure 2-3 A Typical Photograph of I-71 Taken With The KA-62A Aerial Camera.



Figure 2.4 The KA-62A Aerial Camera and Bell Helicopter

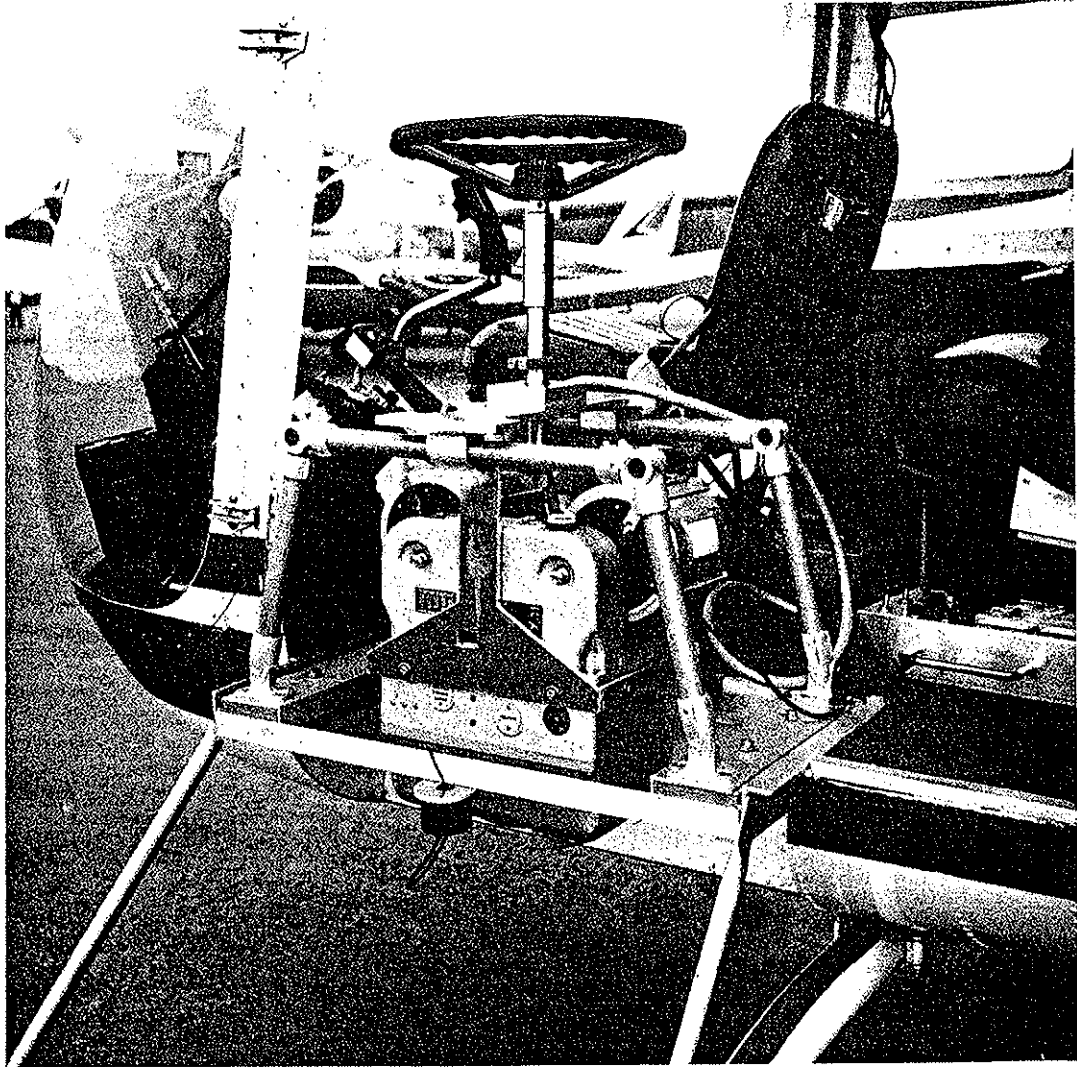


Figure 2.5 The KA-62A Aerial Camera and Bell Helicopter

on the time interval between photographs, not considering the total period of time covered.

- 3) Capacity of Camera -- Traffic surveys are designed to cover a certain period of time, this time being limited by the capacity of the camera. The instrument selected for the work was a KA 62A aerial reconnaissance camera from Chicago Aerial Industries, Incorporated. A typical photograph taken with the KA 62A aerial camera is shown in Figure 2.3.

The KA 62A is fitted with a three-inch lens with an aperture range of f/4.5 to f/11. The diagonal view angle is $93^{\circ}22'$ and the side view angle is $73^{\circ}44'$, giving a coverage of about 6,360 feet and 4,500 feet respectively from an altitude of 3,000 feet. Most of the surveys were flown at an approximate altitude of 3,000 feet, and the length of freeway covered was about 4,500 feet. The camera can take up to six photographs per second at autocycle operation mode.

A special camera mount was designed, constructed, and mounted in the Bell 4752 Helicopter of the Ohio Department of Transportation and a Jet Ranger of the Ohio National Guard. Figures 2.4 and 2.5 show the camera mounted in the Bell helicopter.

Velocities had to be determined within ± 1.0 mph, i.e. ± 1.5 ft/sec., if meaningful data were to be provided by the survey method. Thus, since the maximum acceptable time interval between photographs was determined

to be 1.0 seconds, positions of vehicles in each photograph had to be measured to within ± 1.0 foot. Photographs were taken at nominal scales of 1:23,000 , 1:12,000 , and 1:600 , and it was found that, considering the available equipment, a scale of about 1:12,000 would provide an accuracy of measurement which is better than the required ± 1.0 foot. Many features of the roadway such as light poles, guard rail posts, drainage culverts, manhole covers, and other roadside features can be identified on the 1:12,000 scale photographs and can be used as ground control points in the data reduction process. It is one of the main advantages of the aerial survey method that it may be applied to any roadway or road traffic system without previous preparation of the study location. The flexibility of the survey method, however, is hampered by any scale smaller than 1:14,000 since natural roadside features are frequently not discernible in the photographs, necessitating the preparation of ground control points before flying the survey. However, with the 1:12,000 scale, natural ground control points can be determined from the photographs and their positions can be surveyed on the ground after the flight.

During each survey run, photographs of a specific group of vehicles were taken from the helicopter at intervals of one second while the platoon of vehicles proceeded along the freeway. At the beginning a marked test vehicle, easily discernible from the air, was introduced into the traffic stream and the pilot was instructed to follow the test vehicle. Radio contact

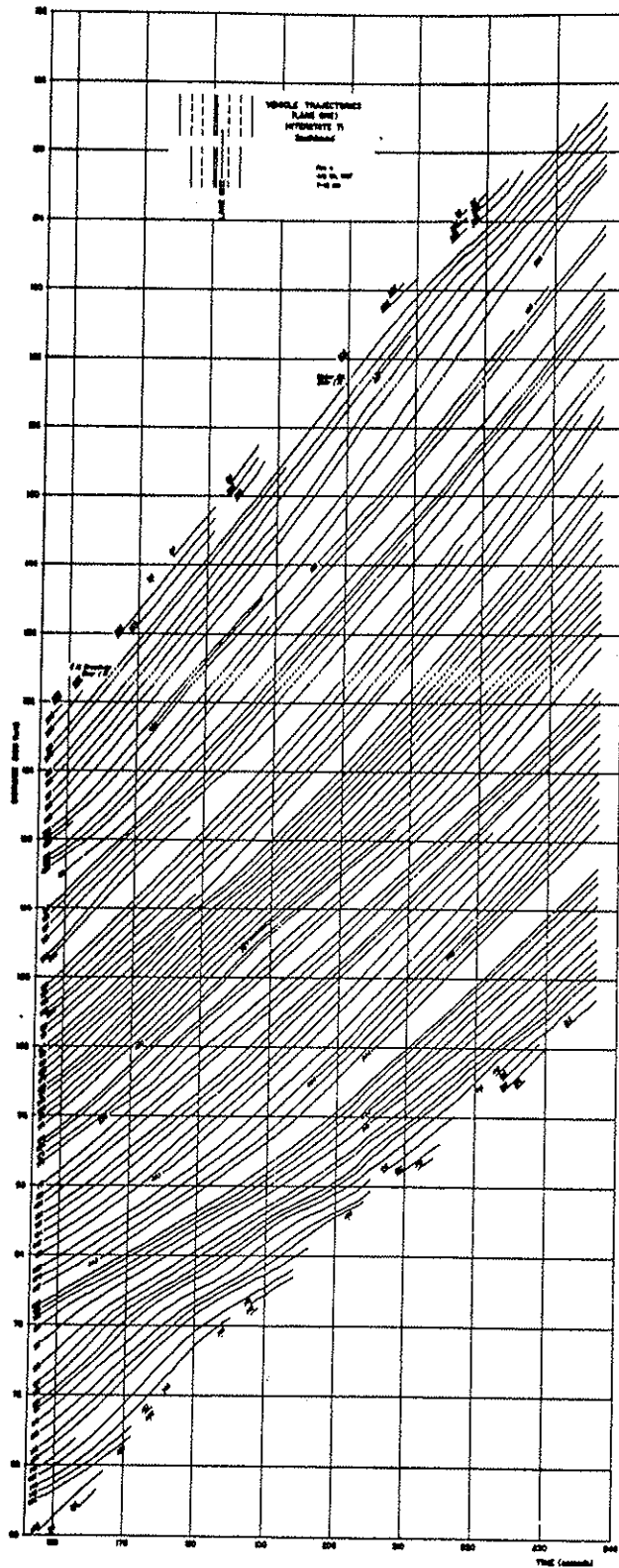


Figure 2.6 Vehicle Trajectories, Photos 218-297, Lane 1

between the test car and the helicopter was available and was used to direct the study program. In later flights no test vehicle was used anymore after it was found that data recorded by the test vehicle agreed very well with the aerial survey data. Pilots did not have any difficulties in selecting a vehicle in a platoon of cars and in following the selected vehicle. The aerial survey method became much more responsive to developing traffic conditions and more flexible in its application after the test vehicle guidance was abandoned.

2.4 DATA REDUCTION

One of the primary goals of the research program was the development of an efficient, accurate, and reliable data reduction system. In previous phases of the research, the data evaluation was accomplished by the Nistri AP/C Analytical Plotter of the Ohio Department of Transportation.

It should be noted that vehicles need not be individually identified and that no vehicle identifications were carried from one photograph to another except for a few cars. Certain easily discernible vehicles, however, were identified and carried along in the reading process to simplify the reading of the computer plotted points of vehicle trajectories. This method to determine the general pattern of vehicle trajectories has shown to be quite reliable since vehicle trajectories cannot cross each other and all trajectories must follow a similar pattern in dense traffic. Figure 2.6 shows the vehicle trajectories of Lane 1, southbound traffic on I-71. It can be seen that, though there is considerable variance in spacing, velocity,

and lane changes, by establishing the general pattern of a few vehicles, it is quite simple to determine the pattern of movement for the other vehicles by using the progress of the identified vehicles as a guide.

The spacing between vehicles on a curved section of highway was measured in straight line segments along the chord line. For this purpose certain vehicles distributed along the arc were chosen as distance control points to provide a close approximation of the actual distance along the section.

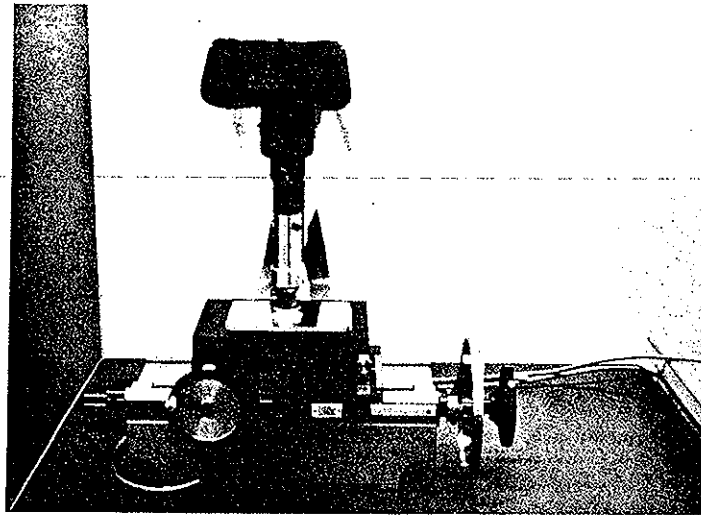
All photo coordinates were measured in microns using the Nistri AP/C Analytical Plotter. The output was then manually transferred to punch cards for further reduction of the photo-data to ground-data by the computer. Depending upon the number of vehicles found on each photograph, this entire process, photo-coordinate reading and manual card punching, could be expected to take between 1-1/2 hours to two hours per photograph. Given that an average traffic film may contain anywhere from 300 to 500 usable photographs, the magnitude of time required for the completion of the reduction process can easily be seen. In addition to the time requirements inherent in this process, further data reduction delays resulted because the AP/C is the property of the Ohio Department of Transportation and thus could be used for the research program only when not in use for the Transportation Department personnel.

To determine the photo coordinates for one film took nearly 570 man hours, this necessitated the development of a simple, more efficient and less time consuming data reduction system. Extensive studies and tests were carried out to develop an automatic data reduction system using very precise high speed cathod ray tube scanning techniques. Some of the tests carried out at the Rocket Research Center in Pasadena, California, and at the Technical University of Karlsruhe, Germany, were most promising. The method used was based on the subtraction or addition of scanning pulses derived from a synchronous scanner which covered two successive photographs simultaneously. This method was intended to eliminate all data of stationary objects and select data on moving objects for storage and further evaluation by the computer. Research on automatic data reduction had to be abandoned when cost estimates showed that about \$3-1/2 million would be required to develop and build a modest system. However, the method was further pursued at the University of Karlsruhe and advanced scanning systems have been developed at that University in the meantime.

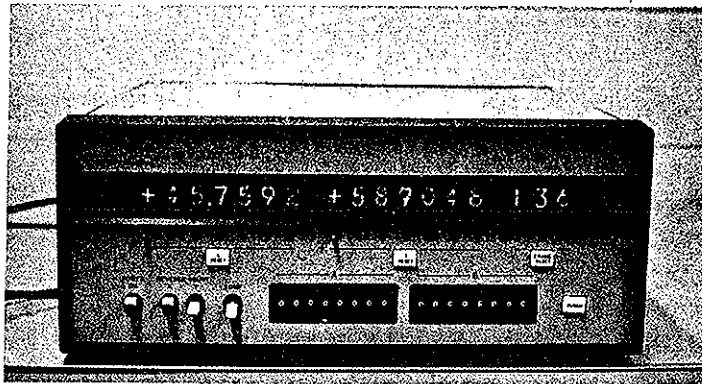
The data reduction system ultimately devised consisted of three basic components:

- 1) Mann Type 829 D Comparator
- 2) Mann Type 1945 Data Logger
- 3) IBM 026 Printing Card Punch

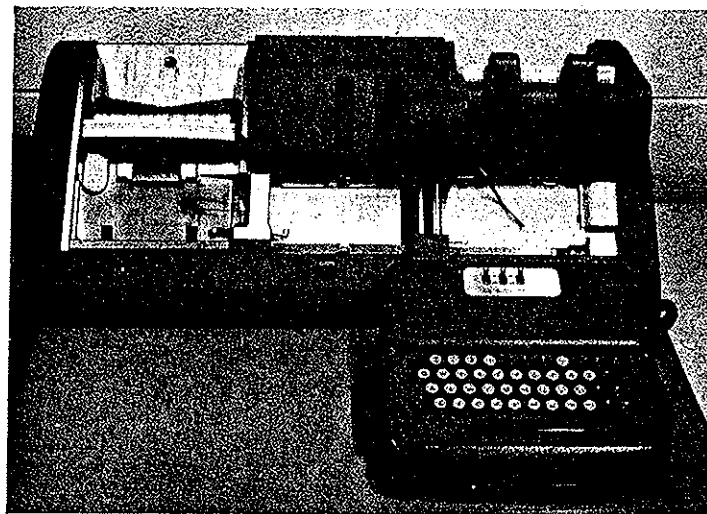
These three components are shown in Figure 2.7. A description of the function of each of the components is provided below.



Mann Type 829D Comparator



Mann Type 1945 Data Logger



IBM 026 Printing Card Punch

Figure 2.7 Basic Data Reduction Equipment

IBM 026 Printing Card Punch

The output element of the data reduction system is an IBM 026 Printing Card Punch. This machine is connected on line with the data logger and allows the photo-coordinate values, the switch register values, and the frame count to be transferred directly to punched card output. This greatly speeds the rate at which coordinates can be taken from the film.

Three computer programs were developed for further data reduction. The data recorded on punch cards was processed on the IBM 7094 computer into a binary card output. The binary card output contained suitable instructions for the IBM 1620-27 digital incremental plotter.

The binary output deck was then used as the input for the plotting system; data points representing the distribution of vehicles in a traffic lane at the time when the relevant photo was taken were produced. Photo coordinate points were then plotted on graph paper of the format 29.5 inches by 120 feet. The distance scale was 1:2406 and the plotting accuracy shown to be better than ± 0.005 inches. Since the pattern of traffic movement can be established by identified vehicles, which were plotted by x's to distinguish them from other vehicles, the vehicle trajectories could be drawn by connecting the consecutive accumulative distance points for each vehicle. Erroneously punched data cards, missing vehicles, or grossly incorrect measurements of photo coordinates could easily be spotted by observing the vehicle trajectories.

With the use of the third computer program, a final record was provided

which contains data corrected to the exact scale factor between ground control points. A printed record and a record on computer compatible magnetic tape was provided which contained the following information:

Vehicle number (code)	
Photo coordinates	
Ground coordinates	
Accumulative distance	
Spacing	of each vehicle on each photograph recorded
Headway	in the appropriate lane
Velocity	
Total number of vehicles	
Average velocity	for each lane on each photograph
Traffic density	
Traffic volume	

Figure 2.8 illustrates the record for lane one of photograph 61, flight number four, film section one. The total record was then used for further research on traffic flow characteristics and the verification of theories of traffic flow.

2.5 PERFORMANCE OF THE SYSTEM

The reduction system was placed in service in 1969 and subjected to operational testing. It was found that on the average approximately 16 photographs could be completely reduced and all data punched on IBM cards during

VEH	PHOTO X	PHOTO Y	GROUND X	GROUND Y	DIST(FT)	SPAC(FT)	HEAD(SEC)	VEL(FPS)	VEL(MPH)
175	123-178	183-784	823-80	1066-38	1072-09	376-98	4.63	81.47	55.55
176	129-416	181-144	1166-05	1449-07	1449-07	384-45	4.05	95.01	64.78
177	135-764	179-228	1515-58	710-29	1833-52	205-00	2.06	99.33	67.72
178	139-230	178-462	1709-43	650-50	2038-52	146-58	1.43	102.21	69.69
179	141-724	178-036	1849-78	608-92	2185-10	292-32	2.88	101.65	69.31
180	146-736	177-626	2133-52	539-48	2477-42	510-78	4.57	111.88	76.28
181	155-566	177-356	2640-30	474-87	2898-40	101-19	1.07	94.49	64.43
182	157-312	177-466	2741-36	469-21	3089-59	161-63	1.74	93.12	63.49
183	160-088	177-778	2902-78	468-25	3211-22	201-17	2.16	93.03	63.43
184	163-560	178-154	3103-93	466-07	3422-39	1189-76	11.35	104.84	71.48
185	184-078	180-694	4293-88	471-48	4642-35	83-54	1.13	74.07	50.50
186	185-520	180-882	6377-42	472-40	472-89	523-87	6.97	75.16	51.24
187	194-568	182-018	4901-29	475-67	475-76	90-85	1.20	75.52	51.51
188	196-140	182-190	4992-13	474-79	5340-61	90-85	0.70	71.18	48.53
189	197-008	182-278	5042-26	473-96	5399-74	196-52	2.78	70.73	46.22
190	200-402	182-722	5238-78	476-39	5587-26	334-94	4.46	75.17	51.25
191	206-190	183-450	5573-71	478-66	5922-20	113-73	1.69	67.45	45.99
192	208-160	183-658	5687-44	477-43	6035-93	59-99	1.08	55.69	37.97
193	209-196	183-794	5747-43	478-20	6095-92	79-73	1.74	45.78	31.22
194	*****DISTANCE	INTERPOLATED*****			6175-65	116-07	2.99	38.79	26.45
195	212-578	184-234	5943-24	480-47	6291-72	90-95	2.77	32.81	22.37
196	216-154	184-396	6334-19	479-08	6382-68	77-02	2.09	36.91	25.16
197	215-484	184-572	6111-21	480-15	6439-70	72-88	2.07	35.18	23.99
198	216-742	184-742	6184-09	481-36	6532-58	67-00	1.92	34.83	23.75
199	217-904	184-852	6251-09	479-79	6592-57	74-33	2.14	34.67	23.65
200	219-186	185-034	6325-41	481-52	6671-90	116-59	3.75	31.08	21.19
201	221-214	185-228	6442-00	479-12	6780-50	49-44	2.99	16.55	11.28
202	222-066	185-398	6491-44	483-03	6839-93	34-10	4.57	7.46	5.09
203	222-660	185-462	6525-54	482-66	6874-03	39-73	5.05	7.87	5.36
204	223-350	185-594	6565-27	483-23	6913-76	43-26	6.07	7.13	4.86
205	224-106	185-614	6608-52	481-55	6937-02	44-54	3.88	11.48	7.83
206	224-878	185-730	6653-06	482-94	7001-35	58-42	3.85	15.19	10.36
207	225-896	185-836	6711-48	482-10	7059-97	39-63	2.06	19.25	13.13
208	226-584	185-930	6751-11	482-80	7099-60	54-16	3.03	17.88	12.19
209	227-524	186-060	6805-26	483-85	7153-76	40-39	2.53	15.99	10.90
210	228-230	186-116	6845-66	482-28	7194-15	51-02	4.35	11.73	8.00
211	229-112	186-268	6896-67	484-97	7245-17	44-86	2.74	16.36	11.15
212	229-894	186-348	6941-54	484-24	7290-03	66-95	3.15	21.25	14.49
213	231-060	186-476	7008-49	483-66	7356-98	77-59	3.77	20.59	14.04
214	232-406	186-668	7086-07	485-49	7434-57	59-83	2.73	21.91	14.94
215	233-448	186-782	7145-90	484-85	7494-40	59-09	3.01	19.64	13.39
216	234-476	186-904	7204-09	484-95	7553-49	41-54	****	****	****
217	235-200	186-978	7246-53	484-28	7595-02	****	****	****	****

TOTAL NUMBER OF VEHICLES = 43
 AVERAGE VELOCITY = 34.30 MILES PER HOUR (FOR 41 VEHICLES)
 DENSITY = 34.81 VEHICLES PER MILE
 VOLUME = 1193.74 VEHICLES PER HOUR

Figure 2.8. Phase 4 Output for Lane 1 of Photograph 61,
 Flight Number 4, Film Section 1

an eight hour work day. This works out to a data reduction rate of about 30 minutes per photograph which compares quite favorably to the 1-1/2 to two hours per photograph required using the Nistri AP/C to read the photo-coordinates and punching the cards manually.

A typical aerial survey film containing 300 usable frames could be completely reduced with all pertinent data transferred to punched card output in about 150 hours. The rate at which data points can be measured in x, y photocordinates is now determined by the processing speed of the IBM 026 Printing Card Punch. The data reduction system could be improved considerably by connecting it to a late model Card Punch.

Two problems, however, must be mentioned which occurred in operating the data reduction system. These are:

- 1) The strain on the eyes of the operator limits working time without a break to about two hours
- 2) Film density must be controlled carefully in the developing process to match the intensity of the light source in the comparator.

Considering the overall performance of the data reduction system it is felt, however, that the goal of developing an efficient data reduction system for the investigation of traffic dynamics by aerial photogrammetry techniques has been realized.

CHAPTER 3
INDIVIDUAL STUDIES OF TRAFFIC DYNAMICS BY
AERIAL PHOTOGRAMMETRY TECHNIQUES

3.1 CONCEPTS AND CRITERIA

Policies of Safe Driving

Little is known about the policy of safe spacing that the major part of the driver population chooses. The factors that influence this decision cover the entire system of driver, vehicle, and road. The choice depends on human attitudes, vehicle capabilities, traffic conditions, and the quality of the road. However, with different levels of risk-taking, these individual choices of driving policies will be distributed around or between two concepts:

- 1) The concept of absolute safety, and
- 2) The concept of marginal safety.

Both concepts represent interpretations of the safe spacing as the critical measure to avoid rear-end collisions. These concepts employ the assumption that a queue of vehicles is traveling in a single lane and that vehicles cannot change lanes. Furthermore, the concepts are based on a

car-following model with two cars following each other.

As a simplification, the rather complex car-following safety concepts have been limited to passenger cars traveling on level roads under the following conditions:

- 1) All vehicles travel at about the same speed,
- 2) Deceleration patterns and capabilities are similar for all vehicles,
and
- 3) Road conditions are identical for all vehicles.

These assumptions are not in accordance with real life conditions but are expected to give reasonable approximations of most existing conditions for the car-following situation.

The Absolute Safety Concept

This may be defined as follows: The leading vehicle is brought to a sudden stop by some object in the roadway (running into a suddenly appearing obstacle; heavy truck or container). The driver of the trailing vehicle reacts on the incidence of the collision and is able to stop his car without hitting the leading car in a rear-end collision. No space is left between the vehicles after the stopping maneuver.

The spacing required by the following car to avoid a collision is known as safe stopping distance and would guarantee absolute safety in the car-following situation. Spacing consists of the distance traveled during the reaction time of the driver and the braking distance:

$$S_{\min} = S_a = VT + \frac{V^2}{2d}$$

where:

$S_{\min} = S_a$ = safe spacing, feet

V = speed, feet/second

T = reaction time of the driver, seconds

d = rate of deceleration, feet/second²

Employing the dimensions generally used:

$$S_a = 1.47 VT + V^2/30f$$

where:

V = speed, mph

f = coefficient of friction or $\frac{\text{percent of braking}}{100}$

The factors influencing safe spacings are:

- 1) Velocity
- 2) Driver's reaction time, and
- 3) Vehicle deceleration rate.

The Marginal Safety Concept

This concept can be defined as follows: The driver of the front car is forced to bring his car to a standstill in an emergency and tries to stop his vehicle in the shortest possible distance. After some delay caused by reacting on the maneuver of the lead car, the driver of the following vehicle duplicates the braking maneuver of the lead car, and both vehicles come to a

safe stop. No rear-end collision will occur although no space is left between the vehicles after stopping.

The distance between the two vehicles required to avoid a rear-end collision is the marginally safe spacing since the basic assumptions imply that both cars travel at about the same speed and are subject to the same deceleration pattern. This spacing is determined by the distance traveled during the reaction time of the driver. Thus:

$$S_{\min} = S_b = 1.47 VT$$

where:

S_{\min} = marginally safe spacing feet

V = speed, mph

T = reaction time of the driver, seconds

Hence, the marginally safe distance between vehicles is determined by:

- 1) Velocity, and
- 2) Driver's reaction time.

The resulting safe and marginally safe spacings are dependent on a variety of factors, one of which is speed. The safe distance at high speeds is greater than at low speeds. Marginal spacing shows only a linear dependence on the velocity, whereas an absolute spacing policy gives quadratic velocity dependence intensified by a continuous decrease of the possible deceleration (friction) with increasing velocities.

The driver's response or reaction time is referred to as the time for

perception, intellection, emotion, and volition (PIEV time). Response time consists of the time to perceive the situation and to apply the brakes. In this research project a reaction time ranging from 0.7 to 2.0 seconds was employed. This seems reasonable considering the fact that drivers adjust their attention and driving habits to the prevailing conditions.

Maximum deceleration rates (1) of modern motor vehicles are as high as 0.8g. Often, for lack of maintenance and adjustment, vehicle brakes in use do not maintain such high rates. In panic stops the minimum stopping distance is obtained by locking all four wheels so that the available friction between tire and road surface will determine the stopping distance.

In an attempt to gain more knowledge on driving conditions in dense freeway traffic and in evaluating the basic condition for the propagation of disturbances 48 vehicles were observed, and the unsafe driving time, applying different safety criteria, was determined. (EES 278-1 Chapter 5)

The following safety concepts were used.

- | | | |
|----------------|-------------------------------------|-----------------|
| A ₁ | Reaction time = 0.7 sec. | |
| | Upper friction limit | Absolute safety |
| A ₂ | Reaction time = 2.0 sec. | |
| | Lower friction limit | |
| B ₁ | Reaction time = 0.7 sec. | |
| | | Marginal safety |
| B ₂ | Reaction time = 2.0 sec. | |
| R | One car length per 10 mph velocity. | |

Table 3.1 Observed unsafe driving time in freeway traffic for different safety criteria.

Safety criterion	Unsafe driving time % of total observation time
A ₁	69.81%
A ₂	90.89%
B ₁	10.97%
B ₂	80.28%
R	37.08%

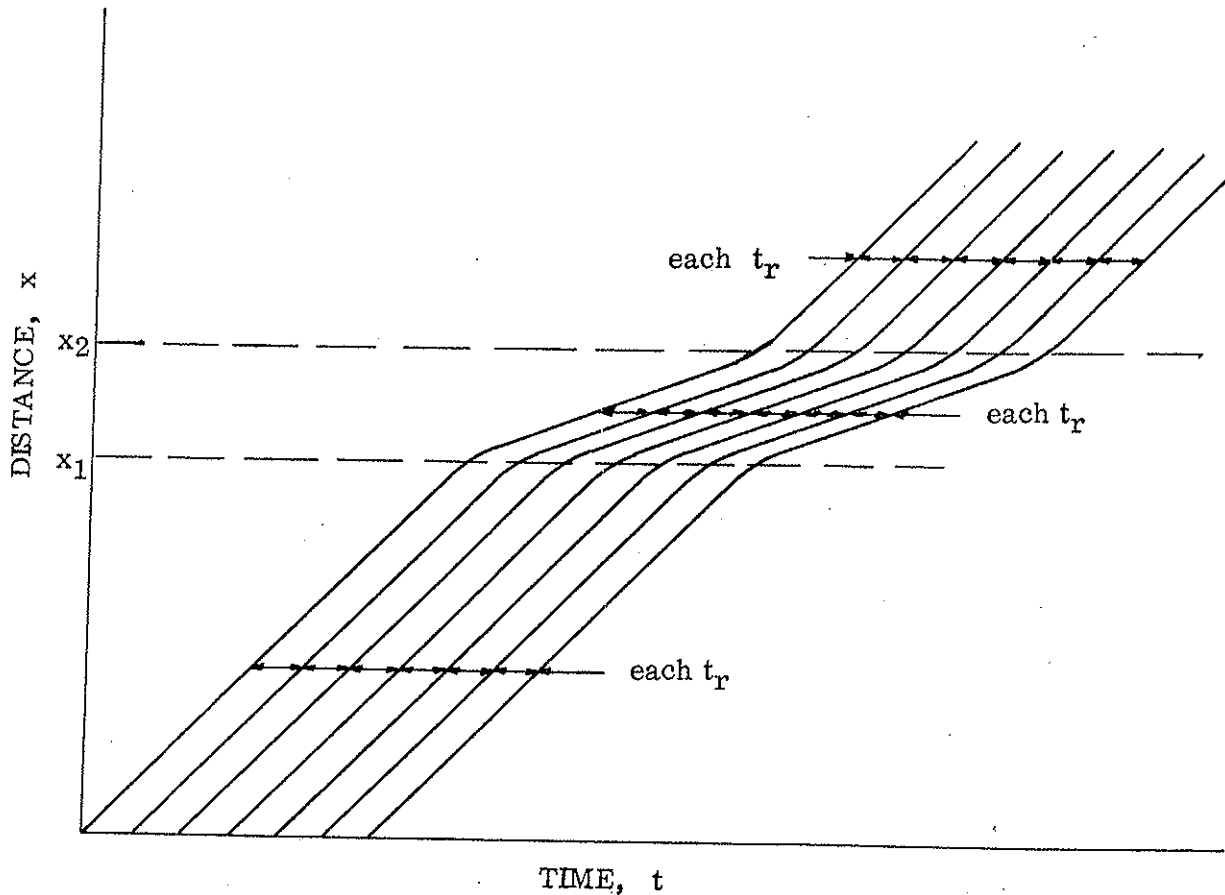


Figure 3.1 Time-distance diagram for marginally safe spacing for vehicles travelling in a platoon, if the response time t_r is kept constant.

Table 3.1 shows the unsafe driving times, i. e. rear end collisions would have occurred in an emergency according to the specified safety criteria.

A major problem of this research project is how to increase traffic flow and how to improve traffic safety at the same time. The magnitude of the problem is confirmed by the findings listed in Table 3.1.

High density freeway traffic is at its best marginally safe assuming almost ideal condition (11% unsafe driving at a reaction time of 0.7 sec.), and for 90% of the time unsafe if the driver is distracted (reaction time 2.0 sec.) and the brakes of his vehicle are average considering the absolute safety concept.

3.2 INVESTIGATION OF THE PROPAGATION OF DISTURBANCES IN A TRAFFIC STREAM

Some Aspects of the Stability of Traffic Flow

Two of the most important factors associated with the instability of traffic flow are:

- 1) The degree of safety in the car-following situation of vehicles traveling in a platoon.
- 2) The change (reduction) in traffic flow.

In this research study marginal safety only was considered for the car following situation. Figure 3.1 is intended to describe this situation for seven vehicles traveling at marginally safe spacings. It should be noted that the locations on the highway where accelerations (x_2) or decelerations (x_1)

occur will be the same for all vehicles traveling in the platoon if the reaction time t_r is kept constant. Disturbances will propagate along the moving platoon of vehicles but will remain stationary with regard to their location in the highway, and vehicles will proceed through similar acceleration patterns when passing these points. It has been proposed that traffic instability arises from the variance in the reaction of drivers to changes in behavior of the leading vehicle. Delayed reaction or too much of a change in velocity by the trailing vehicle may cause following drivers to over-correct errors and thus amplify originally small disturbances. It should be noted that a change in t_r will also cause a shift of the location on the highway where vehicles will encounter disturbances.

It appears that drivers derive their stimulus for controlling the spacing between the leading and trailing vehicle from two observations; an estimate of the distance to the leading vehicle and an estimate of the differential velocity from the range in change in angular vision.

The Propagation of Traffic Disturbances

The Lighthill-Whitham Theory of Traffic Flow on Long Crowded Roads appears to cover the fundamental characteristics of traffic flow found in this research project. This is a macroscopic approach to traffic flow theory. Figure 3.2 shows the theoretical relationship between flow, density, and speed as presented by the theory.

Aerial traffic surveys were carried out on I-71 and I-70 in Columbus,

PLATOON 142

ABS-DENSITY(VPMI;ORD-AVE SPD(MPH)) (L.I.)
 TOTAL NO. OF PTS. PLOTTED IS 227 AND NC. NOT PLOTTED BECAUSE THEY FALL OUTSIDE OF BOUNDS IS 0

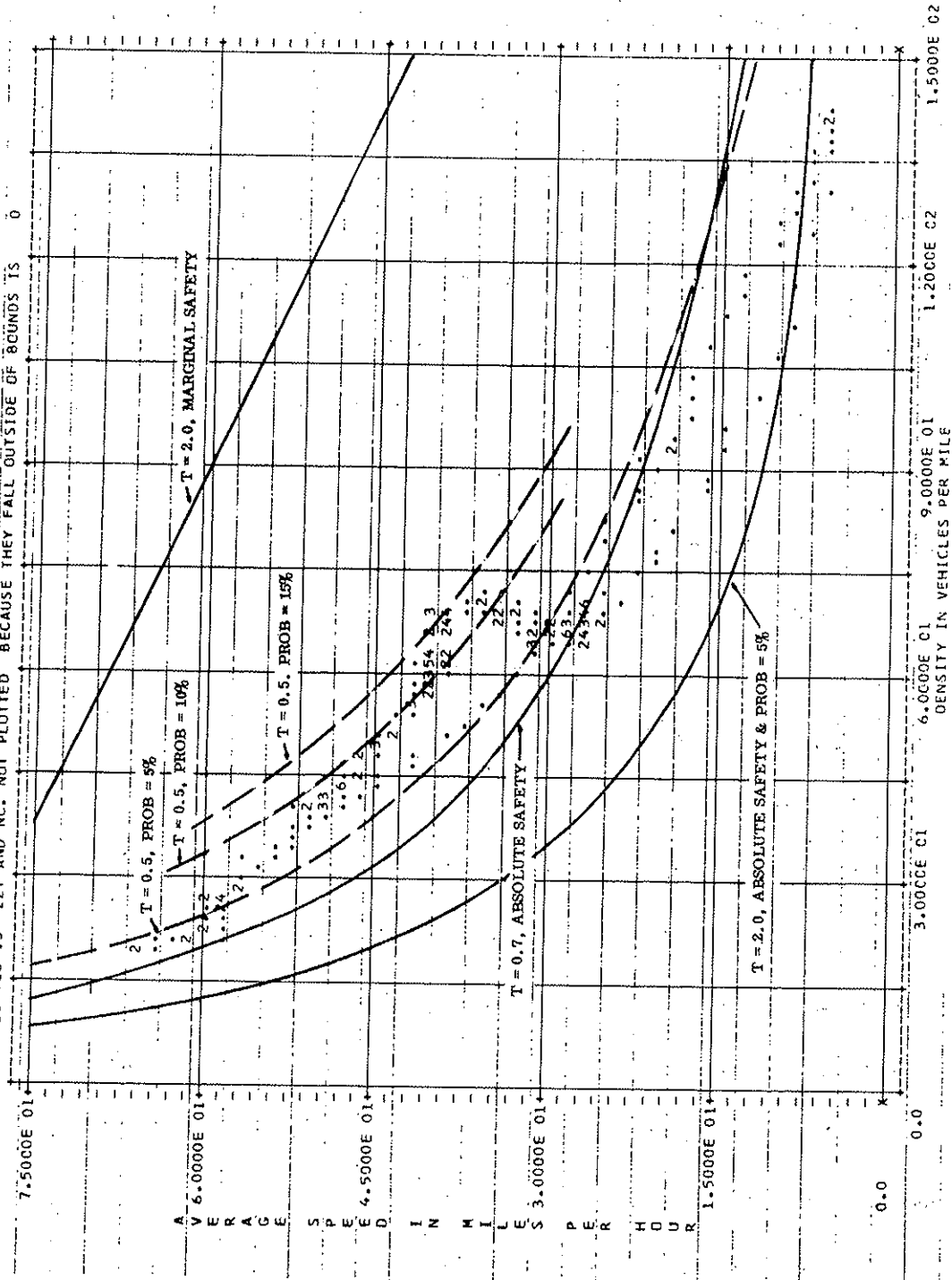


Figure 3.2 Safe Separation Concepts Applied to Speed-Density
 Data of Platoon 142

Ohio, to investigate causes and effects associated with instability in the traffic flow stream. It was found that flow instability can occur for no apparent reason and that the resulting disturbances may affect highway traffic in a number of ways.

During a survey made on southbound, morning peak hour traffic, a kinematic wave was generated and propagated at a velocity of approximately 19 feet per second against the direction of movement of the vehicles traveling in the median lane. The disturbance lasted for about 110 seconds with nearly 40 vehicles being forced to stop for periods ranging from a few seconds to almost 12 seconds. The situation, shown in Figure 3.3, was investigated for general information on volume, density, and stability of traffic flow. The traffic condition shown by the trajectories of Figure 3.4 3.3 comprises the whole range of free flowing traffic at about 60 mph average velocity to a complete breakdown and recovery of traffic movement with traffic densities exceeding 60 vehicles per mile at a speed of about 31 mph.

An attempt was made to determine the relationship of flow, density, and speed as presented by the Lighthill-Whitham Theory. The nine distinctly different areas of Figure 3.4 were chosen for this investigation. The points corresponding to areas 1 to 5 were plotted in Figure 3.5^{3.3}, and it can be seen that the ensuing volume-concentration curve fits rather smoothly. The measured propagation speed of the kinematic wave does meet the requirements

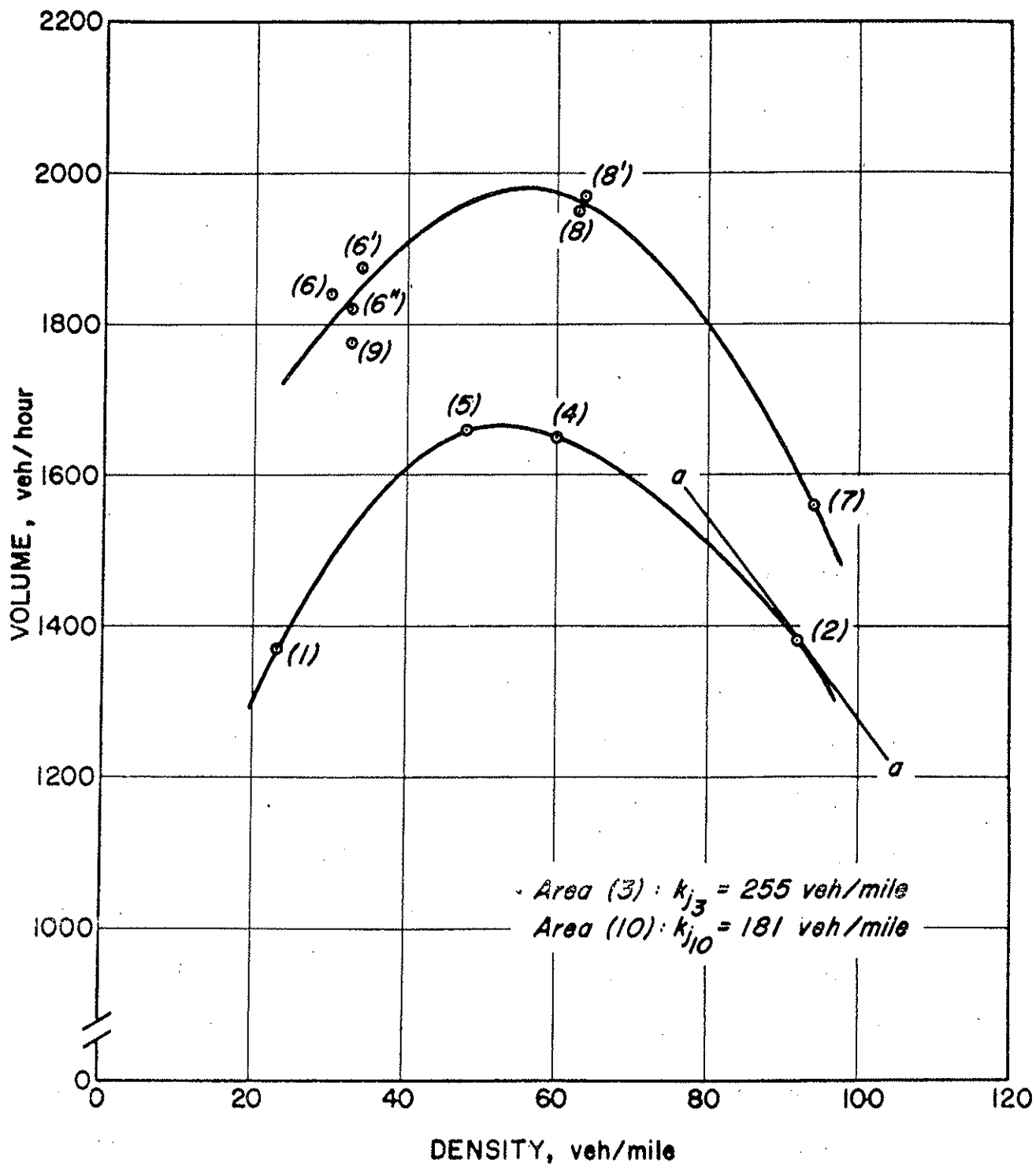


Figure 3.3 Volume-density Relationship

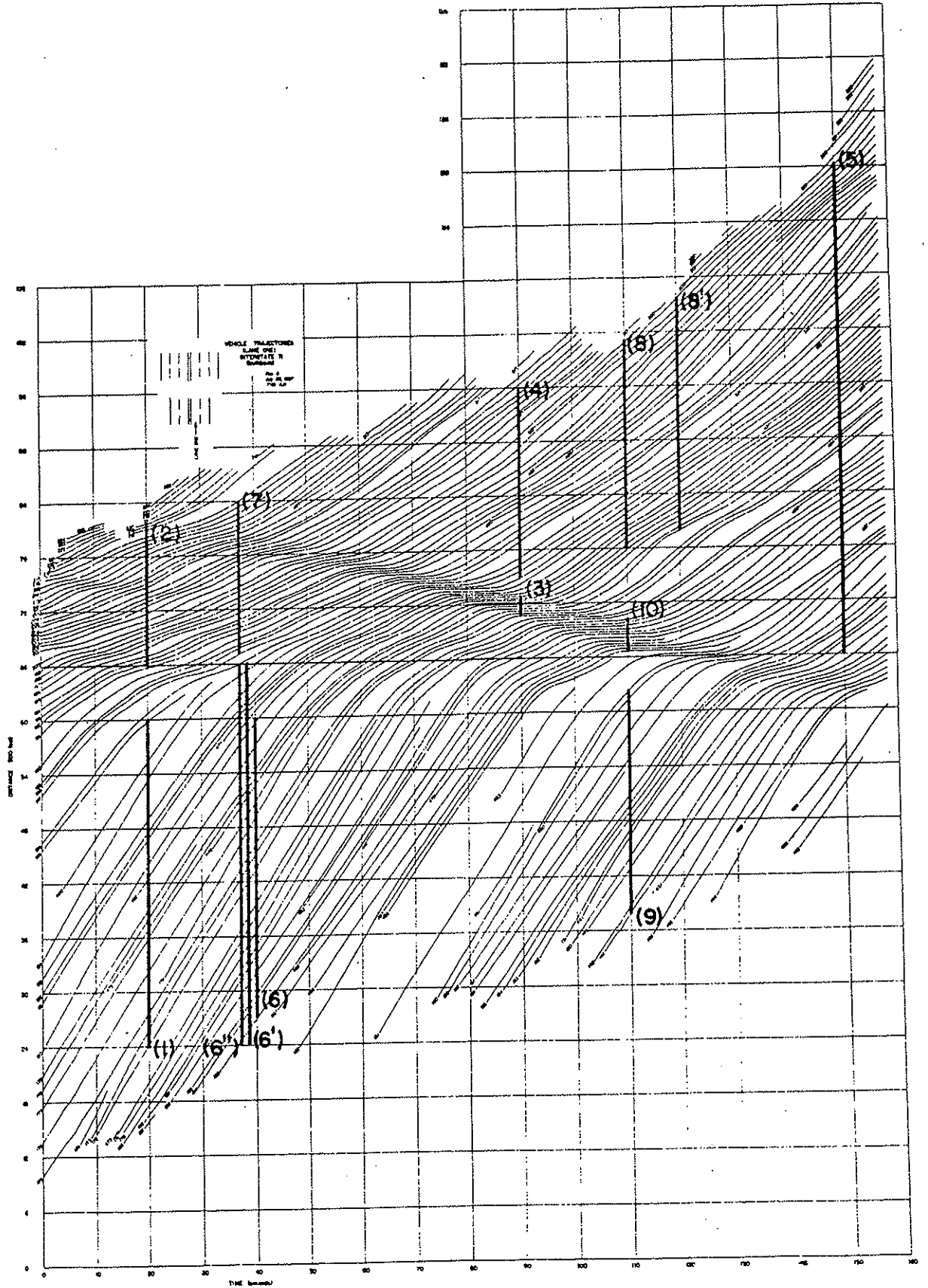


Figure 3.4 Areas Investigated to Determine Volume-density Relationship

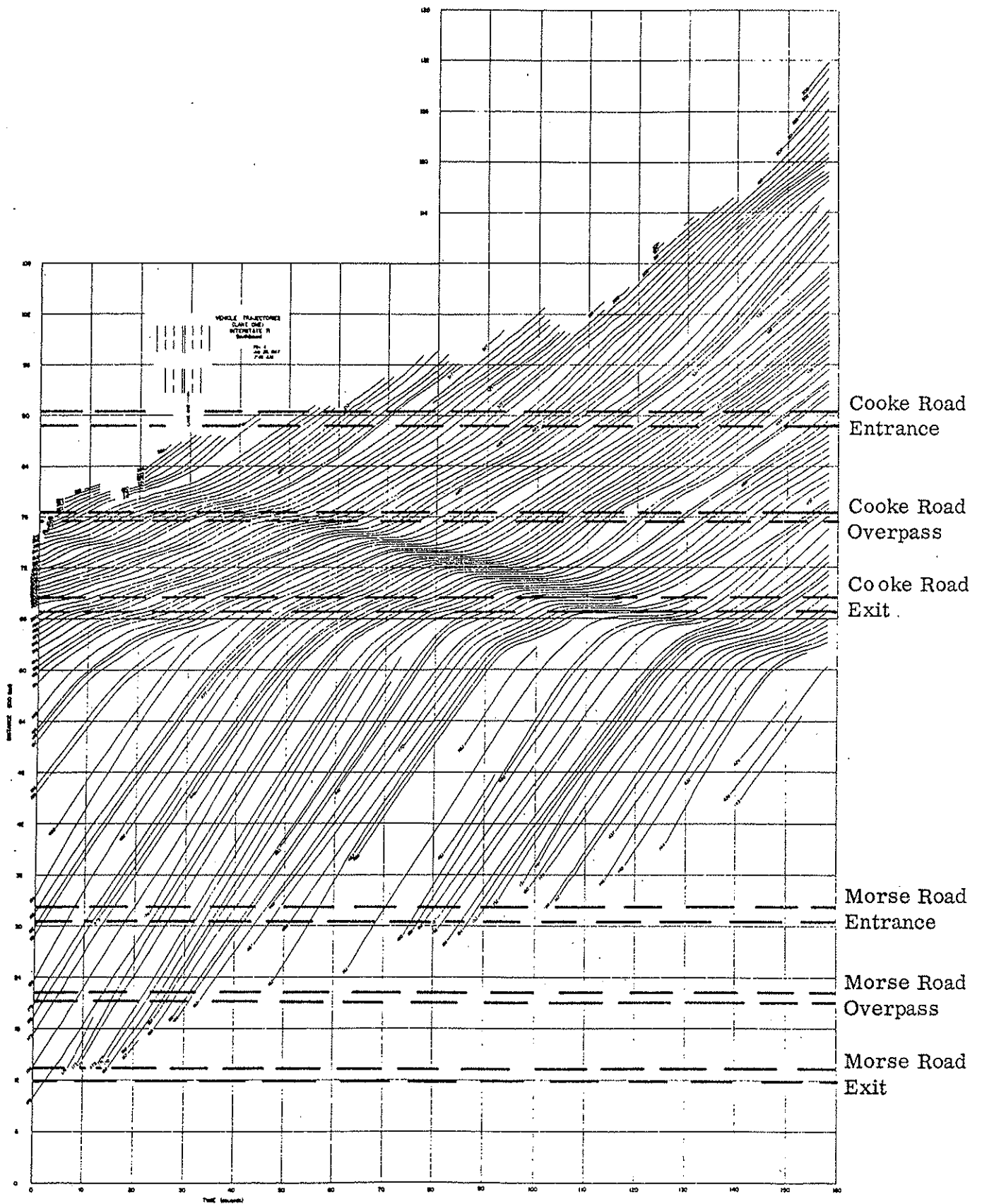
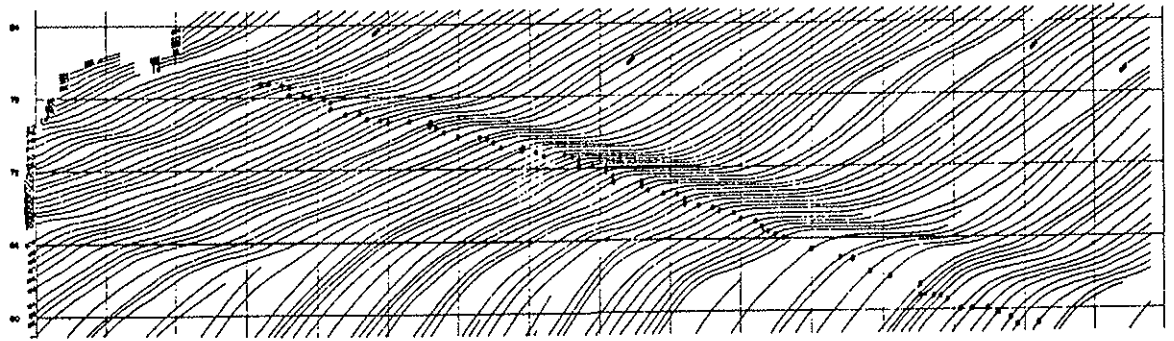
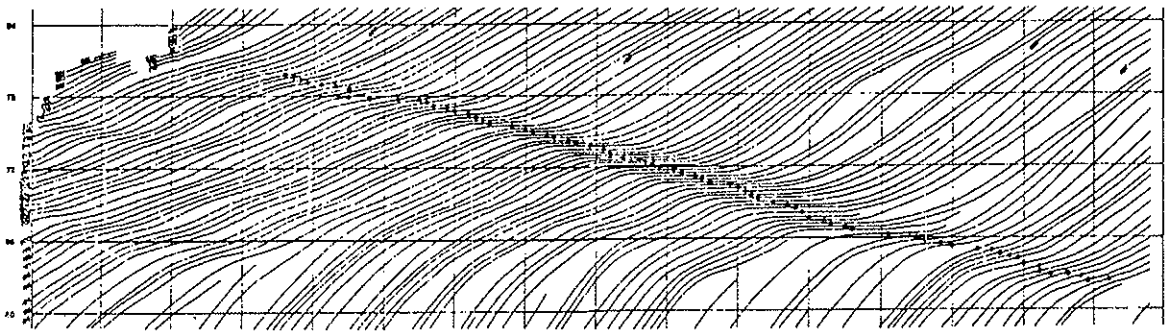


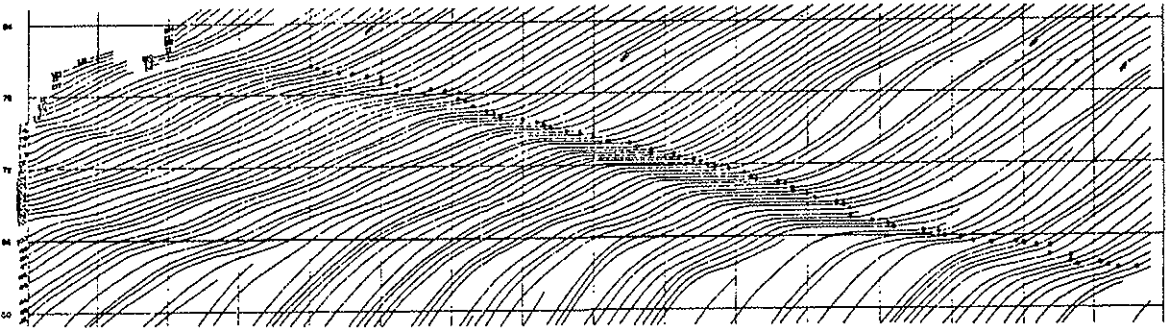
Figure 3.5 Location of Overpasses, Exit and Entrance Ramps
Lane 1



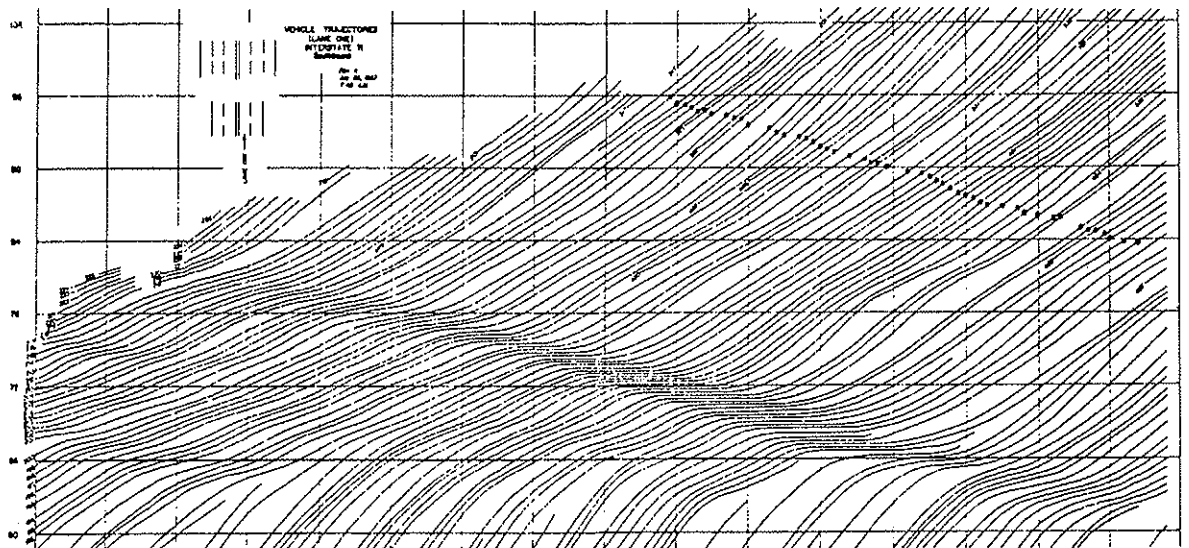
ENTERING DISTURBANCE



WITHIN DISTURBANCE

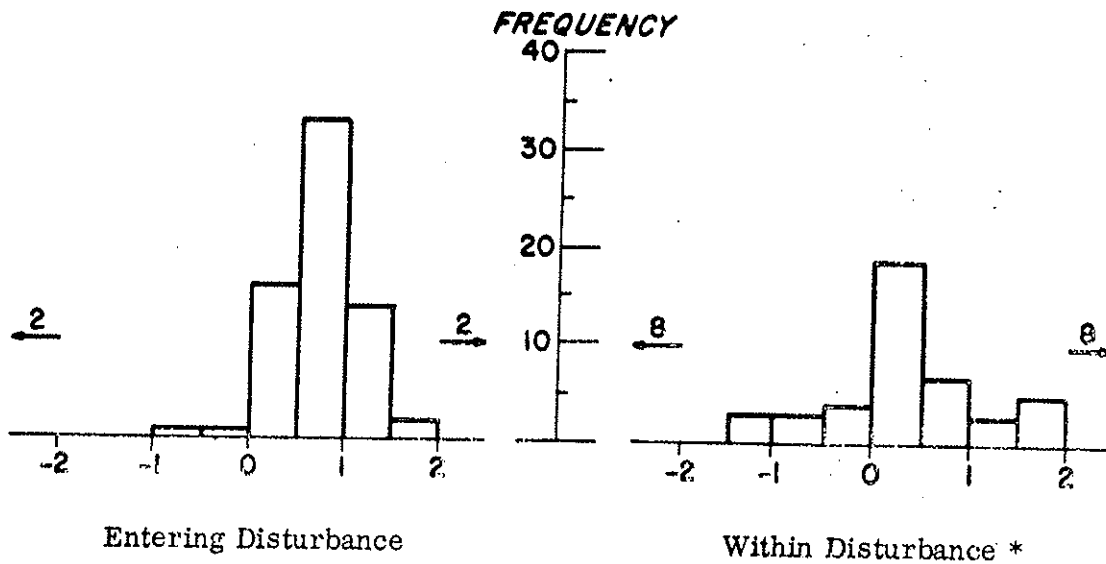


LEAVING DISTURBANCE



UNIFORM TRAFFIC FLOW

Figure 3.6 Location of Data Points



* Also has 9 infinite or undefined values of λ

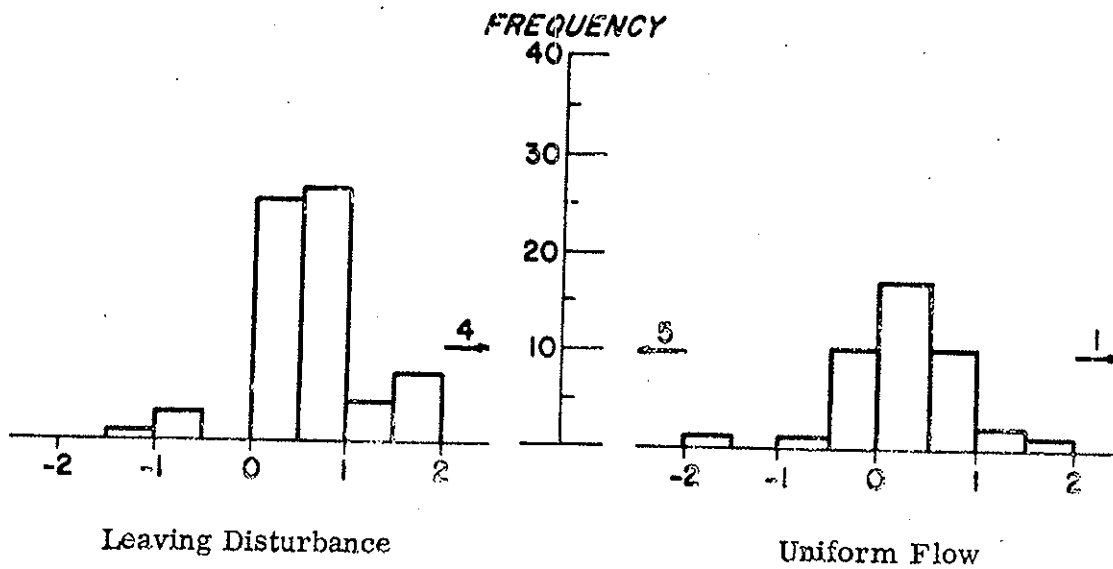


Figure 3.7. Distribution of λ -values

of the Lighthill-Whitham Theory close to point (2) as shown by the tangent a-a. Other points calculated from different areas, however, do not seem to agree with that curve. Points 6 to 9 and the resulting curve gives the distinct impression that traffic is proceeding at two different levels or in between two different levels.

It was decided to test the stability of traffic flow by the distribution of the sensitivity factor f and the distribution of λ . A general form for the sensitivity factor was proposed by Gazis, Herman, and Rothery (2) as

$$\lambda = a \frac{\dot{x}_{n+1}^m (t + r)}{[x_n(t) - x_{n+1}(t)]^L}$$

where:

r = response time and a is a constant of proportionality.

The condition for stable flow is:

$$1 \geq 2 \lambda r$$

Figure 3.6 shows the distribution of data points for vehicles entering, within, and leaving the disturbance, and for uniform traffic flow which exceeds 1700 vehicles/hour in this region. The distribution of sensitivity values λ is given in Figure 3.7; most of the values are concentrated in the area $x < 1$ indicating stability for all conditions, i. e. entering, within, and leaving the disturbance, as well as for uniform flow. It is quite obvious that this result does not agree with actual traffic conditions. The formation of a kinematic wave in itself is an instability which in this investigation is

propagated along the traffic lane causing vehicles to stop.

The distribution of the $2\lambda r$ -values is shown in Figure 3.8. Again stable conditions are indicated within the disturbances with most of the values smaller than unity. In entering quite a number of $2\lambda r$ -values exceed unity, implying the pending generation of a disturbance. More research on the subject appears to be necessary to determine the range of $2\lambda r$ -values to which traffic must adhere to prevent the formation of kinematic waves which frequently cause the breakdown of traffic flow.

3.3 TRAFFIC ENERGY CHANGE: A MEASURE OF THE QUALITY OF FREEWAY TRAFFIC

Drew (5) introduced the energy concept into traffic flow analysis by considering the traffic stream to be analogous to the flow of a compressible fluid in a constant-area duct. The kinetic energy term of the order aku^2 , similar to the fluid mechanics term of $1/2 \rho V^2$ for kinetic energy of a compressible fluid, is used to describe certain properties of a traffic stream. In the traffic case, a is a dimensionless constant, k is the density of the traffic stream, and u is the average speed of the stream.

The internal energy, however, is thought to be related to the interactions among vehicles in the stream and which are rather difficult to define. Drew proposed that a parameter, α_+ = "acceleration noise" be used as this measure.

Total energy for the system would be written as:

$$T = E + I \quad (1)$$

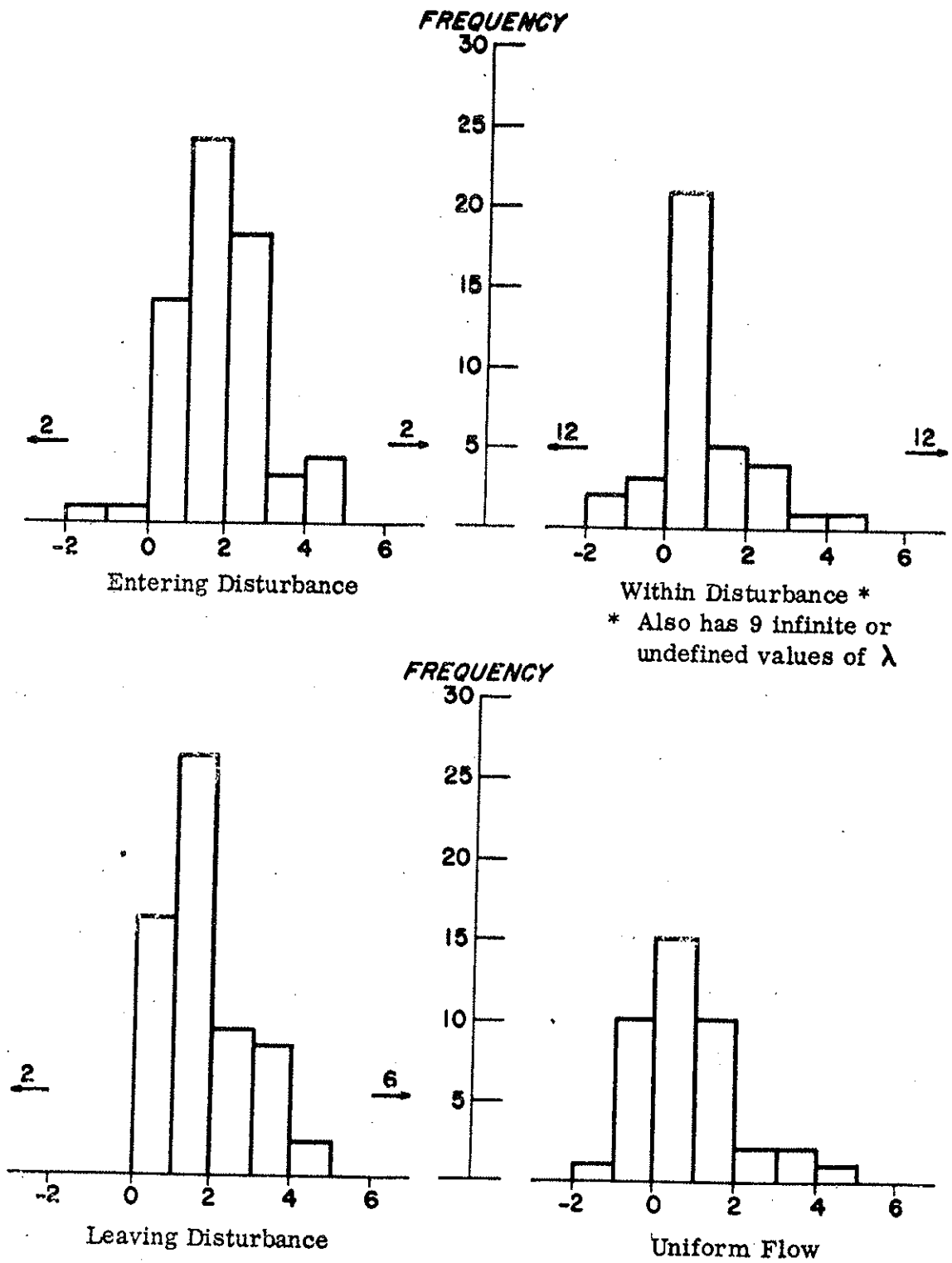


Figure 3.8. Distribution of $2\lambda\tau$ -values

where:

T = total energy of the traffic stream

E = kinetic energy

I = internal energy or "acceleration noise"

Equation 1 can then be rewritten as:

$$T = aku^2 + \sigma_t = \text{constant} \quad (2)$$

Although this expression represents a significant concept for the study of traffic characteristics, the application of the data derived from this research project found certain shortcomings of the energy hypothesis.

If the kinetic energy of the traffic stream is to be defined as aku^2 , the principle of the conservation of energy was shown to not hold. This, therefore, infers that the analogy between traffic flow and compressible fluid flow is not valid in terms of kinetic energy.

A search was undertaken for an acceptable indicator of internal energy. An empirical approach was used utilizing data on traffic movement collected by the aerial photogrammetry technique. Two groups of vehicles, designated as Group A and Group B, were chosen for study. The identification of these two groups of vehicles is shown on the trajectories presented in Figures 3.9 and 3.10 respectively.

Of various internal energy parameters investigated, only the coefficient of variation of speed fulfilled the requirements for the desired parameter. This parameter, CV_u , formed by dividing the standard

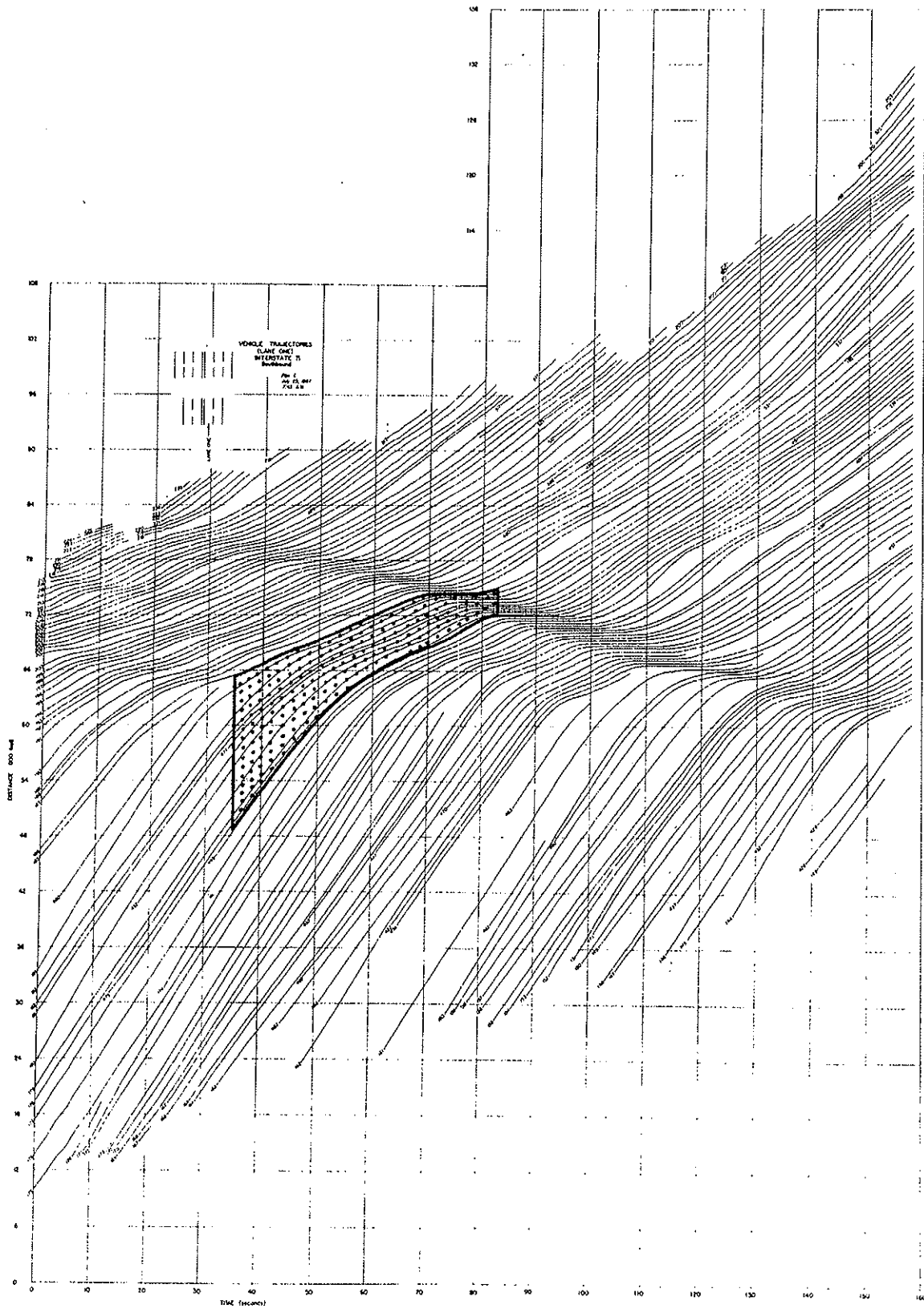


Figure 3.9 Identification of Group A Vehicles (shaded area)

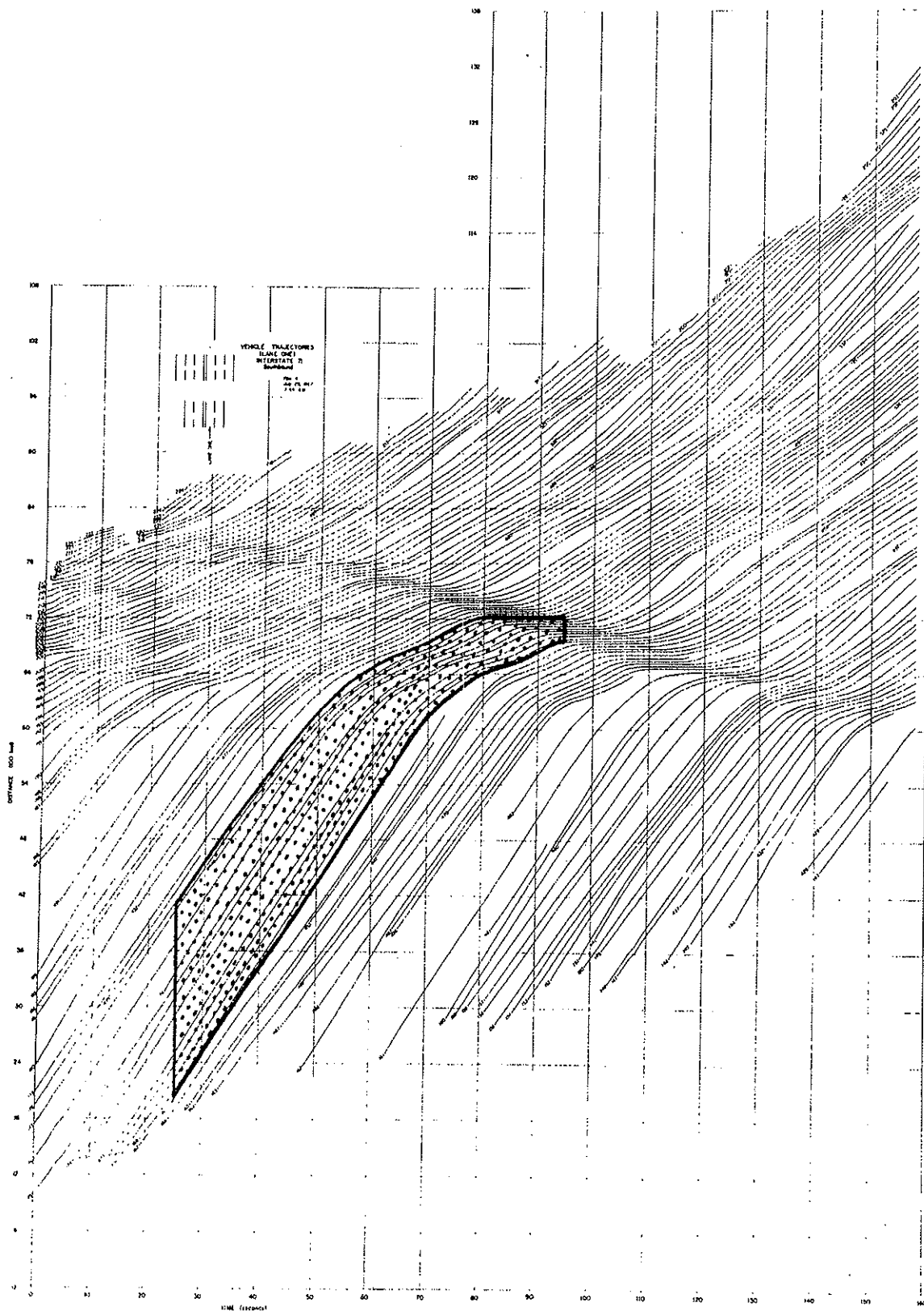


Figure 3.10 Identification of Group B Vehicles (shaded area)

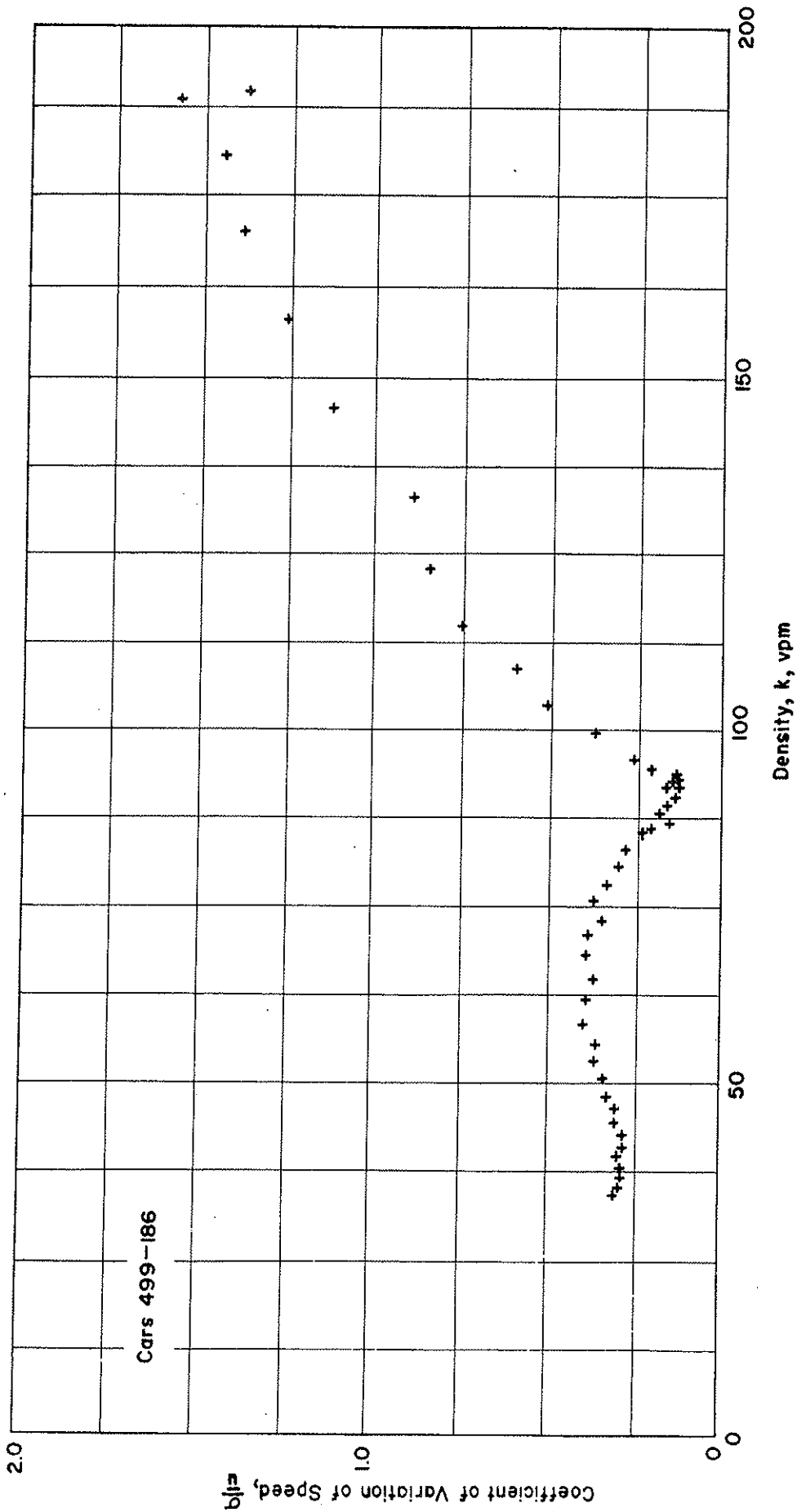


Figure 3.11 Coefficient of Variation of Speed versus Density for Group A Vehicles

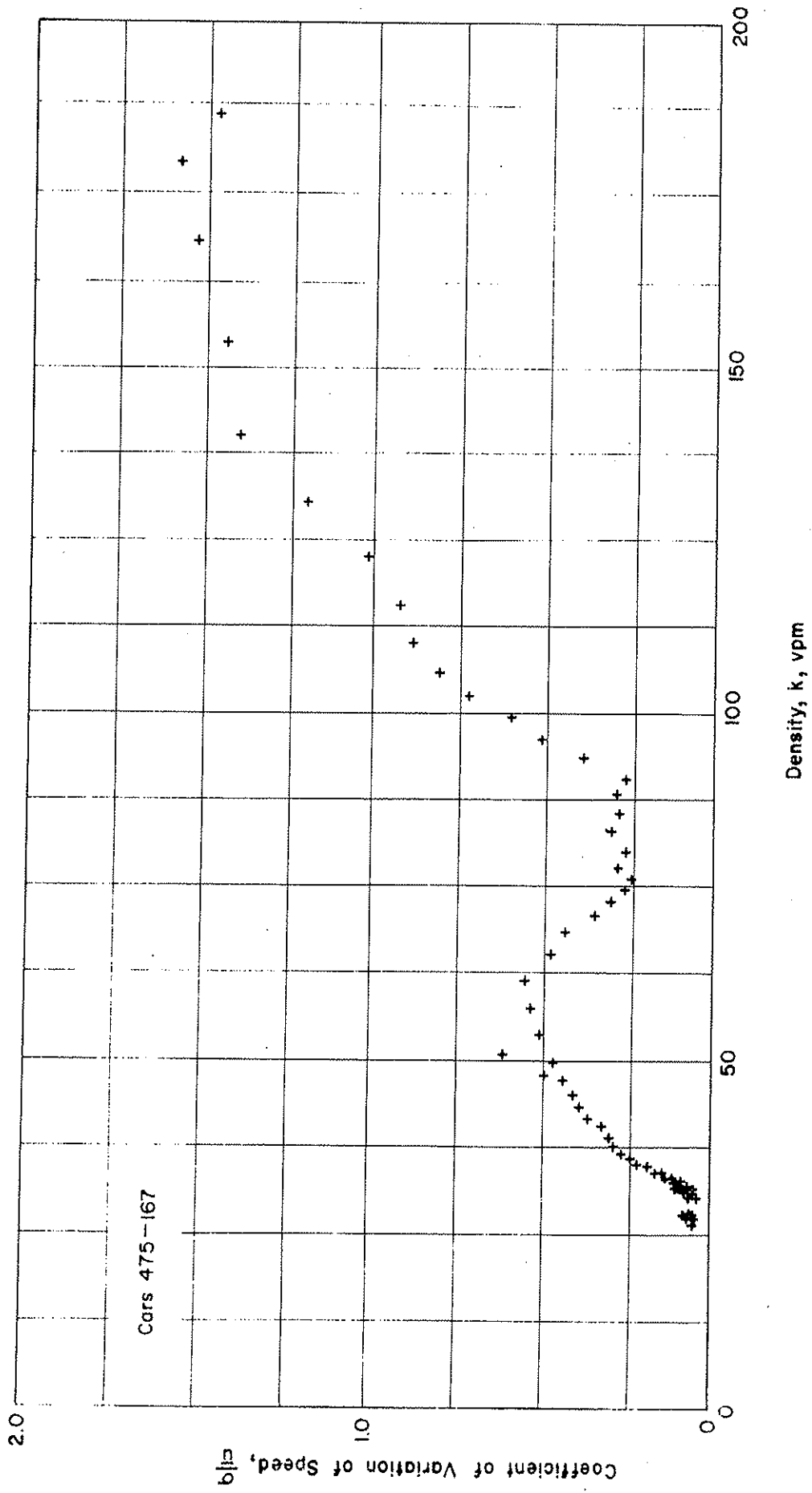


Figure 3.12 Coefficient of Variation of Speed versus Density for Group B Vehicles

deviation of the speed distribution by the arithmetic mean speed at each density level, provides a measure of the relative dispersion of the speed values as a percentage of the mean speed. A plot of CV_u versus density is given in Figures 3.11 and 3.12 for Group A and B vehicles.

This parameter displays almost the same pattern proposed by Drew in Figure 3.13. It is noted that the CV_u displays nearly the same pattern as the standard deviation of the platoon speed distribution σ_5 at the low and medium density levels but increases rapidly to a maximum at jam density.

In spite of the inapplicability of the principle of conservation of energy and compressible fluid flow, the concepts of the kinetic and internal energy of a traffic stream are thought to be important contributions to the understanding of traffic dynamics. The coefficient of variation of speed fulfills the postulated requirements of an internal energy parameter, and is therefore proposed as a suitable measure of that parameter.

3.4 MULTILINEAR SPEED-DENSITY RELATIONSHIPS

A major area of investigation during this research project has been the study of functional relationships between the three fundamental traffic parameters: density, volume, and speed. The basic relationship of traffic flow assumes that traffic volume equals the product of speed (space-mean) and density. Therefore, only one pair of the three basic parameters is needed to study all possible functional relationships. Of the possible pairings, speed-density data seems to exhibit the simplest function pattern and

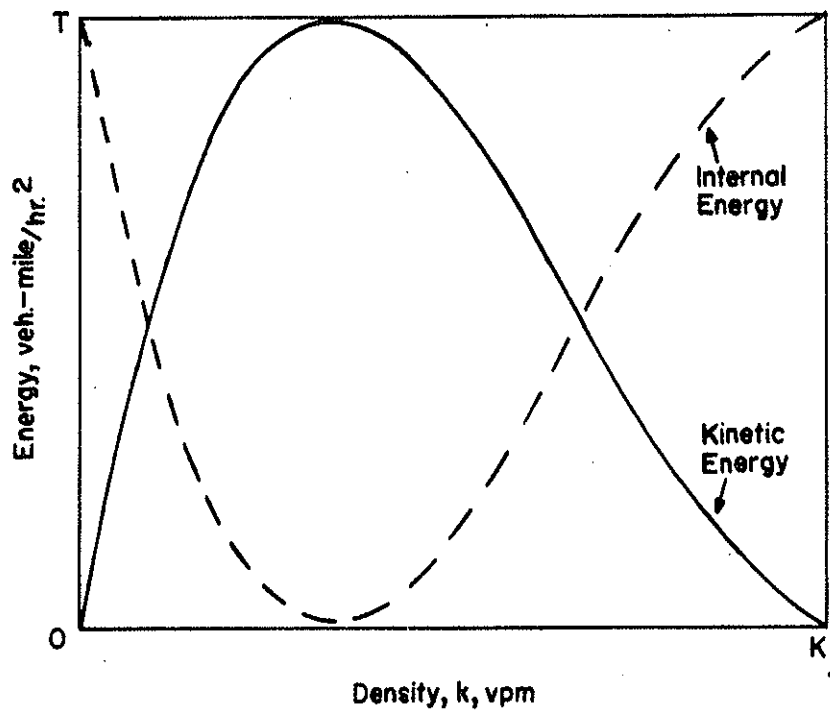


Figure 3.13 Energy System Proposed by Drew, Assuming a Linear Speed-Density Relationship

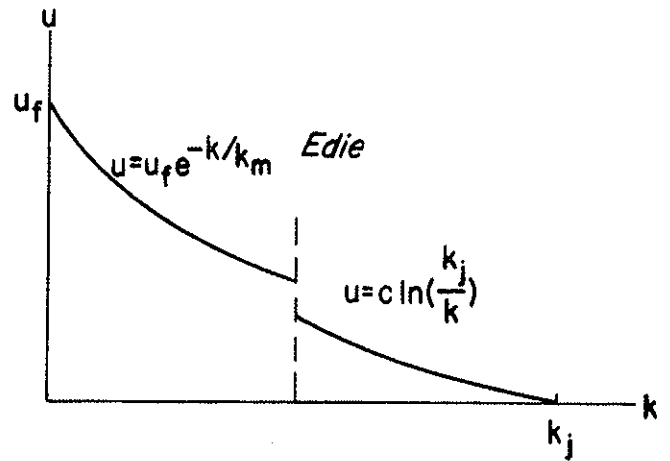
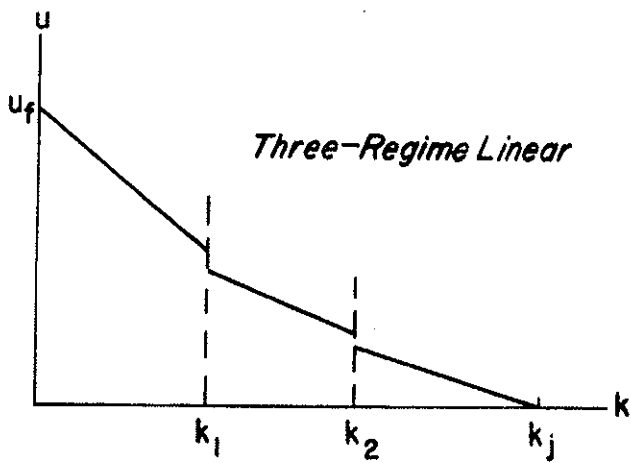
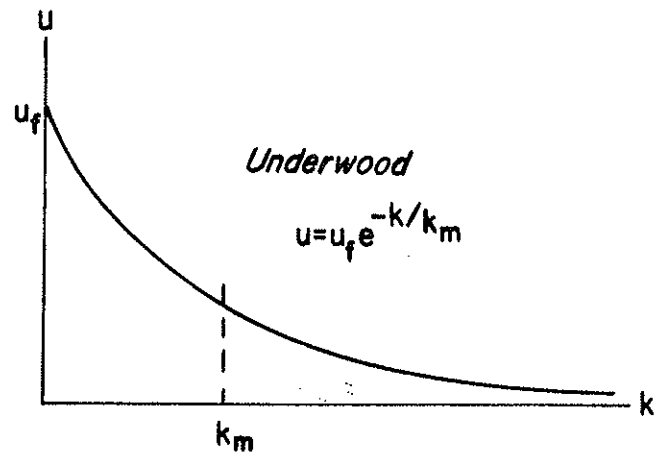
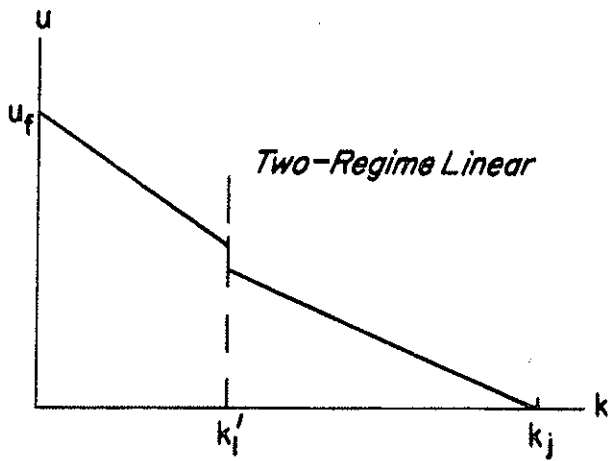
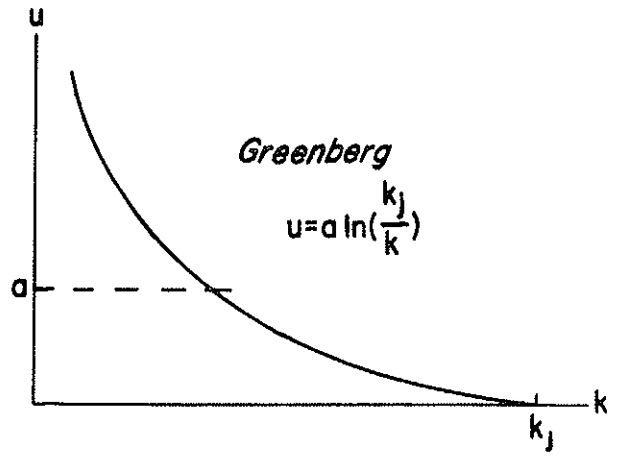
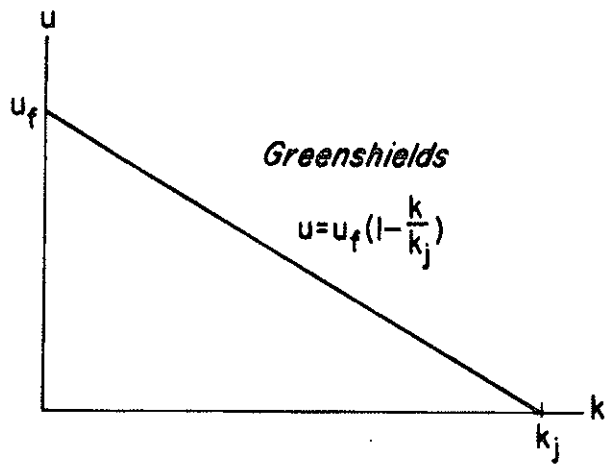


Figure 3.14 Proposed Speed - Density Relationships

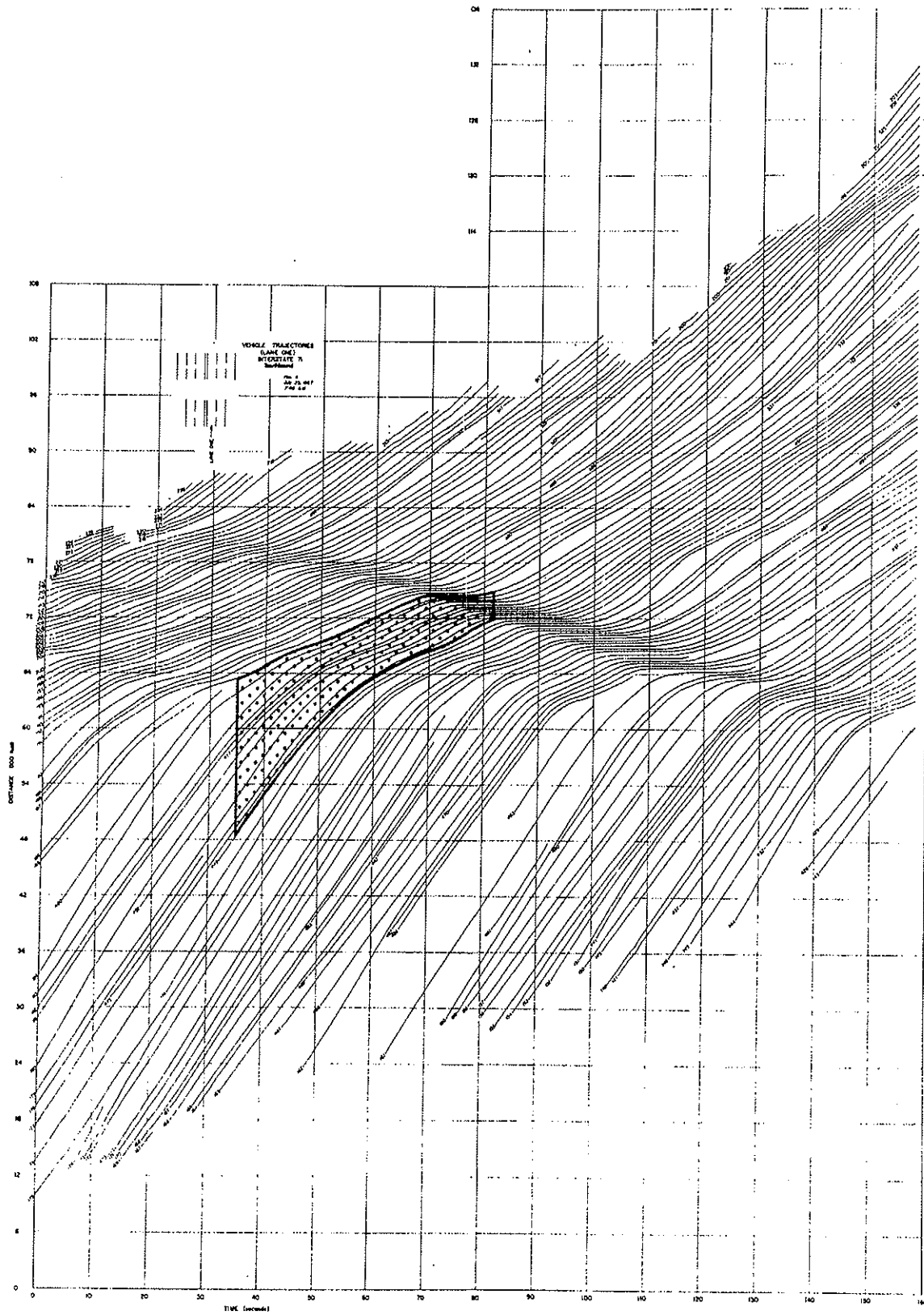


Figure 3.15 Identification of Group A Vehicles (Shaded Area)

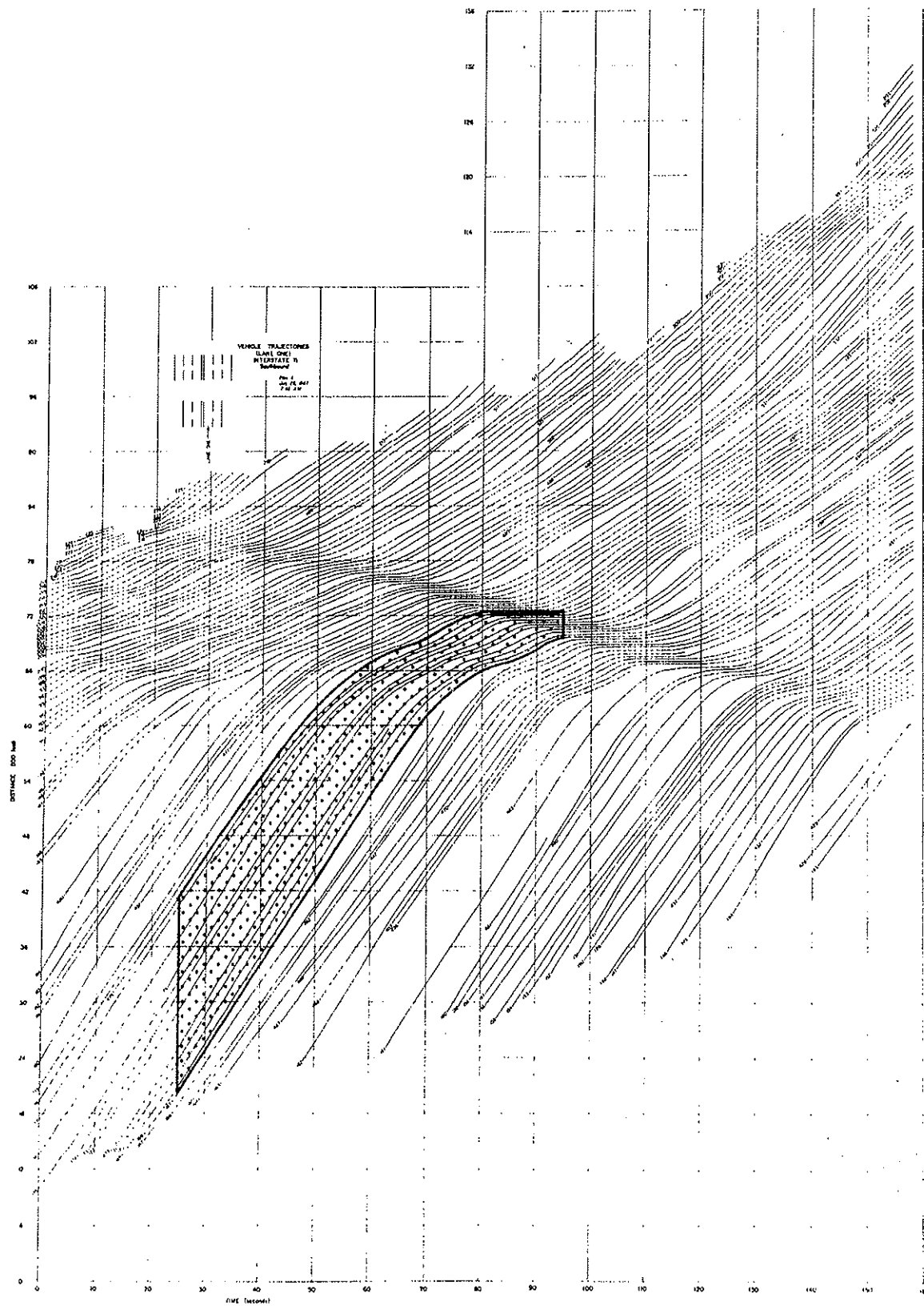


Figure 3.16 Identification of Group B Vehicles (Shaded Area)

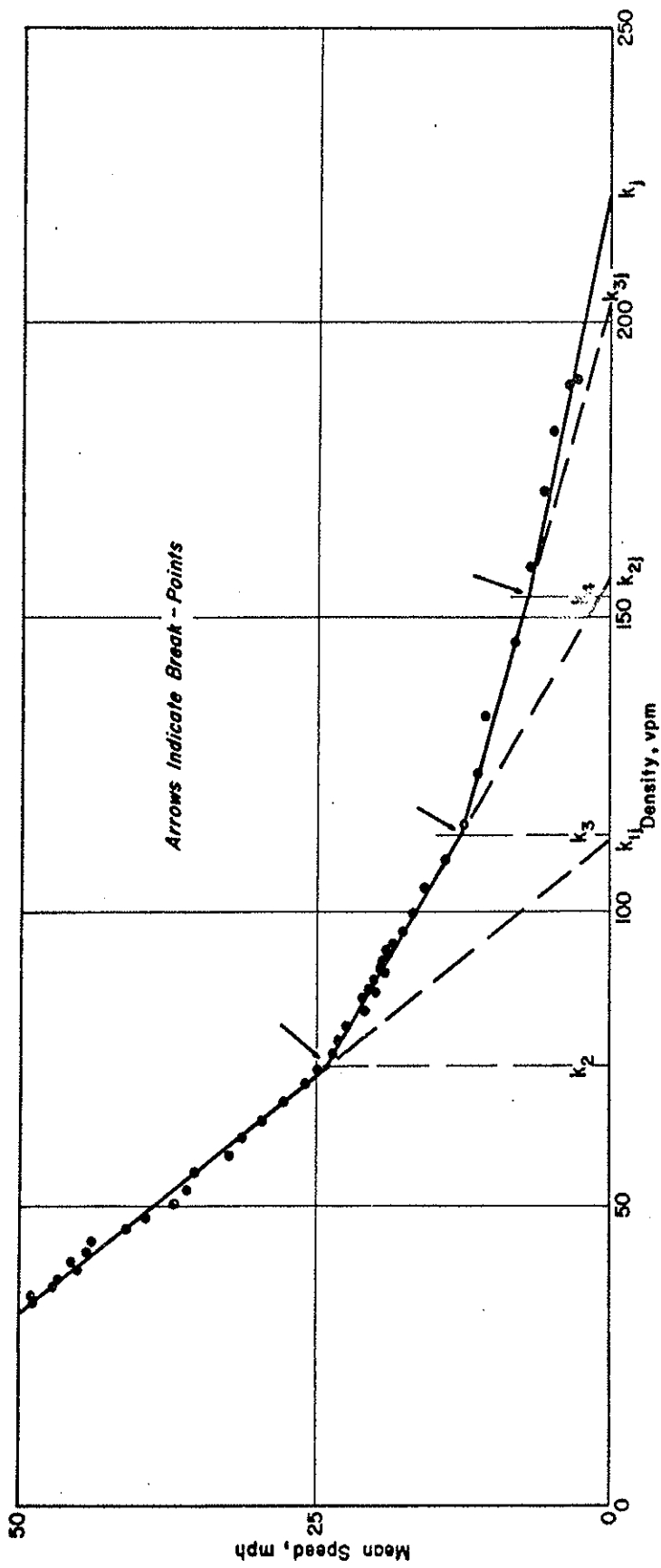


Figure 3.17 Hand Fitted Multilinear Curve for Velocity versus Density Relationship for Group A Vehicles

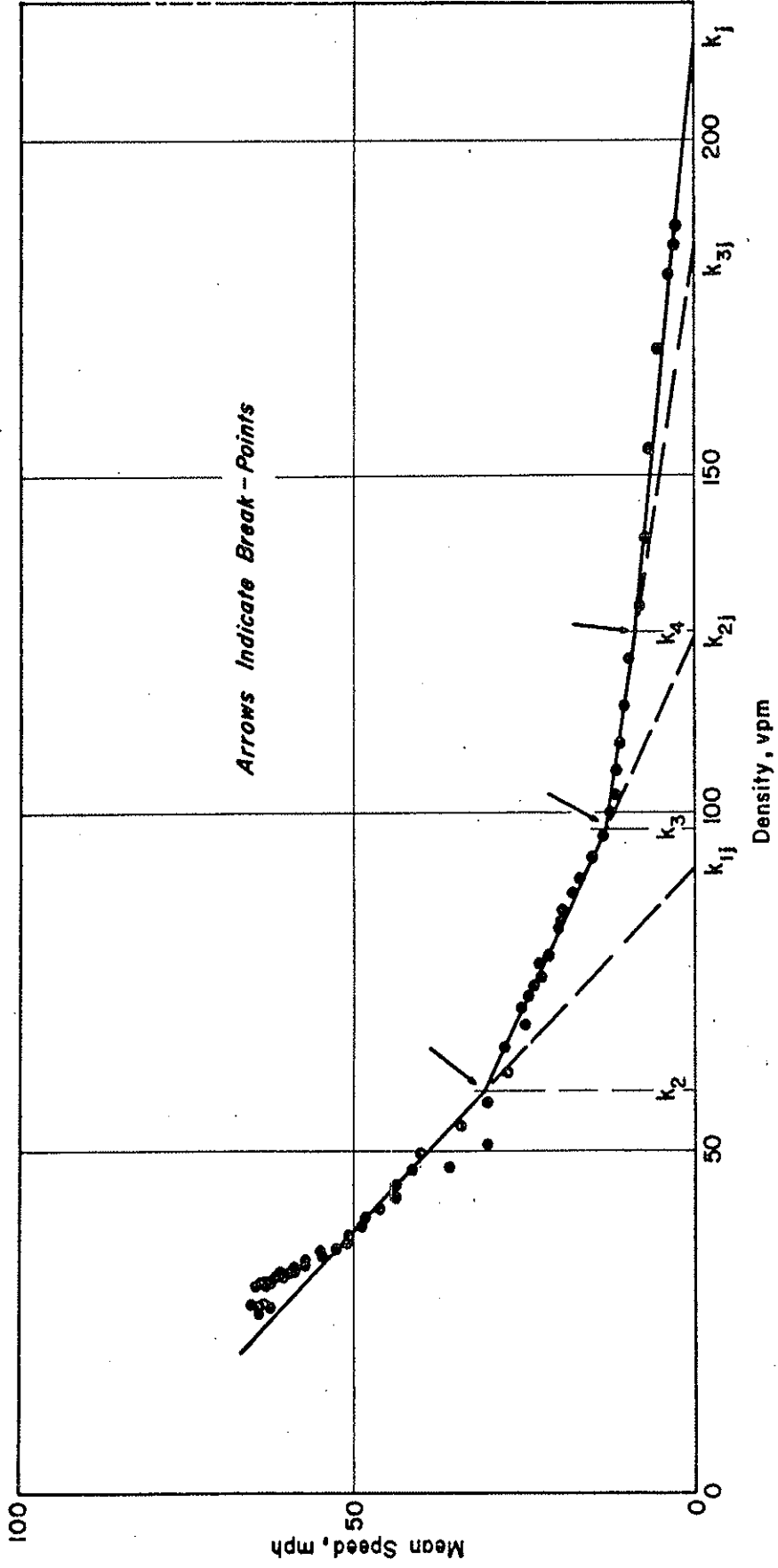


Figure 3.18 Hand Fitted Multilinear Curve for Velocity versus Density Relationships for Group B Vehicles

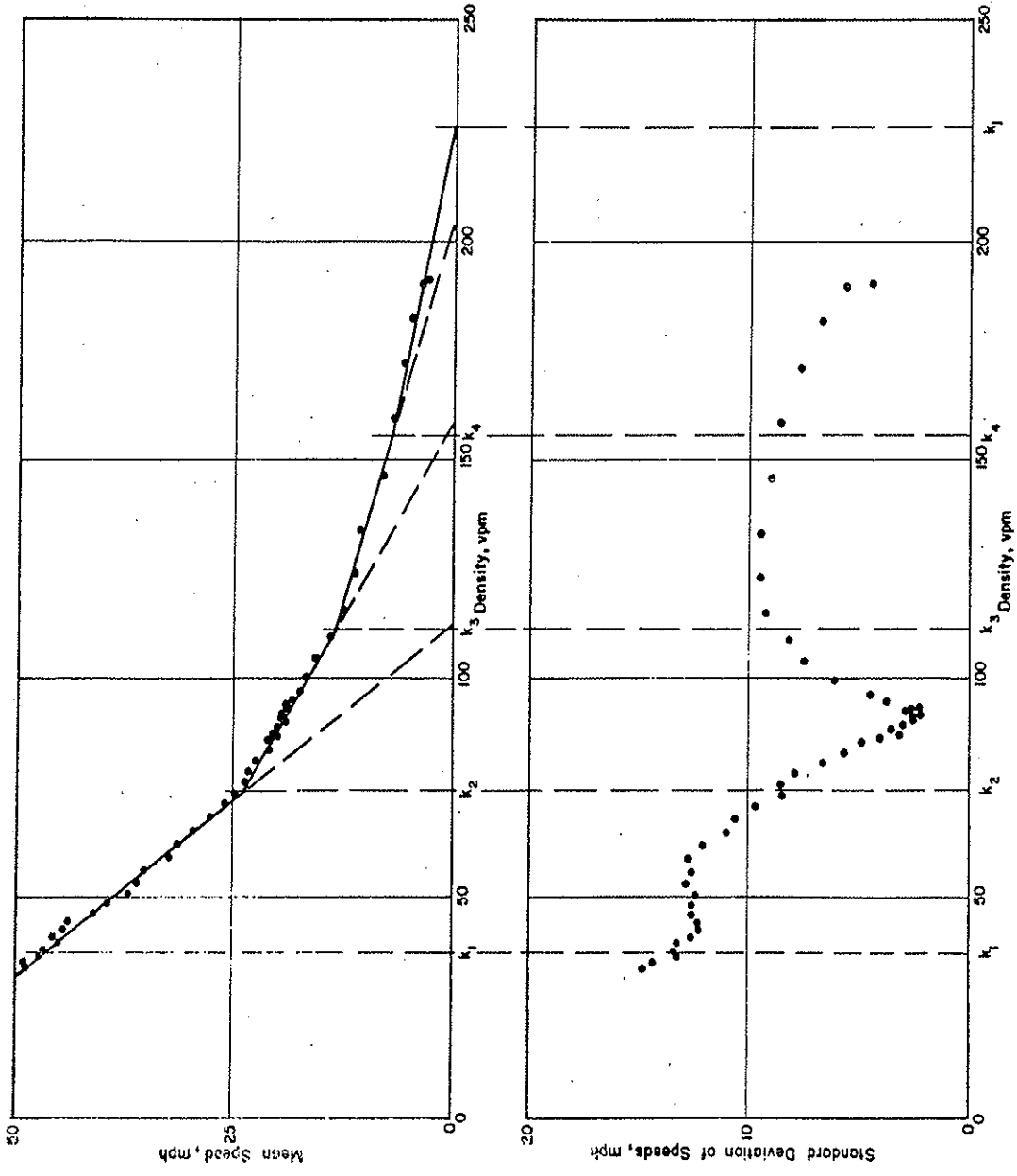


Figure 3.19 Variation of Speed Distribution in Different Density Regions for Group A Vehicles

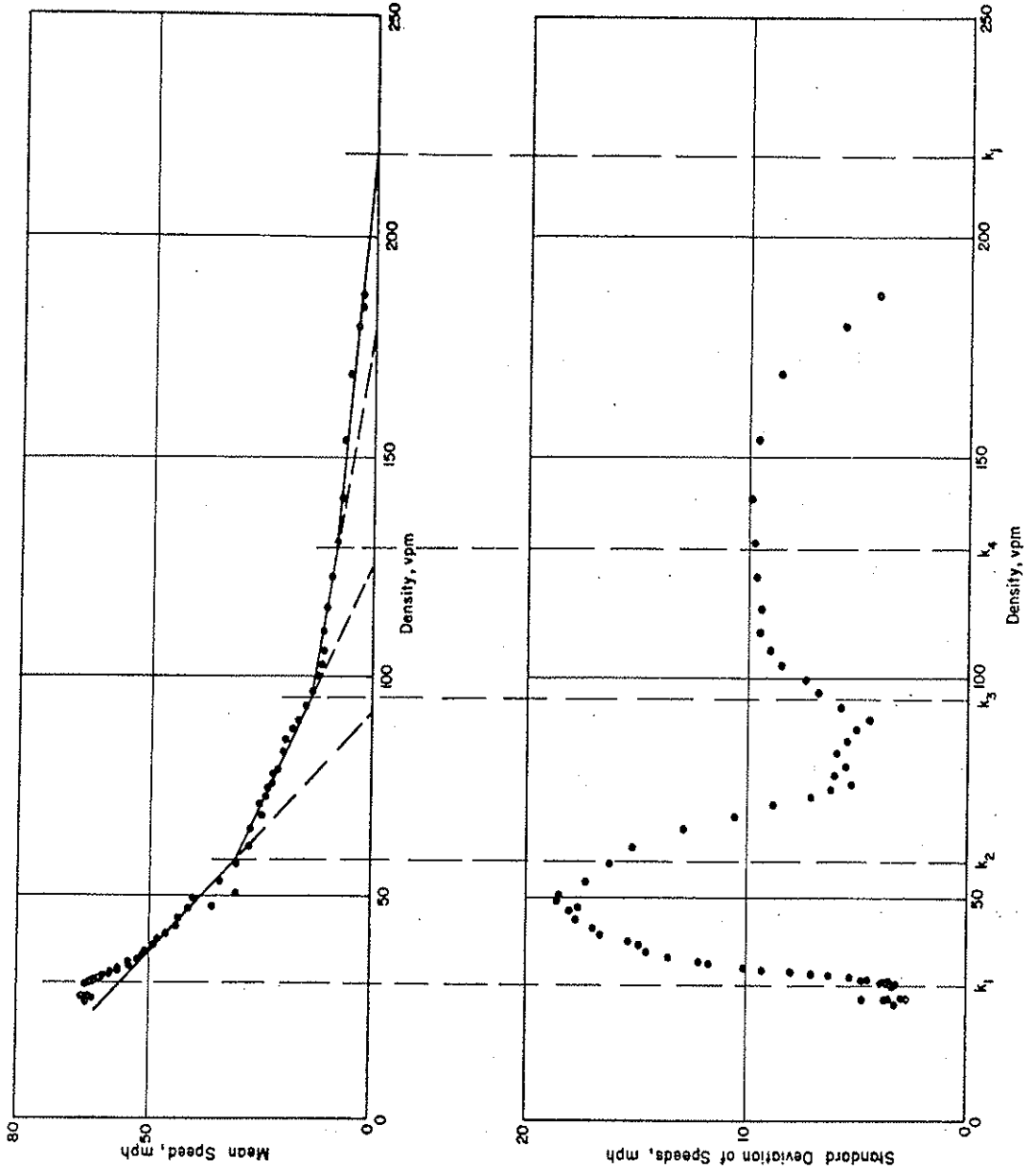


Figure 3.20. Variation of Speed Distribution in Different Density Regions for Group B Vehicles

therefore is used most often to investigate the macroscopic characteristics of traffic flow.

Drake, Schofer, and May (6) evaluated the seven different speed-density hypotheses summarized graphically in Figure 3.14. Results tended to support the three-regime linear hypothesis although all hypotheses performed well enough to warrant use.

The seven hypotheses considered by Drake et al were evaluated using the I-71 Columbus, Ohio data. Data from the two groups of vehicles selected for analysis are shown in the vehicle trajectories of Figures 3.15 and 3.16. From the diagrams it can be seen that the vehicles selected proceed from low density, high speed conditions through medium density, medium speed conditions to a disturbance.

For each group of vehicles, mean speed-density relationships were determined and straight lines were fitted to the data points, as in Figures 3.17 and 3.18. Three obvious points of discontinuity can be readily detected, supporting the use of the multilinear speed-density relationship.

In order to reflect a change in the state of traffic flow in the multilinear speed-density curve, the standard deviation σ of the velocities of each of the two groups of vehicles was calculated and the variation with traffic density for each group was plotted. These relationships are shown in Figures 3.19 and 3.20.

From these curves it is apparent that σ undergoes pronounced variations for the range of traffic density studies. It appears that the entire

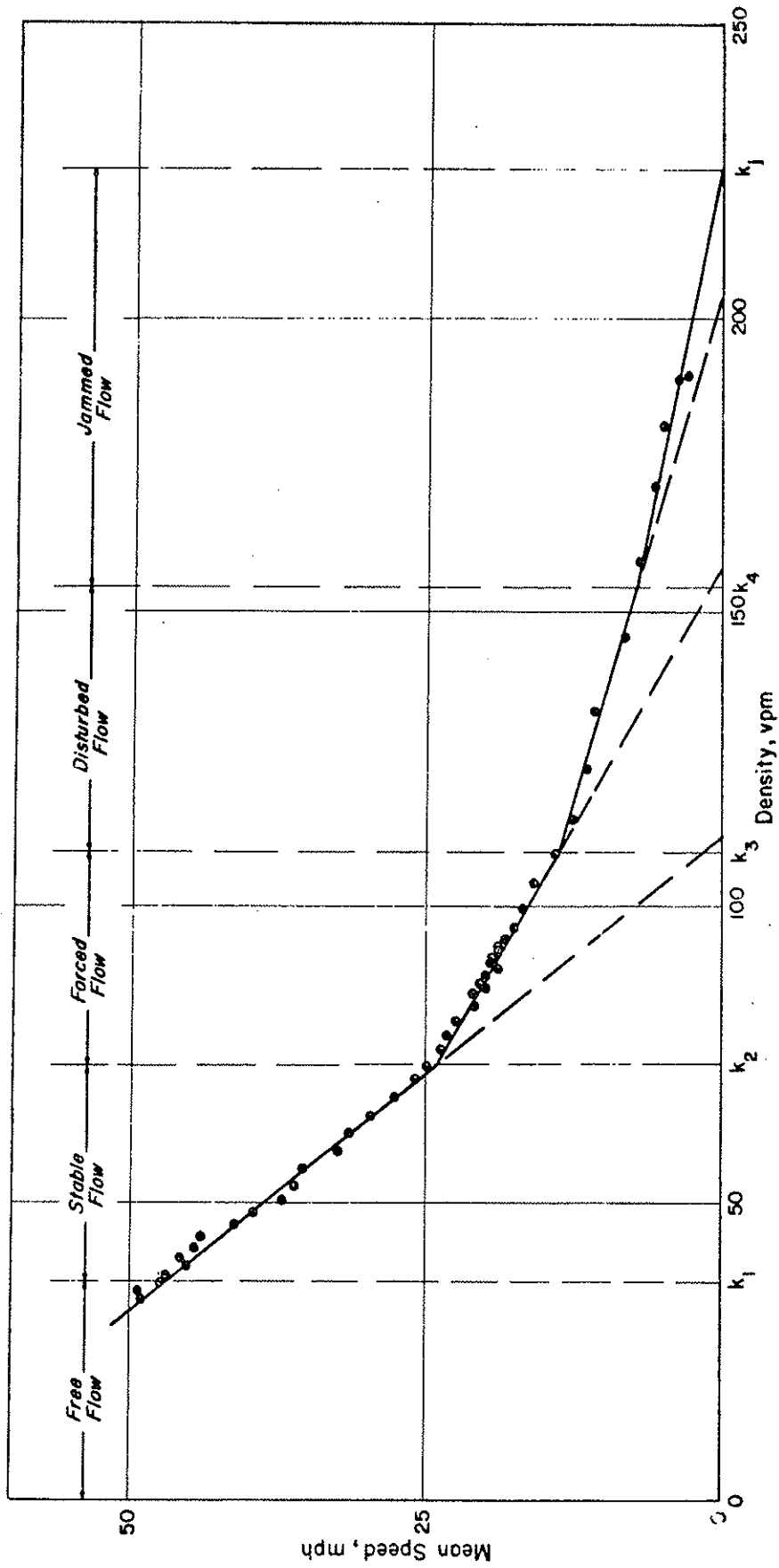


Figure 3.21 Suggested Operational Regions

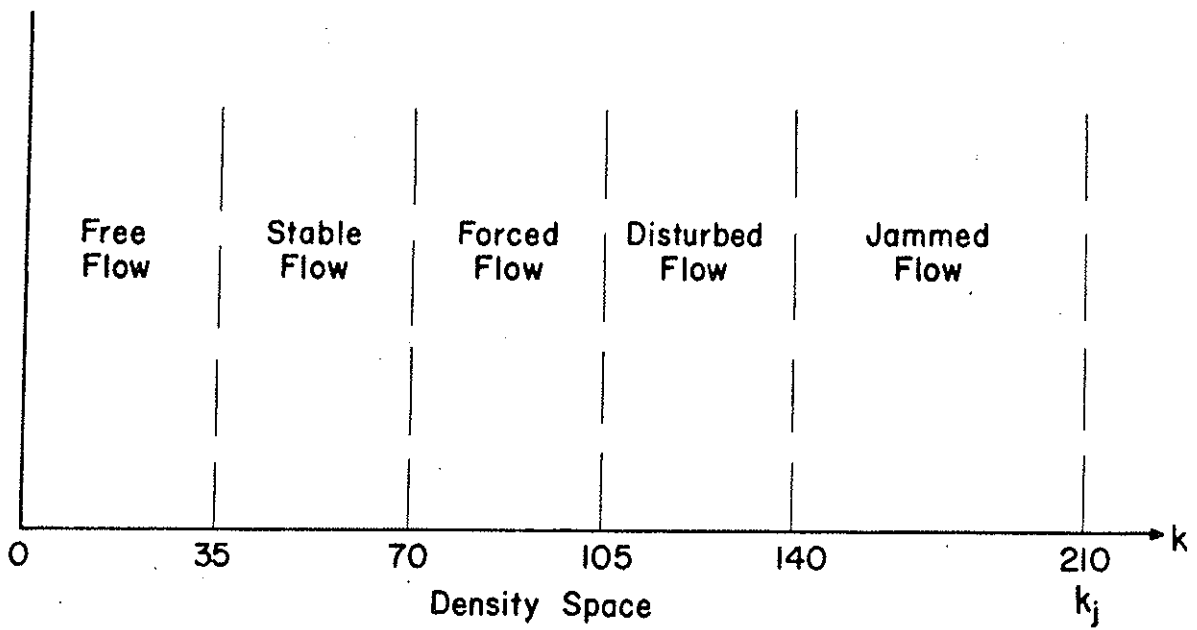


Figure 3.22 Suggested Operational Standards

traffic domain can be divided into six mutually exclusive operational regions; however, the effect of the hysteresis phenomenon on the characteristics of these operating regions is unknown.

The operating characteristics of each density region, as suggested in Figures 3.21 and 3.22, are described below. Those traffic characteristics which are affected by the hysteresis phenomenon are omitted.

Free flow region. This region has a density span from zero to 35 vpm.

Stable flow region. The two curves show different σ patterns, suggesting that traffic density does not have much effect on speed variation in the stable flow.

Forced flow region. When the level of traffic density reaches the forced flow region, in both cases σ begins to decrease quickly. It may be interpreted that the bunching of vehicles restricts the speeds that drivers can maintain and this interaction of vehicles is reflected in the low σ values.

Disturbed flow. The region of disturbed flow is an unstable state and density is apt to increase rapidly. This further increase in density disturbs the platoon as seen by the increase in the speed variation. This increase in σ seems to agree with the aspects of instability associated with the car-following situation.

Jammed flow. Instability results in nearly half the vehicles being stopped as they enter the jammed flow region. A point k_j , projected on the density axis indicates jam conditions.

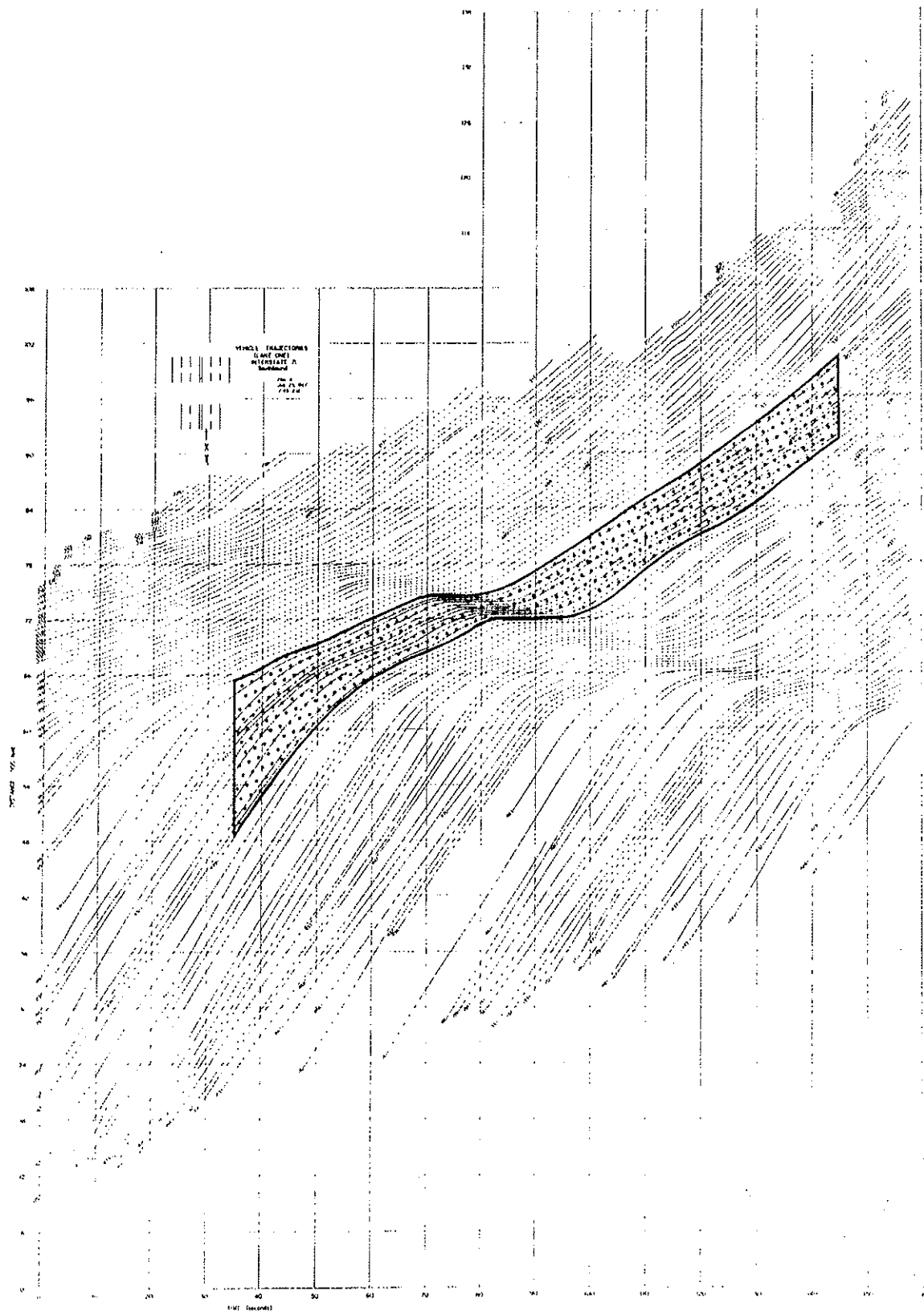


Figure 3.23 Identification of Group A Vehicles (Shaded Area)

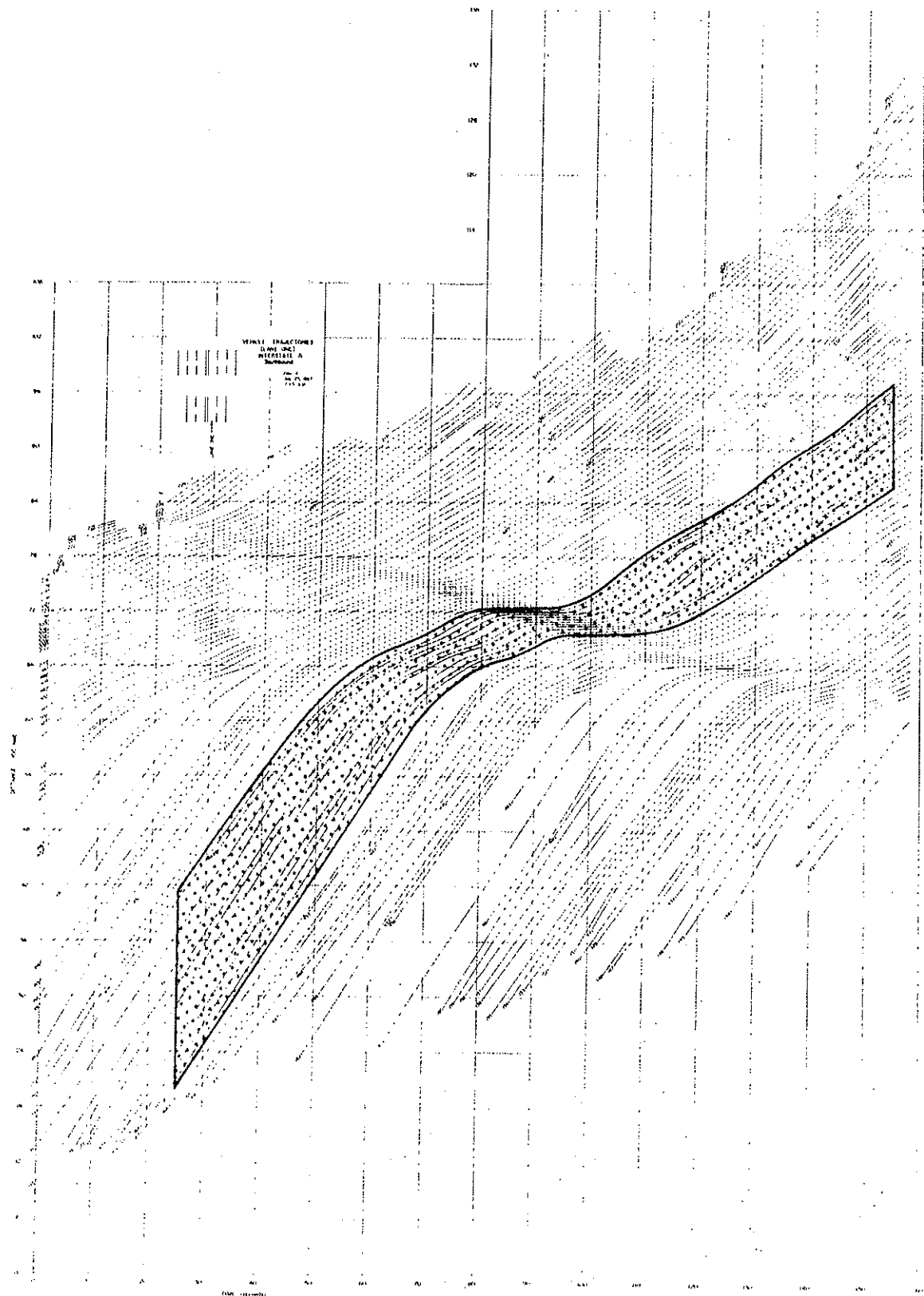


Figure 3-24 Identification of Group B Vehicles (Shaded Area)

The multilinear speed-density function adequately describes the speed-density of the traffic stream. Traffic density breakpoints, determined from the multilinear speed-density relationship, delineate the regions of traffic flow.

3.5 HYSTERESIS PHENOMENON OF TRAFFIC FLOW

An investigation of the different traffic patterns between a queue forming and queue releasing condition was conducted with the photogrammetric data. The two platoons observed are illustrated in Figures 3.23 and 3.24.

Following each of the two platoons of vehicles for a period of two minutes, average platoon velocities and densities were calculated at one second intervals. The kinetic energy of each stream was then calculated for each second and plotted against the corresponding traffic density. These relationships are shown in Figures 3.25 and 3.26. The important feature in the construction of the graphs is to note the time dependence; any two consecutive points connected by a line are separated in time by one second. It is observed that the traffic stream does not recover at the same rate with density as it entered jam conditions. This retardation was called the hysteresis phenomenon of traffic flow.

The standard deviation, σ , of the individual velocities of the vehicles in a platoon is used as an unbiased indication of the interaction between vehicles.

The standard deviations of the vehicle velocities were computed from

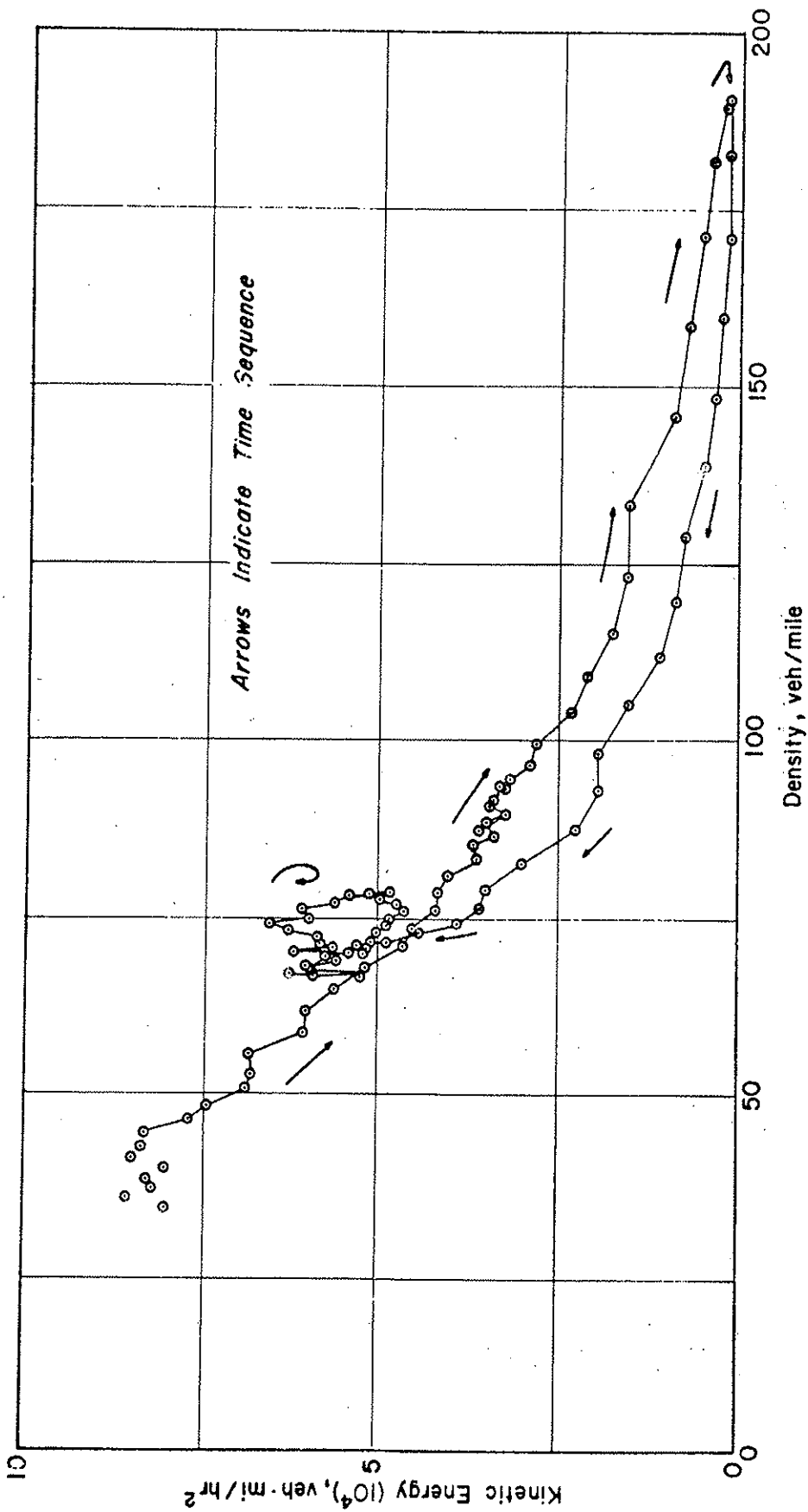


Figure 3.25 Observed Hysteresis Loop Before and After a Jam Condition (Group A Vehicles)

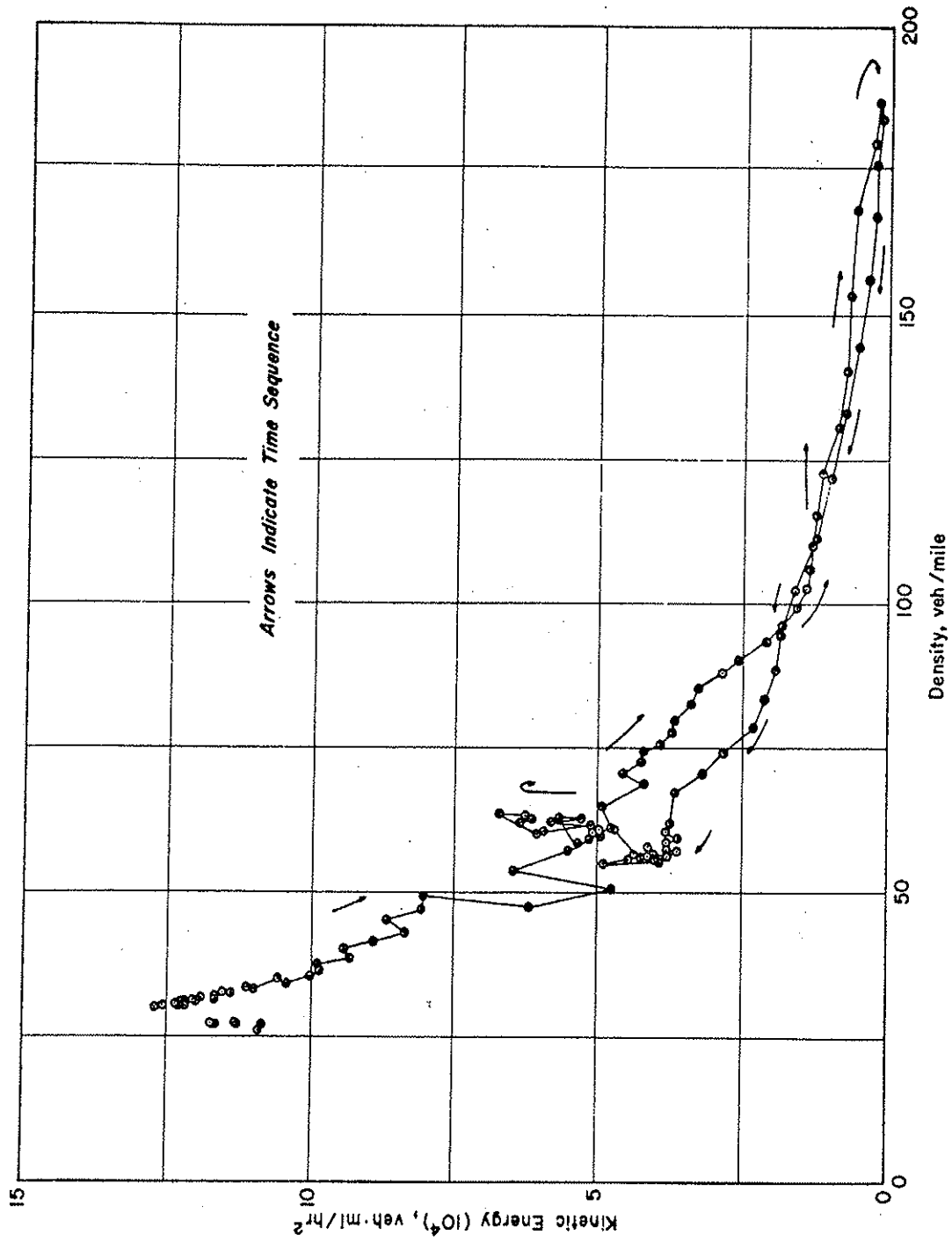


Figure 3.26 Observed Hysteresis Loop Before and After a Jam Condition (Group B Vehicles)

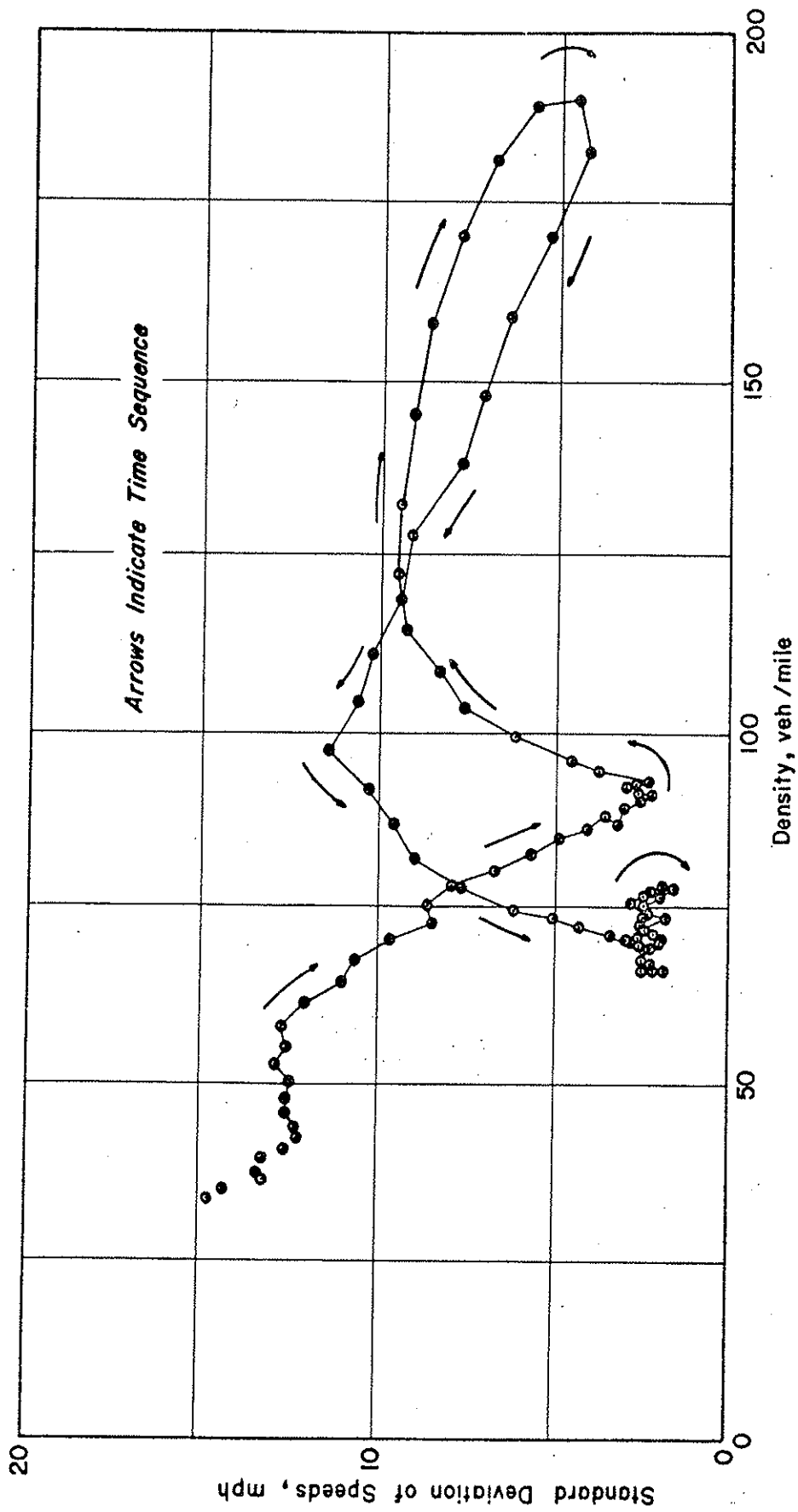


Figure 3.27 Variation of Speed Dispersion Before and After a Jam Condition (Group A Vehicles)

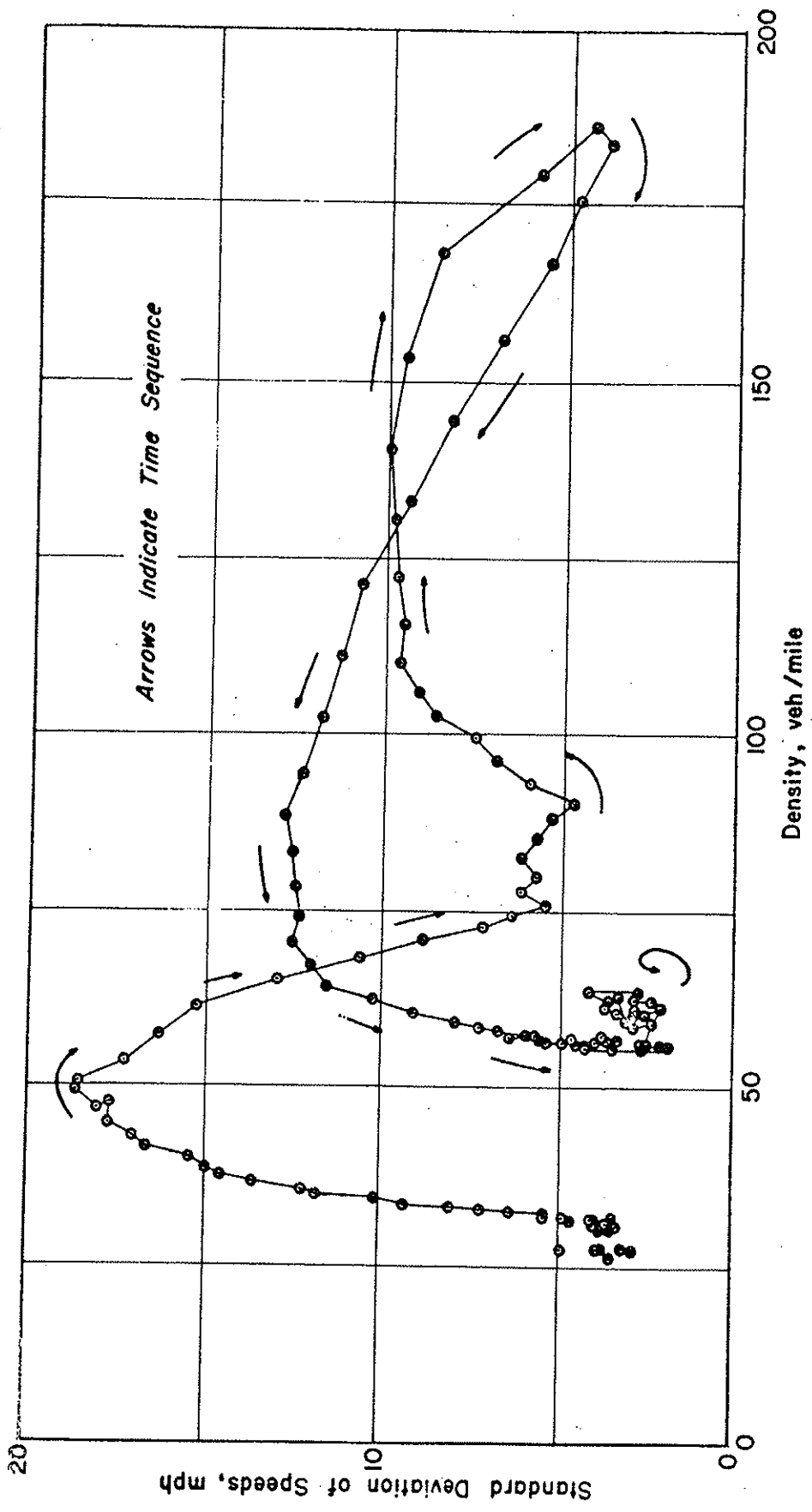


Figure 3.28 Variation of Speed Dispersion Before and After a Jam Condition (Group B Vehicles)

the platoon data, and the variations of σ with traffic density are presented in Figures 3.27 and 3.28. As in the previous graphs, these relationships are also in time sequence.

By comparing the energy-density relationships and the σ -density relationships for each platoon, several significant facts are noted. When the queue releases at a point where the hysteresis effect recovers, the platoon remains at that density and no further decrease in density occurs.

Furthermore, the point of recovery coincides with the point proposed as a breakpoint, in the previous section, between stable and forced flow. It can also be noted that low σ values are generally associated with the higher kinetic energy values, thus tending to support the idea that σ can be representative of internal energy.

From the viewpoint of the change in state of traffic flow, the hysteresis loops observed support the notion of a special traffic density breakpoint in the density space. However, the point of a change in state suggests that in order to change from one state of flow to another, extra energy is needed to make the transition.

CHAPTER 3: REFERENCES

1. Traffic Engineering Handbook, Institute of Traffic Engineers, Editor, J.E. Baerwold, Washington, D.C., 1965.
2. Gazis, D.C., Herman, R., and Rothery, R.W., "Nonlinear Follow-the-Leader Models of Traffic Flow", Operations Research 9, 545-567, 1961.
3. Chandler, R.E., Herman, R., and Montroll, E.W., "Traffic Dynamics: Studies in car-following", Operations Research 6, 165-184, 1958.
4. Chandler, R.E., Herman, R., and Montroll, E.W., "Car-following Theory of Steady-State Traffic Flow", Operations Research 7, 499-595, 1959.
5. Drew, Donald R., Traffic Flow Theory and Control, McGraw-Hill, 1968.
6. Drake, J.S., Schofer, J.L., May, A.D., "A Statistical Analysis of Speed-Density Hypothesis", Highway Research Record, No. 154, 1967.

CHAPTER 4

APPLICATION

Primary emphasis during the subject research program was placed on the application of the aerial photogrammetric data collection technique to solve practical problems of highway design and operation. One such problem is the congestion which plagues urban freeways during morning and evening rush hours.

A series of four general survey flights were flown over the study section of I-71, revealing that the congested area during the morning peak period extends from midway between the Morse Road and Cook Road overpasses to just south of the southbound on-ramps at Hudson Street, Figure 4.1. In this area traffic disturbances were frequent and complete breakdowns of flow were not uncommon. Especially high concentrations were observed near the on-ramps at East North Broadway, Weber Road, and Hudson Street. It was decided that further data collection would be concentrated in the region bounded by Morse Road on the north and Seventeenth Avenue on the south with special emphasis placed on the merging areas of the three on-ramps mentioned above.

Three types of standard traffic engineering studies were conducted for the purpose of further defining operational problem areas on southbound

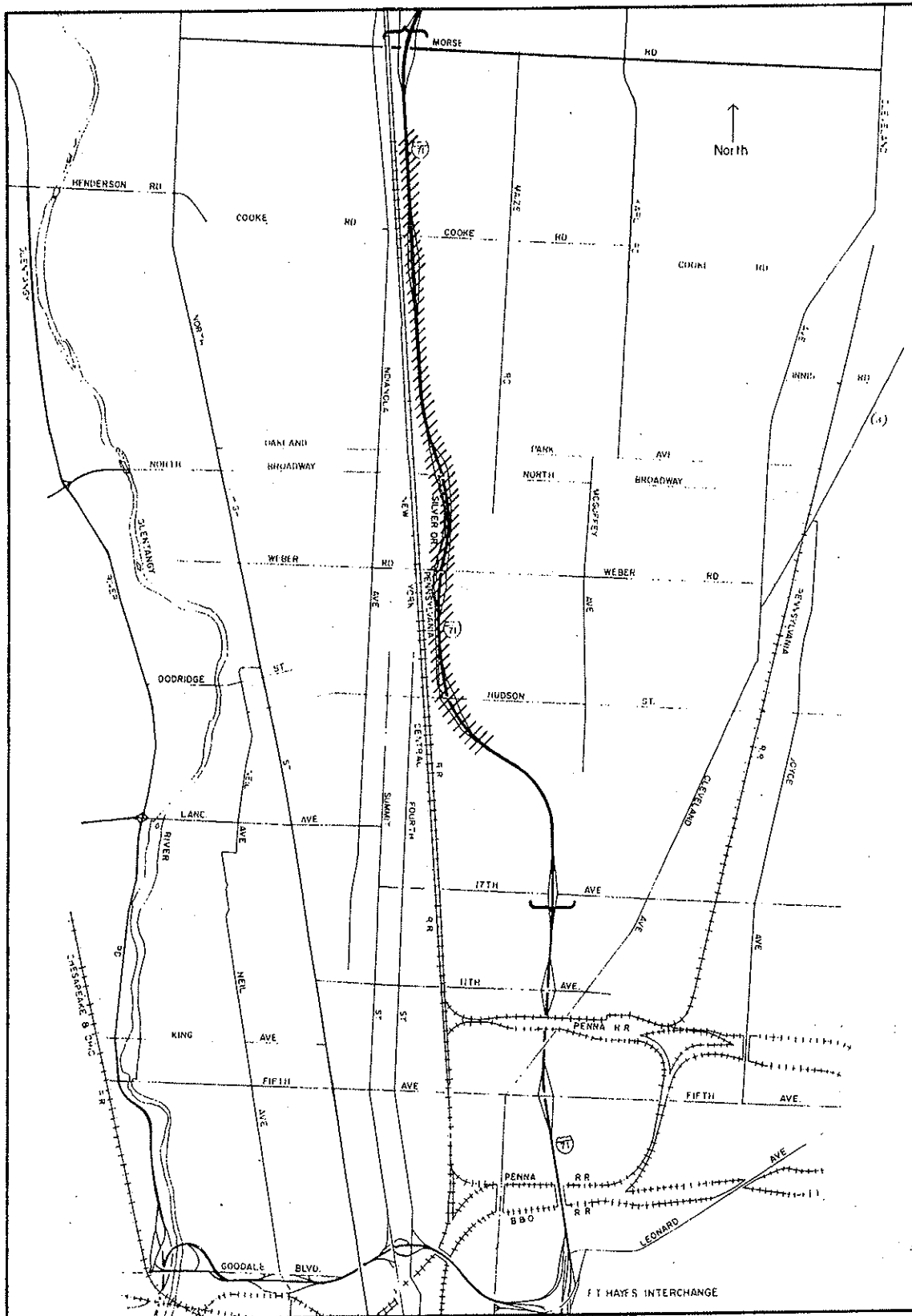


Figure 4.1 Region of Concentrated Data Collection
(Southbound Morning Peak)

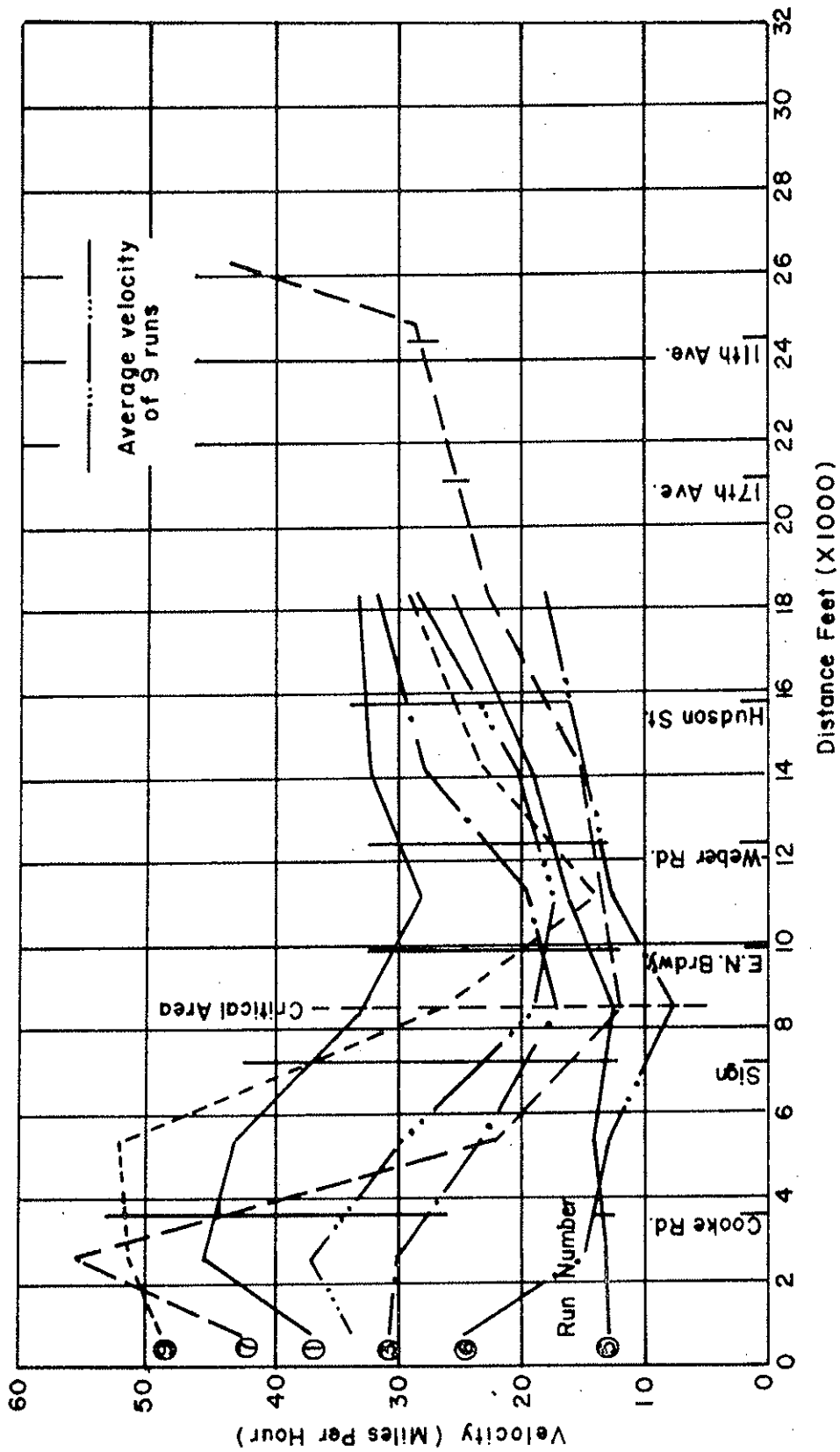


Figure 4.2 Velocity-Distance Profiles for Data of Thursday, February 5, 1970

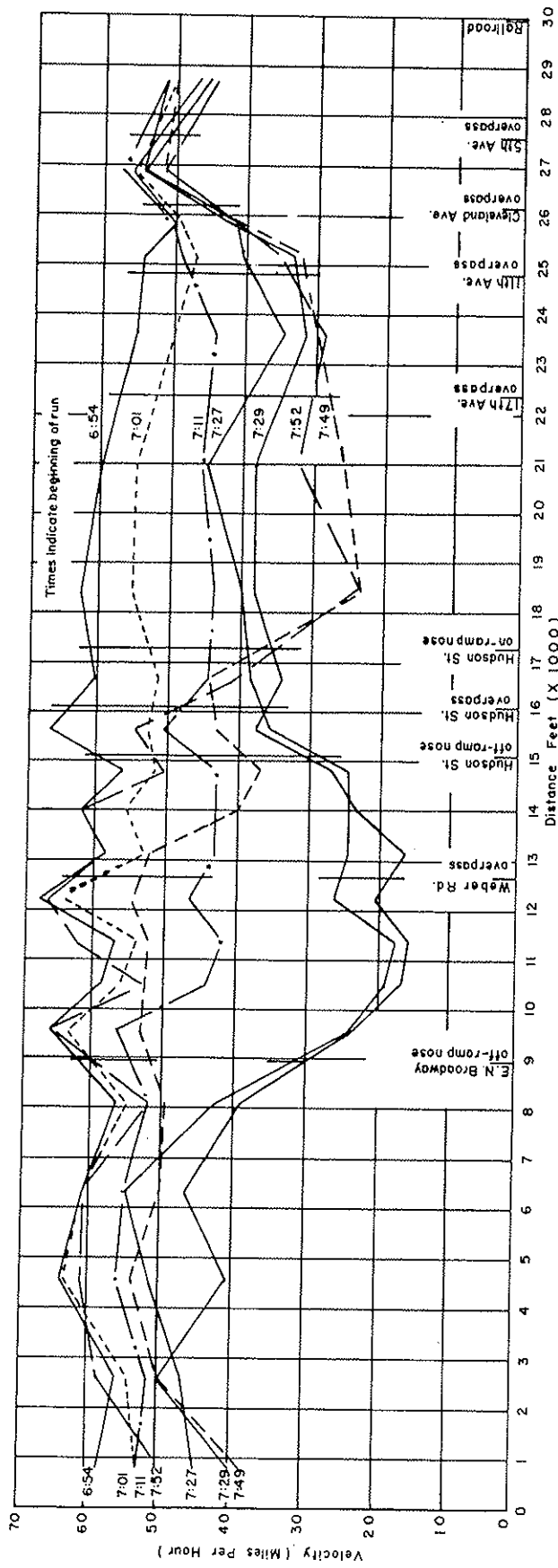


Figure 4.3 Velocity-Distance Profiles for Data of Tuesday, March 24, 1970

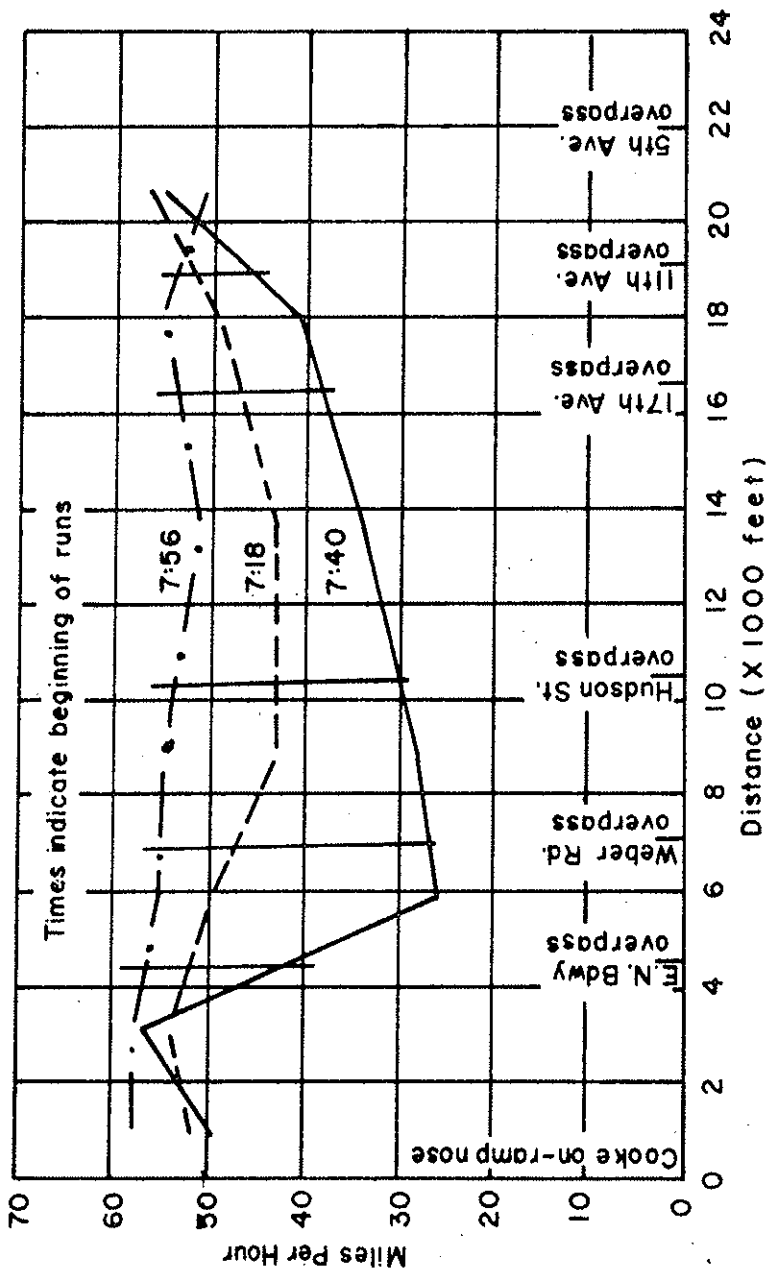


Figure 4.4 Velocity-Distance Profiles for Data of Thursday, June 18, 1970

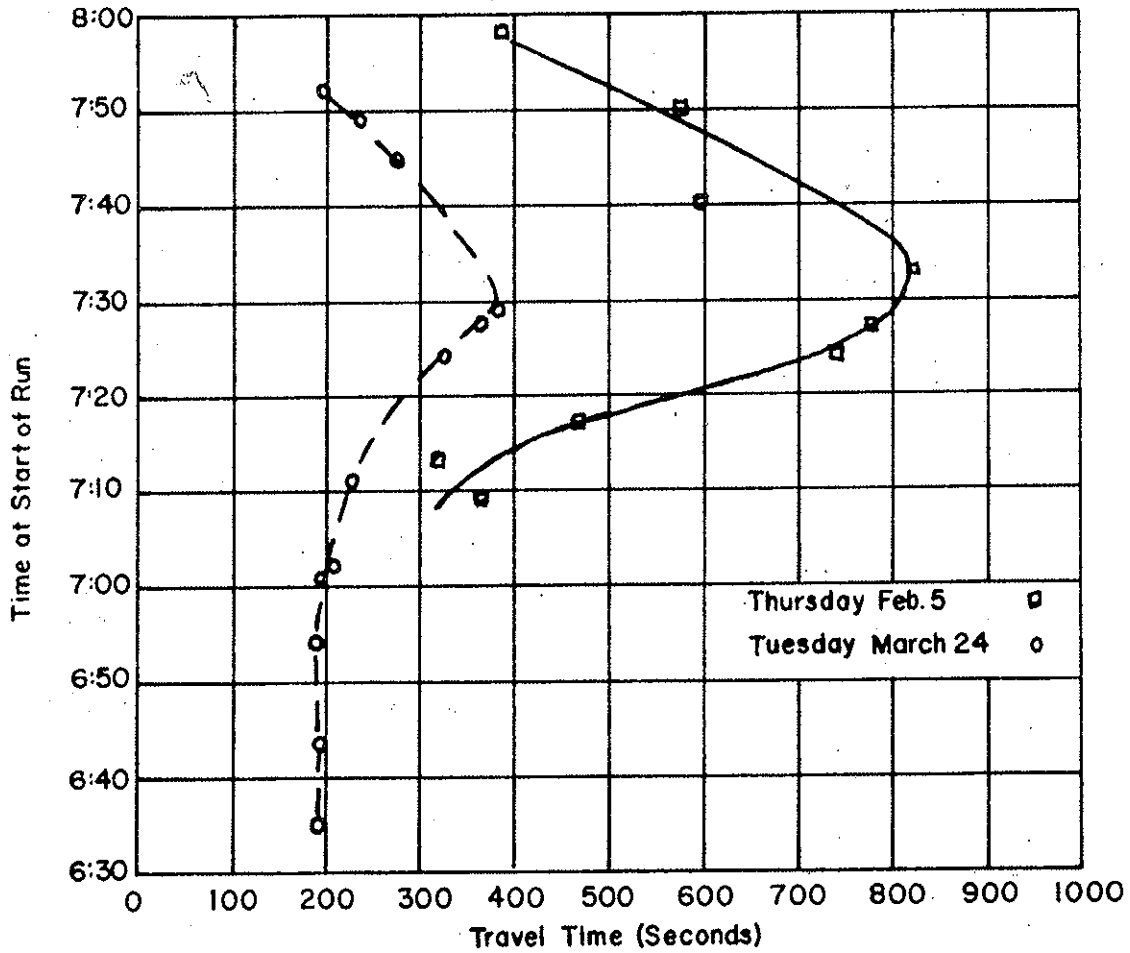


Figure 4.5 Pattern of Travel Time with Time of Day for Travel Time Runs of February 5 and March 24, 1970

I-71. Traveltime runs, density traps, and volume counts were used in investigating probable causative factors leading to traffic congestion.

Travel Time Runs

Travel time runs obtain preliminary indication of the location of operational trouble spots. Since the velocity of a traffic stream is inversely related to traffic density, regions of high density will be reflected as spots of low velocity in a velocity profile of the study section.

The results of the three traveltime runs conducted are summarized in a series of velocity-distance profiles in which the average velocity of the test vehicle between each pair of reading points is plotted against the corresponding position on the freeway for each run. The profiles are shown in Figures 4.2, 4.3, and 4.4. Although the magnitudes of the average section speeds vary for the three days surveyed, the same general pattern is evident in each case. During the period when congestion is the heaviest (7:20-7:50 am) the lowest average speeds are found in the region between the East North Broadway off-ramp and the Hudson Street overpass. Speeds in this region are consistently below 40 mph and drop as low as 10 mph at certain points.

Another interpretation of the data from the traveltime runs is presented in Figure 4.5. In this figure the total traveltimes for the individual runs is plotted versus the time of day at the start of the run. Once again the magnitudes of the values are different for the different days but the pattern is generally the same in each case. Congestion begins between 7:15 and 7:20 am

and lasts until about 7:50 am with the most severe congestion each day occurring at about 7:30 am. During this period of heavy congestion motorist travel-times are anywhere from 25 percent to 100 percent greater than the free flow values for the same section. The time lost by motorists during this 30 minute interval indicates that a significant operational problem does exist on I-71 during the southbound morning peak period.

Density Trap Study (Input-Output)

Although no meaningful density data was obtained from the Input-Output Study due to small counting errors, certain valuable information was collected, including:

1. Composition of traffic (total and by lanes)
2. Lane usage (total and by section of freeway)
3. Ramp usage (total and pattern over time)
4. Traffic volume (total and pattern over time)

This data, summarized in Figure 4.6, is thought to be representative of conditions occurring during each week on Interstate 71. No accidents or inclement weather disturbed the flow of traffic nor were any unusual traffic events noted.

The peak hour volume values calculated for each counting station do not vary greatly from day to day, therefore, it should be possible to obtain a reasonably accurate estimate of the volumes which can be expected at each counting station during peak hour.

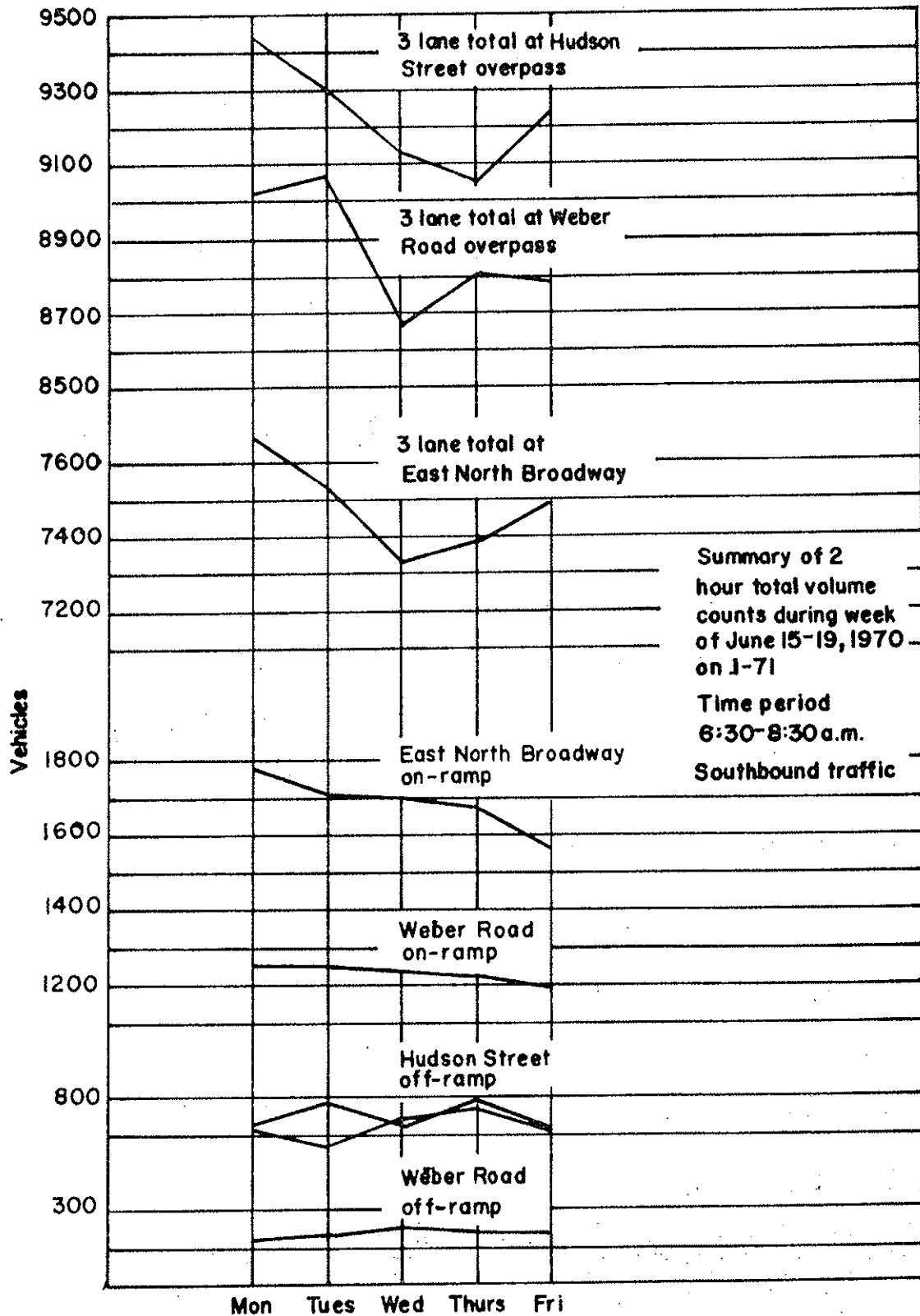


Figure 4.6 Summary of Day to Day Volume Variation at Various Counting Stations for Period June 15 to June 19, 1970 (Study Interval - 6:30 to 8:30 AM)

With the density trap data, the peak hour volumes traveling in the shoulder lane at each overpass can be calculated. The five day average values obtained are:

East North Broadway	1007 vph,
Weber Road	1395 vph,
Hudson Street	1442 vph.

By adding to these shoulder lane volumes the peak hour volume at the three on-ramps, the peak hour demand on the respective ramp merging areas can be established:

East North Broadway	1945 vph,
Weber Road	2135 vph,
Hudson Street	1862 vph.

These high demand volumes provide an explanation for the extreme difficulties experienced by on-ramp drivers in merging into the freeway stream.

Supplementary Volume Counts

Supplementary volume data were collected for each on-ramp merge area between East North Broadway and Hudson Street. Of interest was a volume value known as the merge area capacity. This capacity parameter is measured just downstream from an on-ramp and is a measure of the maximum number of vehicles which can pass through this downstream section. The merge area capacity is thus an indication of the amount of traffic which an on-

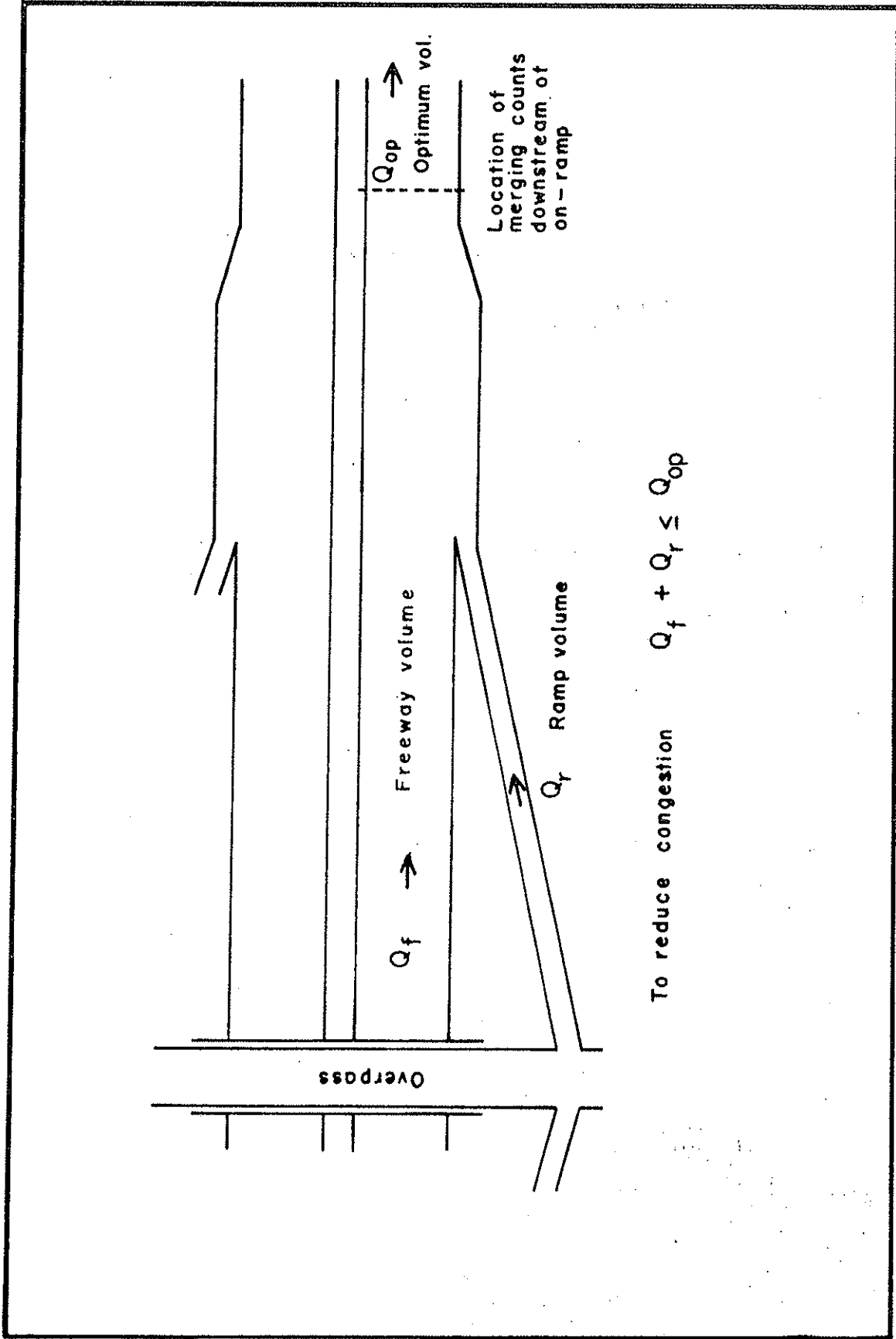


Figure 4.7 Schematic for Merge Area Capacity Study

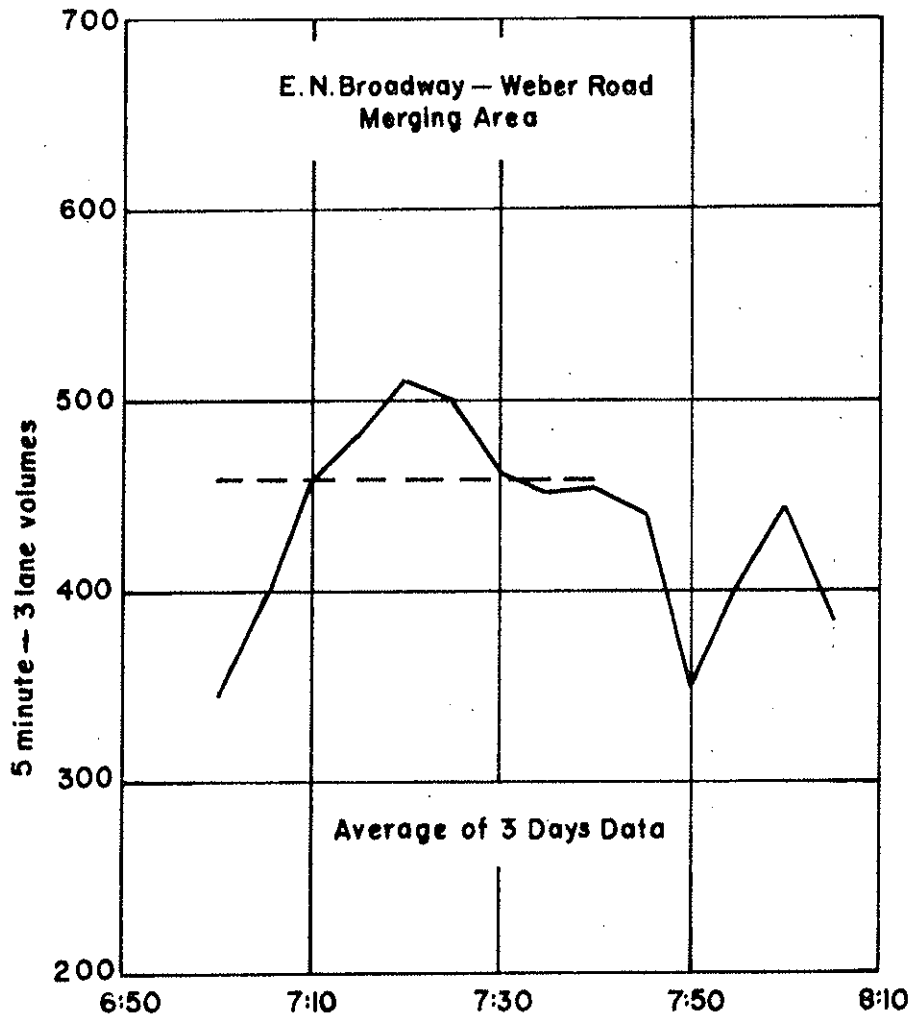


Figure 4.8 Merge Area Capacity Plot for East North Broadway Merge Area

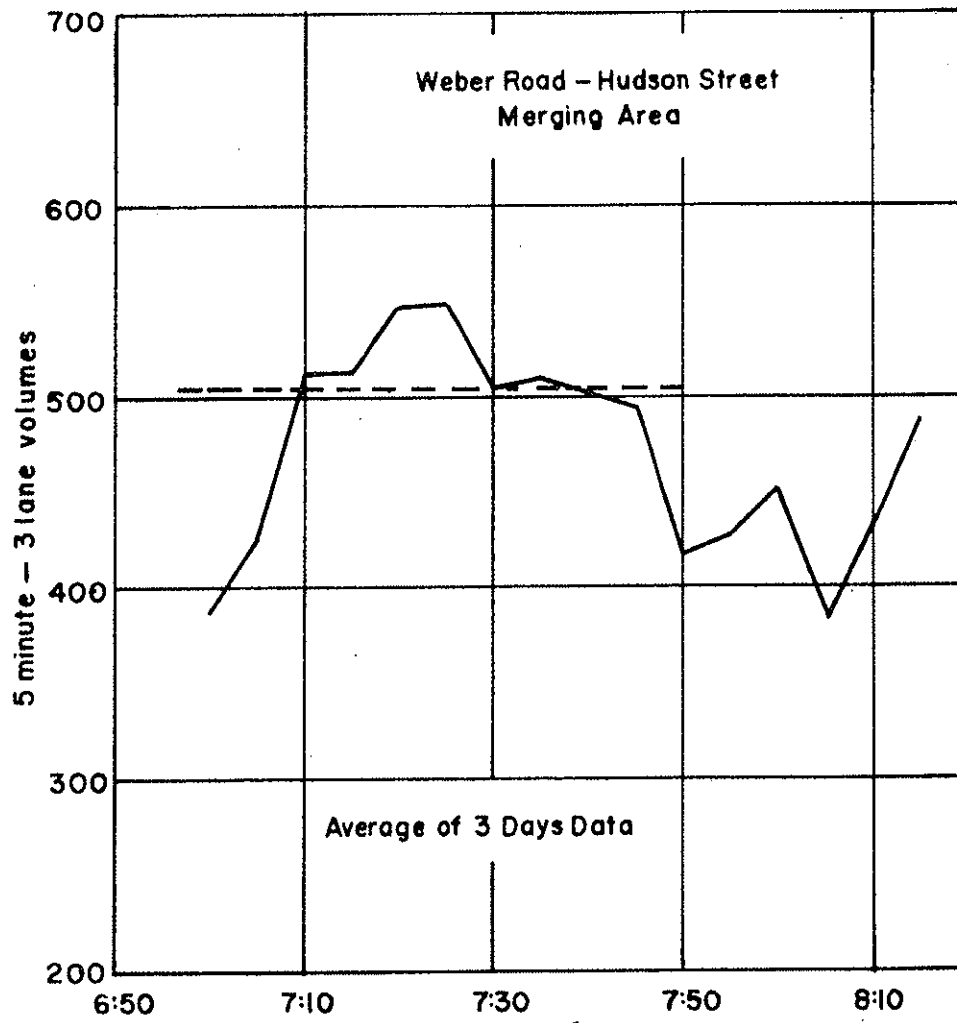


Figure 4.9 Merge Area Capacity Plot for Weber Road Merge Area

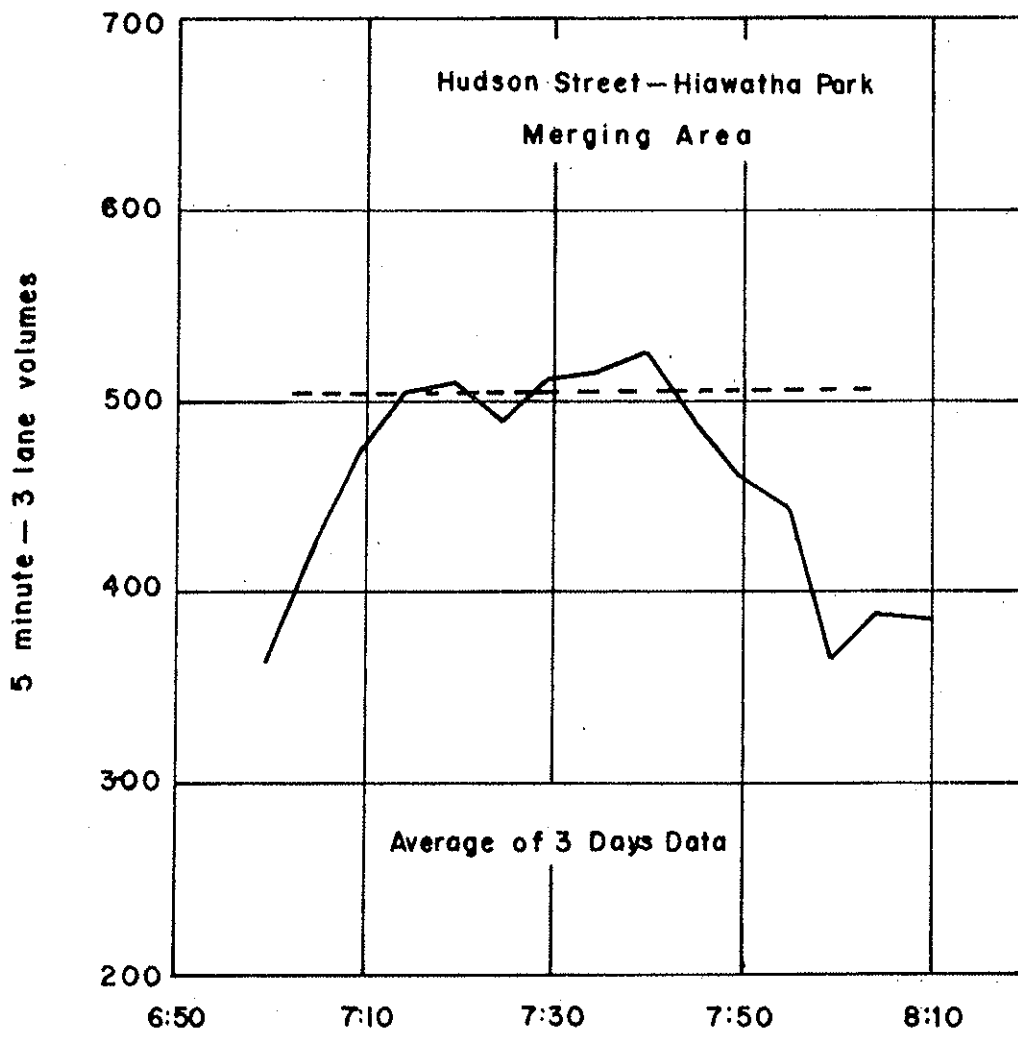


Figure 4.10 Merge Area Capacity Plot for Hudson Street Merge Area

ramp can effectively feed into a freeway stream. Specifically, no more traffic can be efficiently served by an on-ramp than that volume given by subtracting the freeway volume upstream of the ramp from the merge area capacity. (See Figure 4.7). Each merge area has a unique capacity depending upon the horizontal and vertical alignment of the area, the number of lanes, the lateral clearance, the nature of weaving in the area, and the angle which the on-ramp makes with the freeway mainline.

Data collected on the merge areas at East North Broadway, Weber Road, and Hudson Street was plotted as in Figures 4.8 - 4.10. A graphical procedure was then used to provide an empirical estimate of the maximum volume which could consistently pass through each merge area without causing a breakdown in traffic flow. In each case the volume value chosen was between 91 percent and 96 percent of the peak volume for any individual five minute interval. This value was defined as the desirable capacity of the merge area and is presented for each merge area below:

Merge Area	Desirable Merge Area Capacity (5 minute volume for 3 lanes)
East North Broadway	460
Weber Road	505
Hudson Street	505

It was concluded that a freeway control system so designed as to limit the traffic volumes entering the Broadway to Hudson Street section could be of great benefit in alleviating congestion and improving traffic flow during the

morning peak hour. Such a system featuring fixed-time ramp metering and utilizing simple and inexpensive equipment was implemented and is described in the next section.

Implementation of Ramp Metering

Entrance ramp control has consistently been shown to be a viable method for decreasing delay and increasing throughput on congested urban freeway systems. The control strategy proposed for southbound I-71, aimed at keeping the merging volumes just downstream of freeway on-ramps at or below an optimum merging volume such that stable flow would be maintained and traffic breakdown would not occur. This was accomplished by limiting on-ramp volumes when necessary by using fixed-time metering techniques.

The selection of the proper metering rate and the duration of the metering period at each ramp was established using the desirable merge area capacity values determined by the merge area capacity analysis and the volume data collected during the input-output study.

A metering rate of one vehicle per four seconds (900 vph) has been shown to be the maximum allowable metering rate, above which the effect is as though no metering were being done at all. Since this rate defines the threshold of successful metering, it was used in conjunction with the volume data to determine the duration of the metering period at each ramp. The following constant metering rates were derived, each within the limit of one

vehicle per four seconds:

East North Broadway	1 vehicle per 5.0 seconds
Weber Road	1 vehicle per 5.0 seconds
Hudson Street	1 vehicle per 10.0 seconds

Metering of the three on-ramps caused vehicle queues to form on each ramp. The proper treatment of these queued vehicles so as not to disturb traffic flow on the adjacent street was an important part of the overall control problem. It was apparent that a certain number of ramp-bound vehicles would be diverted to the surface street therefore several surface street network improvements were proposed on arterial streets.

It was decided that a control plan field test would be carried out as a joint project of The Ohio State University, the State of Ohio Department of Transportation, and the City of Columbus. The city was responsible for obtaining and installing the required control equipment at its expense and the collection of the necessary data for evaluating the effect of the control plan on traffic flow on the arterial streets in the Interstate 71 corridor. The University was responsible for collecting the required data to evaluate the effect of traffic flow on the freeway itself and aided the city in the evaluation of the effect on traffic movement in the corridor as a whole. The State represented the research project sponsors and aided in an advisory capacity.

The implementation of the field test required effort in three specific areas. First, the necessary control equipment was selected, obtained, and

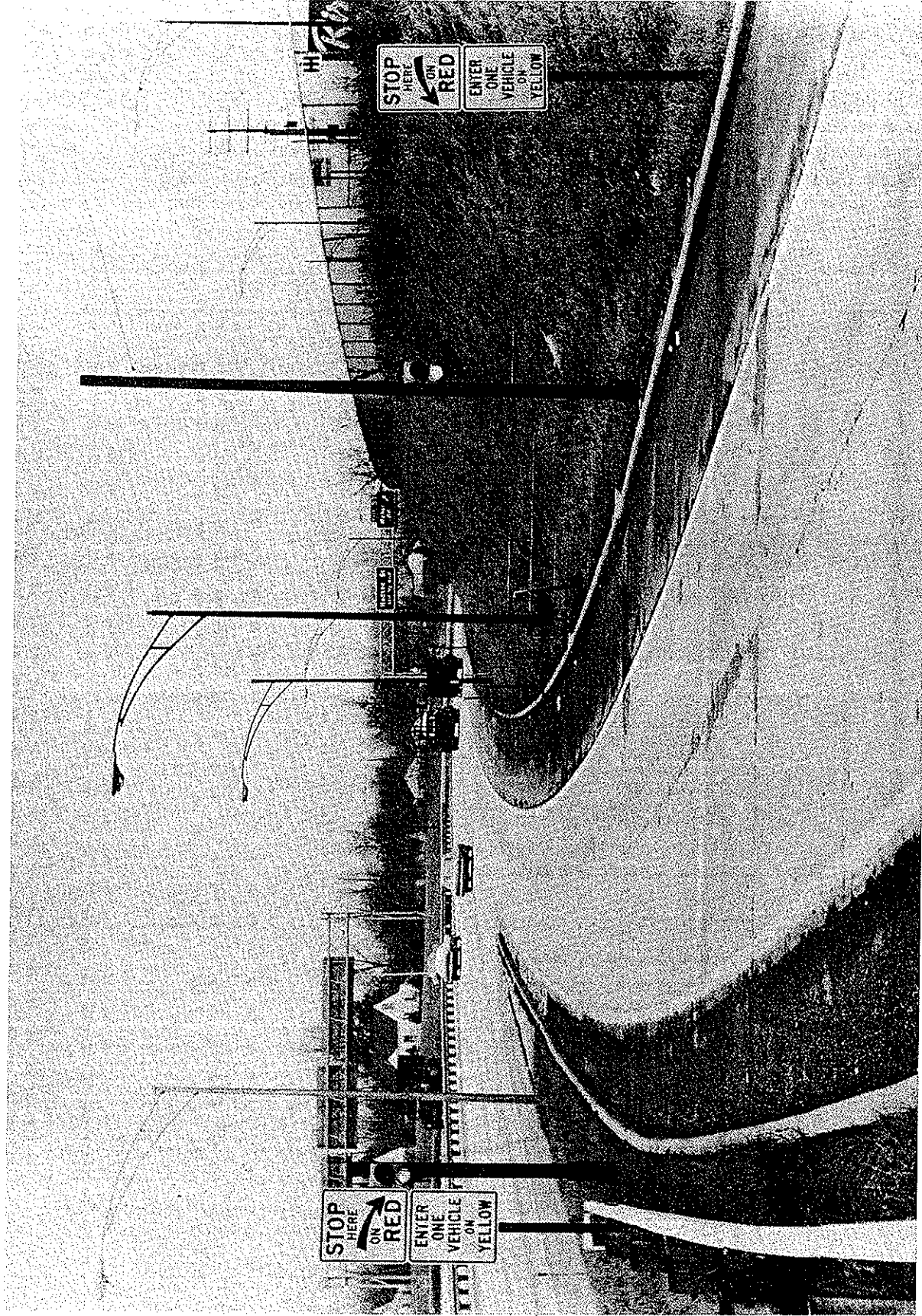


Figure 4.11 Typical Ramp Control Installation: Freeway Terminal

installed at each of the three ramp sites, as in Figure 4.11. Second, the pre-test publicity was prepared for the motoring public explaining the purpose of the control plan. Third, the control equipment was tested and adjusted to insure the proper metering rate and period at each ramp.

The ramp signal at East North Broadway was placed in operation on Wednesday, October 13, 1971. The remaining two signals were activated at one-week intervals with the Weber Road installation becoming operational on October 20 and the Hudson Street signal on October 27, 1971. In each case about a week was required to adjust the signal to operate within the proper time and during the prescribed metering period.

Once the complete system was operational it was allowed to run continuously Monday through Friday and effort was concentrated on the collection of the "after" data on traffic flow required to evaluate the effectiveness of the system.

Evaluation Study: 1971-1972

In order to evaluate the effectiveness of the control steps taken on Interstate 71, an "after" study of traffic operations was conducted with data collection concentrated in the region between the Morse Road overpass and the Seventeenth Avenue overpass. The evaluation covered the period between October 13, 1971 and July 31, 1972.

Data from the traveltime runs on Interstate 71 was summarized in the form of velocity profiles, such as Figure 4.12.

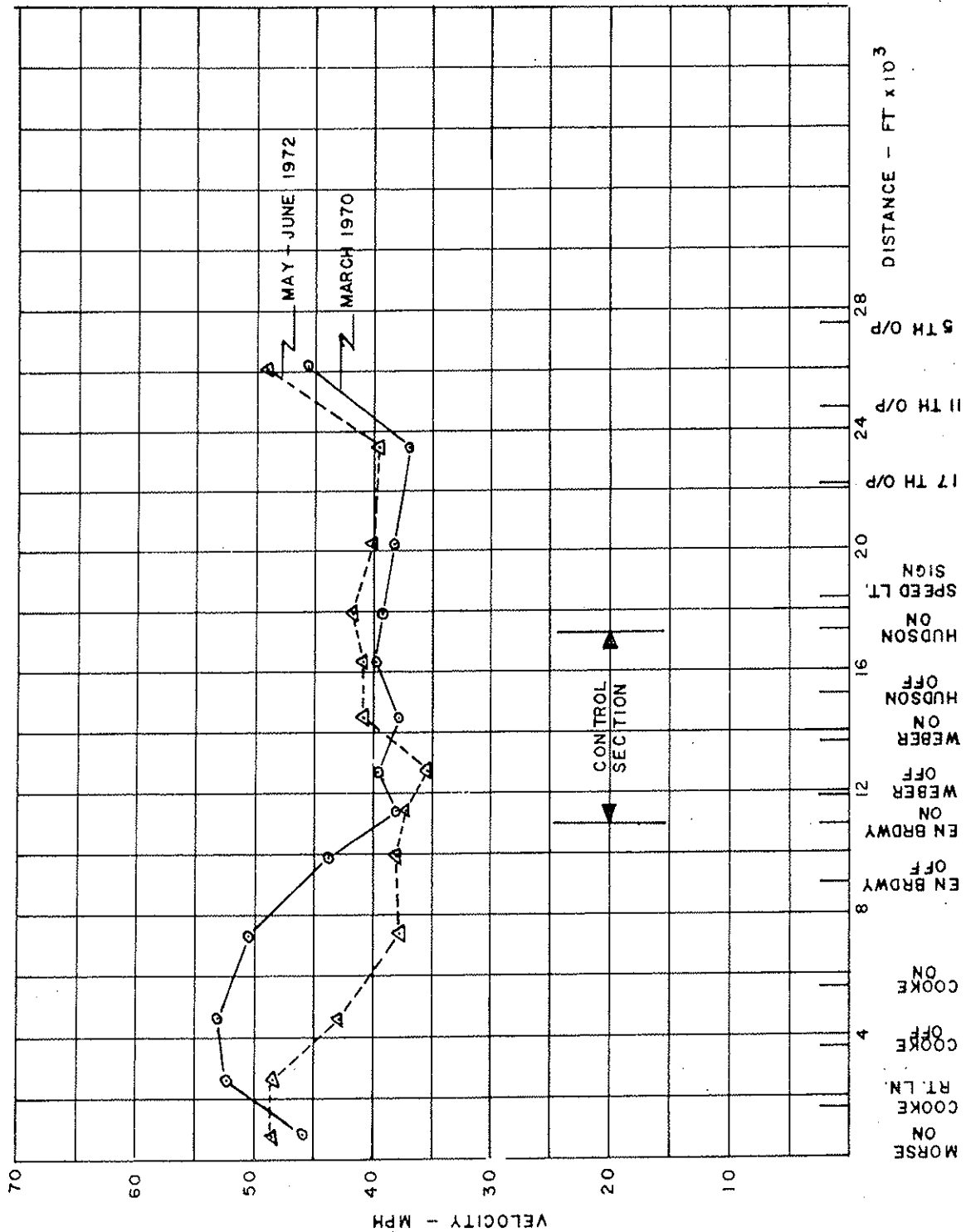


Figure 4.12 Composite Speed-Distance Profiles for "Before" and "After" Travel Time Data

Observation of Figure 4.12 reveals the following interesting phenomenon. Beginning in the middle of the control section, the average speed achieved by motorists during May and June of 1972 shows a constant two to three miles per hour increase over the average speed of March, 1975. Starting at the same point and proceeding northward, the 1972 data show a substantial decline in average speeds for the section upstream of the control areas as compared to the 1970 data. This trend continues until the Cook Road overpass is reached. The average speed for the entire section meanwhile remains virtually the same in 1972 (40.3 mph) as it was in 1970 (40.5 mph).

Analysis of the volume counts conducted in the control section reveals the following relevant facts about Interstate 71 and the associated surface streets in the I-71 corridor.

1. Traffic volumes on I-71 measured at the southern end of the metered section at Hudson Street increased by an average of 615 vehicles (6 percent) since ramp metering was initiated (7:00 - 9:00 am).
2. Traffic volumes in southbound Indianaola Avenue and Summit Street remain basically unchanged.
3. Volumes on southbound Silver Drive have increased significantly. An average increase of 61 vehicles (32 percent) was measured between East North Broadway and Weber Road while the Weber Road to Hudson Street subsection showed an increase of 238 vehicles (305 percent).
4. Volumes on Southbound High Street have also increased significantly

with a net increase of 208 vehicles recorded (11.3 percent).

5. Volumes on Westbound East North Broadway and Weber Road measured just west of I-71 remain basically unchanged.

It appears, therefore, that a substantial increase in traffic volume has been attained on Interstate 71 without adverse effect on surface street roads.

Conclusions

Benefit to freeway drivers in terms of increased flows and reduced congestion can not normally be achieved by freeway control without some resulting cost to the motoring public in general. In the case of the ramp metering this cost appears in the form of (1) delay to motorists using the metering ramps, (2) delay to motorists diverted to alternate routes and (3) delay to surface street motorists caused by the increased traffic load diverted from the freeway. However, the ramp control plan has been effective in increasing the efficiency of southbound Interstate 71 during the morning peak period. Traffic volumes have been increased by six percent without a noticeable decrease in overall travel speeds, thus increasing the throughput of the metered section by almost 8,000 vehicle-miles per hour. Average section densities have increased somewhat but aerial films show that this is a result of improved uniformity in the traffic stream. Vehicles are now traveling at more uniform spacings with less platooning and hence less unutilized space between platoons. As a result flow appears to be more stable.

The present ramp metering, because it is based on a constant metering rate, does not respond to changing freeway conditions. It appears that a more sophisticated system will be needed to prevent minor disturbances from precipitating into major breakdowns. Such a system would include traffic detection and surveillance equipment capable of measuring traffic conditions at several points on Interstate 71.

CHAPTER 5

LOOP DETECTOR FOR DENSITY AND SPEED MEASUREMENTS

5.1 INTRODUCTION: DEFINITION AND DENSITY MEASUREMENTS

The operational difficulties resulting during peak traffic hours due to extreme volumes of traffic on the freeway provide the traffic engineer a twice daily problem of maintaining efficient traffic flow conditions.

When the high peak hour demand is coupled with incidents, the resulting congestion could take hours to disperse. Preventing these daily occurrences or reducing their effects is both a continuing concern and an extremely difficult problem. Physical limitations of the urban freeways coupled with the high traffic volumes create the problem of peak hour congestion for which there is no immediate or inexpensive solution: thus, the logical trend is toward automatic surveillance and control to stabilize and improve traffic flow.

To achieve efficient control of traffic on urban freeways, it is essential that the control system be provided with the necessary information for determining the prevailing condition of flow, that information being speed, volume and density.

The most simple attempts to describe traffic flow in mathematical

terms have been applied to single queues of traffic in a stream, i. e. it is assumed that no vehicles enter or leave the stream and that no vehicles change position by overtaking; under these circumstances, all the vehicles in the stream will be traveling at approximately the same speed. To arrive at a mathematical expression for flow per unit time of this stream; the distance between following vehicles must be known. Spacing is the distance measure and headway is the time measure from head to head of successive vehicles. These two measures describe the longitudinal arrangement of vehicles in a traffic stream.

Space mean speed is the average speed of all vehicles on a given length of roadway at an instant in time. Density also describes the number of vehicles on a given length of roadway for an instant of time. If both are expressed in comparable units (density in vehicles per mile and space mean speed in miles per hour), their product is a rate of flow or volume. Therefore, a basic relationship exists between volume, speed, and density

with: $Q = VK$

Q = volume or rate of flow (veh/hr)

V = Space mean speed (mph)

K = density (veh/mile)

In this sense, the derived flow is the rate for the instant in time being studied, although it may be expressed in vehicles per hour.

The fundamental speed-volume relationship for a given population

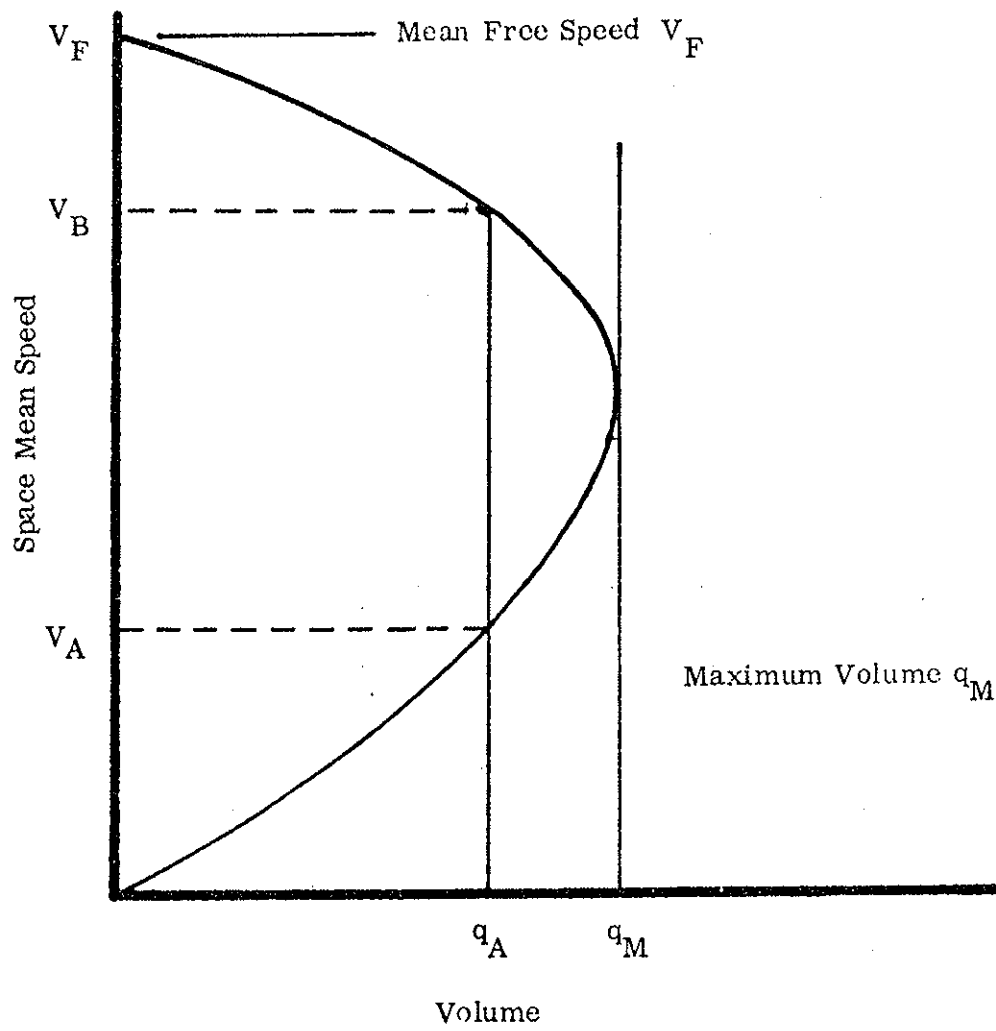


Figure 5.1 General Form of Speed-Volume Relationship (3)

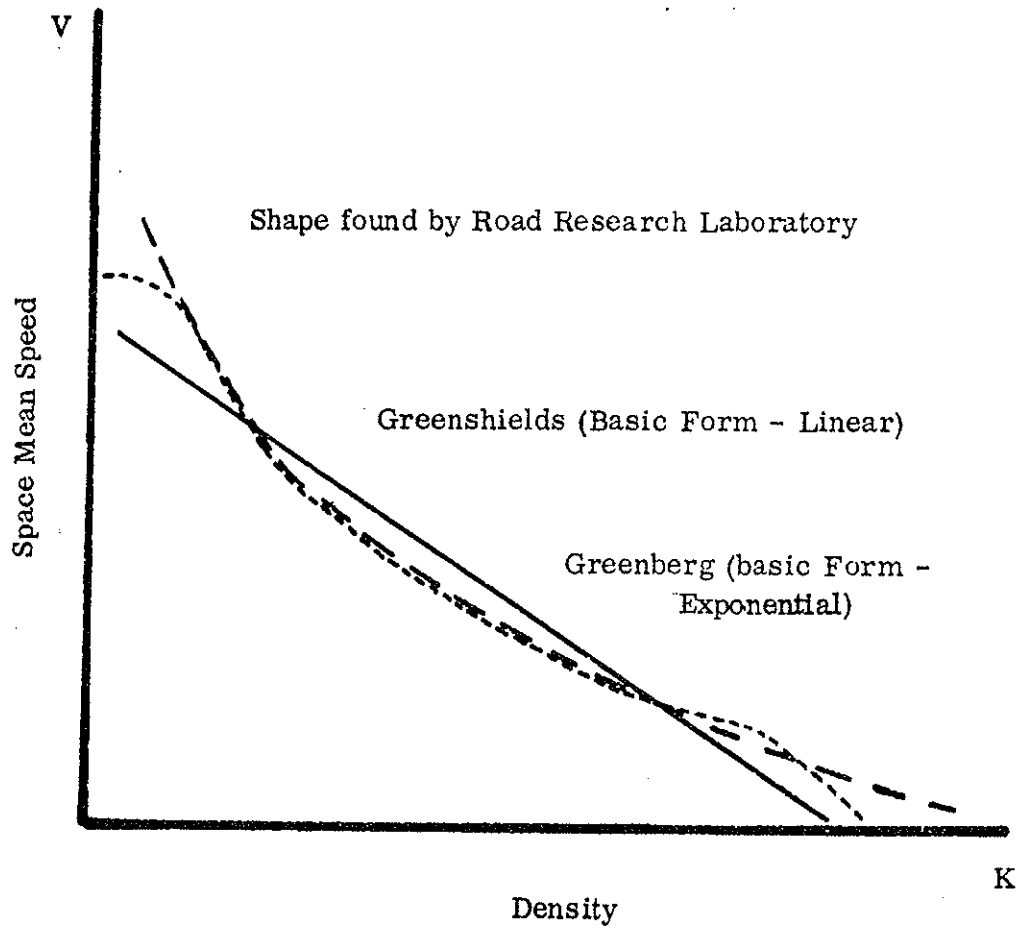


Figure 5.2 General Form of Speed-Density Relationship (5)

of drivers can be simply stated as follows: as speed decreases, volume increases. This relationship holds true throughout the range of free flow and impending congestion, up to the point of critical density, or the density at maximum flow. At and beyond this point, however, it no longer applies; both rates of flow (volume) and space mean speed then decrease with an increase in density. This relationship applies to a roadway section, rather than a point, and is shown in the general form in Figure 5.1. It is the lower portion of this curve which most involves the traffic engineer, for this portion represents what happens due to disturbances or during the peak hour when demand exceeds the capacity of the freeway.

The speed-density relationship simply states that as density increases, speed decreases. Greenshields in a 1934 study on traffic capacity, found that a linear relationship existed between speed and density (1). Subsequent studies by Greenberg found that the relationship under uninterrupted flows departs from linearity. It should be noted that if the speed-density relationship is linear then the speed-volume and volume-density relationships are parabolic, and if it is not linear then they are curvilinear. The differences, perhaps of greater theoretical than practical significance, are shown in Figure 5.2.

The important fact pertaining to freeway operations is that if the speed-density relationship can be approximated by a straight line, then speed and density obviously give a better indication of flow conditions than does volume.

Another reason why density is a better measure of flow conditions than volume is shown by analysing the speed-density and speed-volume relationships. Both of these relationships are similar in that in the upper speed range speed decreases with both increasing volume and density. However, density continues to increase past the point of critical density, which makes it a more reliable predictor of speed than volume because of the simple decreasing relationship that exists between speed and density. Speed prediction is important because it is the best indicator of the level of service of the highway.

Density appears to be the better measure of the prevailing flow conditions on a roadway than volume since density continues to increase as congestion increases. For any given volume, the efficiency of flow can be determined by observing the density. The smaller the density, the quicker the movement of traffic and the greater the efficiency of flow.

The method of density measurement employed in this study closely approximates the actual density existing in a section of roadway by measuring directly that number of vehicles occupying a section of roadway at a given instant in time.

Loop detectors are not free from all problems but considering the types of errors it is subject to, the inductive loop detector is still the most accurate and economical source of the required type of flow information available in the electronic industry today. The current method of determining density with loop detectors is to measure the occupancy time of a

vehicle passing over the loop. The method employed by this study was not to measure the occupancy time but rather to measure directly the number of vehicles actually occupying the loop at an instant in time. It is shown that the magnitude of the differential voltage of a loop circuit at any instant of time created by vehicles passing through the loop's zone of influence is directly related to the number of vehicles in the loop at that instant. The longer the loop, the more vehicles it is capable of measuring. The longer the section of road it covers, the greater the accuracy of the measured density, assuming accurate calibration of the differential voltage output.

This study investigated the feasibility of measuring per lane traffic density on a real-time basis using inductive loop detectors as the sensing element. This was attained by:

- 1) investigating various loop sizes and configurations for the development of the most accurate density measure,
- 2) identifying the important parameters relevant to loop detector measurements, and
- 3) developing a reliable calibration with the selected loop configuration for use in the real-time freeway prototype system.

5.2 DESCRIPTION OF THE LOOP DETECTOR

The loop detector, as shown in the preceding section, offers the

most reliable method of detecting the presence of vehicles on a roadway. The loop of wire is excited by an AC voltage and the resulting current flow establishes a magnetic field. When metal objects enter this field, induced eddy currents act to decrease the magnetic field. The field change may be detected as either:

- 1) A change in inductance of the loop,
- 2) A change in resonant frequency of the circuit of which the loop is a part, or
- 3) A change in phase between the current flowing in the loop and a reference signal.

A representation of a loop tuned circuit is shown in Figure 5.3. All currently available inductive loop detectors use a single coil, with one or more turns of wire, as the vehicle sensing element. A typical loop is rectangular in shape and can be located over one or more lanes depending on the data required.

The loop detector tuned circuit is illustrated in Figure 5.4. "L" represents the inductance of the loop. The resistance, R, comprises the series resistance of the loop plus an eddy current power loss, which is caused by the presence of a vehicle. R_d represents the dielectric loss of the material (insulation, asphalt, water, air) between the loop wires. R_f is due to series resistance of the feeder cable. The circuit is tuned by capacitance C, which is located in the electronic unit. In parallel with C

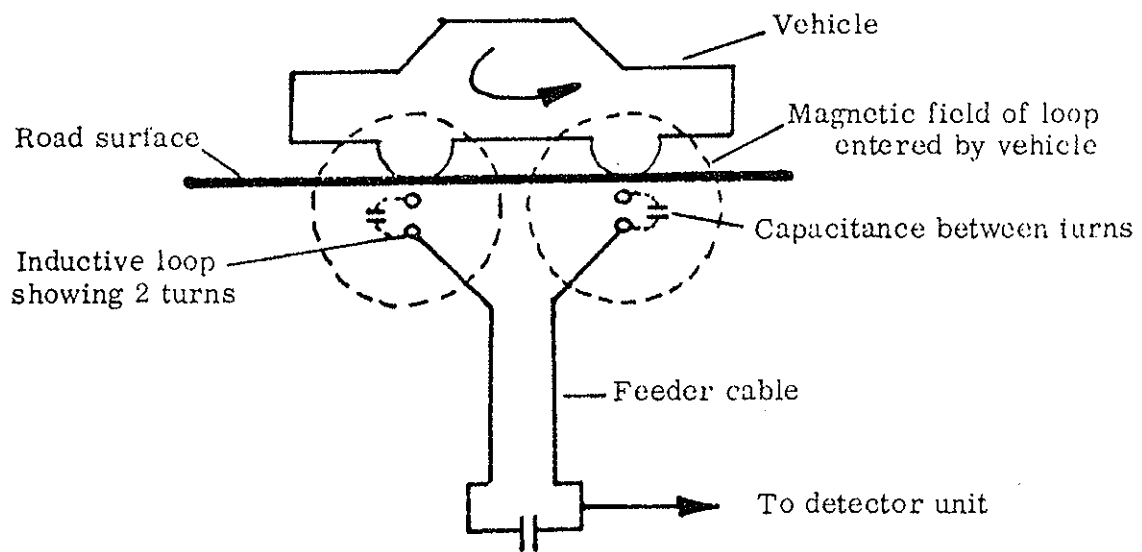
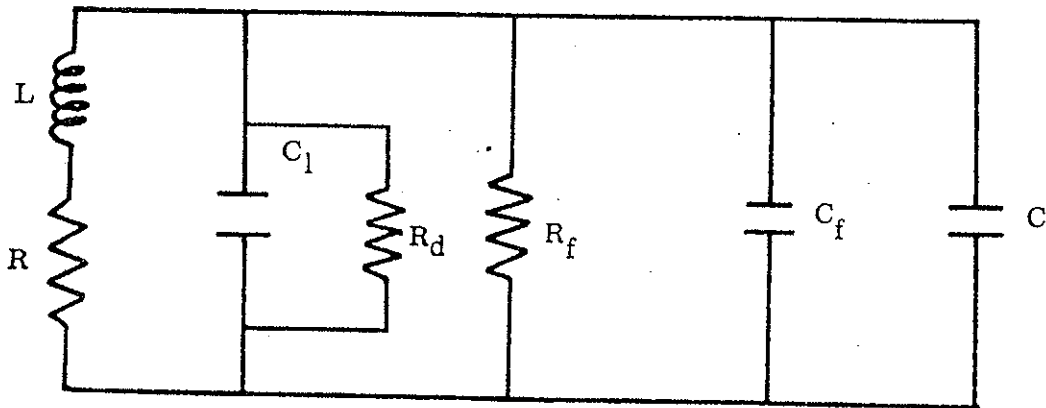


Figure 5.3 Representation of a loop tuned circuit (7)



5.4 A Typical Loop Detector Circuit Diagram (7)

and affecting the tuning are the self-capacitance of the loop and feeder cable,

C_L and C_f (2).

When a vehicle enters the magnetic field of the loop, the following three changes occur:

- 1) Eddy currents are induced in the metal of the vehicle. The magnetic field which is set up by the eddy currents opposes the main field and reduces the inductance. There is also a power loss caused by the flow of eddy currents, which increases the series resistance both contribute toward a reduction in the value of Q , quantity of electric current.
- 2) The presence of iron in the vehicle body increases the magnetic flux density and hence tends to increase inductance and offset the demagnetizing affect of the eddy currents. This effect is smaller than the eddy current effect.
- 3) There is a small increase in capacitance, due to the proximity of the loop wires and the vehicle body. This effect is considered to have a negligible influence on reducing inductance.

In practice, the eddy current effect predominates and this results in an increase of resonant frequency due to a decrease of inductance and to reduction in the value of Q .

5.3 DESCRIPTION AND RESULTS OF THE EXPERIMENTS

Laboratory tests were conducted to determine promising loop

configurations for field testing. The field test program was scheduled to proceed in three phases:

The first phase included the measurement of the density of a static queue of vehicles. This phase allowed for familiarization with the various parameters related to loop operations and with some of the problems likely to arise in making density measurements.

The second phase was concerned with measurements of a small platoon of vehicles moving at a moderate speed (15-30 mph). This phase was to give an indication of the problems caused by vehicle movement in making density measurements.

The final phase was to involve density measurements over the entire speed and density range likely to occur on a freeway (i. e. 0-70 mph, 0-225 vpm).

On the basis of finer adjustment capabilities, the loop detector Model LD-1 of Automatic Signal Division was selected for this investigation. This is an older, proven model which detects by change of phase. The LD-1 has three adjustments for turning and sensitivity and an external volt meter to denote presence and tuning. The detector was available through the Ohio Department of Transportation.

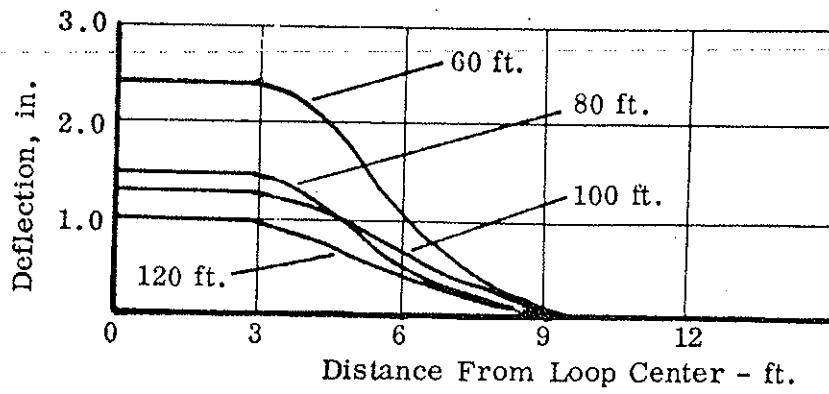
The preliminary tests were conducted by the Traffic Research Center at The Ohio State University. The major conclusions derived from these tests are listed below.

Lateral and longitudinal placement

- 1) Vehicles must break the zone of influence of the loop to be detected (This zone extends less than one foot beyond the wire loop).
- 2) A vehicle must be completely inside the loop to get full detection. It was found that as more and more of the vehicle is located laterally outside the loop, the loop voltage output is lessend accordingly. This effect is illustrated for both configuration shapes and the various loop sizes tested, as shown in Figure 5.5.
- 3) Output is basically constant throughout the entire length for rectangle loops. Fig. 5.6 shows the plot of detection versus longitudinal position.
- 4) Fig. 5.6 also shows somewhat different results due to the crossovers in the Figure "8" loop configuration. For short section lengths the crossovers produce areas of lower sensitivity and thus a wave effect as the vehicle passes over them.
- 5) Lane changes will create difficulties in obtaining accurate density measurement.

Vehicle Size

- 1) Regular passenger cars produce a consistent output.
- 2) Small passenger cars produce an output only 75% that of the regular passenger car and the sports car produced only 67%.



Rectangular Configurations

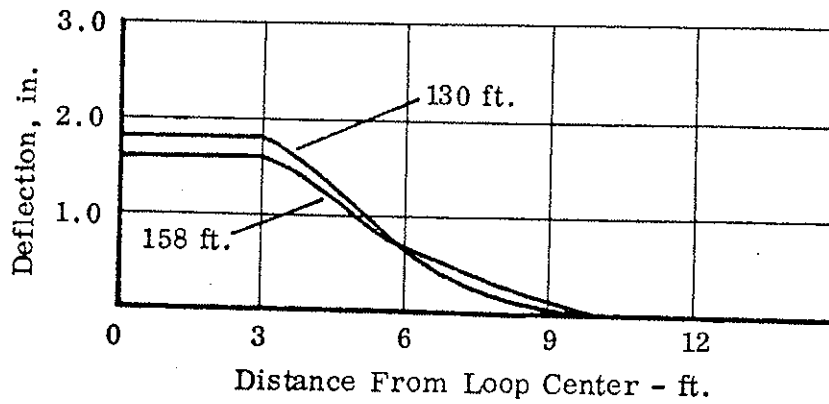
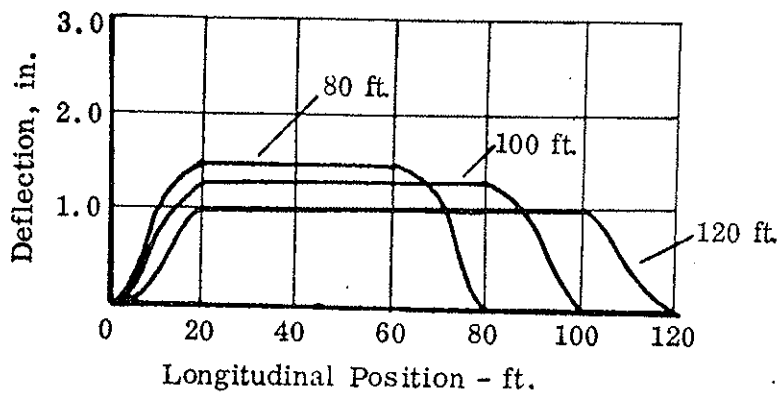


Figure "8" Configurations - 18 ft. Sections

Figure 5.5 Plots of Deflection Versus Lateral Placement



Rectangular Configurations

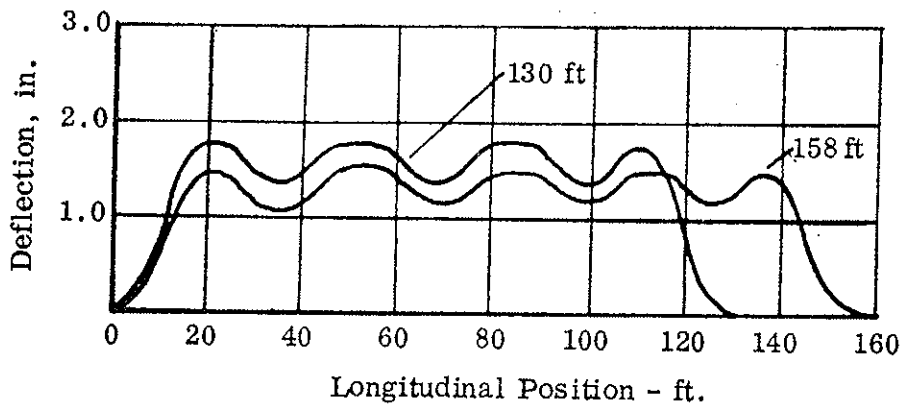
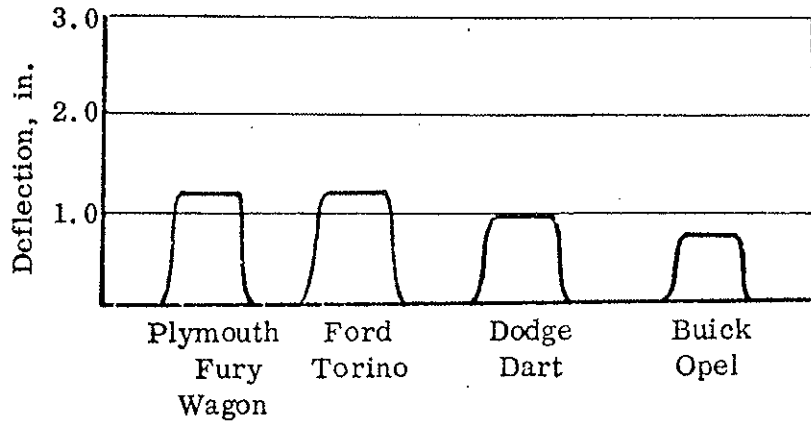


Figure "8" Configurations - 18 Ft. Sections

Figure 5.6 Plot of Deflection Versus Longitudinal Placement



Rectangular Configuration - 100 Ft.

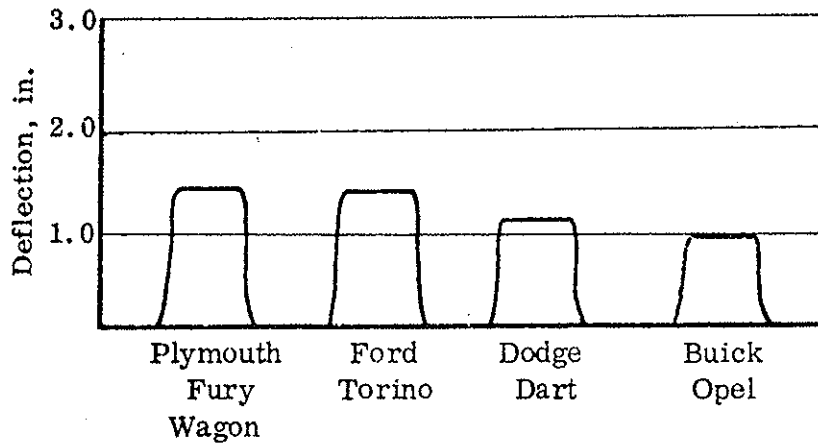


Figure "8" Configuration - 158 Ft.

Figure 5.7 Comparison of Outputs for Varying Vehicle Sizes

This can be seen in Fig. 5.7, where the outputs of two loop configurations for various vehicle sizes are compared.

- 3) The effect of various sized trucks and buses would have to be determined.

Rectangular loop configuration

- 1) The maximum length of detection possible with low sensitivity was 160 feet.
- 2) 40 feet to 80 feet lengths require two turns of wire; 100 feet to 160 feet lengths require one turn.
- 3) The optimum operating length is either 100 or 120 feet.
- 4) Speed affects the output of a rectangular loop such that the output of the static tests is greater than the output of the dynamic tests.
- 5) Fig. 5.8 shows that the pickup and discharge characteristics of the rectangular loop are unequal thus creating inconsistency in density measurement and making reliable calibration unlikely.

Figure "8" loop configuration

- 1) Section length is a variable length that influences sensitivity; shorter length produces greater sensitivity.
- 2) Longitudinal wave variations were created by the crossovers.
- 3) The wave effect is reduced by increasing section length.
- 4) The wave effect could be used as an indication of traffic

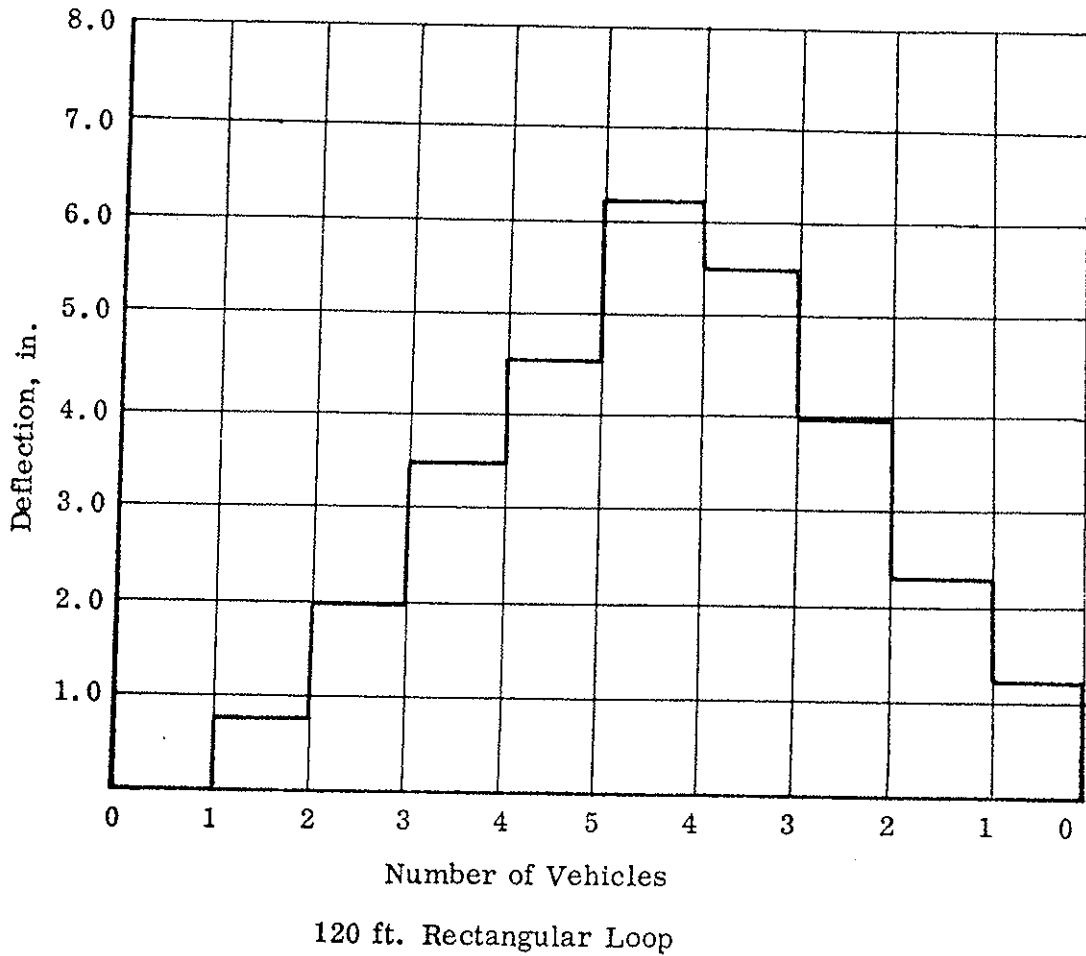


Figure 5.8 Density Measurement with Rectangular Loop
Showing Pickup-Discharge Variations

movement.

- 5) The larger the section length the more the loop behaves like a rectangular loop; the shorter the section length the more it behaves as a series of small loops connected in parallel.
- 6) Pickup and discharge characteristics for density measurement are shown in Fig. 5.9 to be identical for shorter section lengths while longer section lengths produce density characteristics similar to those of the rectangular loop.
- 7) Speed does not affect output; static and dynamic test results were identical.
- 8) Maximum length of detection with low sensitivity was 186 feet (18 feet section length).
- 9) Optimum operating length was 150 feet (18 feet section length).

Comparison of configurations

From the results of the tests on the two alternative configurations it is quite evident that the Figure "8" with 18 foot sections is the superior sensing element for the purpose of measuring density. Besides providing better length and sensitivity it was found that the Figure "8" produces the most consistent and reproducible density measurement. The wave effect at the crossover of the Figure "8" loop could also be cued to indicate movement of vehicles through the loop, thus supplying an additional measure of speed as well as density.

From the results of the preliminary testing, it was recommended that the 158 foot length Figure "8" loop configuration with 18 feet section lengths be used for testing in phase 3.

Site Selection

Once the preliminary tests were completed and the configuration of the loop was developed, a possible test site where such loop could be installed in the freeway was selected. The following criteria were applied for the site selection.

- 1) Variation of vehicular density should range from very low densities to jam density conditions.
- 2) Following criterion 1, speed should vary between free flow speed to stop and go operation.

The study section on I-70, from 18th Street to Hamilton Road, was divided into six sections and density flights were made to obtain aerial data. The flights were made for east and westbound traffic during both the morning and the evening peak hours. From this study, it was concluded that the preferable location would be the traffic lane next to the shoulder lane i. e. the traffic lane next to the gore area, where I-70 splits to merge with northbound I-71. Fig. 5, 10 shows traffic conditions at 7:48 a. m. on May 20, 1974, at this location.

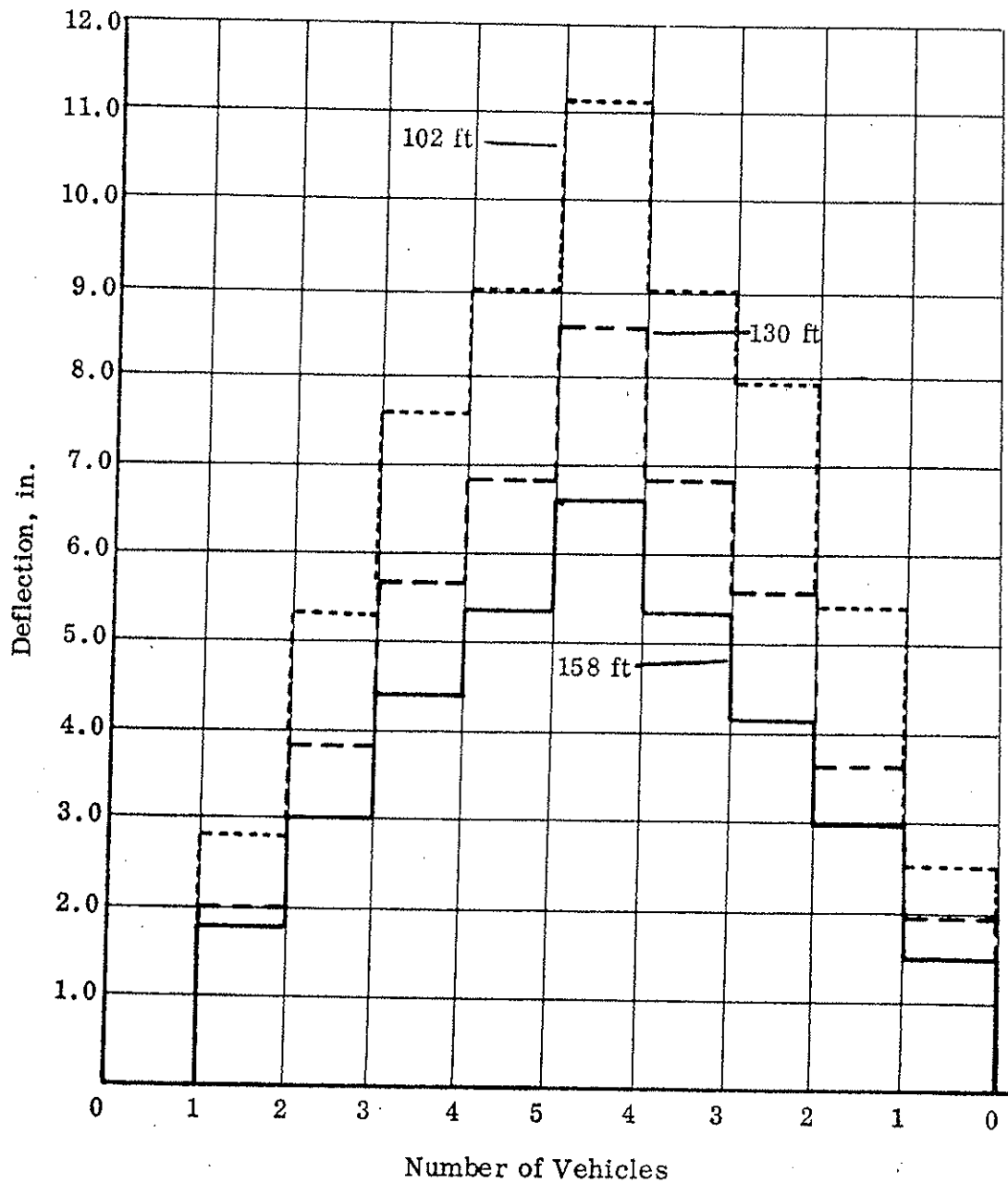


Figure 5.9 Density Measurement with Figure "8" Loop (18 ft. Section Length) Showing Consistent Pickup-Discharge Characteristics

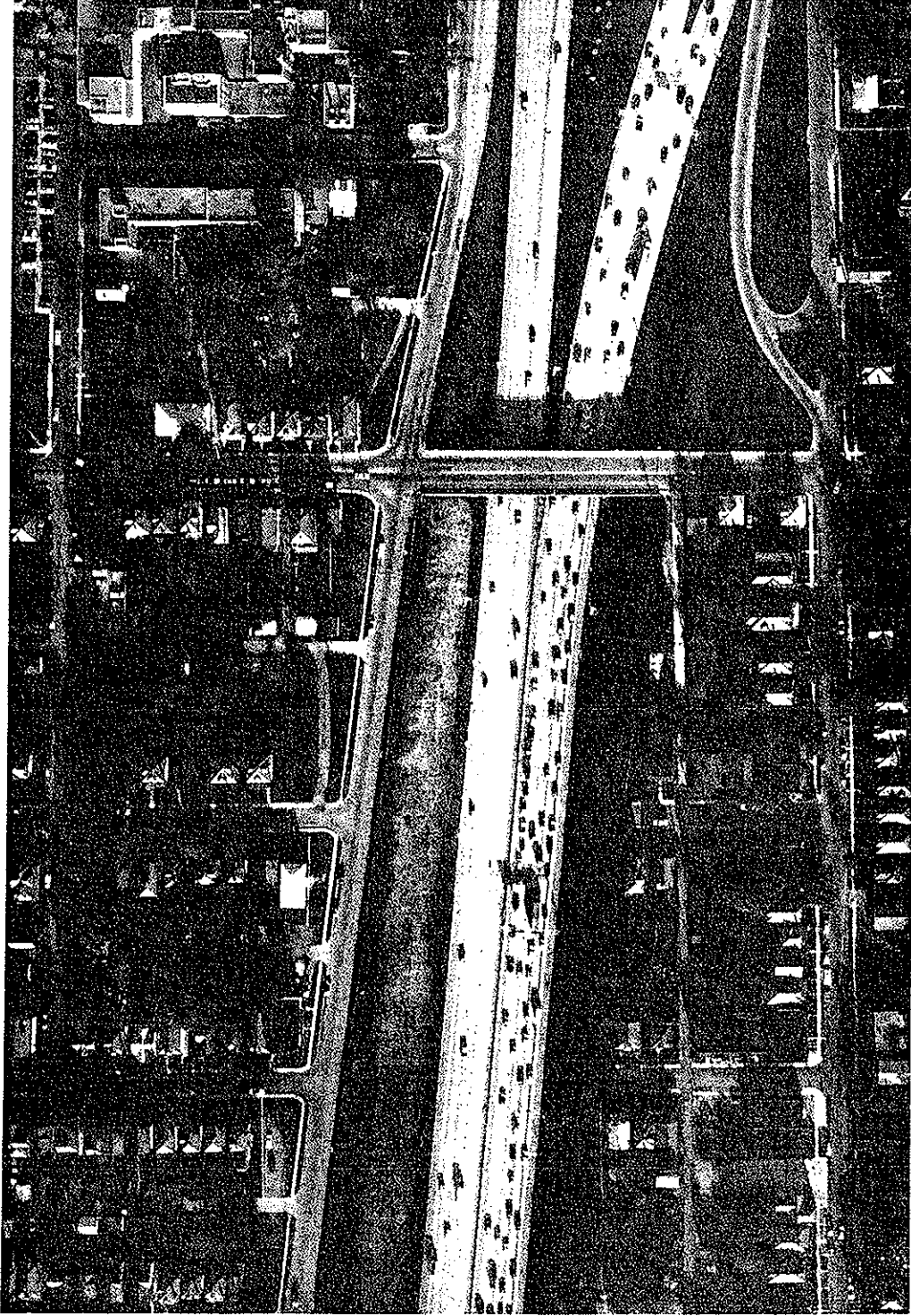


Figure 5.10 Traffic Density on I-70 at the test site
of Loop Detector

18th Street Overpass

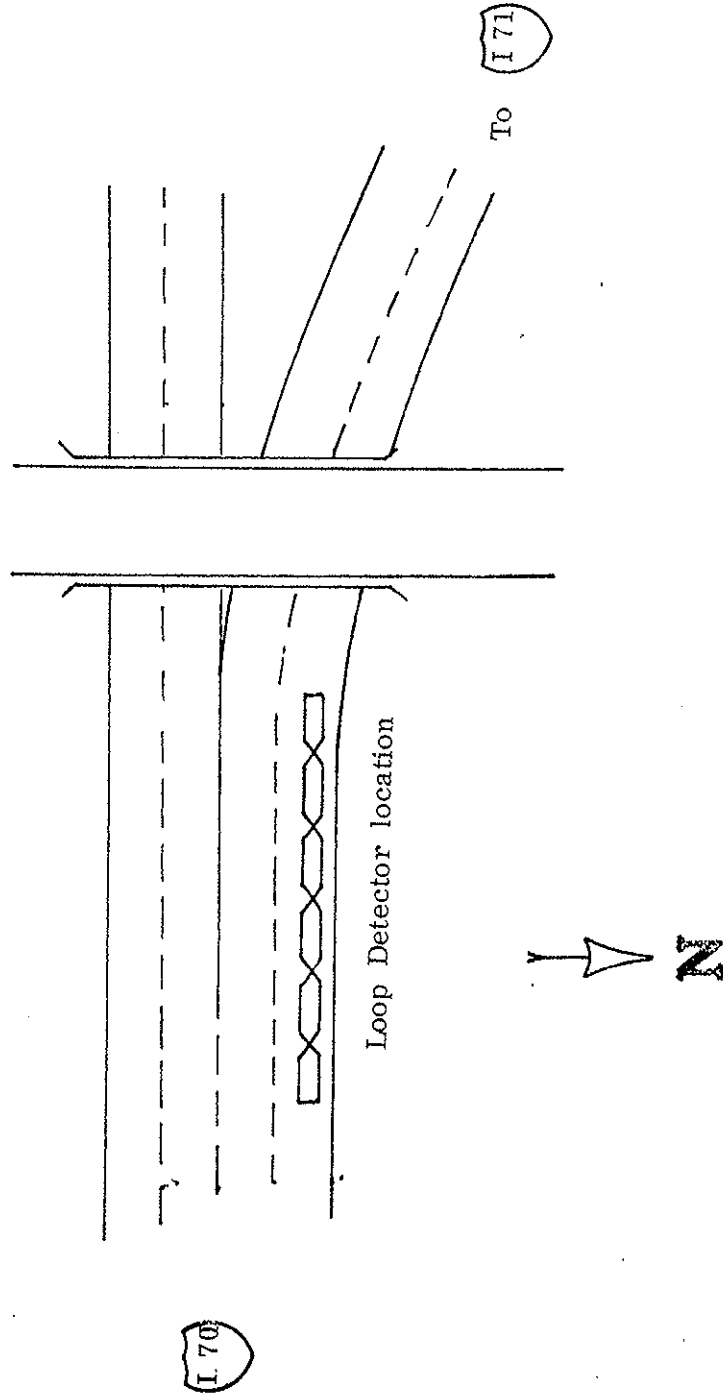


Figure 5.11 Location of Loop Detector on the freeway

Equipment for Field Tests

The loop wire terminals were brought from the freeway into a box which also housed the power supply for the tuner and pen recorder. The connections contained in the box are shown in Figure 5.12.

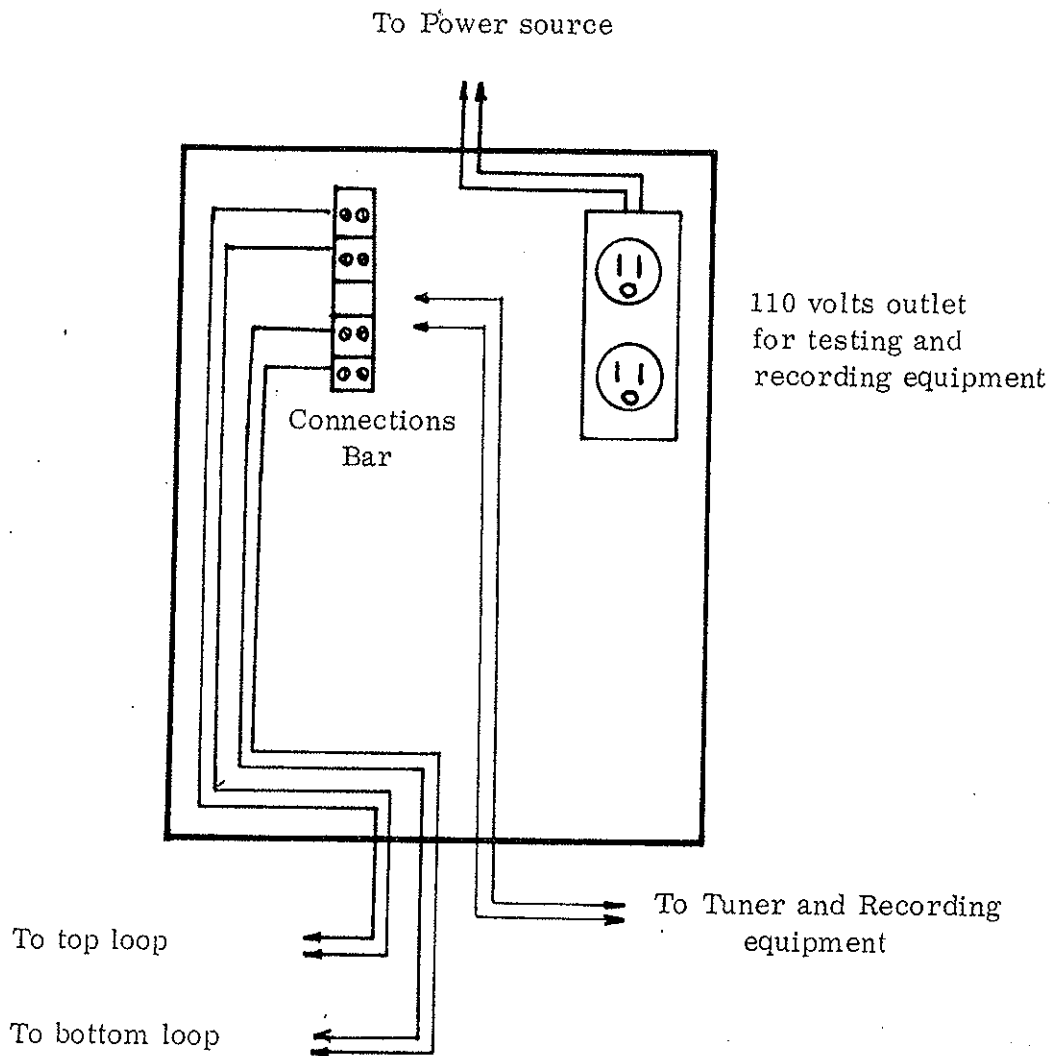


Figure 5.12 Control box connections for field tests of Loop Detector.

Installation

Because of difficulties in controlling traffic during the installation of the loop and in order to avoid serious disruptions which could have lead to traffic accidents it was agreed that the test loop should be installed in the shoulder lane. Fig. 5.11 and Fig. 5.15 show the final location of the loop detector.

The installation was carried out by the Traffic Engineering Division of the City of Columbus who also provided a connection for the 117 V power supply. Two loops of neopren insulated A W^G 14 wire were installed in the groove which was cut about 1 inch deep into the concrete surface. The four leads from the two independant loops were brought out to the connection box to permit tests of different configurations and to provide a spare loop in case that one of the loops should be damaged. For the record of the installations the terminal arrangement in the connection box is shown in Figure 5.12.

Field Tests

The dimensions of the loop detectors are shown in Fig. 5.13. This configuration was developed in previous lab tests with an Electro Matic Model LD-1 tuner, Serial No. 6618248, with a crystal frequency of 90 KHZ. The LD-1 tuner was selected from a range of different tuners since the research project specifically calls for the use of production equipment and not for the development of new equipment. It was found that the Model LD-1

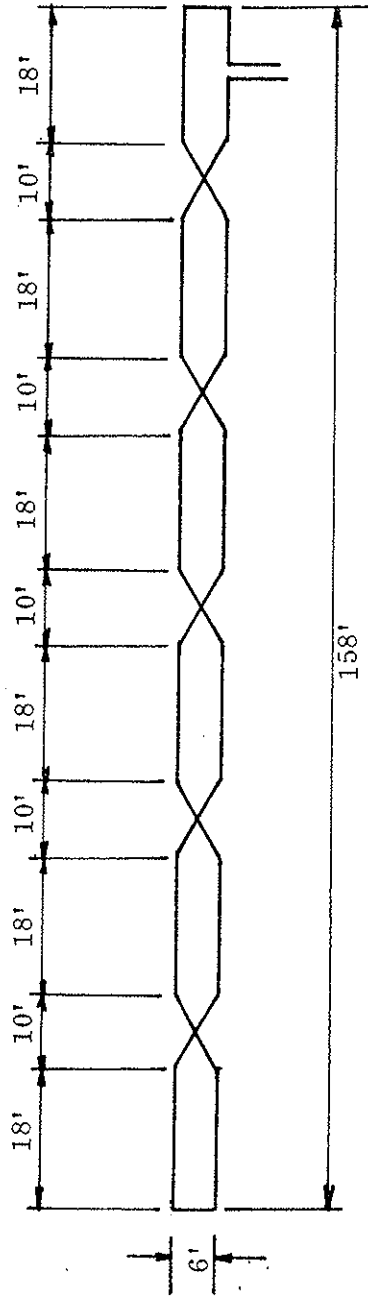


Figure 5.13 Dimensions of the Loop Detector installed on I-70

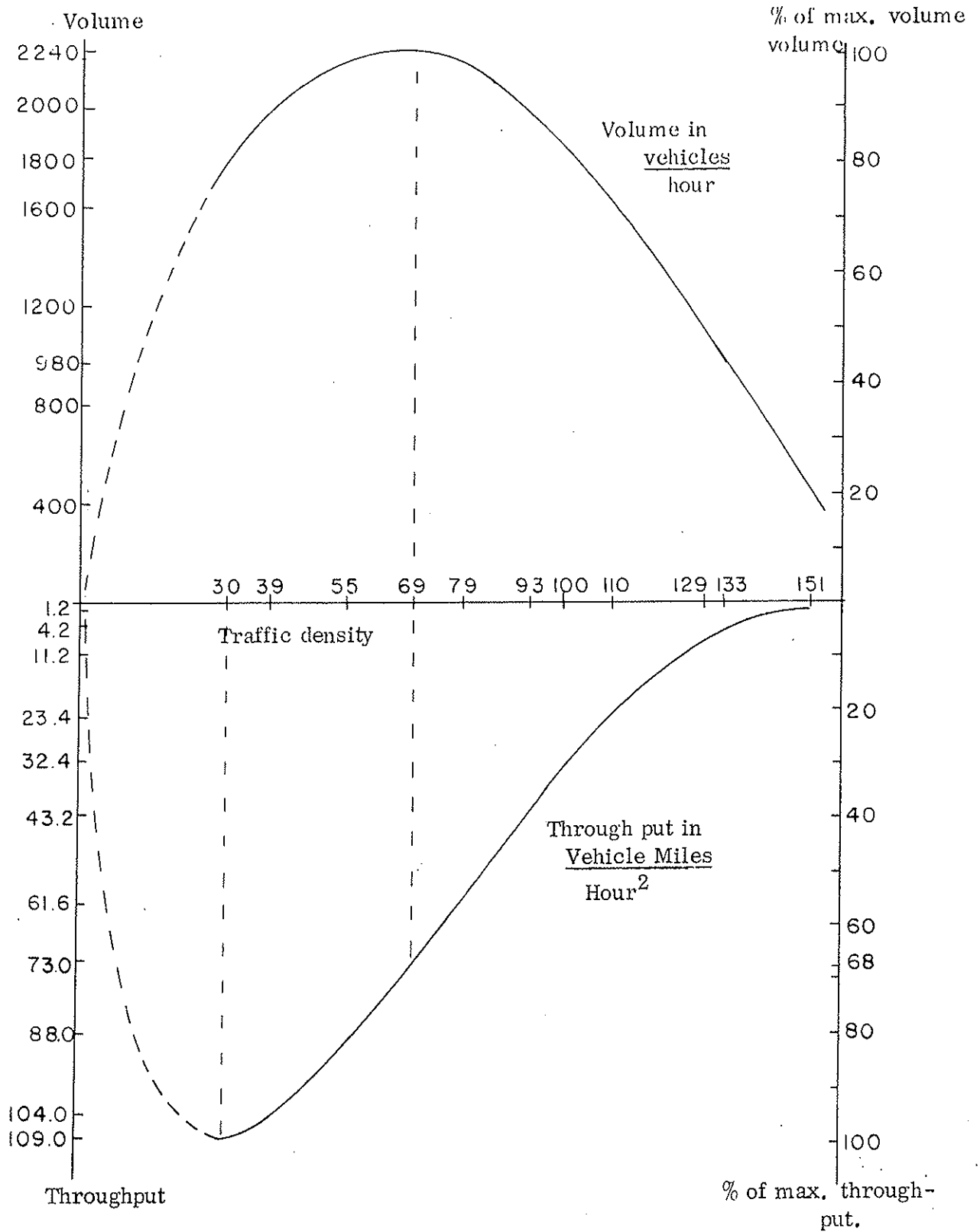


Figure. 5.14 : Traffic Volume and Throughput, a comparison of operating conditions.

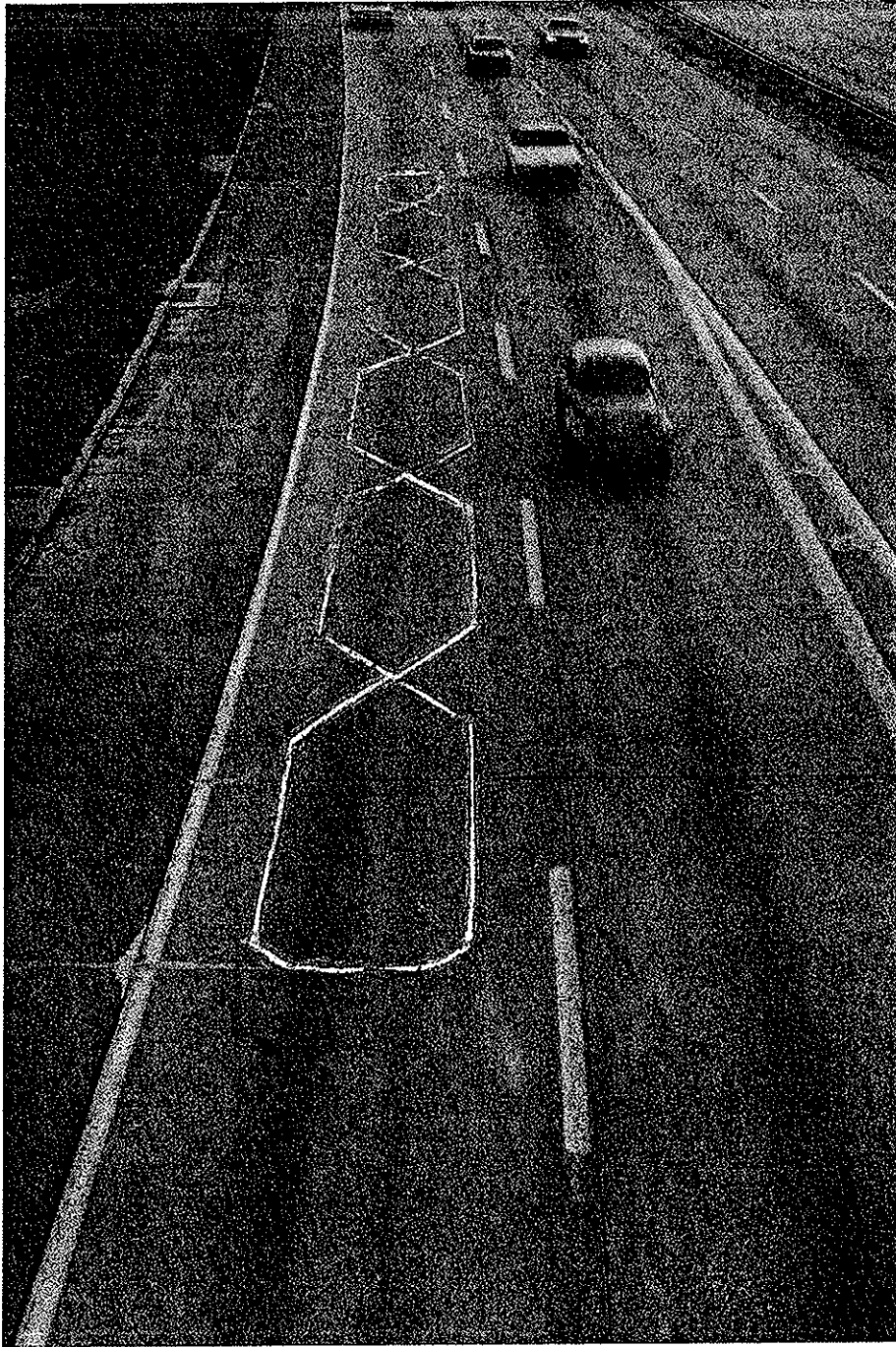


Figure 5.15 Loop Detector observed from the 18th Street Overpass

could best be adapted to the new multiple Figure "8" loop configuration.

Though a loop longer than 158 feet would be desirable this was the maximum length which could be tuned without too much loss of sensitivity and a good range in the output voltage. It appears, however, that it will be possible to extend the loop by making some minor modifications to the tuner.

Data Collection

A super 8 time laps camera Fig. (5.16) was used to record traffic conditions which were thus matched with the output of the loop detector as recorded by the Brush Pen Recorder. (Fig. 5.17) Time from synchronized stop watches was also recorded by the camera and marked on the graph paper of the pen recorder to facilitate the comparison of traffic conditions and loop output.

Data Evaluation

The recordings by the pen recorder and the time lapse photographs were matched with the help of a movie editor.

From these studies nine representative situations were selected for this report to show the following effects.

- 1) Size of vehicle.
- 2) Number of vehicles inside of the loop.
- 3) Clearance between vehicle body and road surface.
- 4) Type of vehicle.
- 5) Effect of lane changes.

Table 5.1 lists the traffic conditions which were selected for presentation. It can be observed from Table 5.1 that both density and speed may be obtained from the output shown in the graphs of Fig. 5.18 to Fig. 5.26. Traffic densities can be obtained from the peak output recorded by the pen recorder. Full size passenger cars show a maximum deflection of about 7 to 8 units (Fig. 5.18, 1-A), and three full size cars show a maximum deflection of 13 to 15 units. The recording of three vehicles was the maximum observed in the loop at one time since no traffic jam was recorded in the traffic lane.

In the present set up of the test loop three successive peaks are generated by a single passenger car when travelling through the loop with the center peak showing the biggest deflection. No explanation can be given at this time why the six loops provided by the multiple Figure 8 configurations produce three peaks of different magnitudes and more research and possibly some modifications are required. At traffic volumes with a density of up to 33 vehicles per mile cars will be recorded as single units with the three peak characteristics.

This is the free flow region where the maximum throughput occurs (Fig. 5.14) on urban freeways. Higher densities change the output characteristic completely and the magnitude of maximum peaks becomes the indicator for traffic density. It was not possible to calibrate the test loop since photographic recording was restricted because of the low light level during traffic peak hours. The principle however was clearly established as

Fig. No.	Situation No.	Time	Type of Cars	Description of effect
5.18	1	2:43.56 2:34.58 to 2:44.04 2:44.06 2:44.09 to .11	A Full size car B Consecutive cars (1 at a time) C Full size car D Truck	1-A shows a full size passenger car with a low center of gravity. 1-B is two consecutive cars with a small headway between them. 1-C is another heavy car and 1-D is 20 ton truck with a higher center of gravity.
5.19	2	2:45.14 2:45.22 2:45.25	A Car B Heavy truck in lane C Full size car	2-A is one car. 2-B is dump truck travelling in adjacent lane with graph showing no side effects on loop. 2-C is a full size car.
5.20	3	2:45.40 2:45.43	A Pick-up truck B Car changing lane	3-A is a pick-up which causes a smaller effect than a car. 3-B is the effect of a car changing lanes. 3-C is the effect of a full size passenger car. 3-D is the effect of two full size passenger cars, a second one entering as the first one is leaving.
5.21	4	2:45.41 2:45.48	A Compact car B Car changing lanes	4-A is the effect of a compact car. 4-B is a car changing lanes plus one car in the loop.
5.22	5	2:47.20	A Two cars over loop	5-A shows the effect of two cars in the loop at the same time which are travelling in adjoining traffic lanes and no effect is recorded by the loop detector.
5.23	6	2:49.45 2:49.51	A Pick-up truck and trailer B Truck	6-A indicates graph of a pick up with a trailer and 6-B shows the effect of a 20 ton semi trailer power horse. (full size passenger car signals are included on the graph for comparison with the other vehicles).
5.24	7	2:50.38 2:50.41	A Van B VW Micro Bus	7-A and 7-B display two different types of vans, the first one has a lower center of gravity than the VW Microbus.
5.25	8	2:54.45	A three cars over loop	8-A represents three cars crossing the loop in a short time.
5.26	9	2:58.49 2:58.55	A car over half loop B three cars over loop	9-A depicts a car crossing only the loop's right half. 9-B shows three cars on the loop at one time.

Table 5.1 Different traffic conditions in actuating the loop detector.

can be seen from the recording of three vehicles crossing the loop simultaneously (Fig. 5.25, 8A and 5.26).

Average speed can be obtained by multiplying the time interval between max. output peaks with a constant which was about 100 to arrive at the speed in feet/sec. In situation 1-A Fig. 5.18 the speed was determined as 72 ft/sec or 49 m. p. h.

Equipment considerations for the practical use of the modified loop detector

The equipment required to read the output of the loop detector must perform two functions. It must determine the mean output peak over a certain time interval. The optimum time interval has not been determined yet but it appears to be in the range of 3 to 10 seconds. Thus it can be expected that density readings can be provided every 10 seconds or less which should suffice a computer controlled traffic surveillance and control system. It also must measure the time interval between two consecutive peak values which again can be averaged over the basic time interval to determine the mean speed of traffic.

Conclusions

The extended multiple Figure '8' loop detector did perform very well in the field tests carried out so far, and it appears that it can provide reliable density and speed information for a computer controlled traffic system. The field tests however, did produce some significant differences from the lab tests. More tests and more research is required to explain

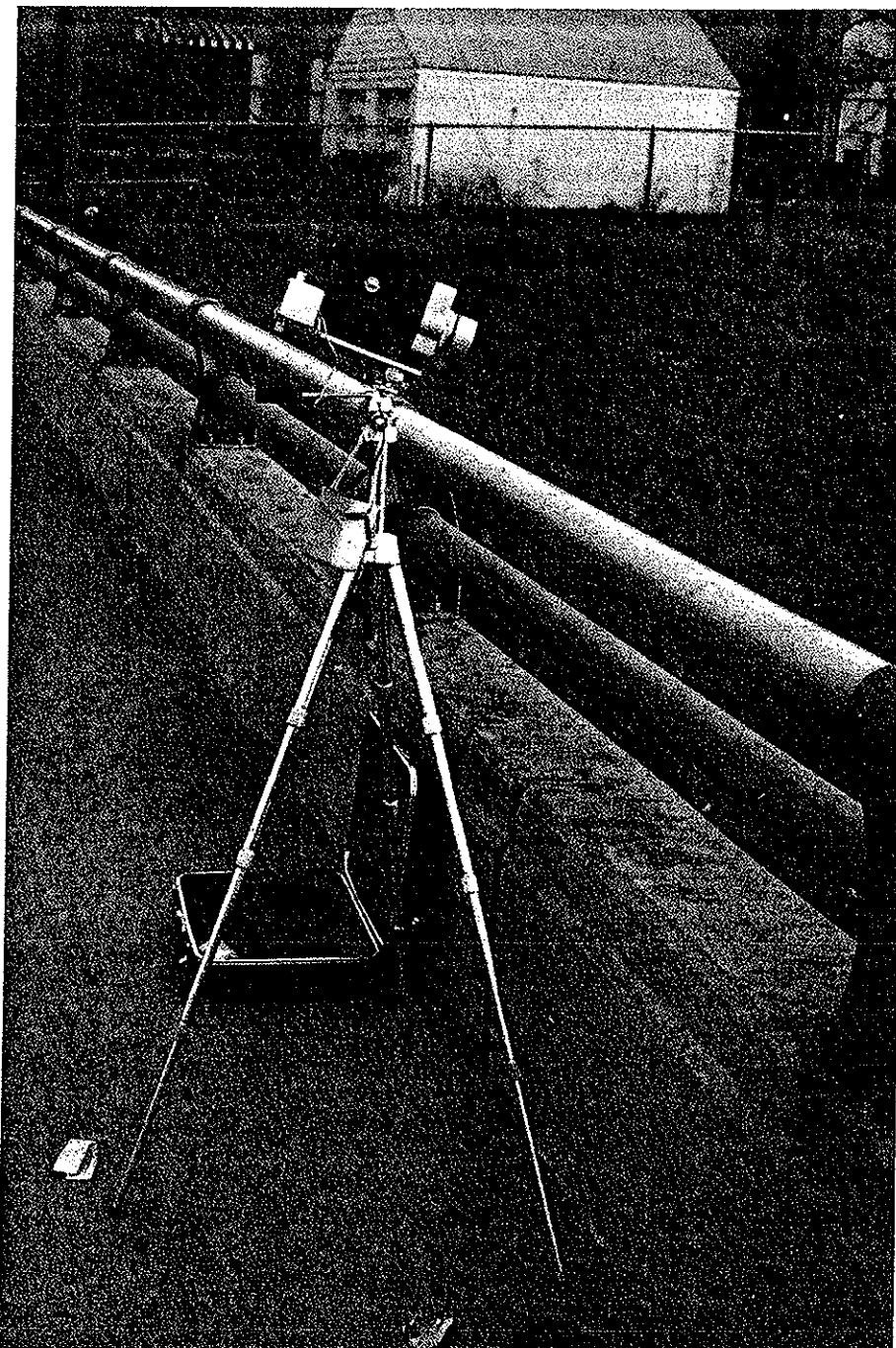


Figure 5.16 The 8 mm Time Lapse camera used to collect the film data

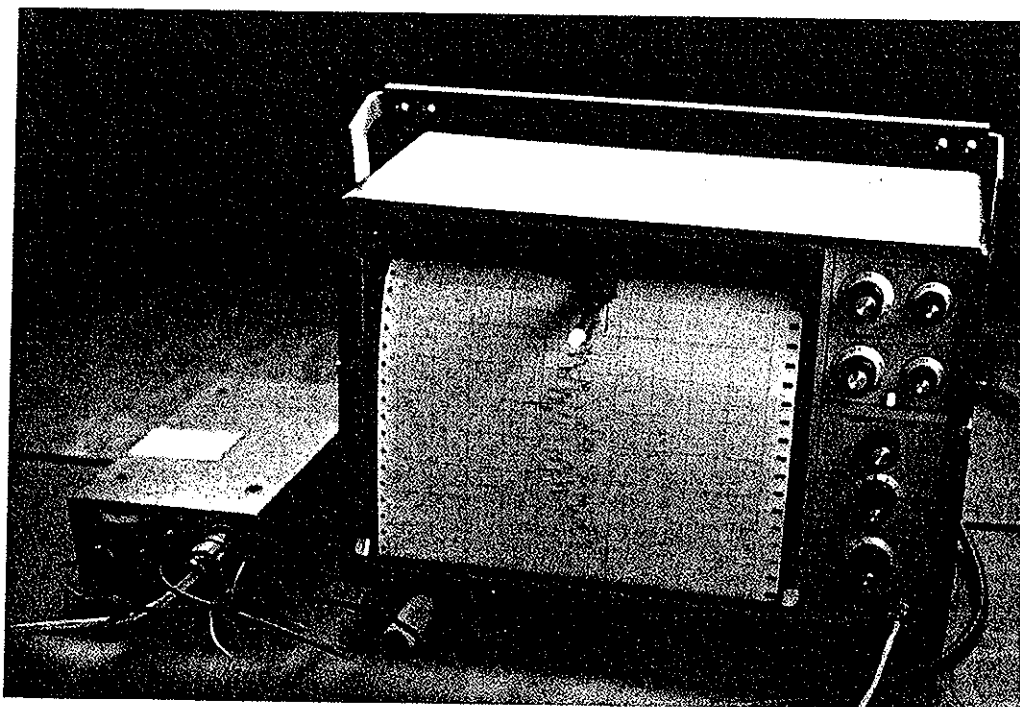


Figure 5.17 The LD-1 tuner and the Brush pen recorder during tests.

15

18

:21

:24

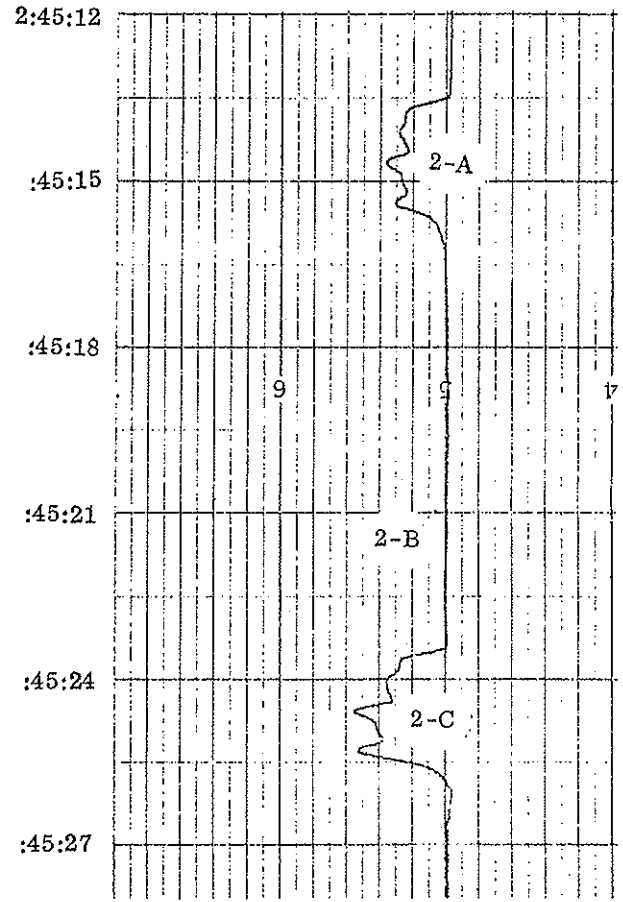
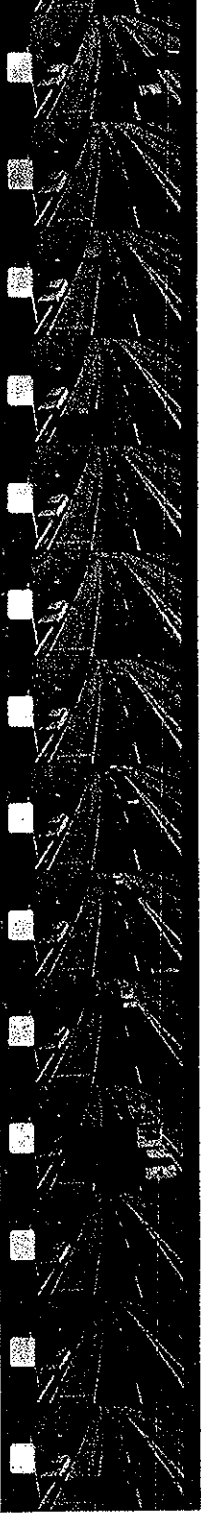
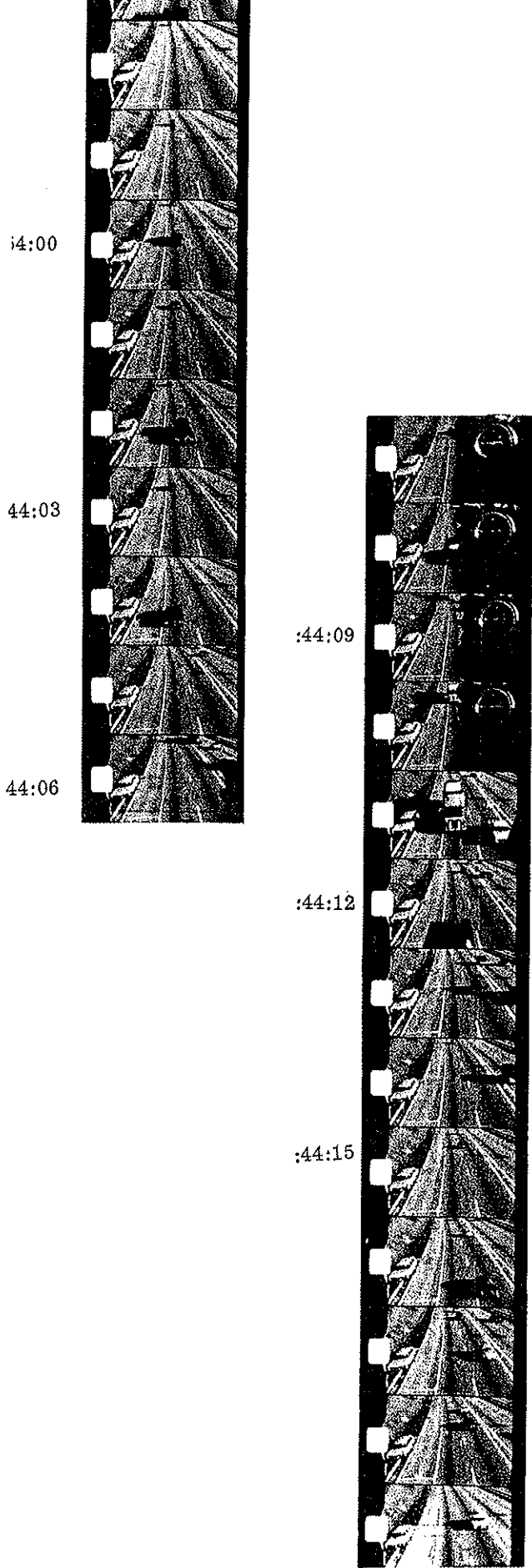


Figure 5.19 Situation Number 2



2:43:54

:43:57

2:54:00

:44:03

:44:06

:44:09

:44:12

:44:15

1-A

1-B

1-C

1-D

Figure 5.18 Situation Number 1

:45:42

:45:45

:45:48

:45:51

:45:54

:45:57

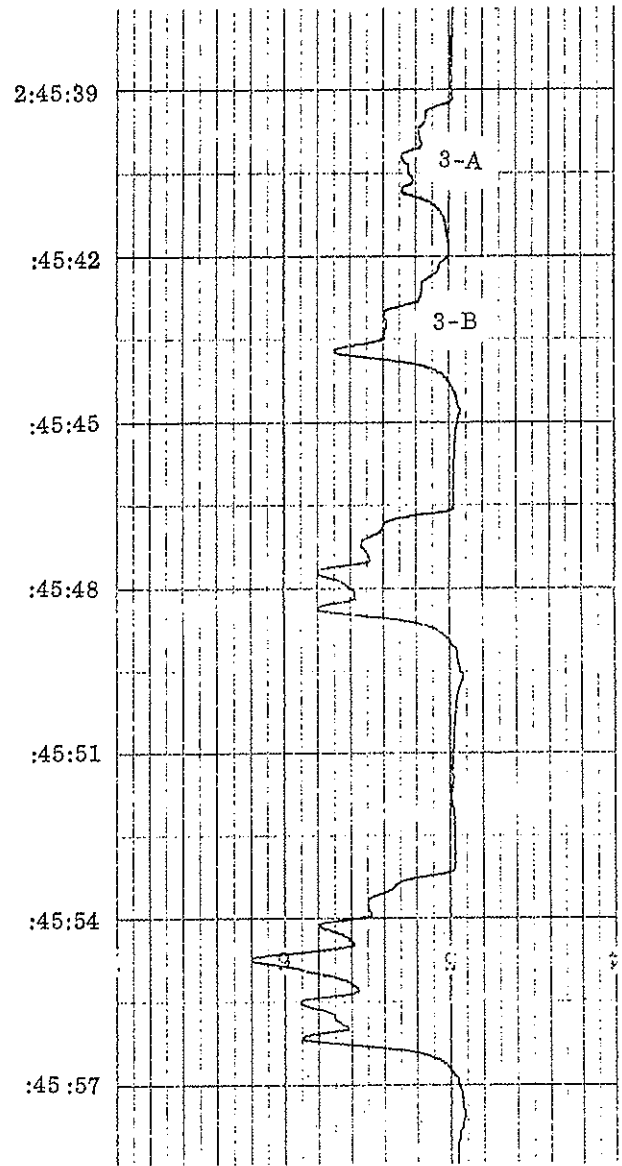
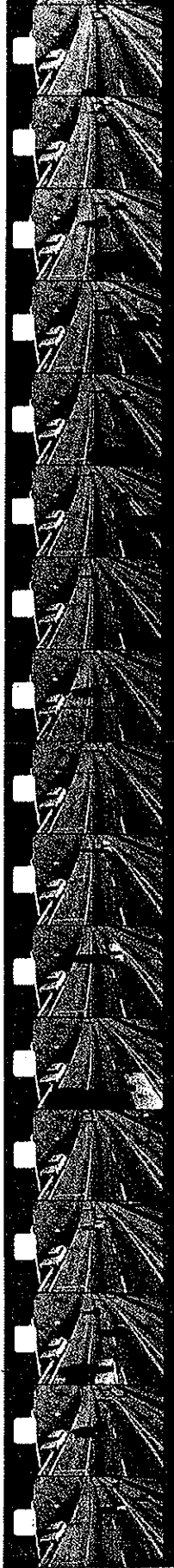
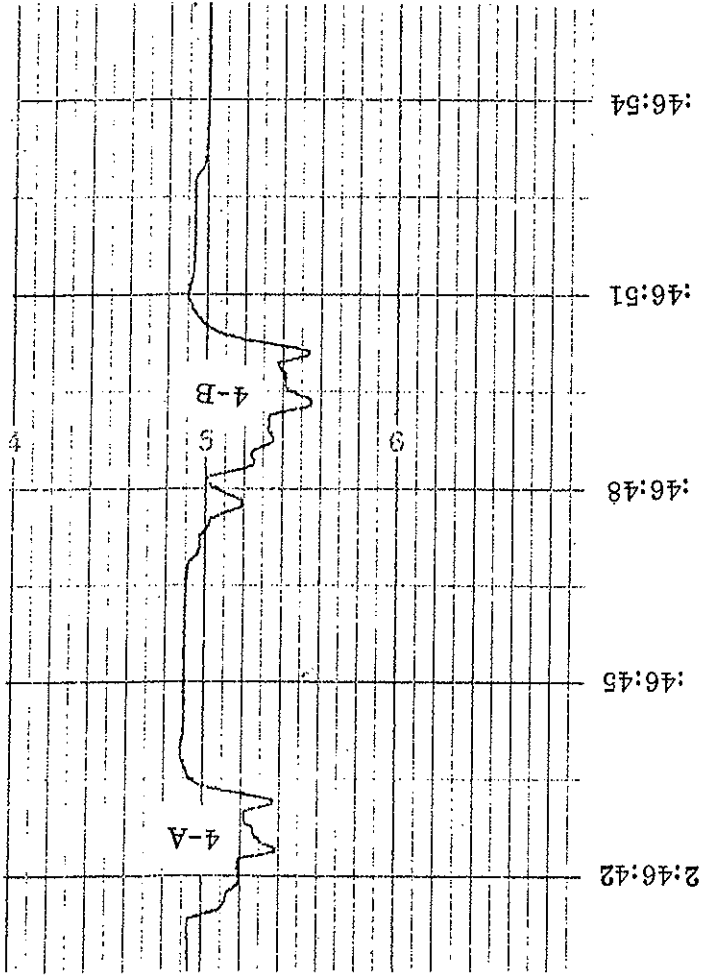


Figure 5.20 Situation Number 3

Figure 5.21 Situation Number 4



:46:51

:46:48

:46:45

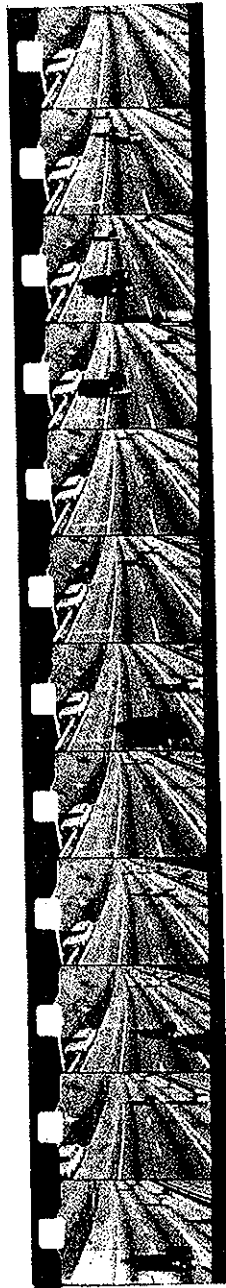
2:46:42

5

8



:47:21



:47:24

:47:27

:47:30

2:47:12

:47:15

:47:18

:47:21

:47:24

:47:27

:47:30

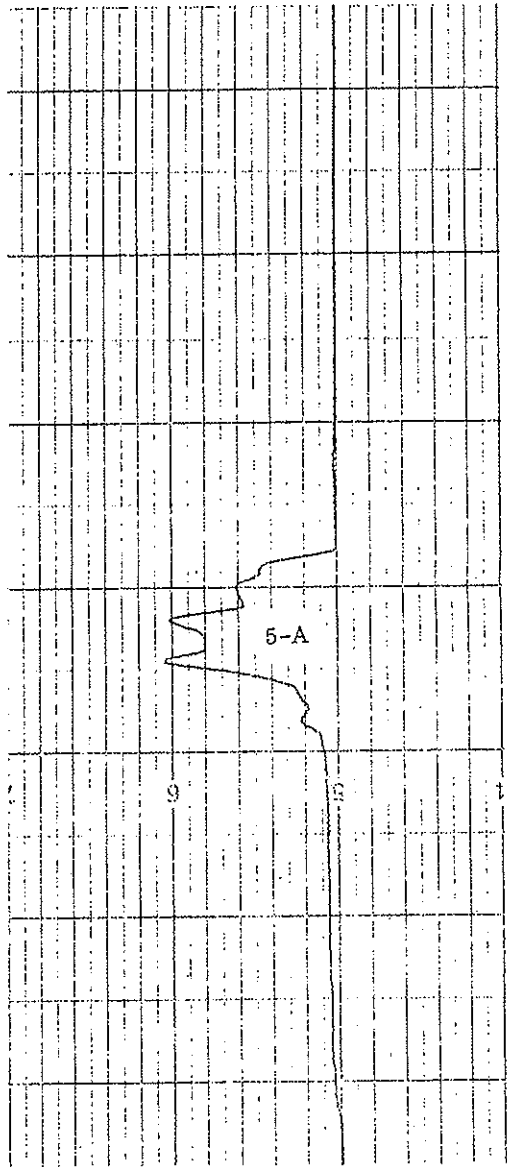
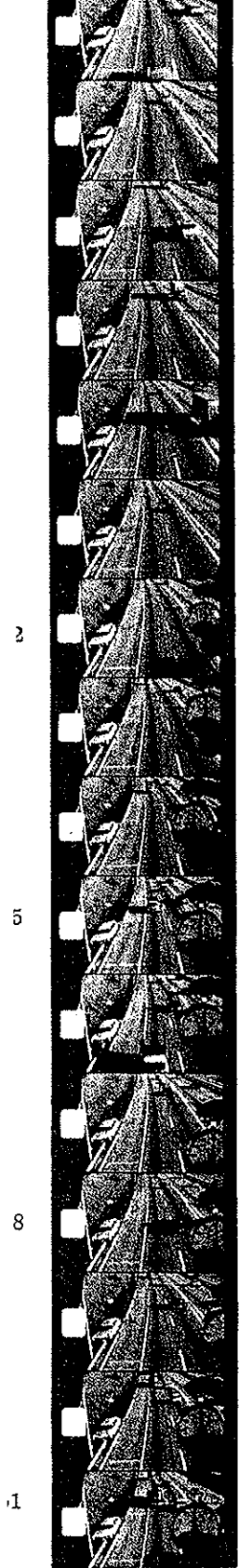


Figure 5.22 Situation Number 5



:49:54

:49:57

2:50:00



:49:36

:49:39

:49:42

:49:45

:49:48

:49:51

:49:54

:49:57

2:50:00

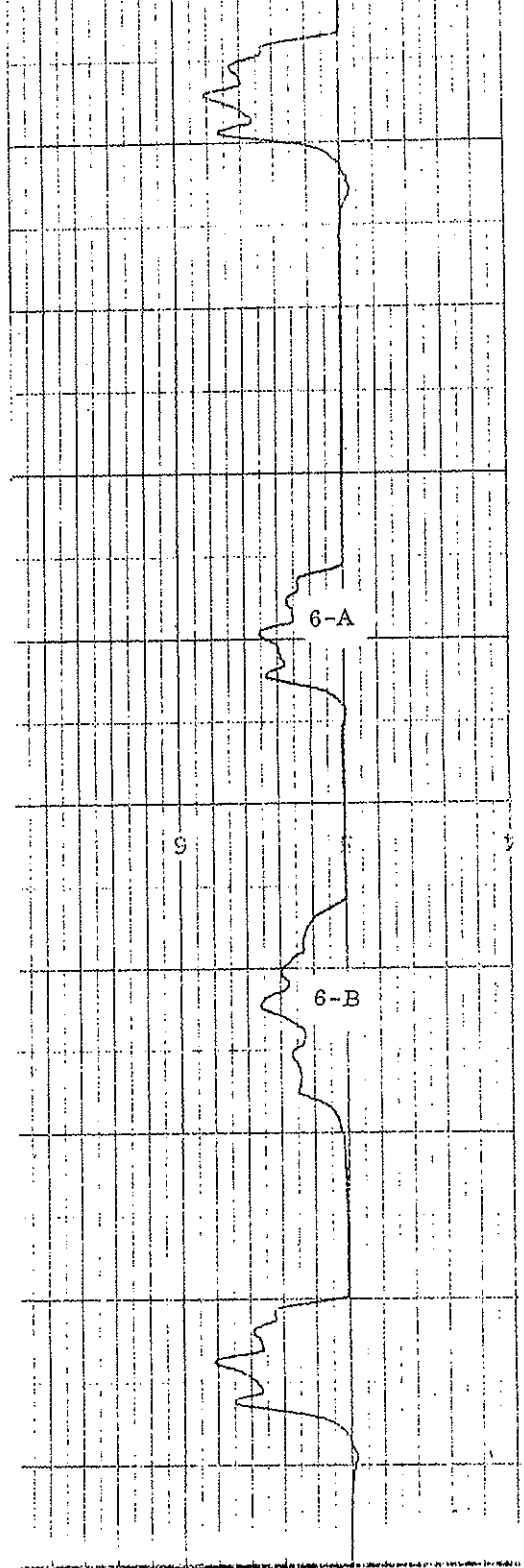


Figure 5.23 Situation Number 6

2:50:36

:50:39

:50:42



2:50:36

:50:39

:50:42

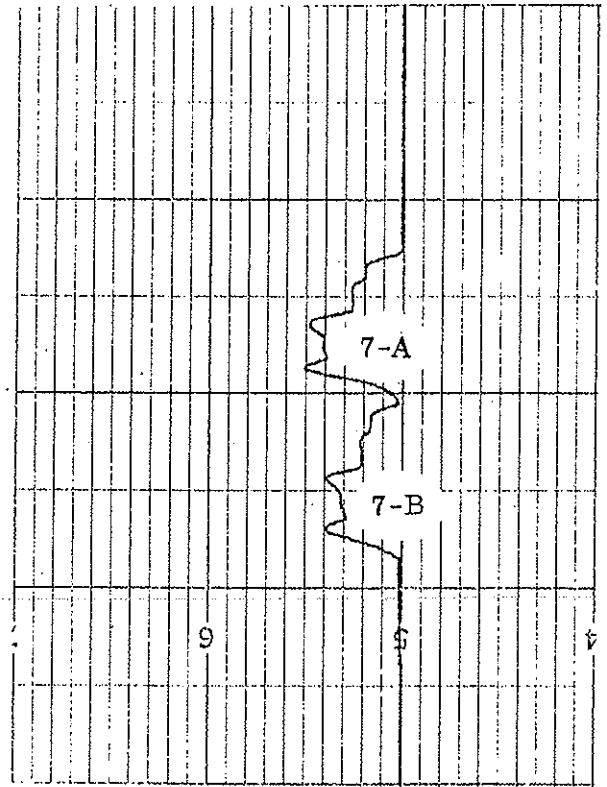


Figure 5.24 Situation Number 7

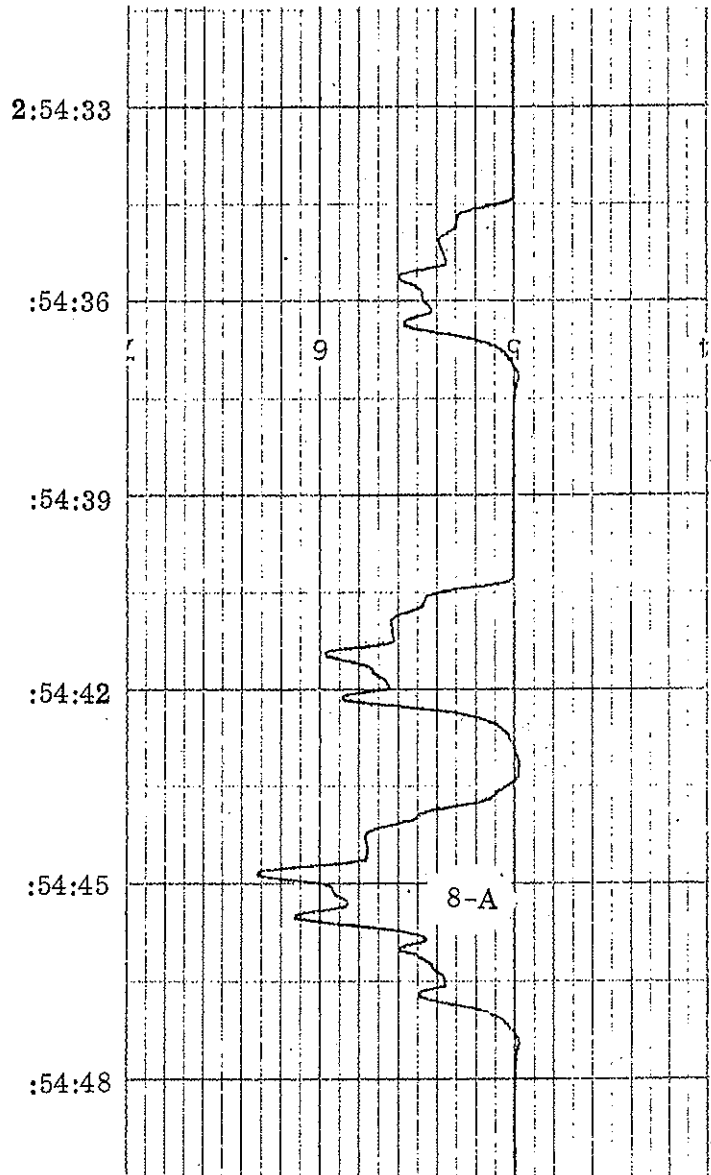
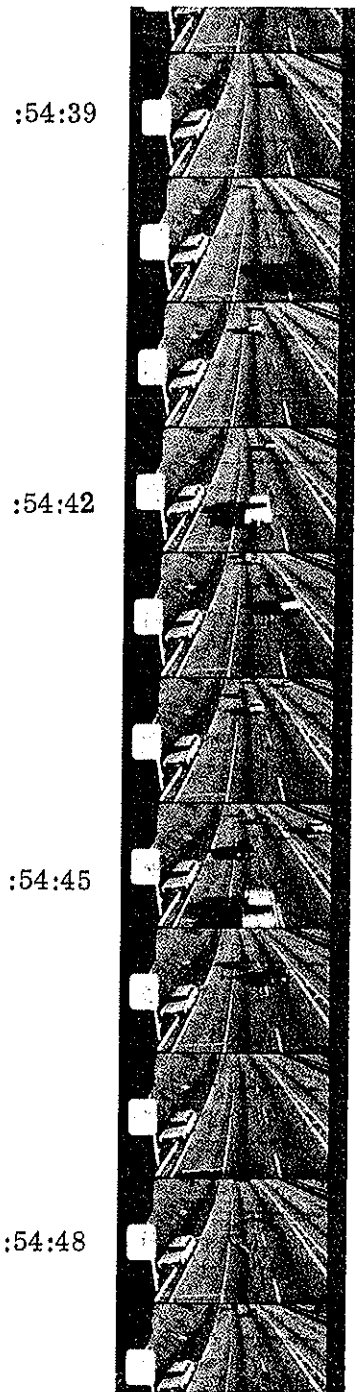


Figure 5.25 Situation Number 8

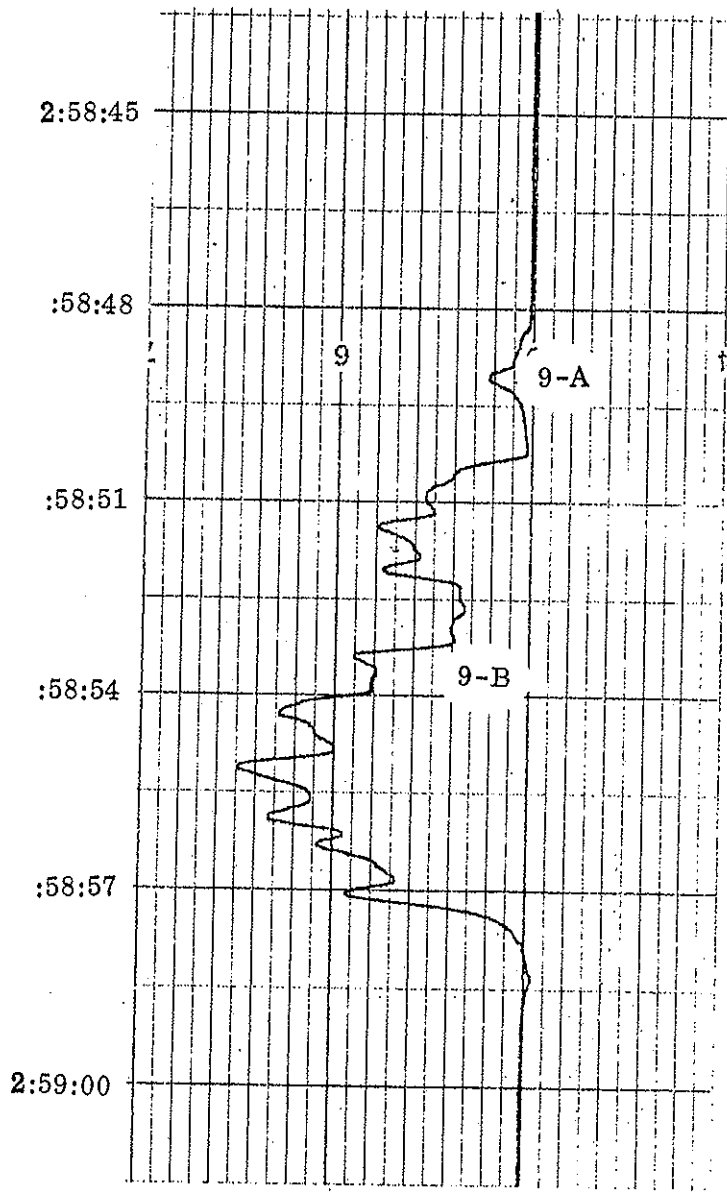
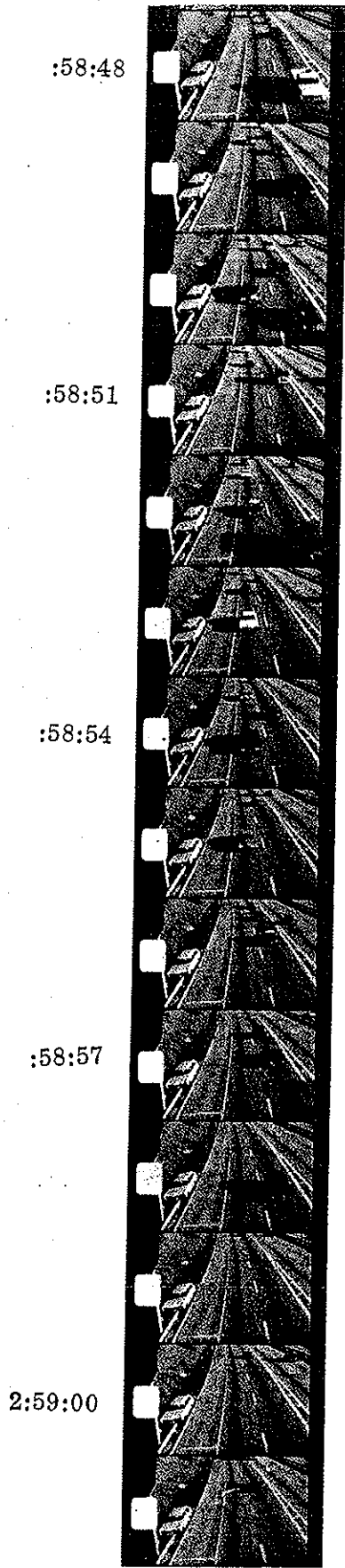


Figure 5.26 Situation Number 9

and modify these differences for practical applications of the loop detector.

The most important factors are :

- 1) Output varies in shape and magnitude for different types of vehicles. This characteristic is more pronounced for single vehicles, i. e. at traffic densities below 30 vehicles per mile, and the data on high density traffic are not sufficient to evaluate the influence of the traffic composition on density measurements.
- 2) The detector, consisting of six fields, produces only two distinctive peaks at present. Though two consecutive peaks are sufficient for speed measurements, it is desirable that more uniform and more pronounced peaks are obtained. This probably can be achieved by better turning, or solidstate amplifiers as integral parts of the field sections.

The test installation of the extended multiple field, loop detector (EMFLD) can already provide traffic density and speed data which are required for a computer controlled traffic surveillance and control system. However, the performance differs from previous lab tests and more research is desirable to understand and improve the system for full scale applications.

Chapter 5: References

1. Greenshields, Bruce D. , Statistics with Applications to Highway Traffic Analysis. , Saugatuck, Connecticut: Emp Foundation, 1952.
2. Head, J.R. , "The Operation of the Inductive Loop Vehicle Detector", Traffic Engineering and Control , Vol. 12(July, 1970), 135-138.

CHAPTER 6

COST ANALYSIS OF AERIAL SURVEY DATA

6.1 INTRODUCTION

In the proposal for continuing research project EES 278 B, it was stated that the researcher would present an economic assessment of the costs for analysis and reduction of aerial data used in the research project.

The economic study should provide the Ohio Department of Transportation with information for an adequate analysis and enable the Department to explore the possibilities of employing this type of data collection for the operation and analysis of freeway traffic in the State of Ohio.

6.2 METHODOLOGY

The figures presented in this analysis are those found in the records of the Engineering Experiment Station. For the equipment purchased by the University, the values reflect the price paid at the time of purchase. No investigation was conducted to actualize the prices of the equipment used.

For equipment on lease and/or with maintenance agreements, the

current costs of those leases and agreements were used in the calculations of the analysis. Equally, for the equipment used on rental basis, the hourly or monthly rates were used.

To simplify the analysis, the costs were subdivided into the following categories

- 1) Fixed costs
- 2) Variable costs
- 3) Labor costs
- 4) Materials and supplies
- 5) Costs not included

This breakdown should make the calculation and understanding of the cost structure of the process easier. In the above divisions, the most complex is that of labor and personnel costs as it will be explained in the following section.

1) Fixed Costs

This section includes all equipment used in the process of aerial traffic surveys. The equipment value is that at the time of purchase, annual costs are calculated on linear depreciation, with a lifetime depending on the type and cost of the instrument or equipment. A Capital Recovery Factor of 8% was used in the calculation of yearly costs.

2) Variable Costs

In this category, the costs which vary with the altitude of flight,

traffic density, length of study section and other variables, are included for an average traffic situation. However, to determine the traffic related costs it appears that one study situation per roll of film could be used to calculate costs.

3) Labor and Personnel Costs

For these costs it was difficult to assign either value per hour or per activity. It was also complex due to the difference in salaries paid by the University to the graduate research assistants and that of a full time employee of ODOT. It therefore was decided to present the time needed for each activity which would enable the department to estimate its own costs according to their salary schedule, as well as assign representative costs of their present organizational structure.

4) Materials and Supplies

In this section all the materials needed for the preparation of the sites, ground control points, projector lamps for the comparator and small office supplies are included.

5) Costs not included

If this activity is fully developed as a permanent operation of any division, ODOT would need logistic support, both on the field and in the office. However, this service could be obtained from the present organizational structure of ODOT and

is therefore not included in the analysis. It should be considered however to an extent depending on the intended scale of operations.

6.3 DESCRIPTION OF THE EQUIPMENT AND PROCEDURE

Although the reader may be referred to previous reports describing the equipment in detail, this report will describe briefly the equipment which is included in the cost study. Therefore, the description herewith should be considered for identification purposes only, and not as an exact description of the equipment used in the collection and reduction of aerial data.

Camera The camera used for the aerial surveys is a KA 62A arial reconnaissance camera, manufactured by the Chicago Aerial Industries. The capacity of this camera is 600 frames of 5" x 5" photographs, which can be taken at intervals regulated by control instruments designed and built by the Transportation Research Center.

Comparator Once the photographs have been developed, a comparator manufactured by the David Mann Company of Burlington, Massachusetts, is used to establish the location of the ground control points and the location of vehicles in relation to these control points. This comparator uses movie projector lamps with a life of approximately 25 hours.

Data Logger The location of the ground control points and the vehicles is translated in terms of coordinates by a Data Logger Type 1945 manufactured

by the David Mann Company of Boston, Massachusetts. In addition to the X and Y coordinates, the Data Logger provides the means of identifying the points entered as control points or vehicles, flight identification numbers, photograph numbers of flights, lane numbers of the freeway or roadway and frame numbers.

Key Punch The information supplied to the Data Logger by the comparator is fed to an IBM 026 Key Punch, which punches all this information in one card per vehicle for computer processing at a later stage. Each card represents then, one point i. e. a vehicle or a control point in a photograph.

Auxiliary Equipment i. e. equipment needed in addition to the equipment described above, which can either be purchased or has to be built to fit specific needs. Some of these items are, for example, the camera mount which is attached to the helicopter and supports the camera during flight. This mount was designed and built to attenuate vibrations and to fit the camera and the helicopter.

Light Table This table is a rectangular glass top table, lighted by fluorescent tubes, with film supports, at each end of the table. This table is used to analyze and mark the film before it is processed in the comparator.

Camera Control Instruments This control equipment was designed and built specifically for the camera used. It consists of a 400 cycle 110 V inverter and a set of meters relays switches and an intervalometer for camera and exposure control.

Card Files The processing of each film usually results in the collection of a few thousands cards which have to be stored. Ample storing space must be provided if this is to be a full scale operation.

Computer Programs The amount of data obtained from the aerial photographs is so large that the complete process requires a number of programs in order to obtain the final plot of vehicle trajectories and other parameters such as speed, acceleration, deceleration, headway, spacing and energy level of traffic flow.

This process is divided into four phases which are briefly described below.

Phase 1 Binary plotting

The data recorded on punch cards are processed on the IBM 360 computer using a program similar to the program used for Phase 3. The only difference between the two programs is that Phase 1 has a binary card output and Phase 3 has a printed output. The binary card output contains suitable instructions for the IBM 1620/27 digital incremental plotter.

Phase 2 Plotting of data points

The output deck obtained in Phase 1 is used as the input for the IBM 1620/27 plotting system. Phase 2 produces data points representing the distribution of vehicles in a traffic lane at the time when the relevant photograph was taken. Eighty photographs are plotted on graph paper of the format 29.5 inches by 120 feet.

Phase 3 Vehicle identification

The computer output of Phase 3 are photo coordinates, ground

coordinates, and accumulative distances for each vehicle and photograph being processed. During the verification process of the vehicle trajectories, erroneously punched cards, missed vehicles, or grossly incorrect measurements are detected. All corrections, insertions, or deletions are made at this point before Phase 4 is processed.

Phase 4 Final record

The computer program for Phase 4, provides a final record which contains data corrected to the scale factor between ground control points. A printed record and a record on computer compatible magnetic tape is provided which contains the following information:

vehicle number (code), plot coordinates, ground coordinates, accumulative distance,

Spacing, headway, velocity of each vehicle on each photograph recorded in the appropriate lane

total number of vehicles, average velocity, traffic density, and traffic volume for each lane on each photograph.

6.4 COST ANALYSIS

	Fixed costs per year
Camera - Initial cost \$ 24,000.00	\$2,560.
Life 18 years, 8% CRF	\$2,560.80
Maintenance and repairs	555.75
Data Logger & Comparator	
Initial Cost \$19,180.00	
Life 10 years, 8% CRF	2,857.82
Maintenance and repairs	236.20
IBM Key Punch	
Rental and Maintenance	1,011.60
Additional Equipment	
Total Estimate \$6,000.	
10 years, 8% CRF	894.00
	<hr/>
	\$8,116.17
	Variable costs per flight
Film (black and white)	\$ 55.00
Processing	25.00
Computer Programs per situation	
Phase I computer time (avg.)	\$ 100.00
Phase II computer time (avg.)	175.00
Phase III computer time (avg.)	100.00
Phase IV computer time (avg.)	80.00
Helicopter cost per hour \$100.00	
Normally 1-1/2 hour of flight per film	\$ 150.00

	Labor costs per study situation
Principal or project supervisor	160/man/hr
Reduction time per situation 50 man hours*	50 man/hr
Data Processing-Supporting Activities	
Phase I	40 man/hr
Phase II	75 man/hr
Phase III	40 man/hr
Phase IV	30 man/hr
Analysis of Results	75 man/hr

* Based on an estimate of 150 frames per study situation, with high density traffic, 2 mile length of study section and 3 lanes in one direction.

	Materials and Supplies* per study site
25 Ground Control Points at \$29.50 each	\$ 737.50
Installation	30 man/hr
Office Supplies	\$ 25.00

* Based on an estimate study section 2 miles long.

CHAPTER 7

STUDY OF TRAFFIC DYNAMICS ON I-70

Traffic studies on I-70 have been carried out by aerial surveys and travel time studies using the moving vehicle method.

The objective of these studies were

- 1) To obtain traffic density distributions for inbound and outbound traffic on I-70 during peak traffic hours.
- 2) To evaluate traffic conditions (travel times) for peak hour traffic.
- 3) To collect more data on the hysteresis phenomenon of traffic flow which has been observed on I-71.

7.1 TRAFFIC DENSITY STUDIES

Density studies were carried out on Mondays, Wednesdays, Thursdays, Fridays for east and westbound traffic during peak hours. These days were chosen to represent typical weekly variations. A summary of the general survey flights is given below.

Flight Identification	Date	Time of coverage	Exposure Interval
Film # 39 E. bound	Fri., Jan., 25, 1974	4:20 pm-5:40 pm	2-3 sec.
Film # 40 E. bound	Wed., Feb., 13, 1974	4:20 pm-5:40 pm	2-3 sec.
Film # 41 W. bound	Thur., May, 16, 1974	7:01 am-8:04 am	most 5 sec; 1-3 sec. at 7:25 7:25 am disturb- ance.
Film # 42 W. bound	Mon., May, 20, 1974	6:59 am-8:10 am	most 5 sec.
Film # 43 E. bound		4:06 pm-5:30 pm	all 5 sec.

General Survey Flights

Observations and aerial photographs from the general survey flights were used to define critical sections on I-70.

For eastbound traffic it was found that highest densities were reached in the section between the traffic signs LA-AC and WB-LA(mi) on all weekdays with a maximum average density on Friday of almost 50 vehicles/mile/lane. (Fig. 7.1)

For westbound traffic the highest value was recorded for the section James Road - US. 33 overpass with 56 vehicles/mile/lane on Monday. Rather high values of about 50 vehicles/mile/lane were also recorded at the following sections :

Sign LA to RR WBR

RR WBR to Kelton overpass

Kelton overpass to Linwood overpass.

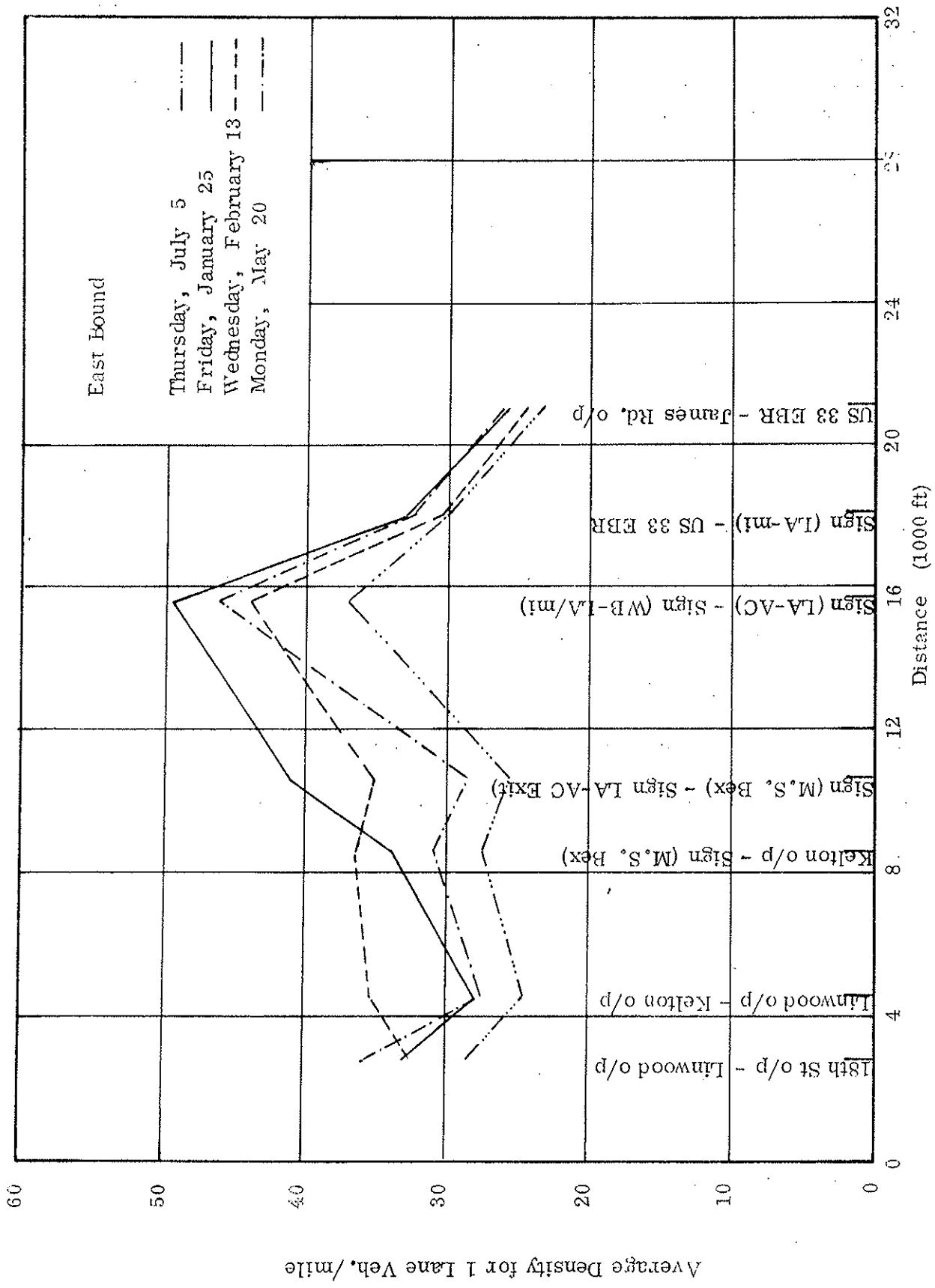


Fig. 7.1 : Traffic Density Versus Distance

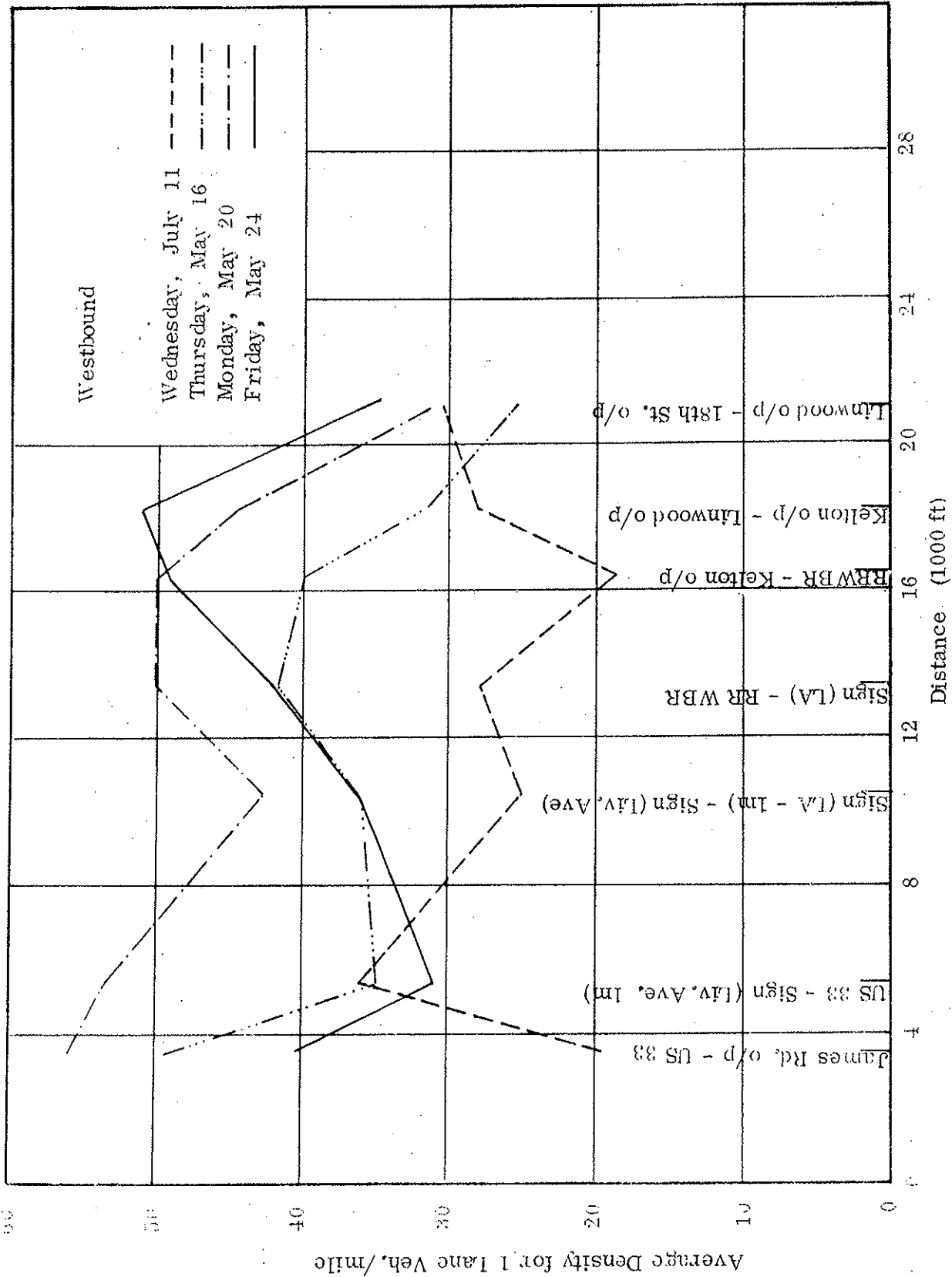


Fig. 7.2: Traffic Density Versus Distance.

The survey data for westbound traffic are shown in Fig. 7.2.

Peak hour traffic density

Density distributions for westbound traffic during the morning peak hours are given in Figures 7.3 to 7.9. On Wednesday July 11, a jam condition developed and the survey had to be broken off at 7.45 am. when peak densities reached the average level of 90 vehicles/mile/lane in sections 4 and 5.

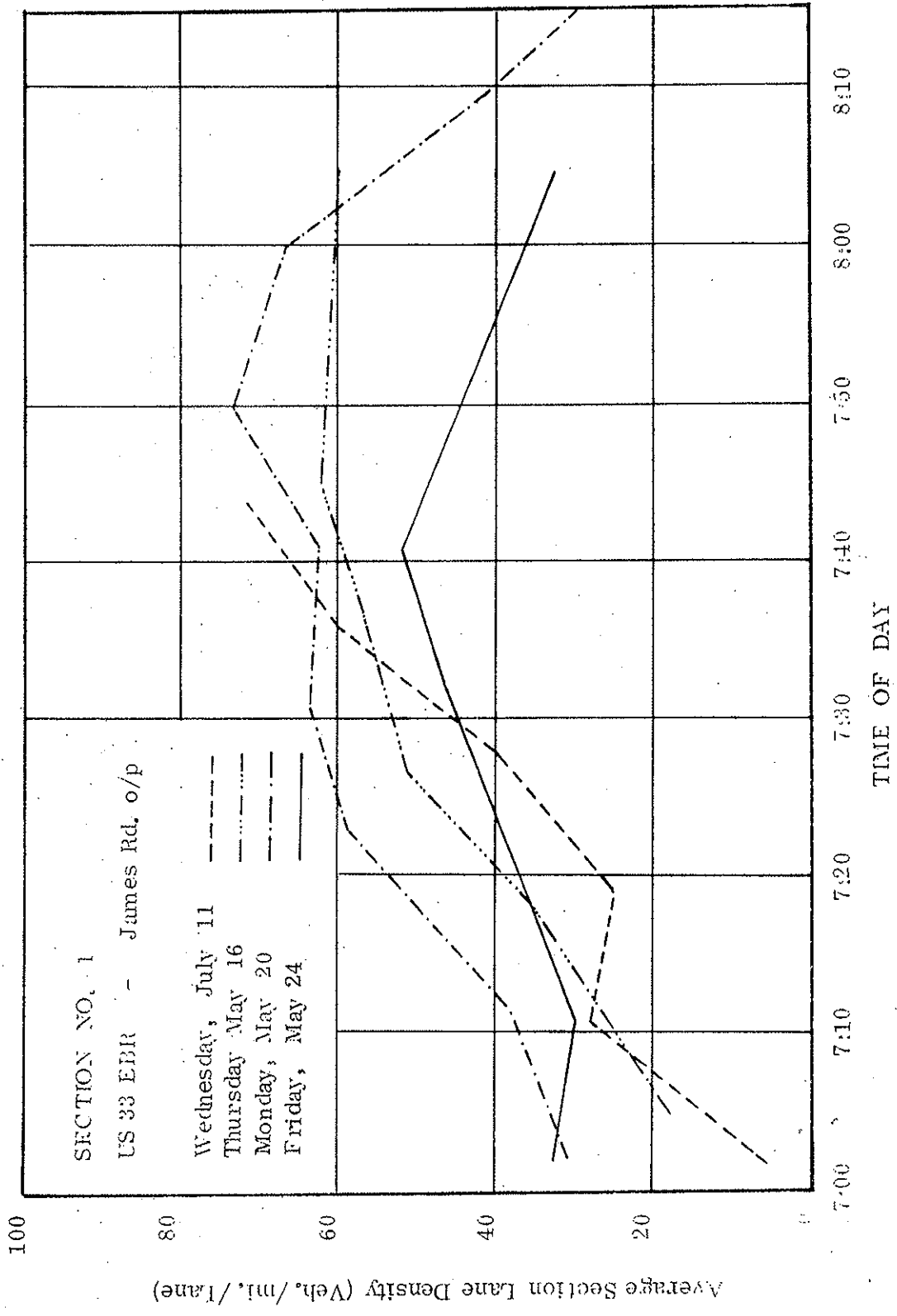


Fig. 7.3 : Traffic Density Versus Time of Day for US 33 EBR -- James Rd. Overpass Subsection.

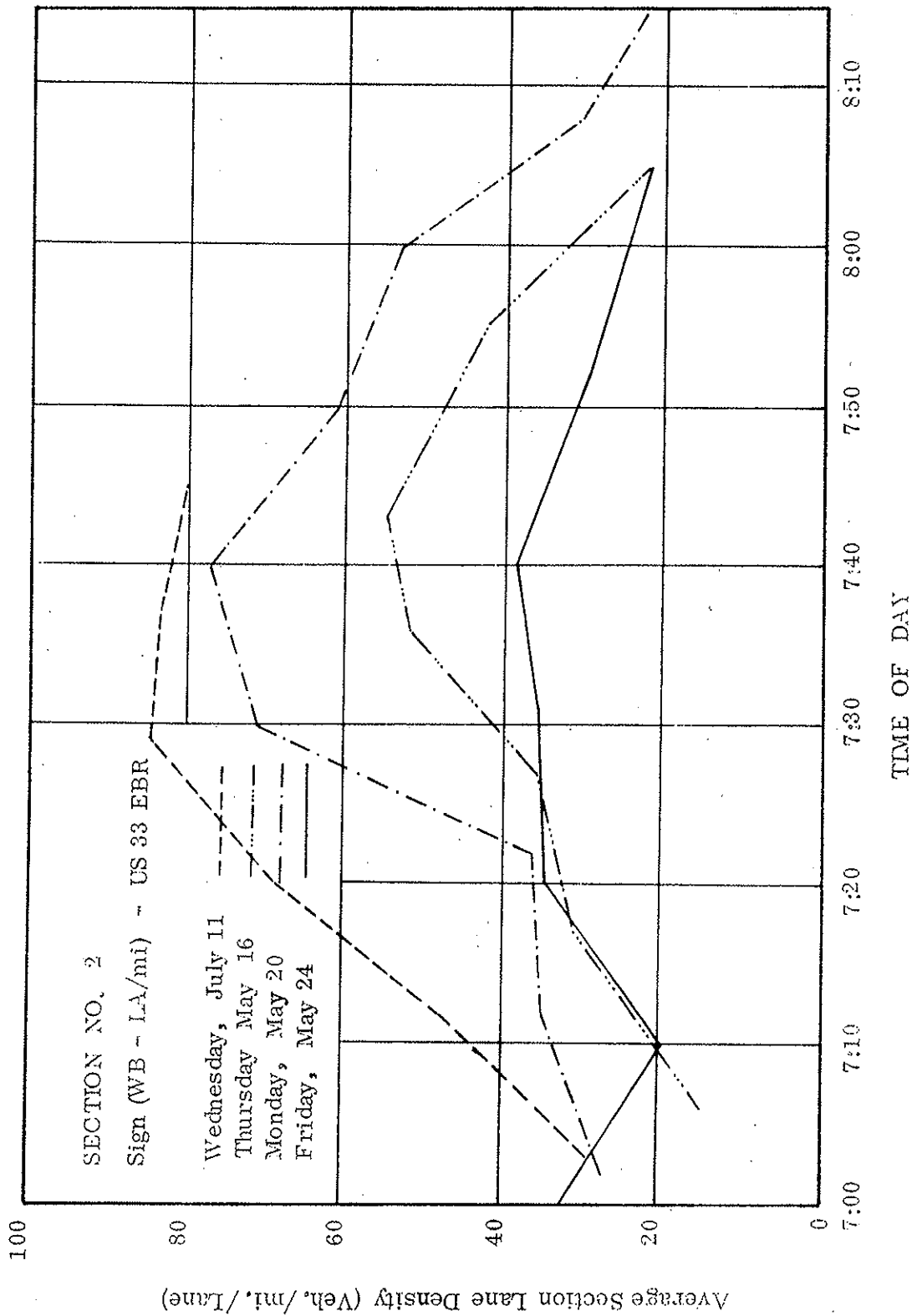


Fig. 7.4: Traffic Density Versus Time of Day for Sign (WB - LA/mi) - US 33 EBR Subsection.

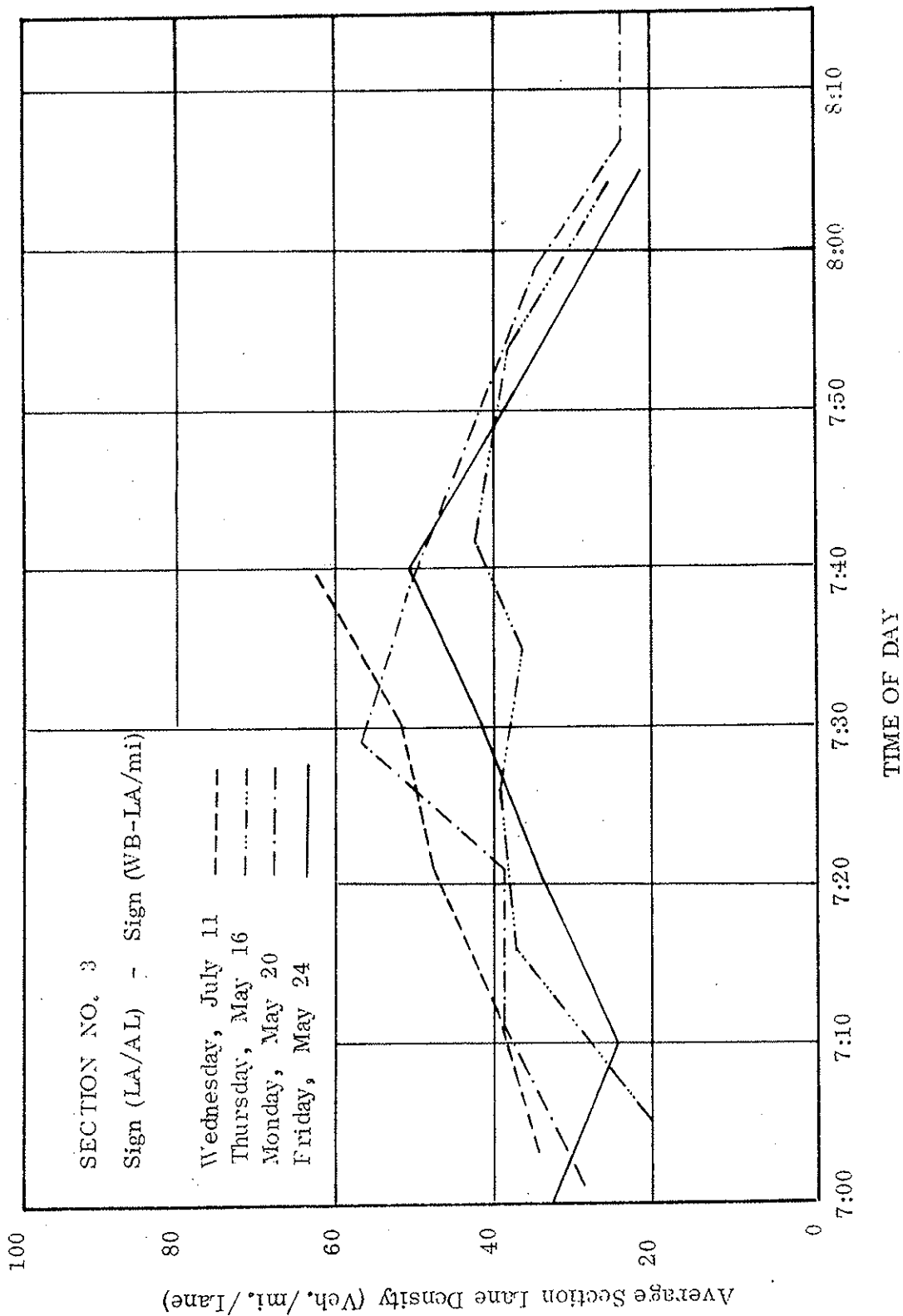


Fig. 7.5: Traffic Density Versus Time of Day for Sign (LA/AL) ---
 Sign (WB - LA/mi) Subsection.

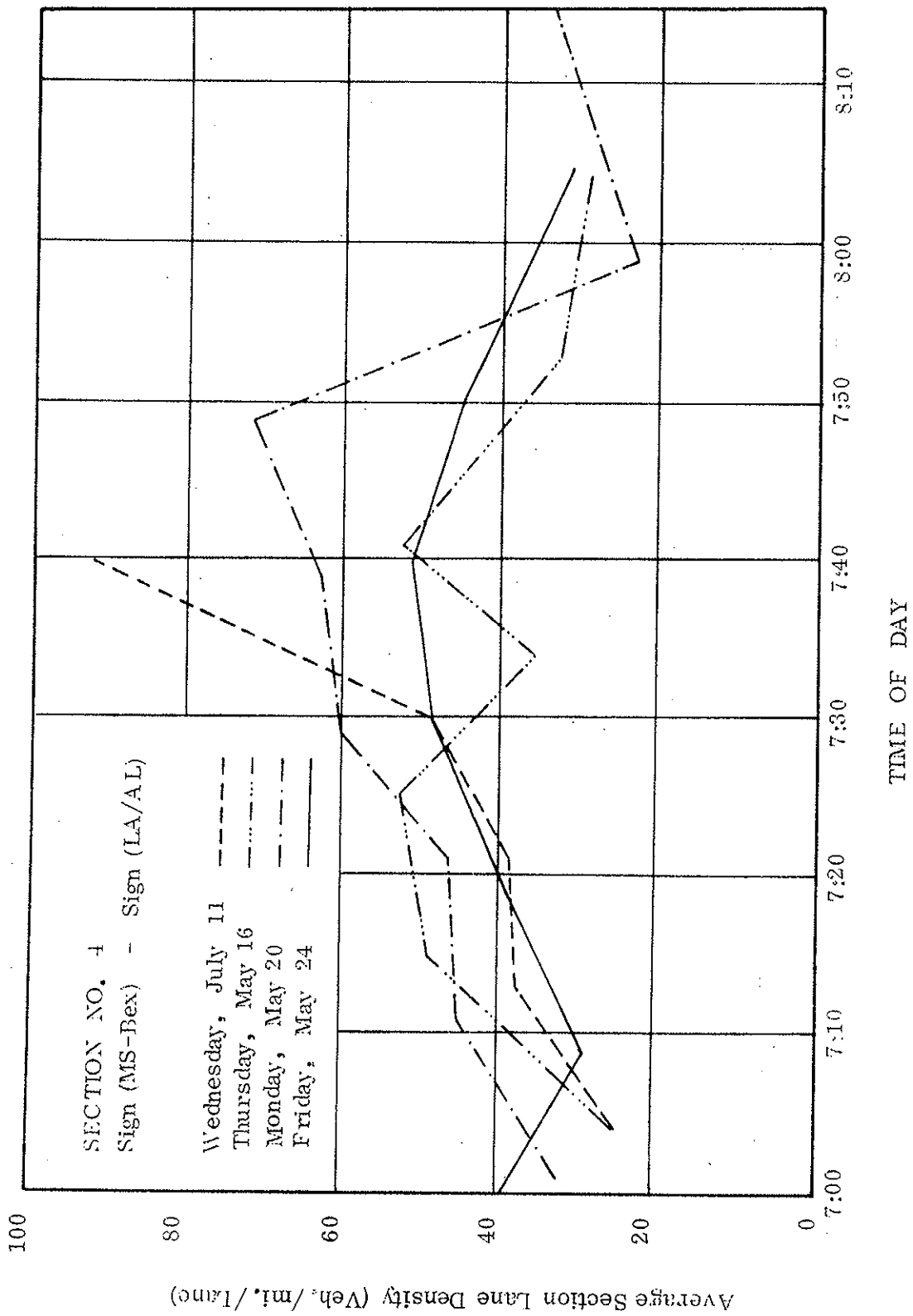


Fig. 7.6: Traffic Density Versus Time of Day for Sign (MS - Bex) --
 Sign (LA/AL) Subsection.

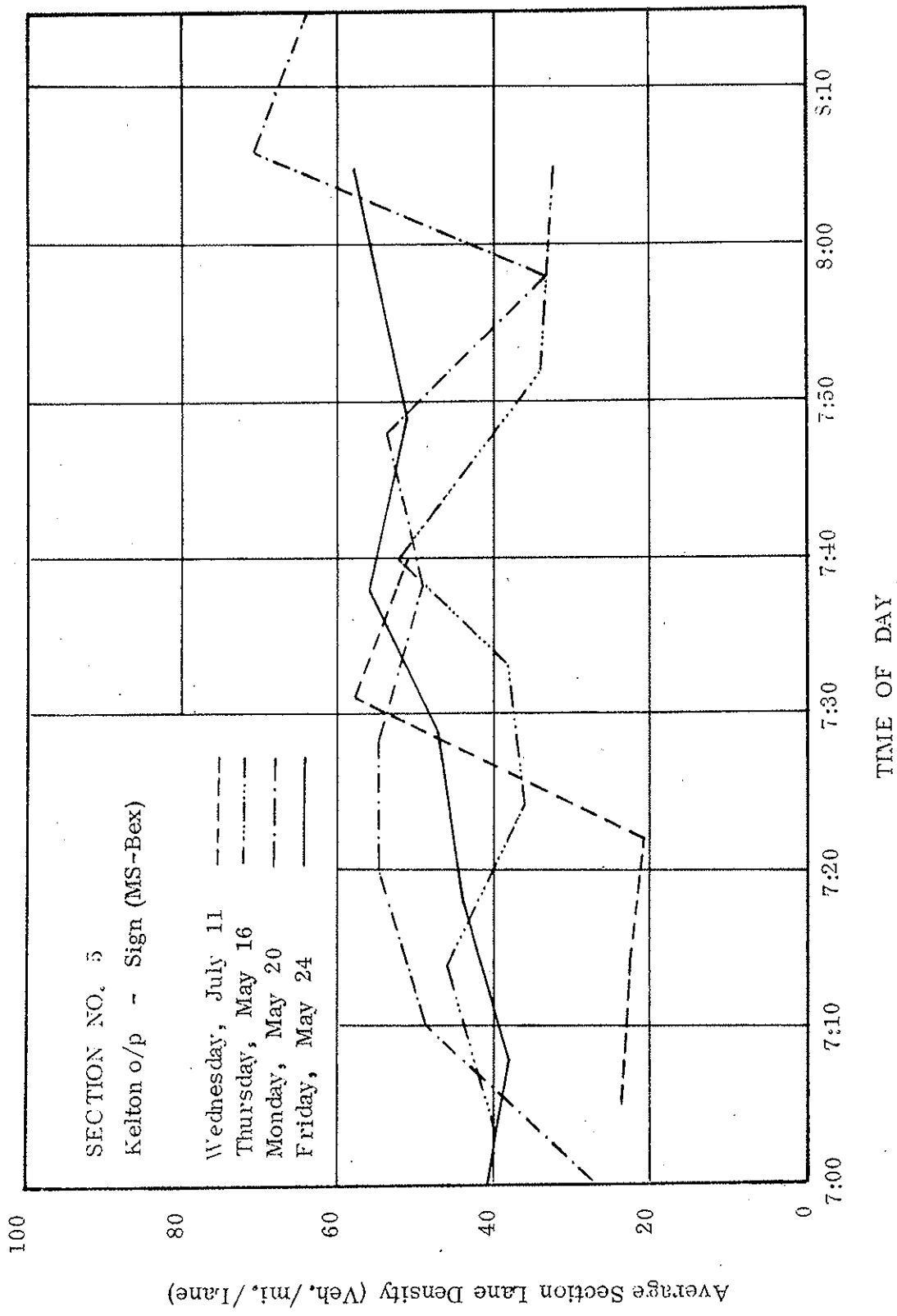


Fig. 7.7: Traffic Density Versus Time of Day for Sign (MS - Bex) Kelton Overpass Subsection.

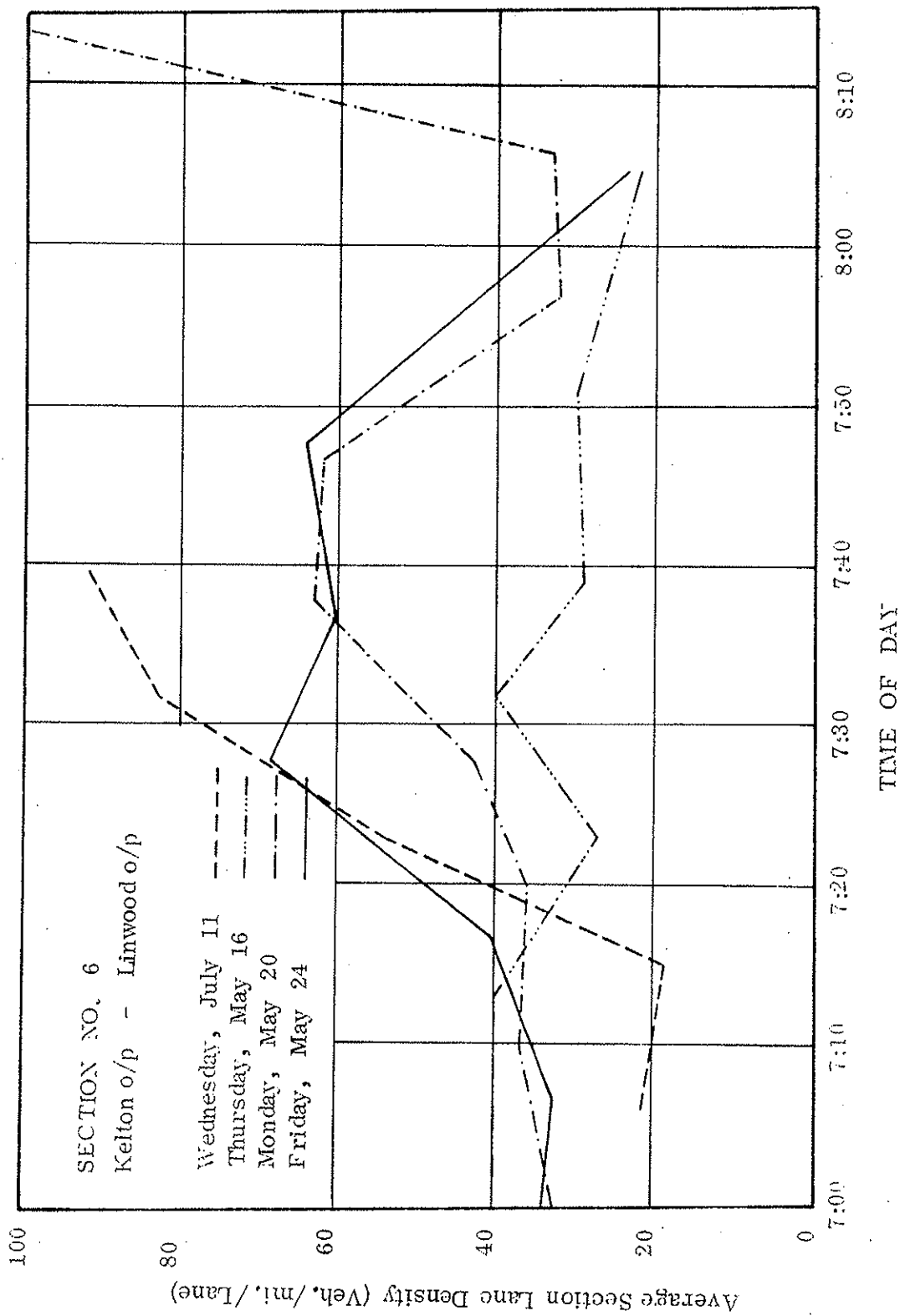


Fig. 7.8: Traffic Density Versus Time of Day for Kelton Overpass ---
Linwood Overpass Subsection.

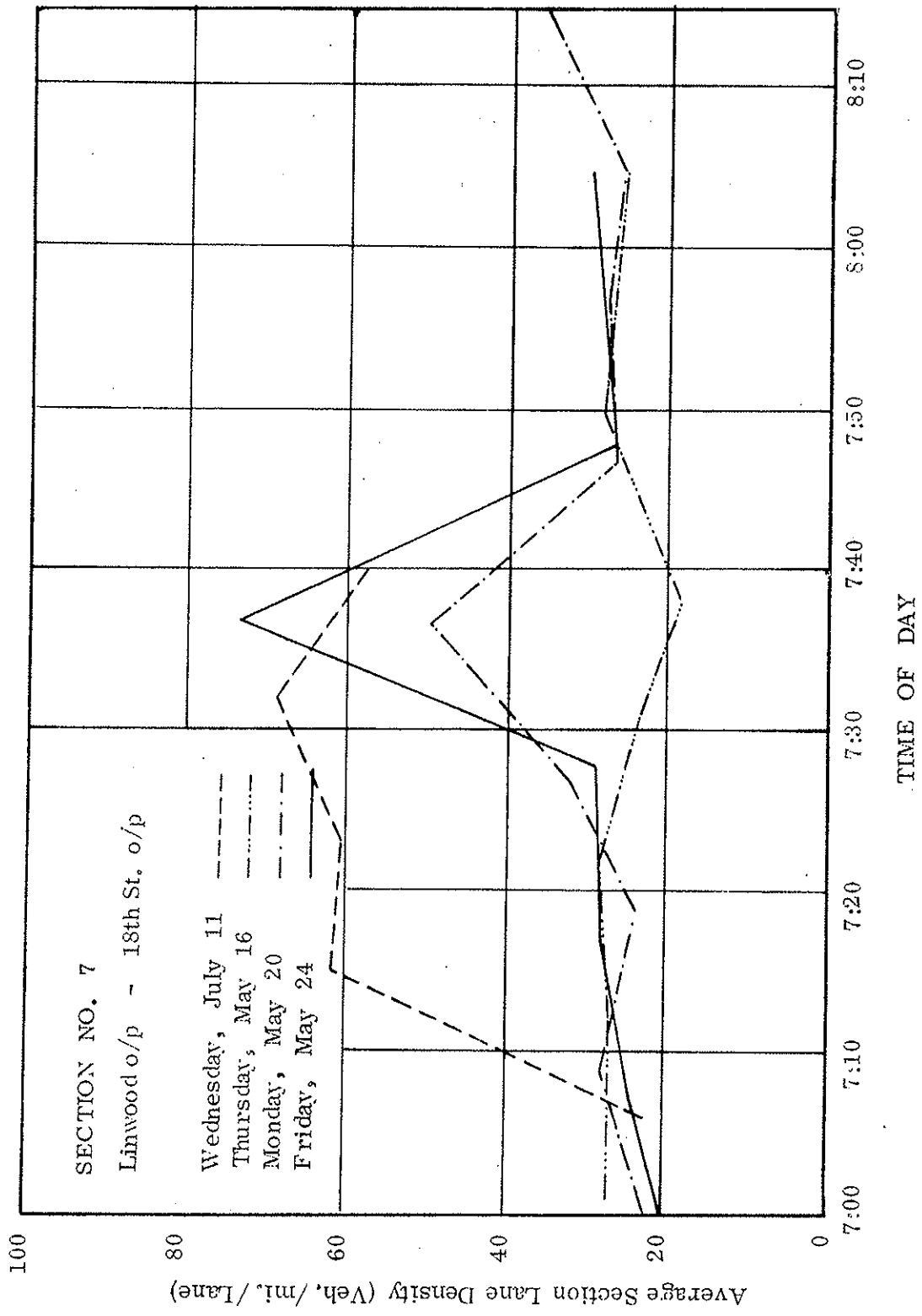


Fig. 7.9: Traffic Density Versus Time of Day for Linwood Overpass --
 18th St. Overpass Subsection.

Density distributions for eastbound traffic during the evening peak hour are given in Figures 7.10 to 7.16. It can be seen that traffic density during the evening peak hour is more uniformly distributed and peak densities are less than those recorded during the morning peak hour.

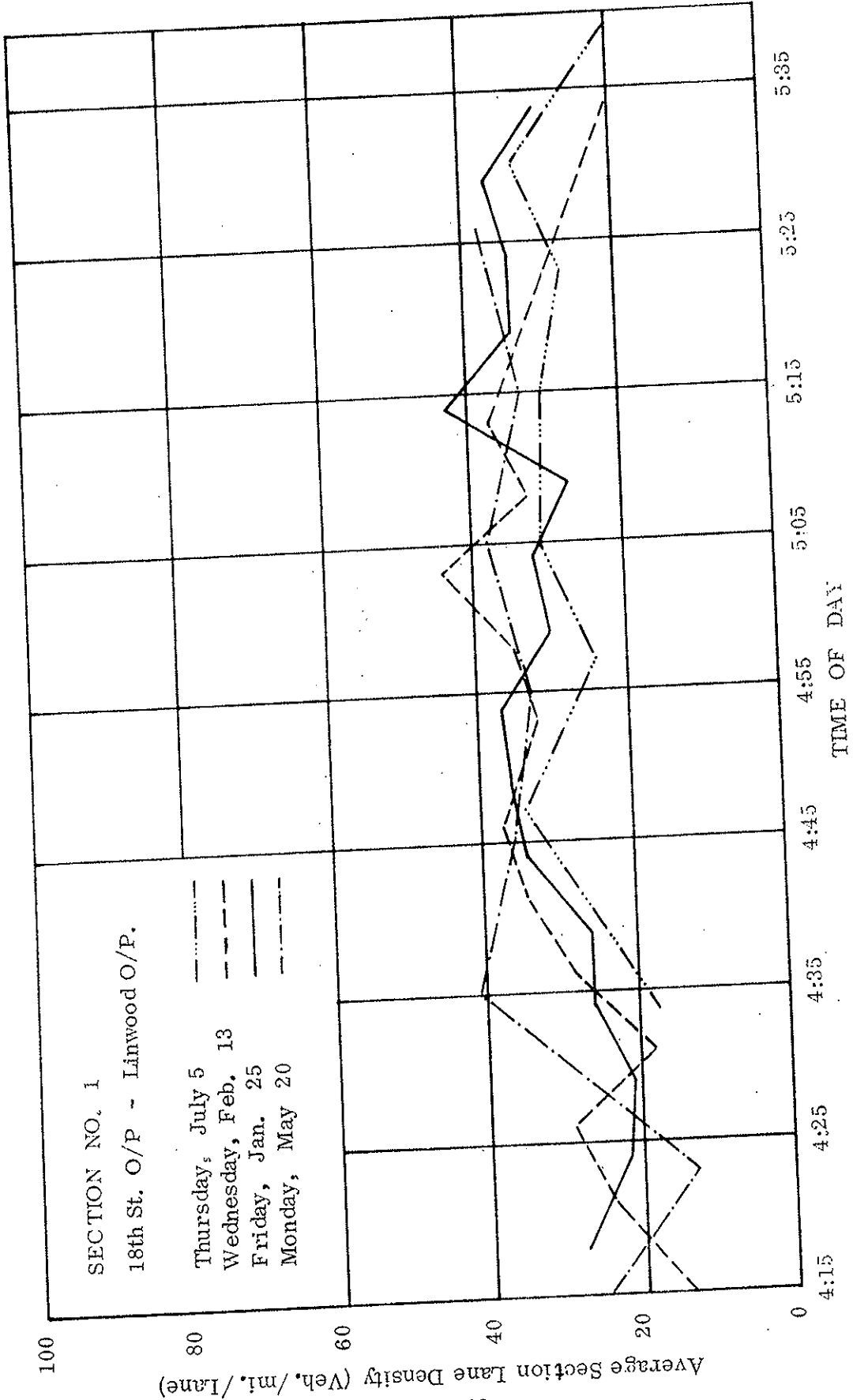


Fig. 7.10: Traffic Density Versus Time of Day for 18th St. Overpass --
Linwood Overpass Subsection.

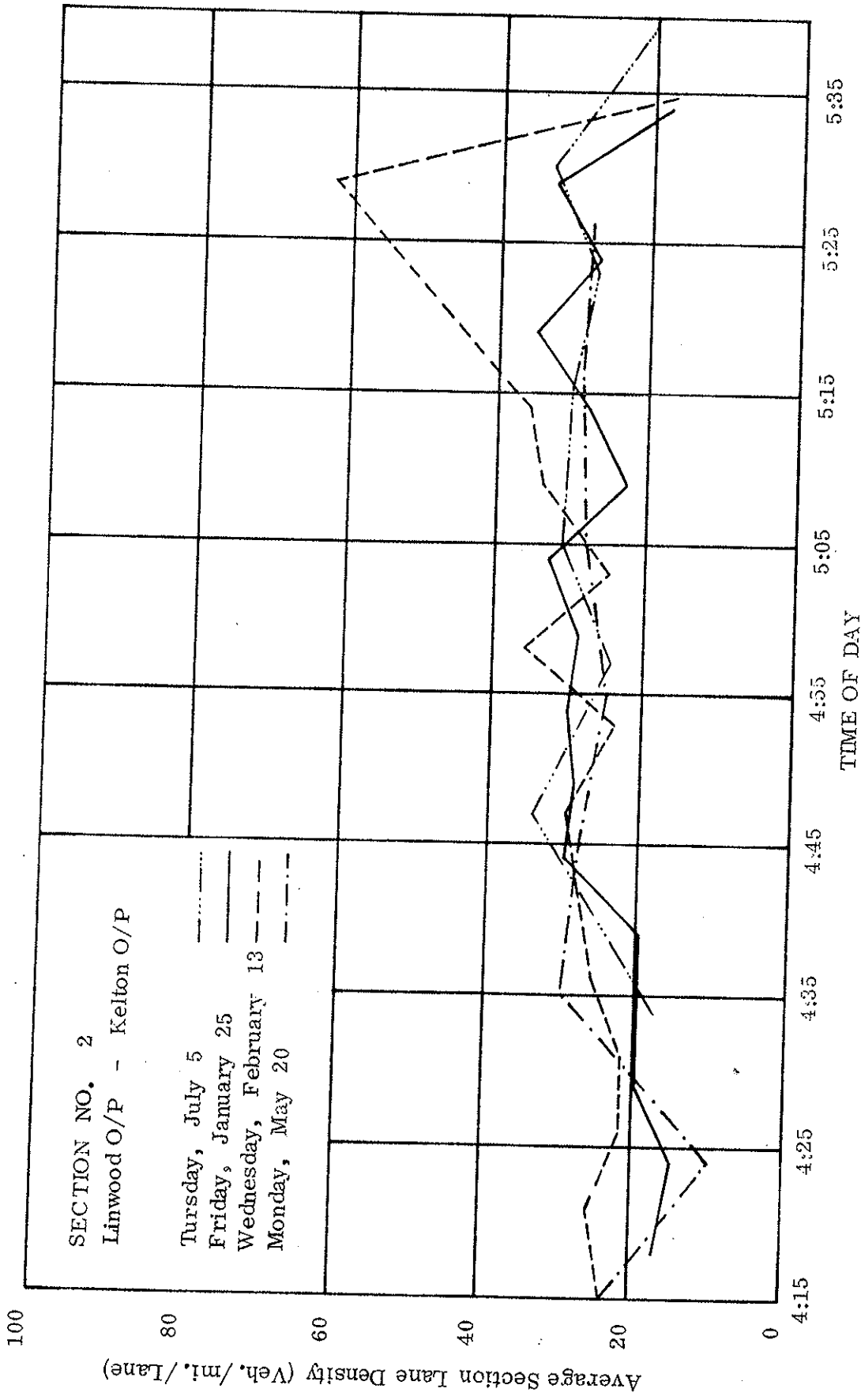


Fig. 7.11: Traffic Density Versus Time of Day for Linwood Overpass ---
Kelton Overpass Subsection.

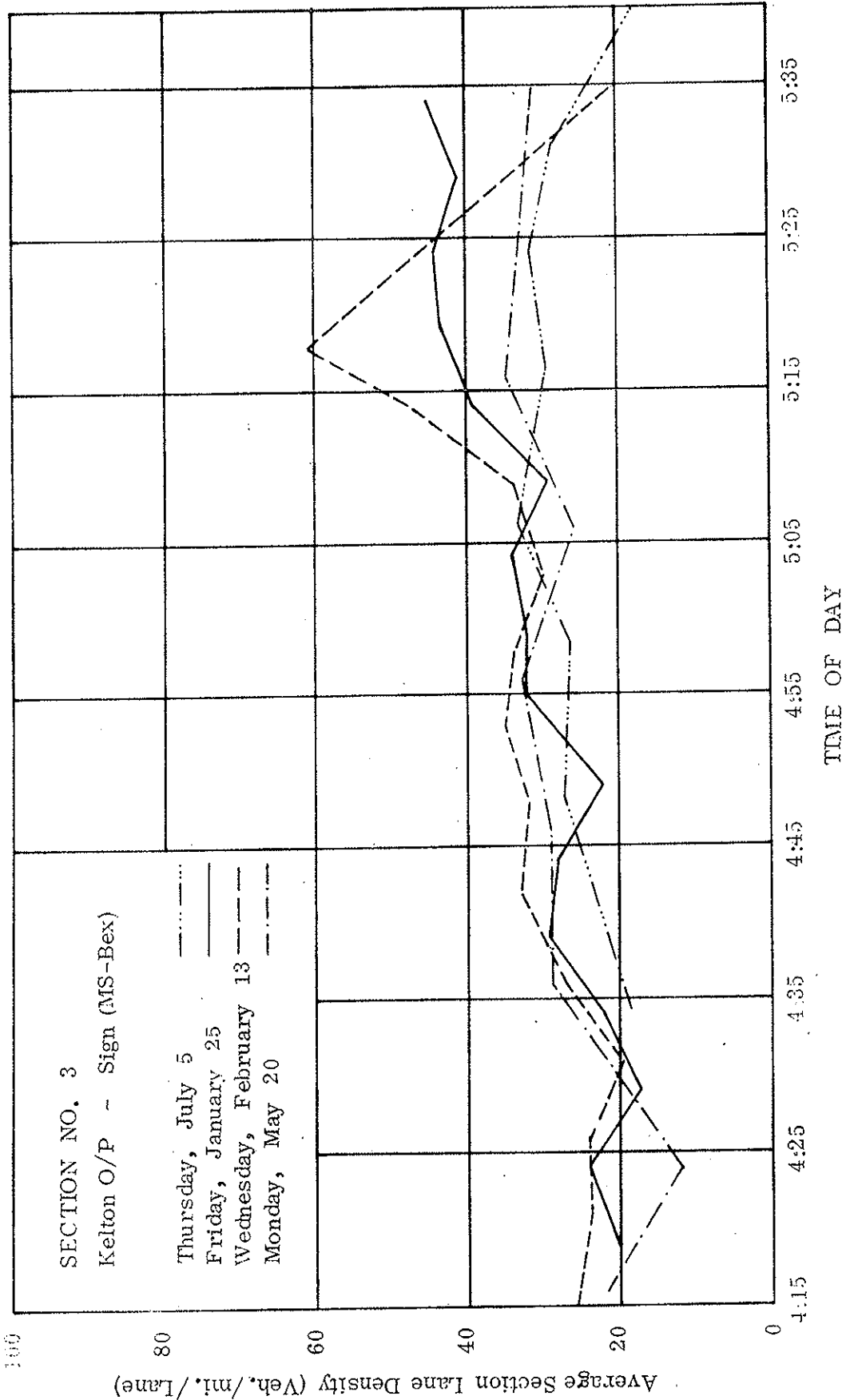


Fig. 7:12 Traffic Density Versus Time of Day for Kelton Overpass --
 Sign (MS - Bex) Subsection.

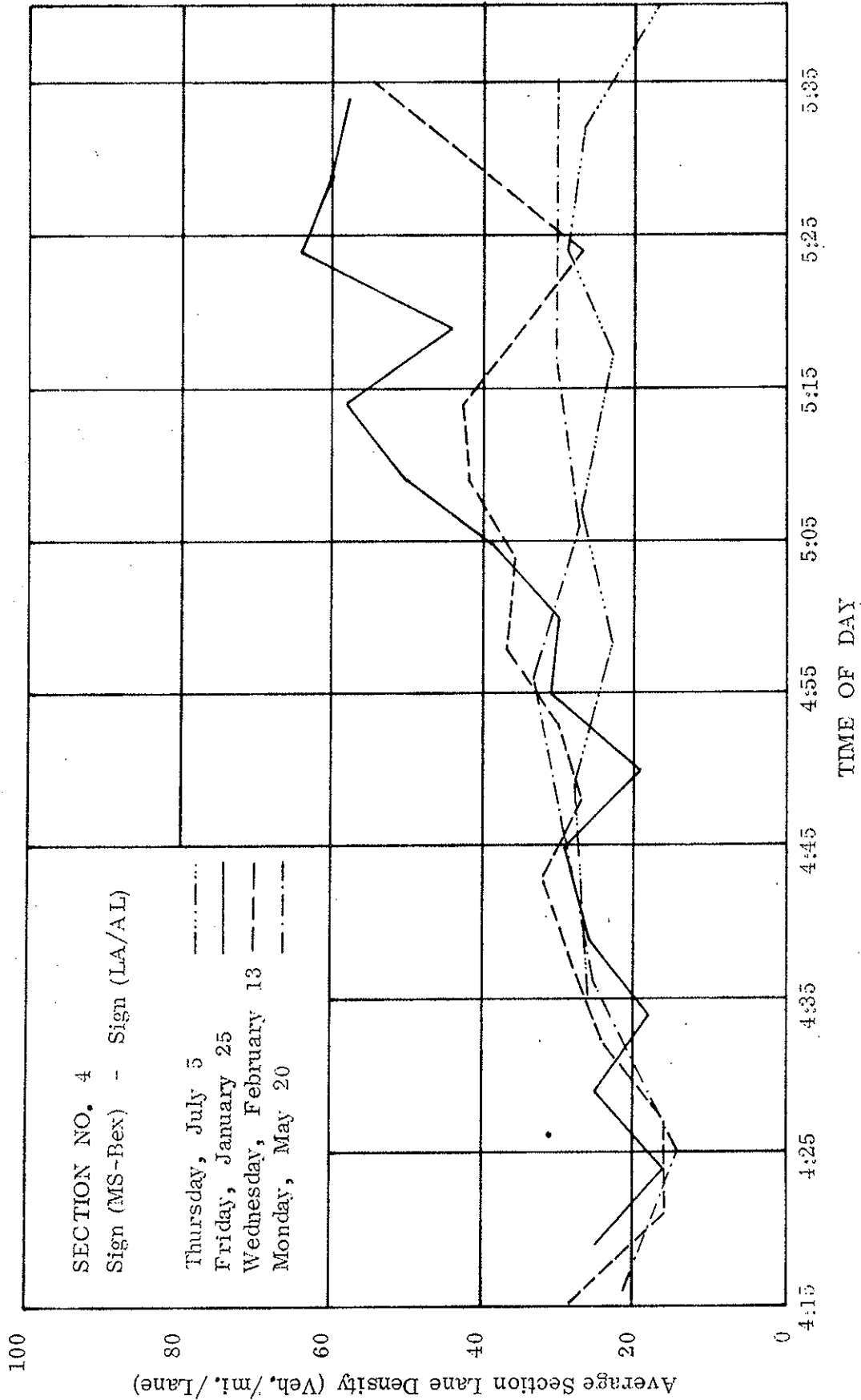


Fig. 7:13: Traffic Density Versus Time of Day for Sign (MS - Bex) --
Sign (LA/AL) Subsection.

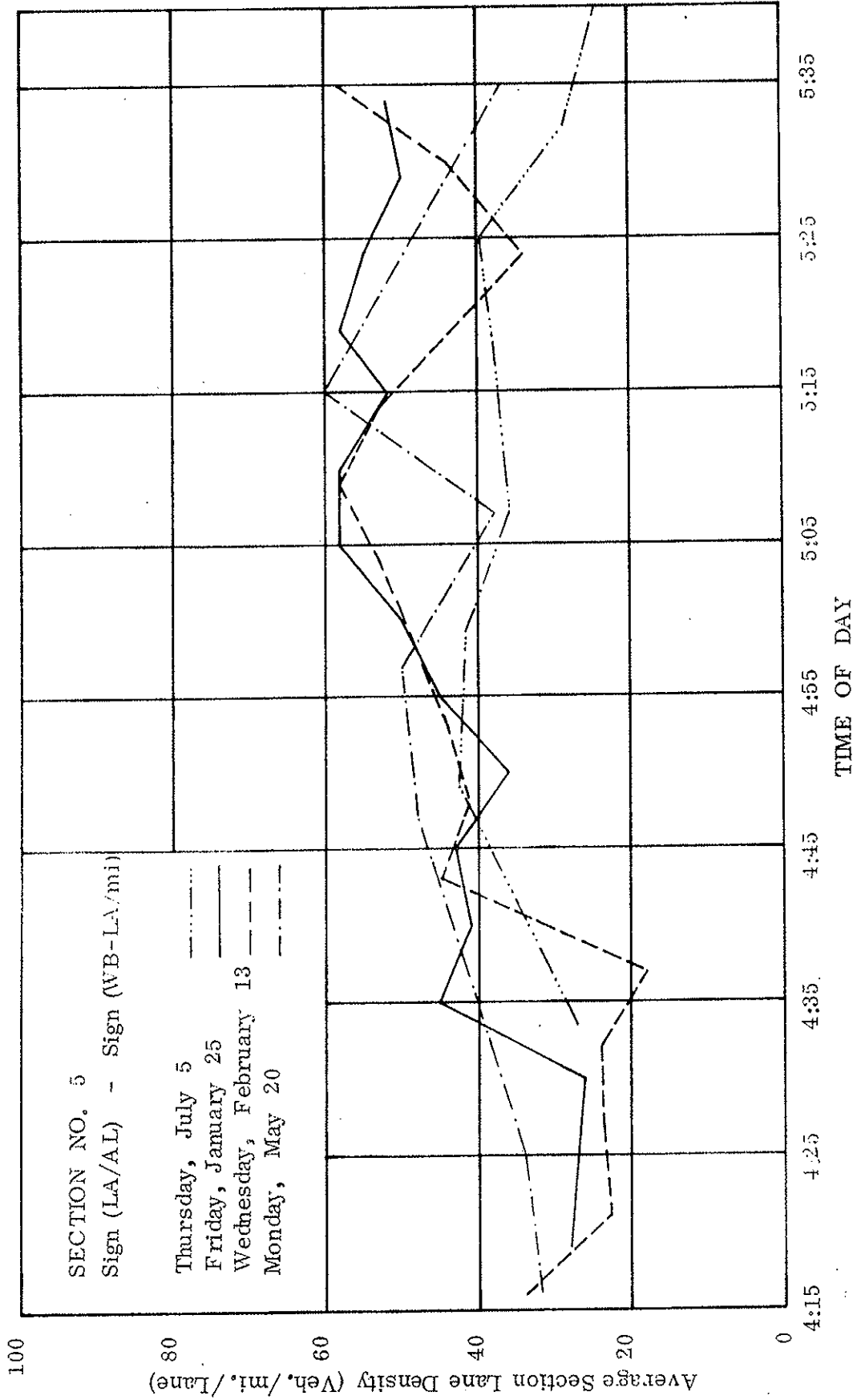


FIG. 7.14: Traffic Density Versus Time of Day for Sign (LA/AL) -- Sign (WB - LA/mi) Subsection.

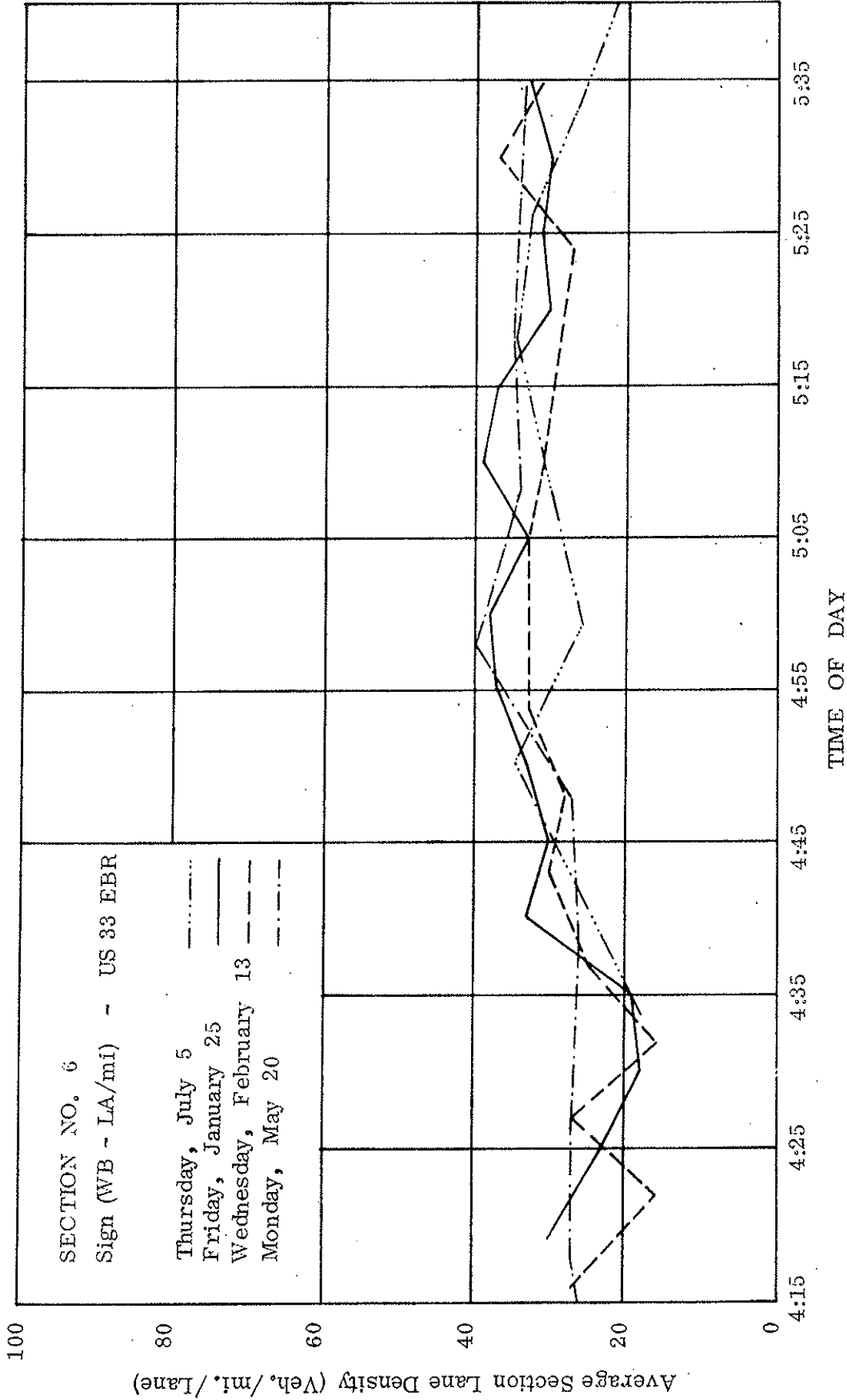


Fig. 715: Traffic Density Versus Time of Day for Sign (WB - LA/mi) --
US 33 EBR Subsection.

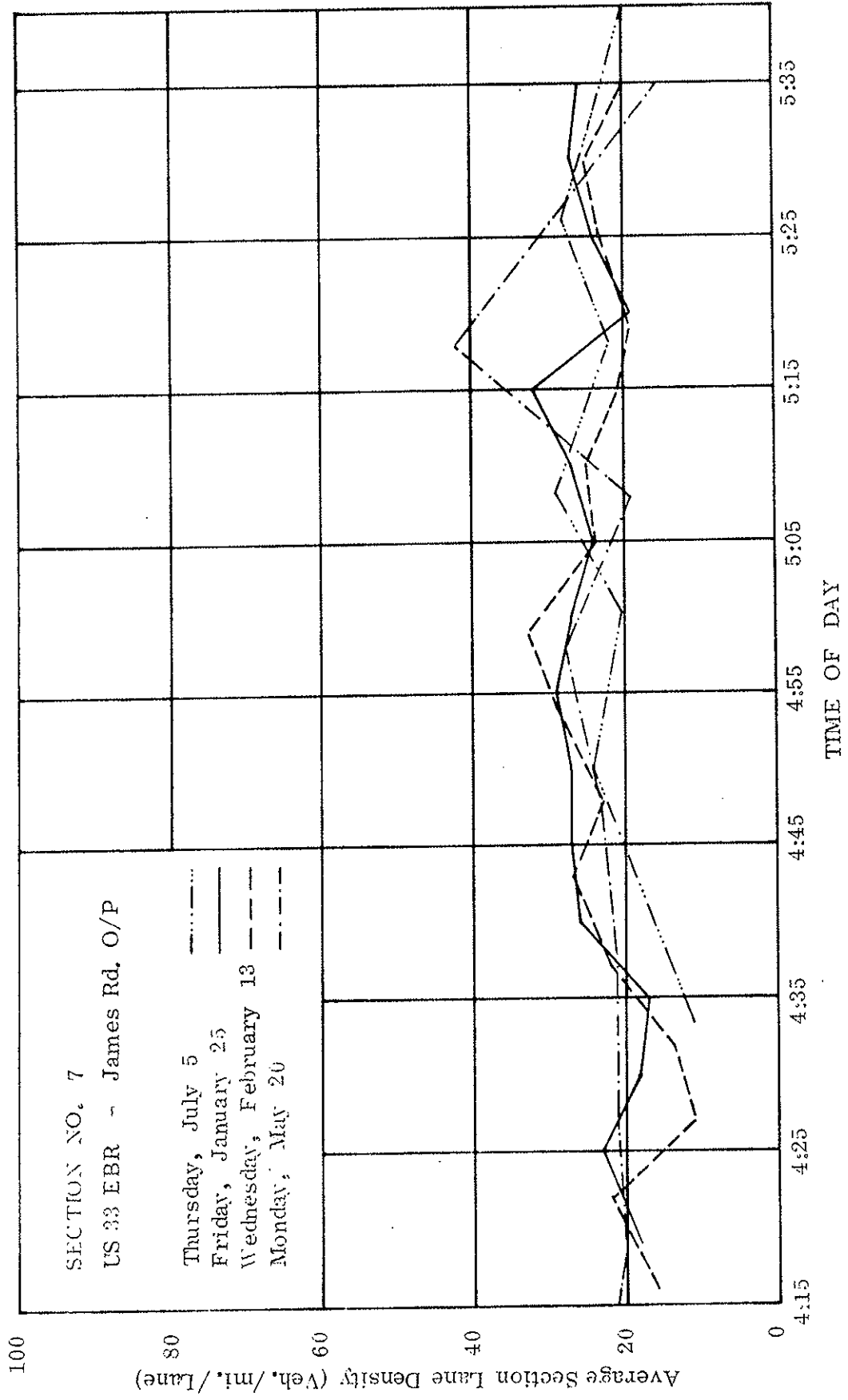


Fig. 7.16: Traffic Density Versus Time of Day for US 33 EBR -- James Rd. Overpass Subsection.

7.2 GROUND BASED DATA

Speed-Distance profiles for peak traffic hours were obtained for Mondays, Tuesdays, Wednesdays, Thursdays and Fridays from the 18th Street overpass to the James Road overpass. This length of I-70 was subdivided into 16 subsections as shown in Figs. 7.17 to 7.26. The subsections are:

For Eastbound (evening peak)

- 1) Ohio Ave. o/p
- 2) Champion Ave. o/p
- 3) Linwood Ave. o/p
- 4) Miller Ave. o/p
- 5) Kelton Ave. o/p
- 6) Sign (Livingston Ave. Merge Sign, Alum Creek Dr, Bexley st)
- 7) Sign (Merge Sign Bexley St)
- 8) Sign (Livingston Ave Exit)
- 9) Speed Limit Sign
- 10) Distance Sign to Zanesville and Wheeling
- 11) E. Bridge Alum Creek
- 12) E. Bridge US. 33
- 13) James Road o/p
- 14) Speed Limit Sign
- 15) Courtright Rd. o/p

16) Hamilton Rd. o/p

For Westbound (morning peak)

- 1) Hamilton Road On Ramp Nose
- 2) Courtright Rd. o/p
- 3) James Road o/p
- 4) 2nd. Merge Sign
- 5) W. Bridge Rail US. 33
- 6) Sign (Livingston Ave. 1 mile)
- 7) Speed Limit Sign
- 8) Sign (Kelton-Miller 1 mile)
- 9) Overhead Sign EB
- 10) W. Bridge Rail (RR Nelson)
- 11) Kelton-Miller Sign
- 12) Kelton Ave. o/p
- 13) Miller Ave. o/p
- 14) Linwood Ave. o/p
- 15) Champion Ave. o/p
- 16) Ohio Ave. o/p

Comparing the morning peak data with the evening peak data it becomes quite obvious that the morning peak presents the more serious problem and a traffic control system appears to be urgently needed for the westbound traffic. The most critical sections are between section 3 (James Road o/p)

Explanation of velocity distance profiles

An average of 9 runs was made for each section and was timed independently.

These runs are denoted as follows in Figs. 7.17 to Figs. 7.26.

Run No.	Symbol
1	-----
2	-----
3	-----
4	-----
5	-----
6	-----
7	-----
8	-----
9	-----
Average of all runs	-----

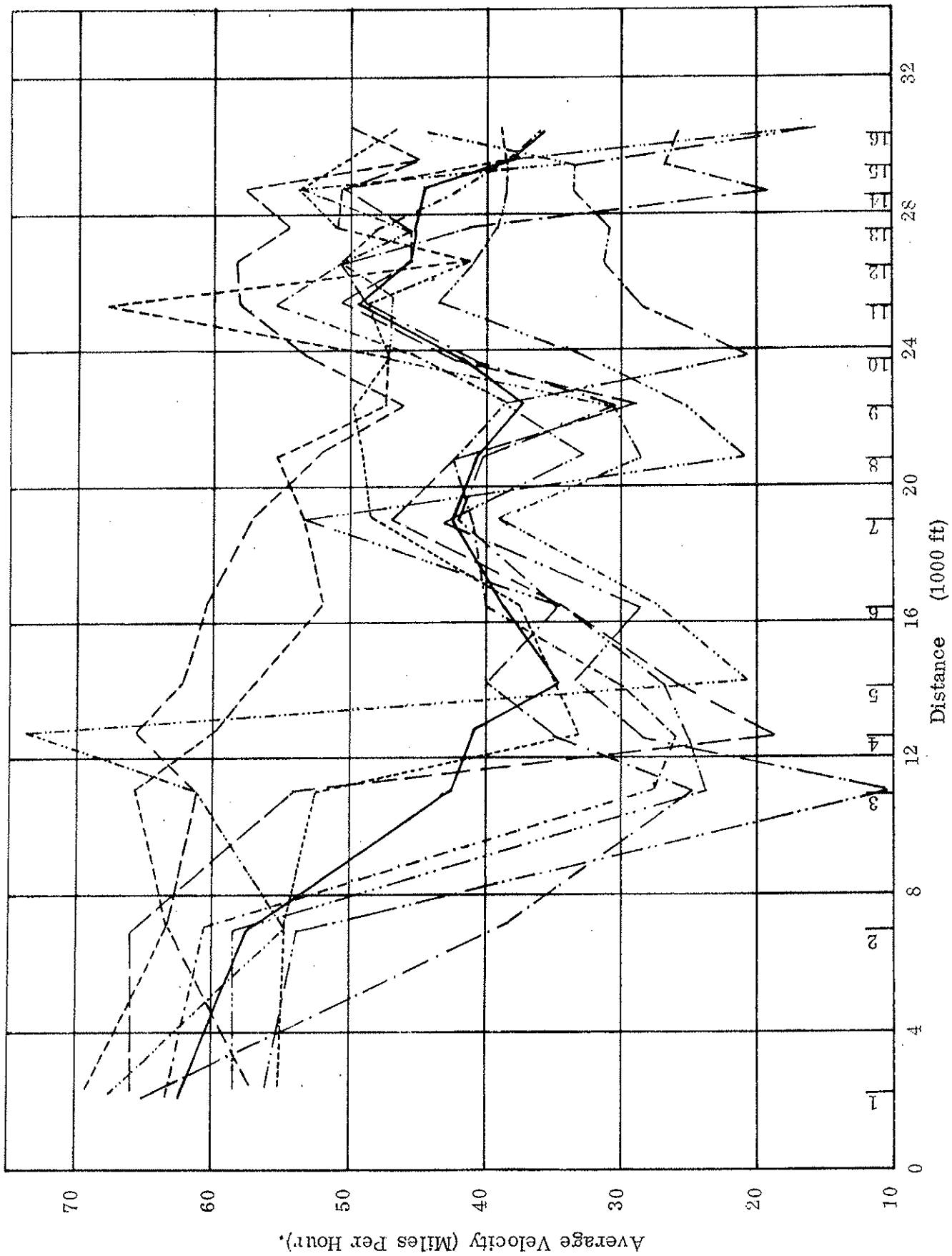


Fig. 7.17: Velocity-Distance Profiles for Data of Monday, May 7, 1973.

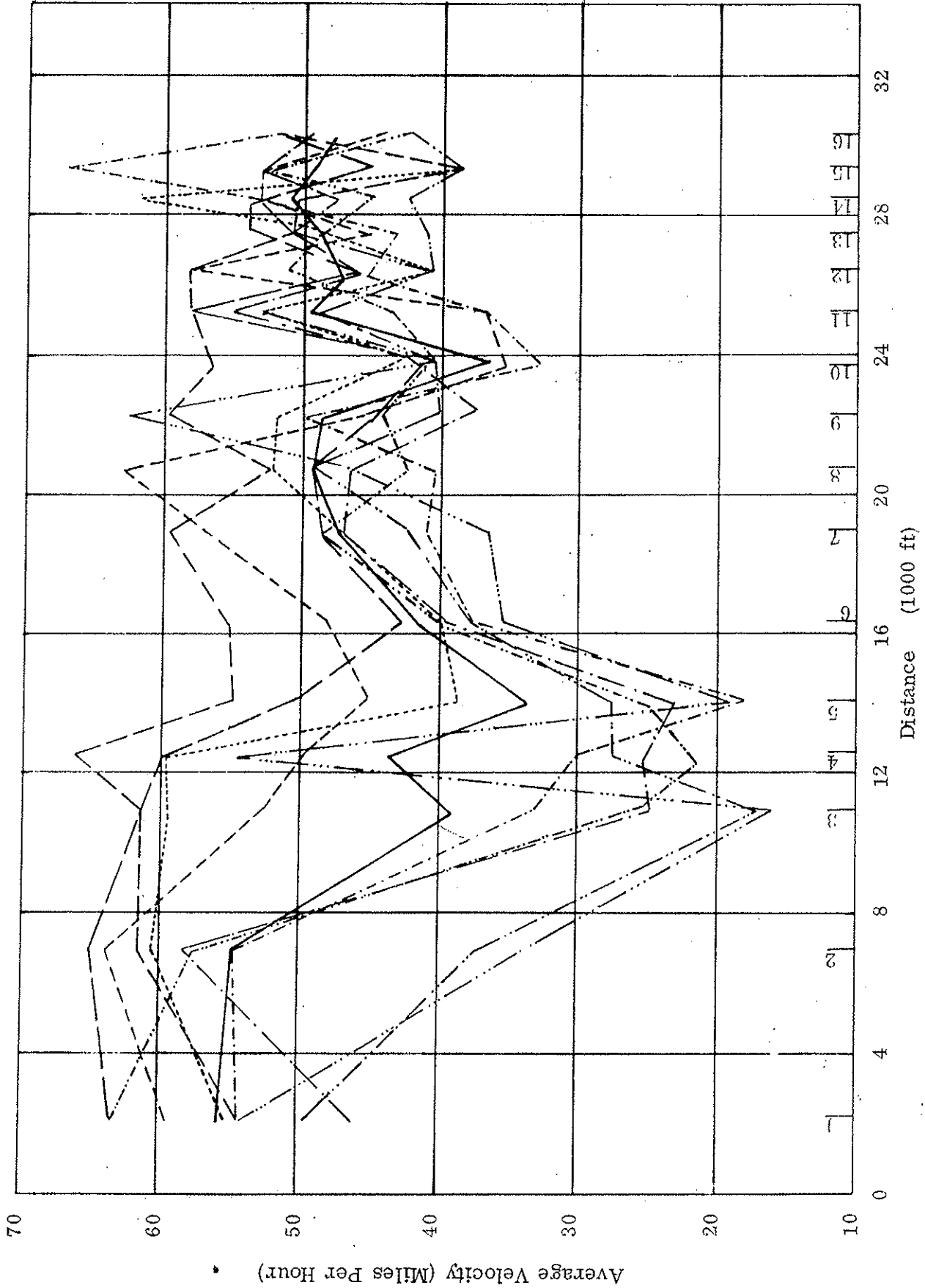


Fig. 7.18: Velocity-Distance Profiles for Data of Tuesday, April 24, 1973.

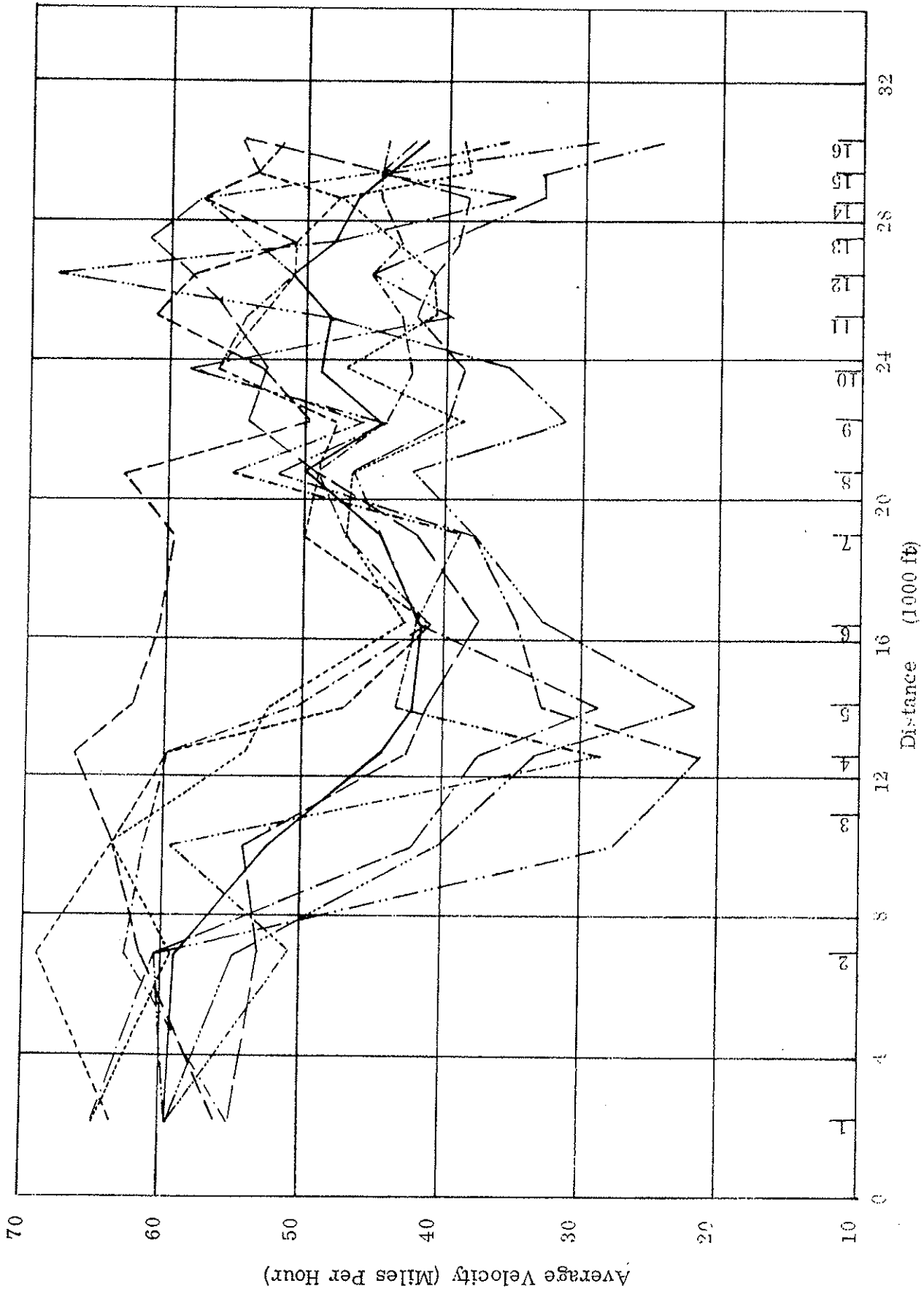


FIG. 7.19: Velocity - Distance Profiles for Data of Wednesday, May 9, 1973.

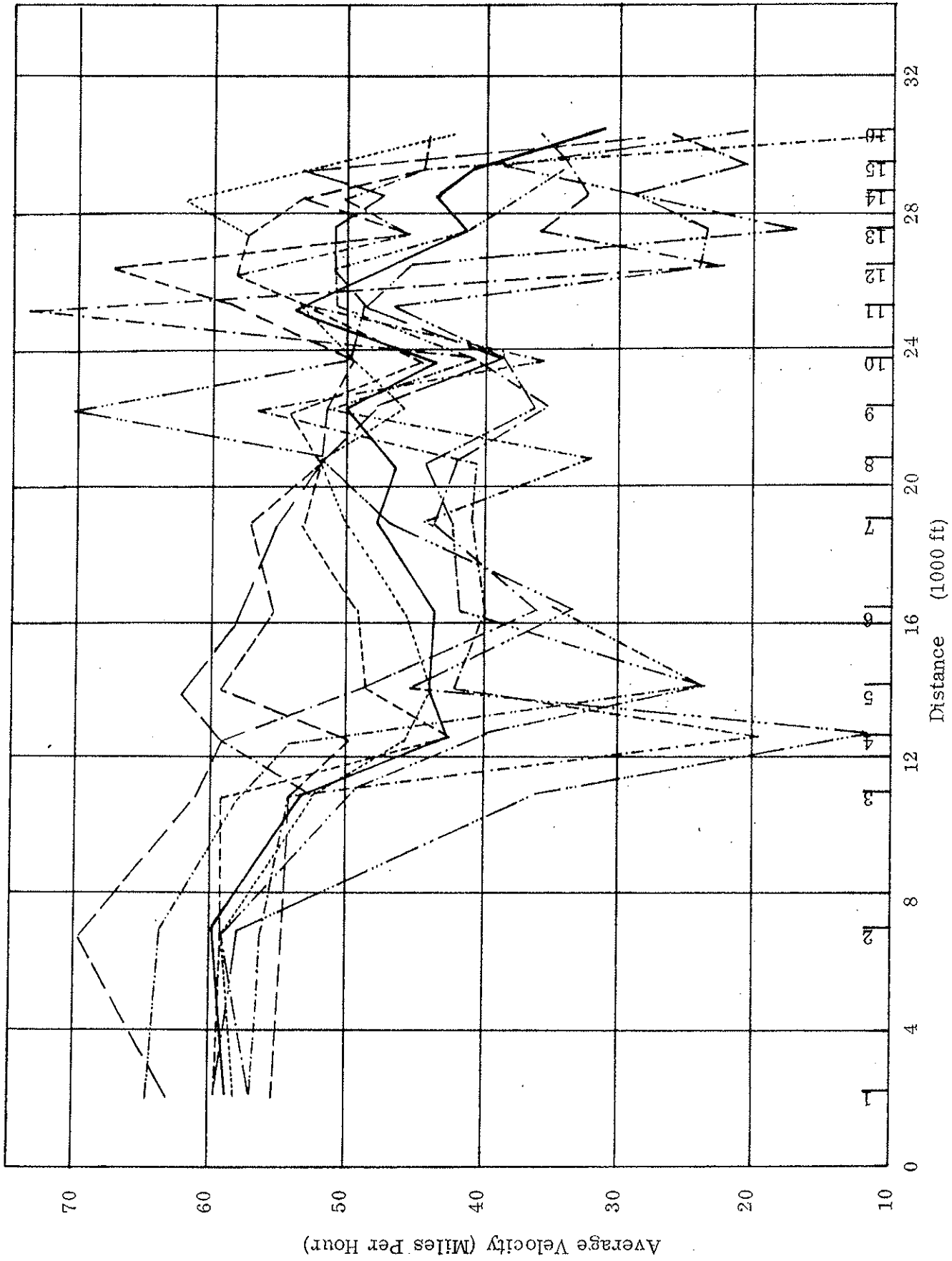


Fig. 7.20: Velocity-Distance Profiles for Data of Thursday, April 26, 1973.

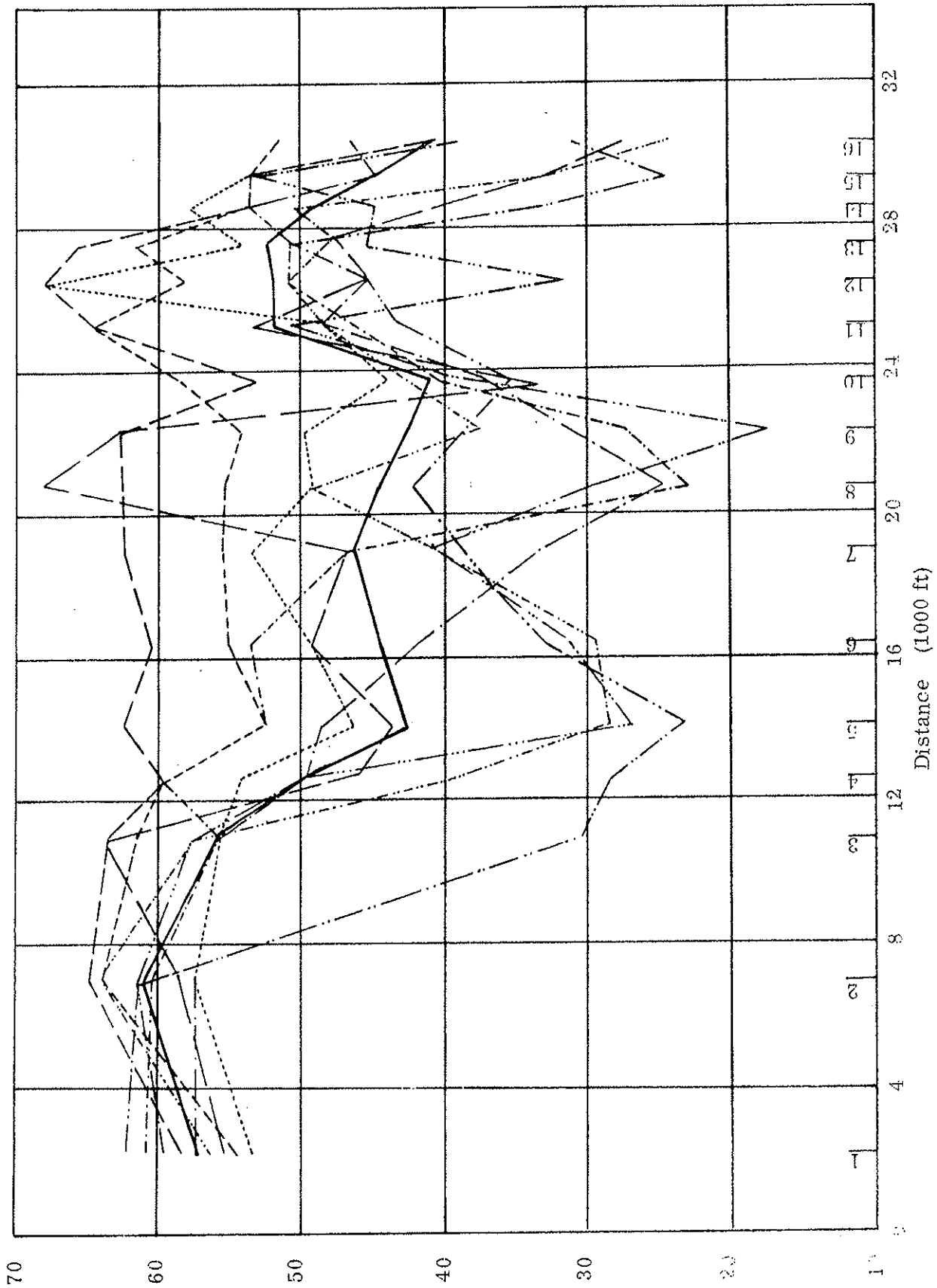


Fig. 7.21: Velocity-Distance Profiles for Data of Friday, May 4, 1973.

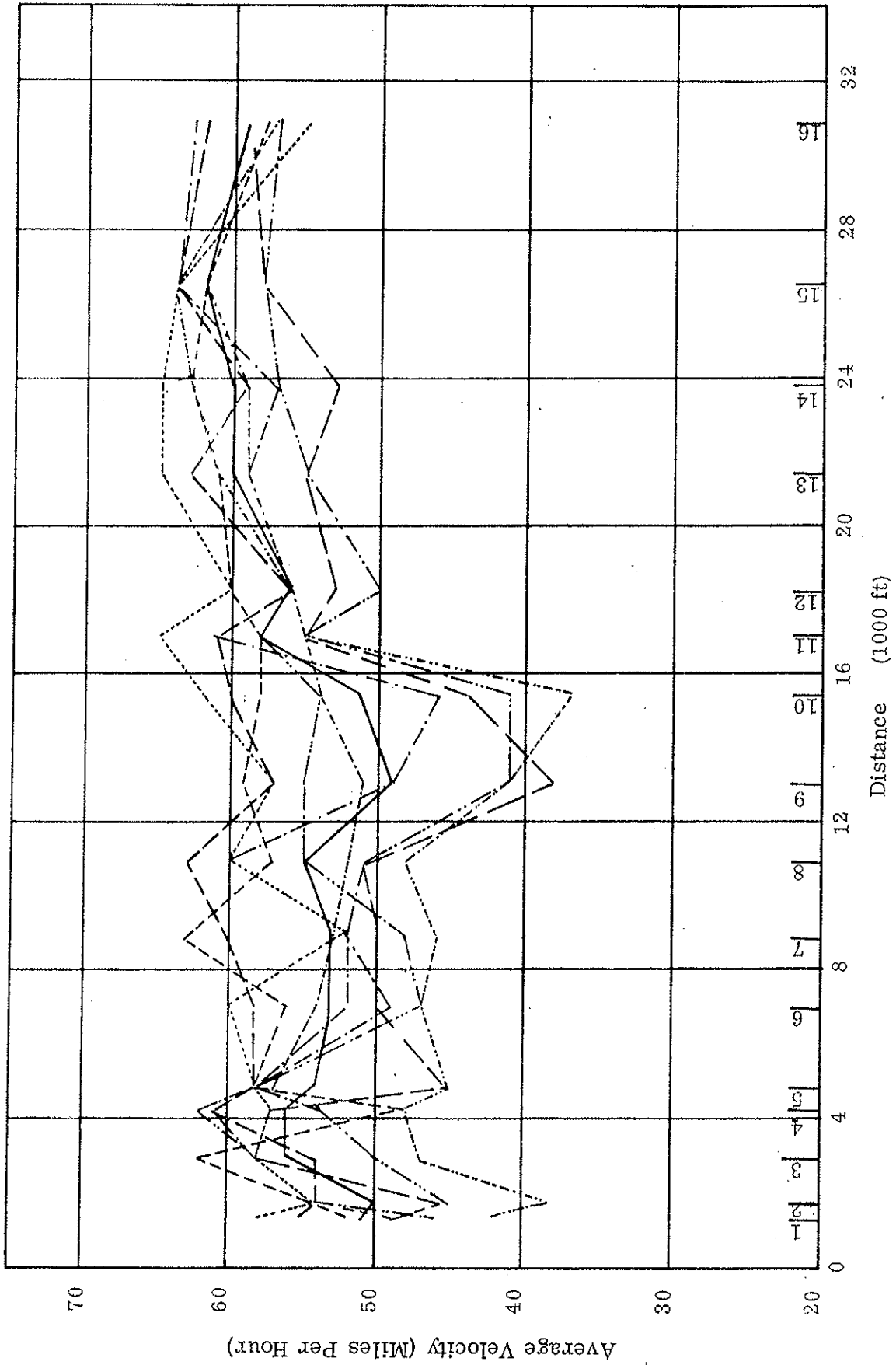


Fig. 7.22: Velocity-Distance Profiles for Data of Monday, June 18, 1973.

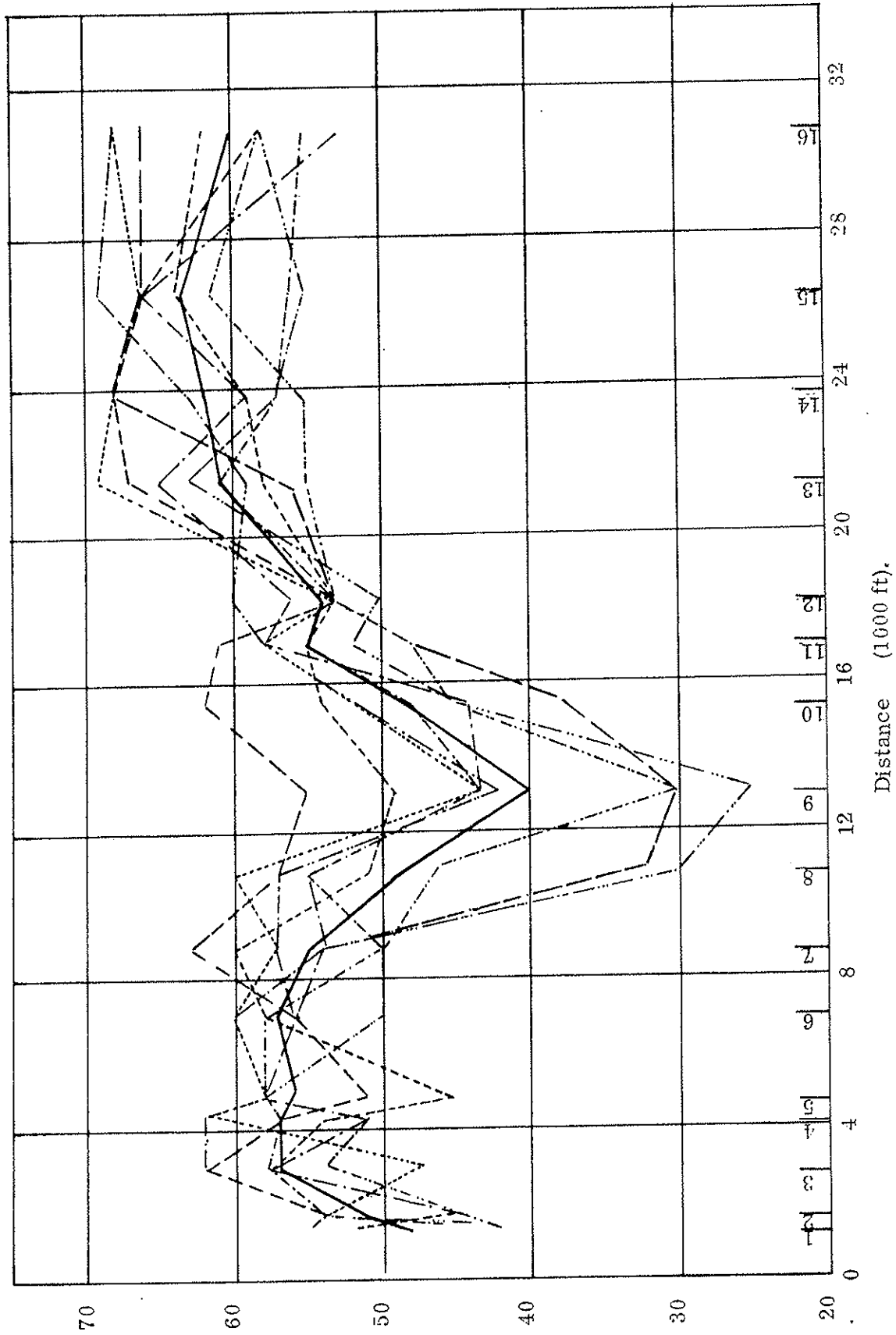


Fig. 7. 23: Velocity - Distance Profiles for Data of Tuesday, May 15, 1973.

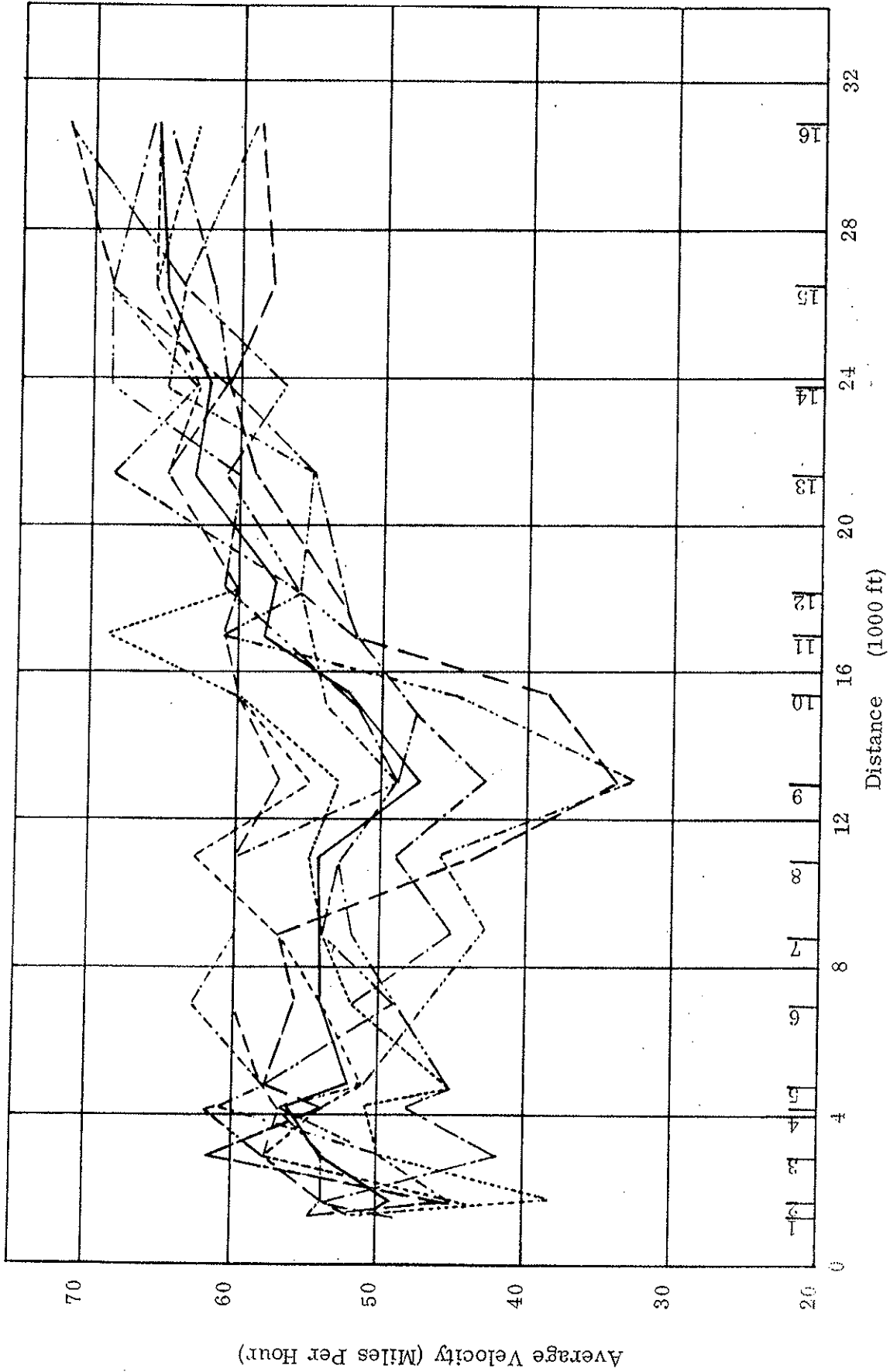


Fig. 7. 24: Velocity-Distance Profiles for Data of Wednesday, January 24, 1974.

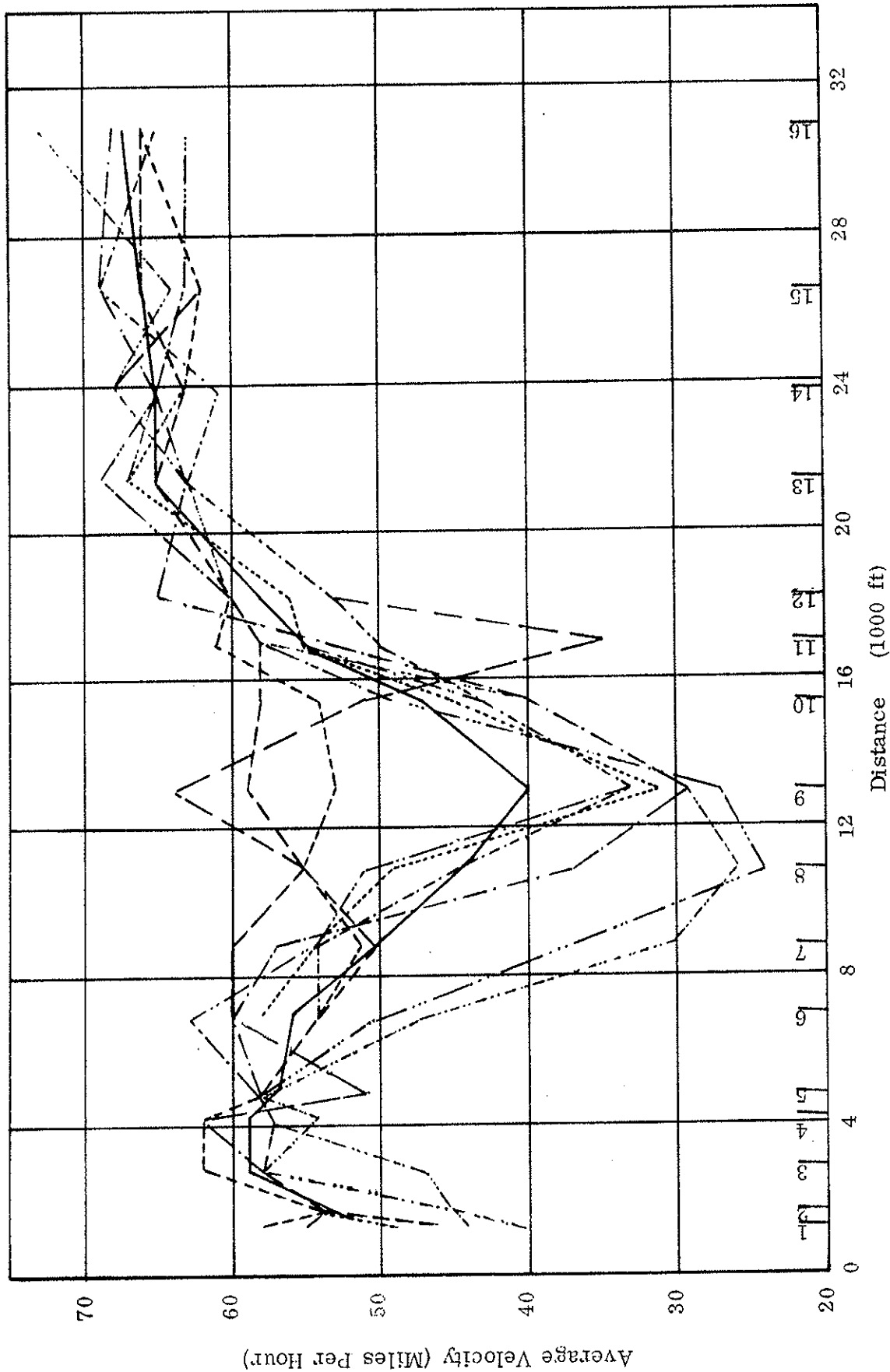


Fig. 7.25: Velocity-Distance Profiles for Data of Thursday, April 5, 1973.

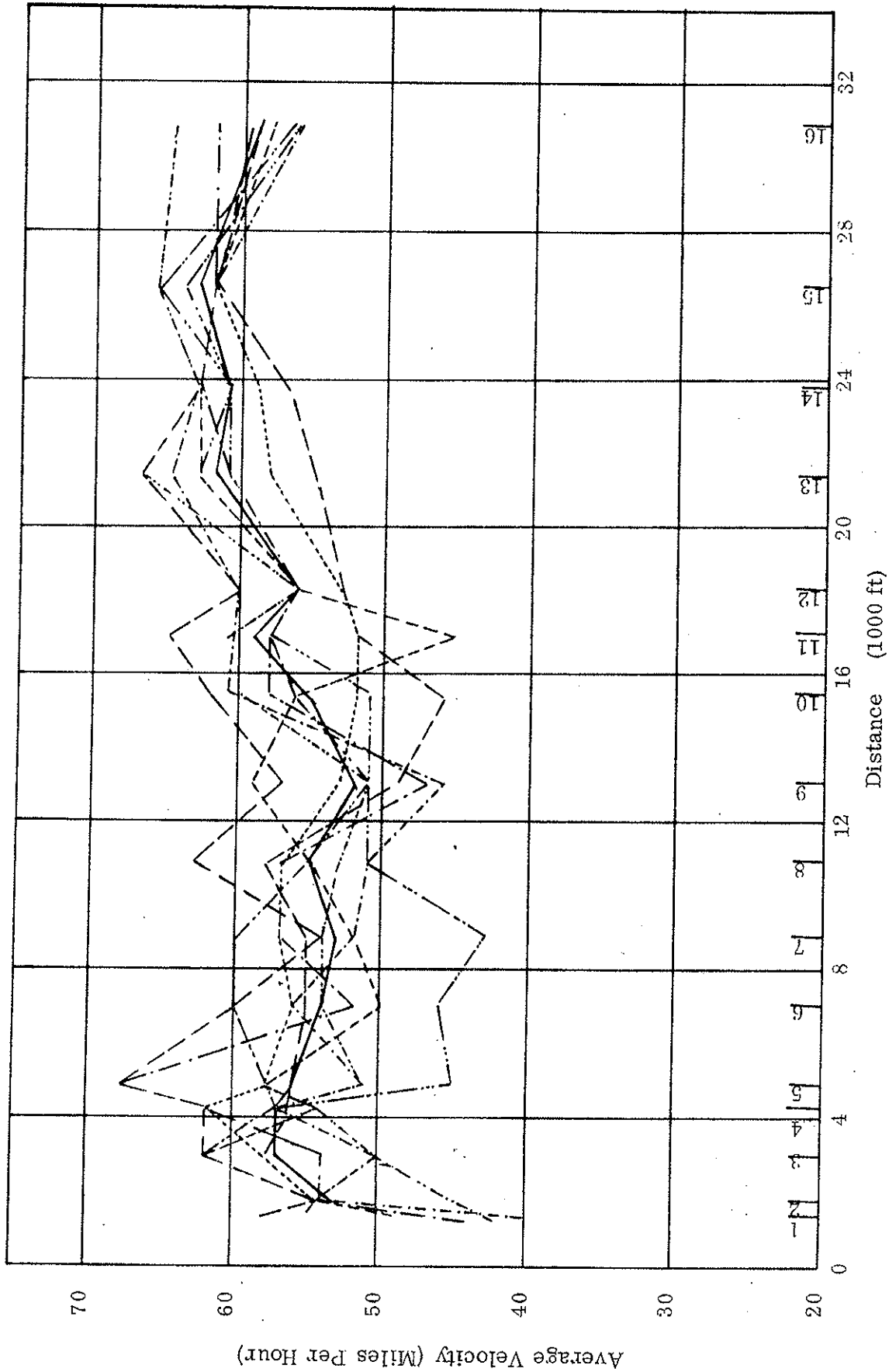


Fig. 7.26: Velocity-Distance Profiles for Data of Friday, June 22, 1973.

and section 5 (W. Bridge Rail US 33) and from section 12 (Kelton Ave o/p) to the inner belt. For the evening peak hour from section 7 (Merge sign Bexley St) to section 9 (Speed Limit Sign) where found to cause some problems on a Tuesday and Thursday, though section speed stayed above 20 m. p. h.

7.3 EVALUATION OF HYSTERESIS DATA

Conditions for aerial traffic surveys were different for I-70 since air control restricted flying to an altitude of about 2000 ft. The coverage is therefore about 3000 ft as can be seen in Figs. 7.27 and 7.28 which show the vehicle trajectories for two adjacent traffic lanes between Nelson Road and 18 th Street.

For westbound traffic . Mean traffic density for traffic approaching the disturbance in lane three is about 78 vehicles per mile and 87 vehicles per mile after recovering from the disturbance. The average speed in approaching the disturbance is 21 mph prior and 23 mph after going through the disturbance.

Traffic flow in lane four is less disturbed. The approach speed is about 30 mph and the speed after recovery is about 29 mph. The more pronounced disturbances in lane three were chosen for further evaluation. There were numerous disturbances, along that section of the freeway and traffic was moving in a typical stop and go operation. Unfortunately, due to a strong tailwind component the helicopter was not able to follow one

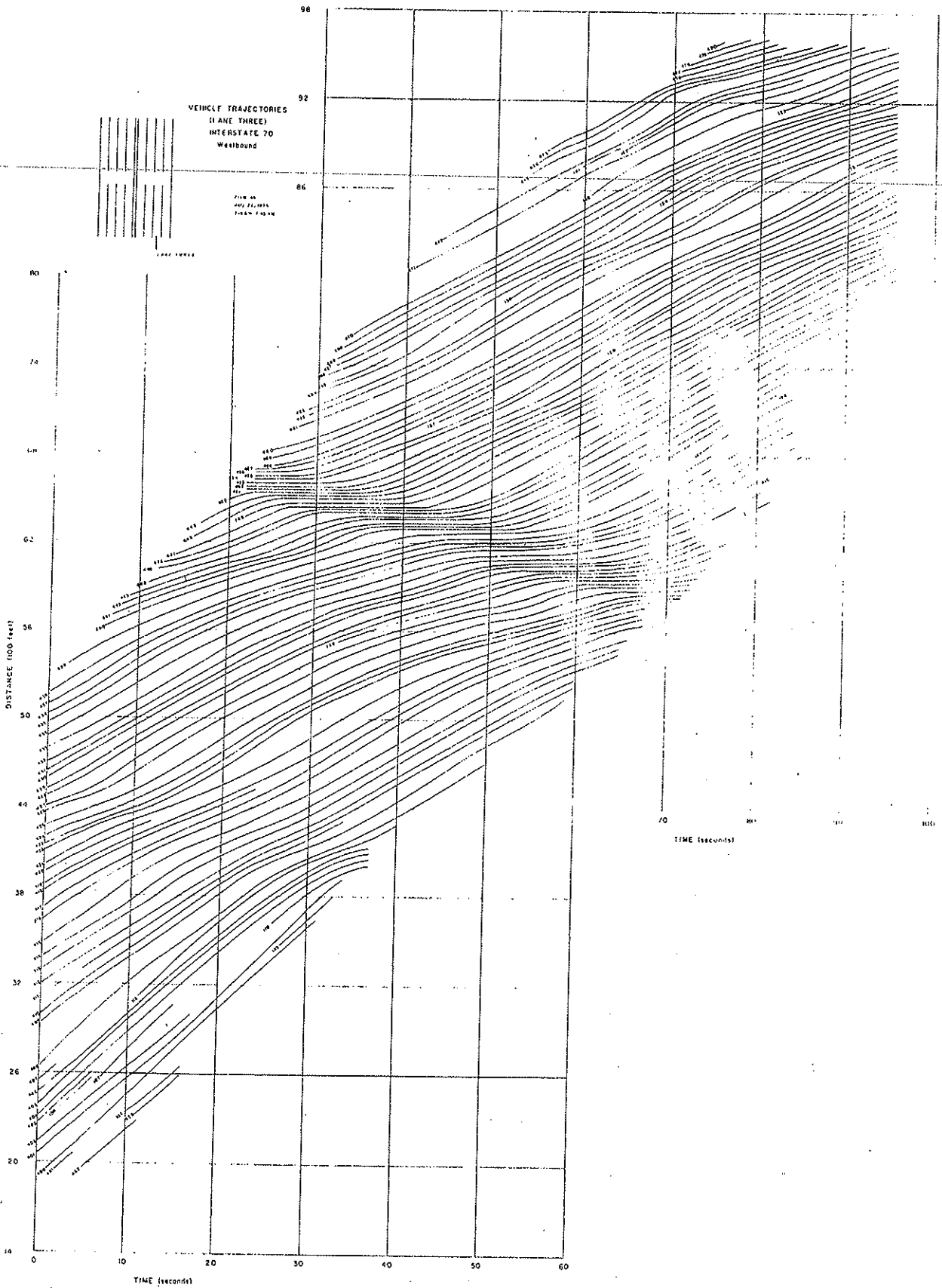


Fig. 7.27 Vehicle trajectories of a kinematic disturbance between Nelson and 18th Street. (Lane 3)

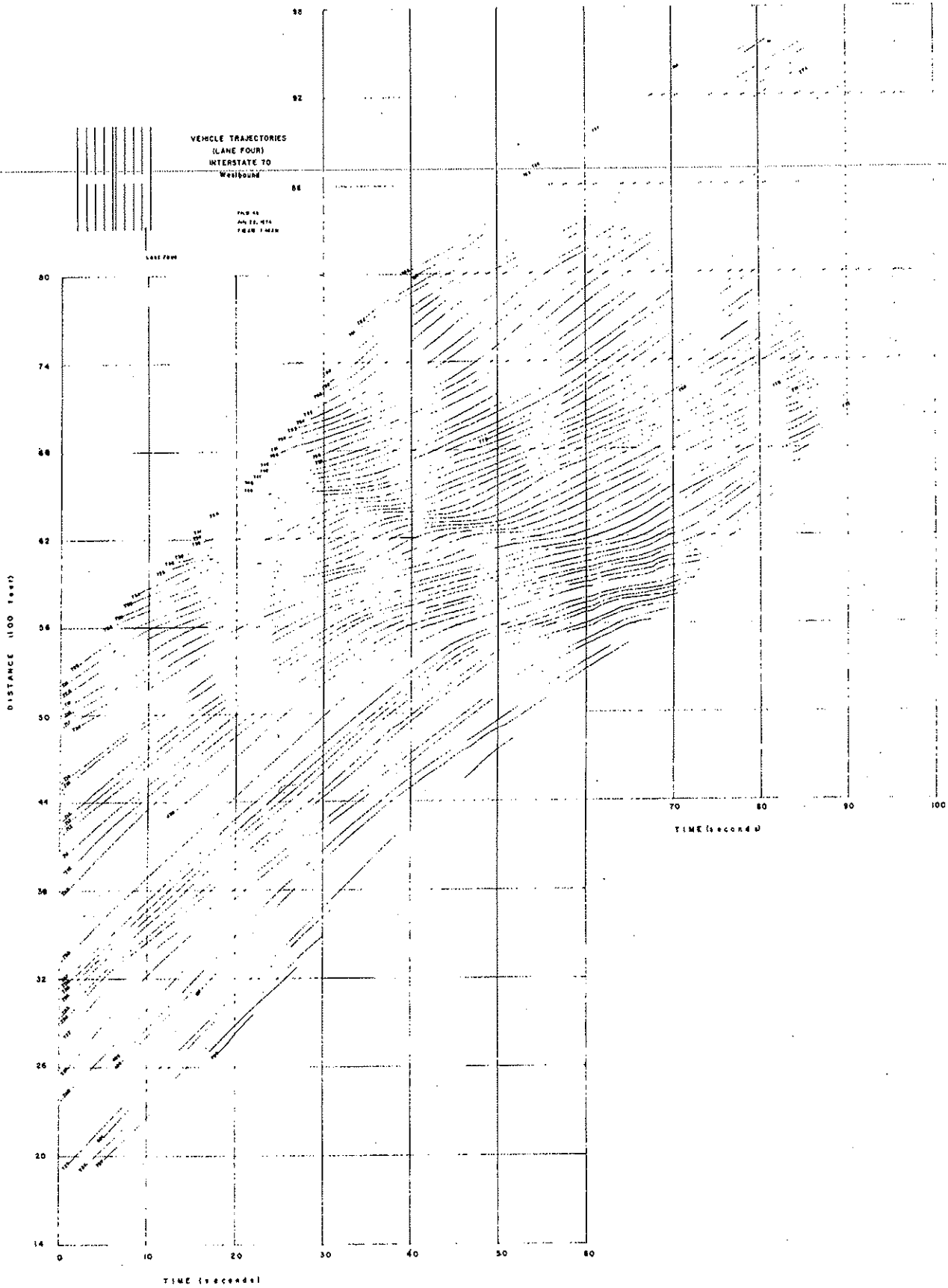


Fig. 7.28 : Vehicle trajectories of a Kinematic disturbance between Nelson Road and 18th Street, (Lane 4)

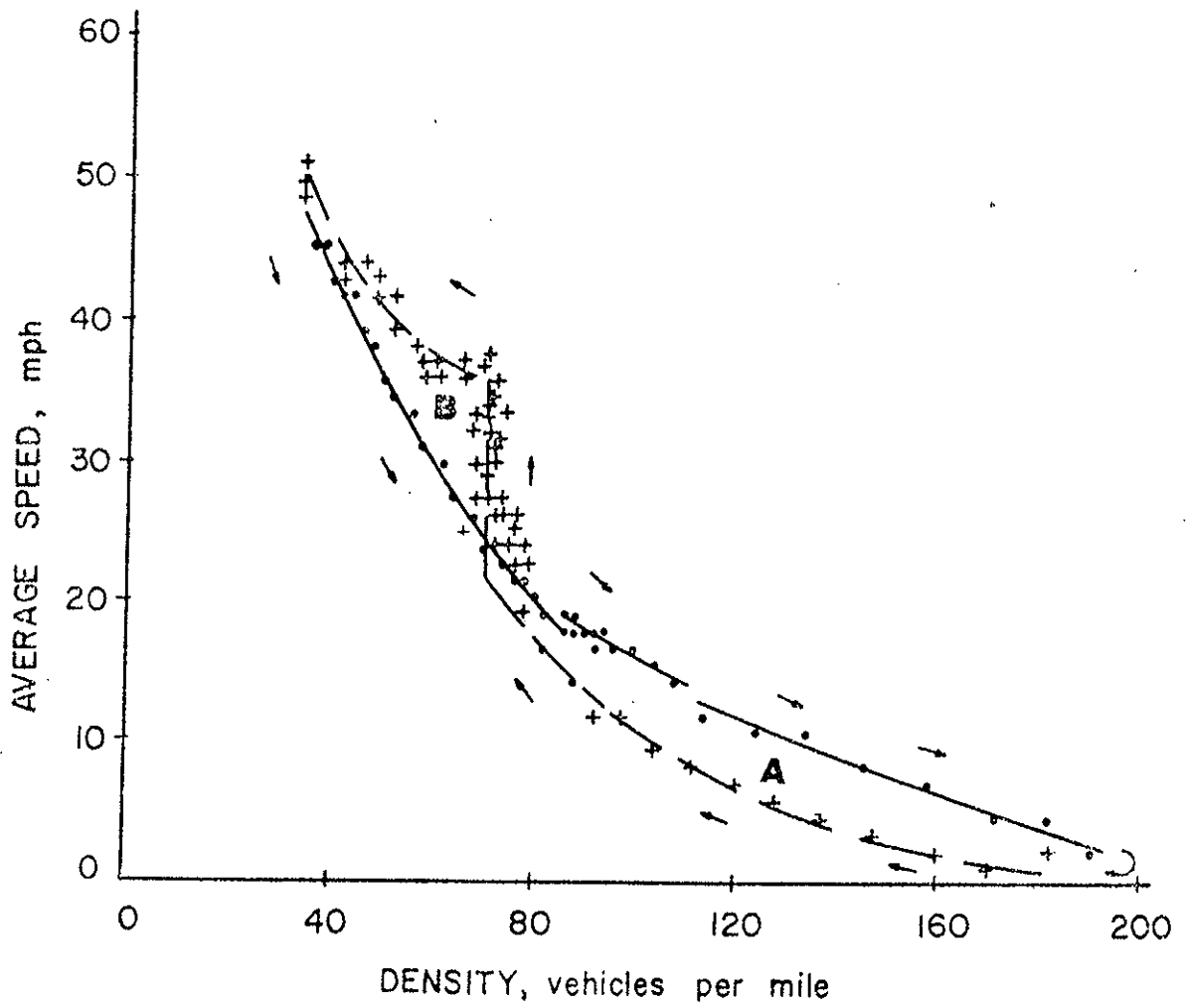


Fig. 7.29 Continuous record of the speed density relationship of a platoon of cars going through a kinematic disturbance. (Aerial survey data, morning peak hour, I-71)

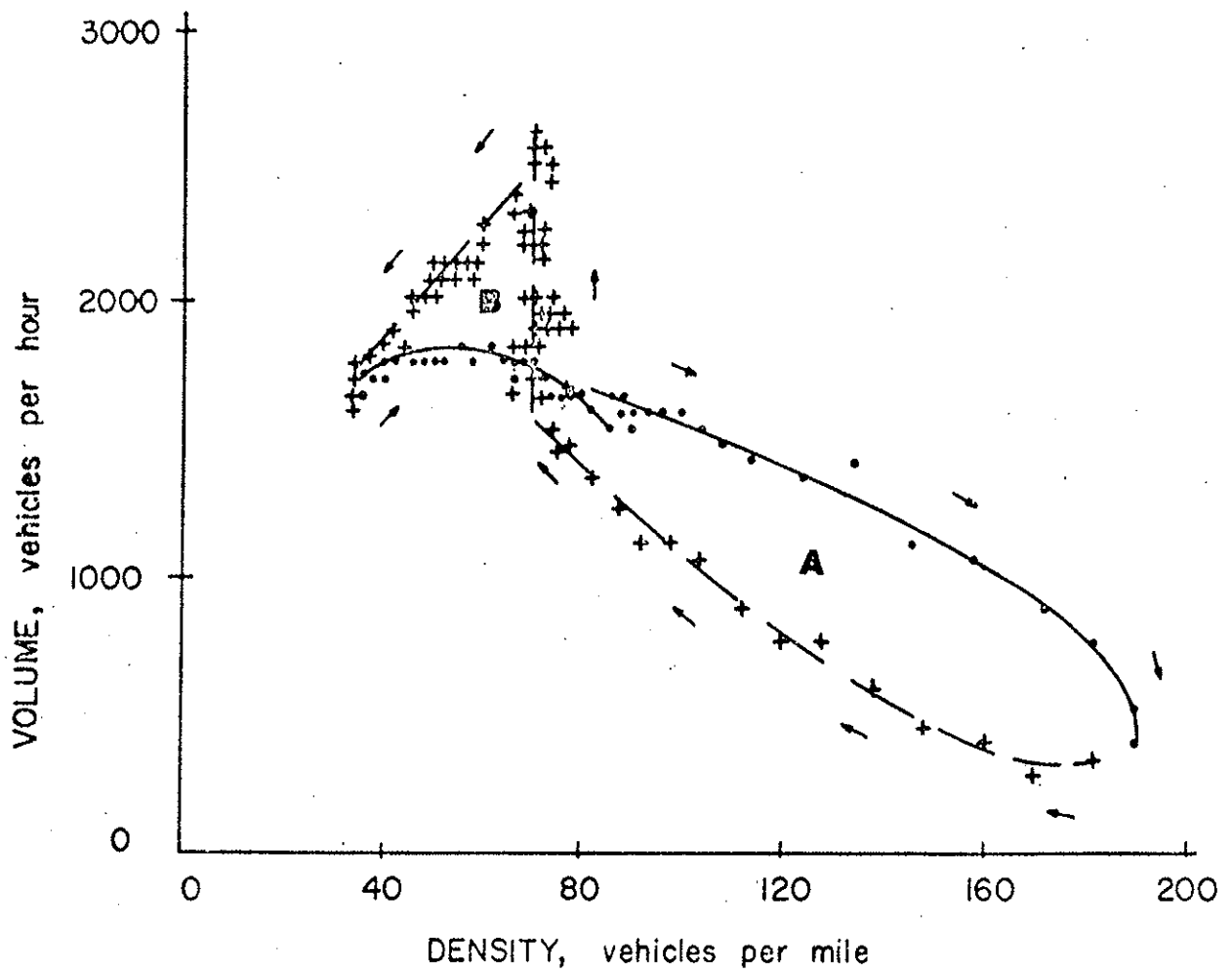


Fig. 7.30 Continuous record of the volume-density relationship of a platoon of cars going through a kinematic disturbance. (Aerial survey data, I-71, morning peak hour.)

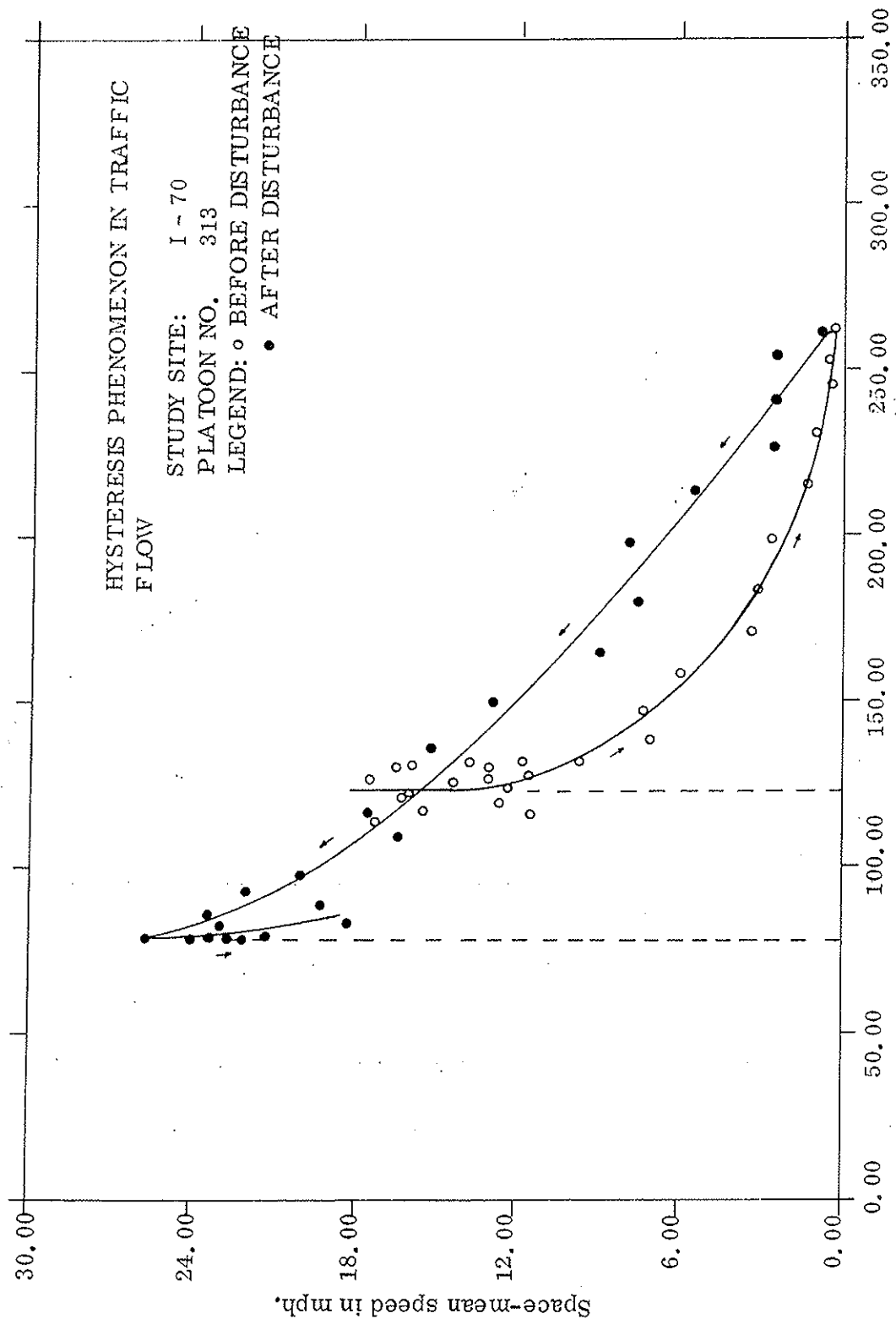


Fig. 7.31: Continuous record of the speed density relationship of a platoon of 8 vehicles going through a kinematic disturbance.

platoon of cars through the disturbances. The aerial survey data therefore, represent small platoons of about 7 to 11 vehicles over a limited distance.

The stoppage time of about 14 seconds in the disturbance however, is similar to the delay observed previously on I-71. Figs. 7.29 and 7.30 are typical for the hysteresis phenomenon observed on I-71 which is to be compared with the data from I-70. The A and B hysteresis loops are clearly defined for both the speed-density and volume density relationship. Comparing Fig. 7.29 with Fig. 7.31 (both Figures depict mean speed-density relationships) traffic conditions on I-70 show the A-loop but no B-loop was observed for platoon 313. Maximum traffic densities on I-70 were higher than that on I-71 and values as high as 280 v.p.m. were observed for small platoons. It appears that the "stop and go" operation mode has a compressing effect on traffic flow since jam densities on I-70 exceeded in most cases 250 v.p.m. The most important difference from previously analysed disturbances on I-71, however, is that the A-loop is reversed. Traffic is entering the disturbances at a lower speed than the speed gained in the recovery phase. The deterioration of traffic flow occurs at a density of about 125 v.p.m. whereas the recovery occurs at a density of about 80 v.p.m. which density is close to the density of recovery phases observed on I-71 (Fig. 7.29). No B-loop is formed though it appears that the recorded situation is a typical example of recycling around the A-loop which does result in "stop and go" operations. This observation is also

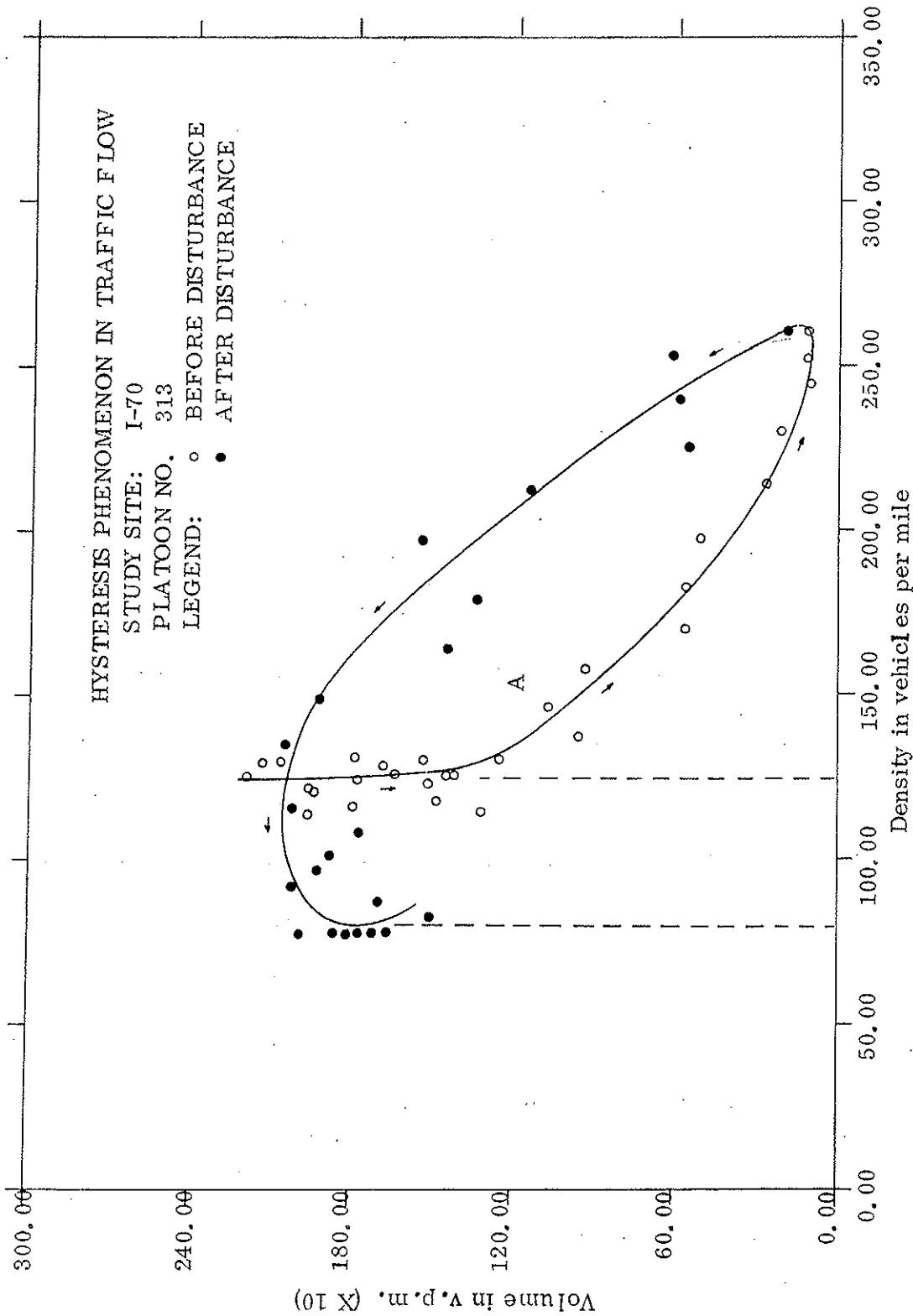


Fig. 7.32: Continuous record of the volume density relationship of a platoon of 8 vehicles going through a kinematic disturbance.

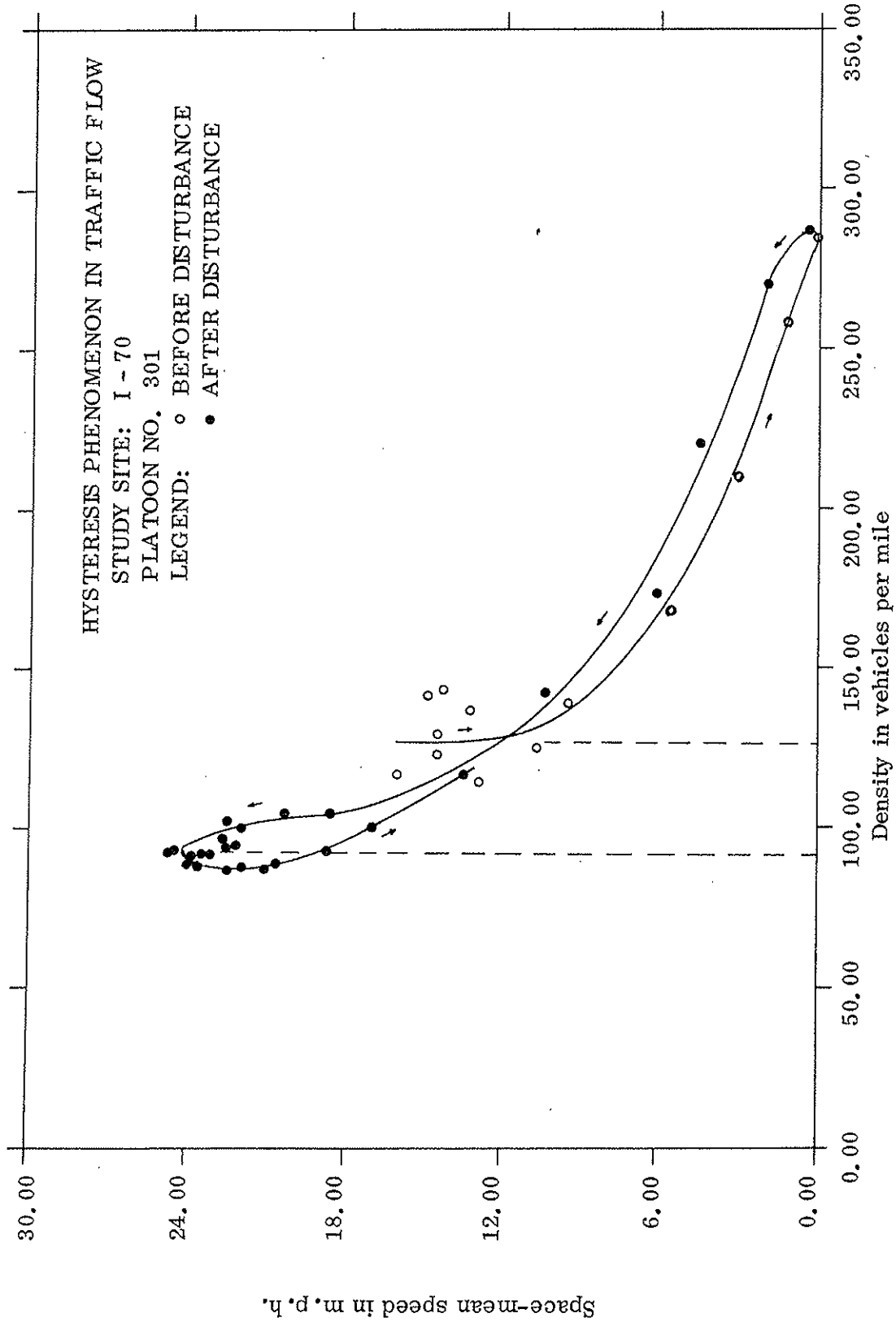


Fig. 7.33: Continuous record of the speed-density relationship of a platoon of 8 vehicles going through a kinematic disturbance.

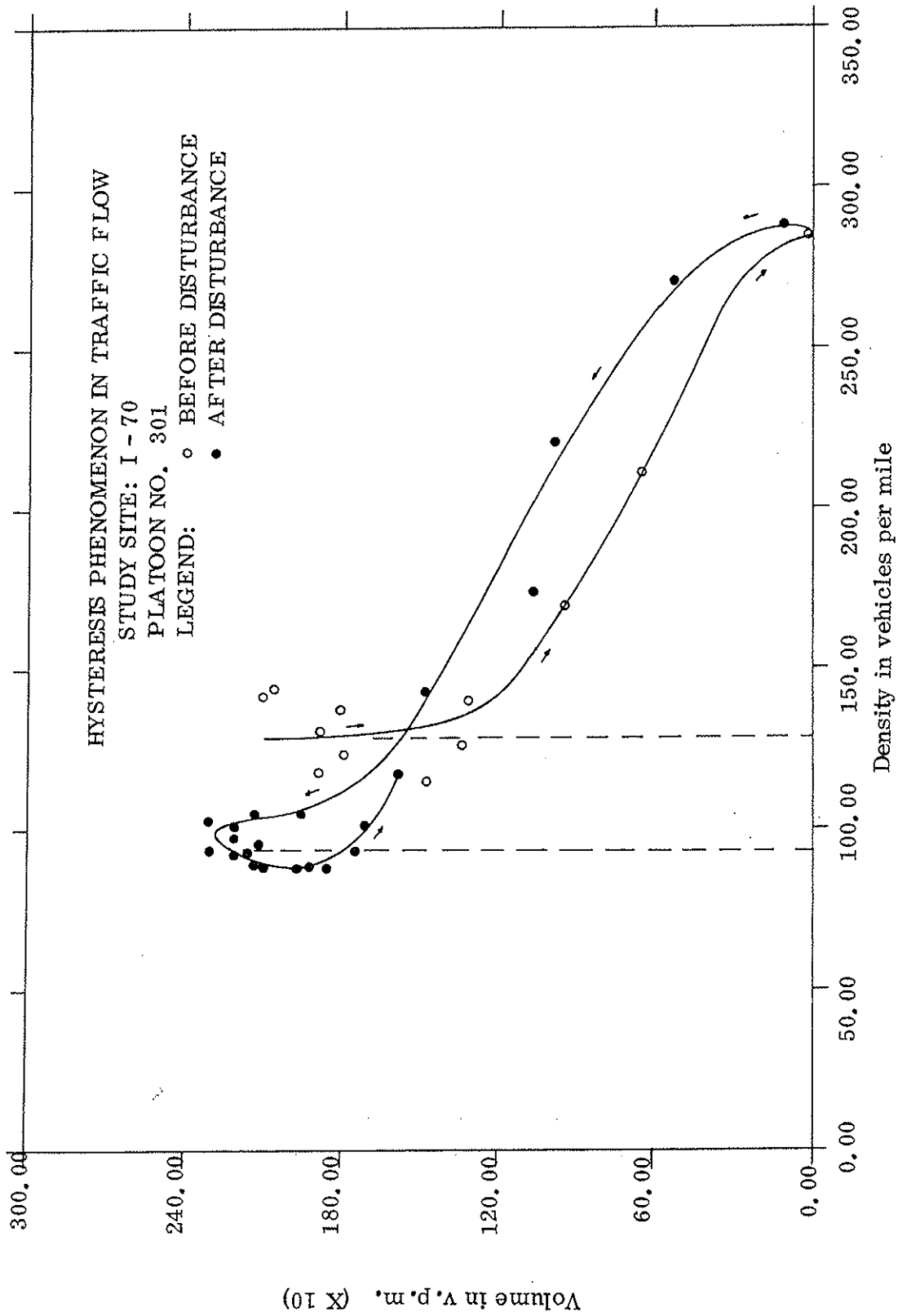


Fig. 7.34: Continuous record of the volume-density relationship of a platoon of 8 vehicles going through a kinematic disturbance

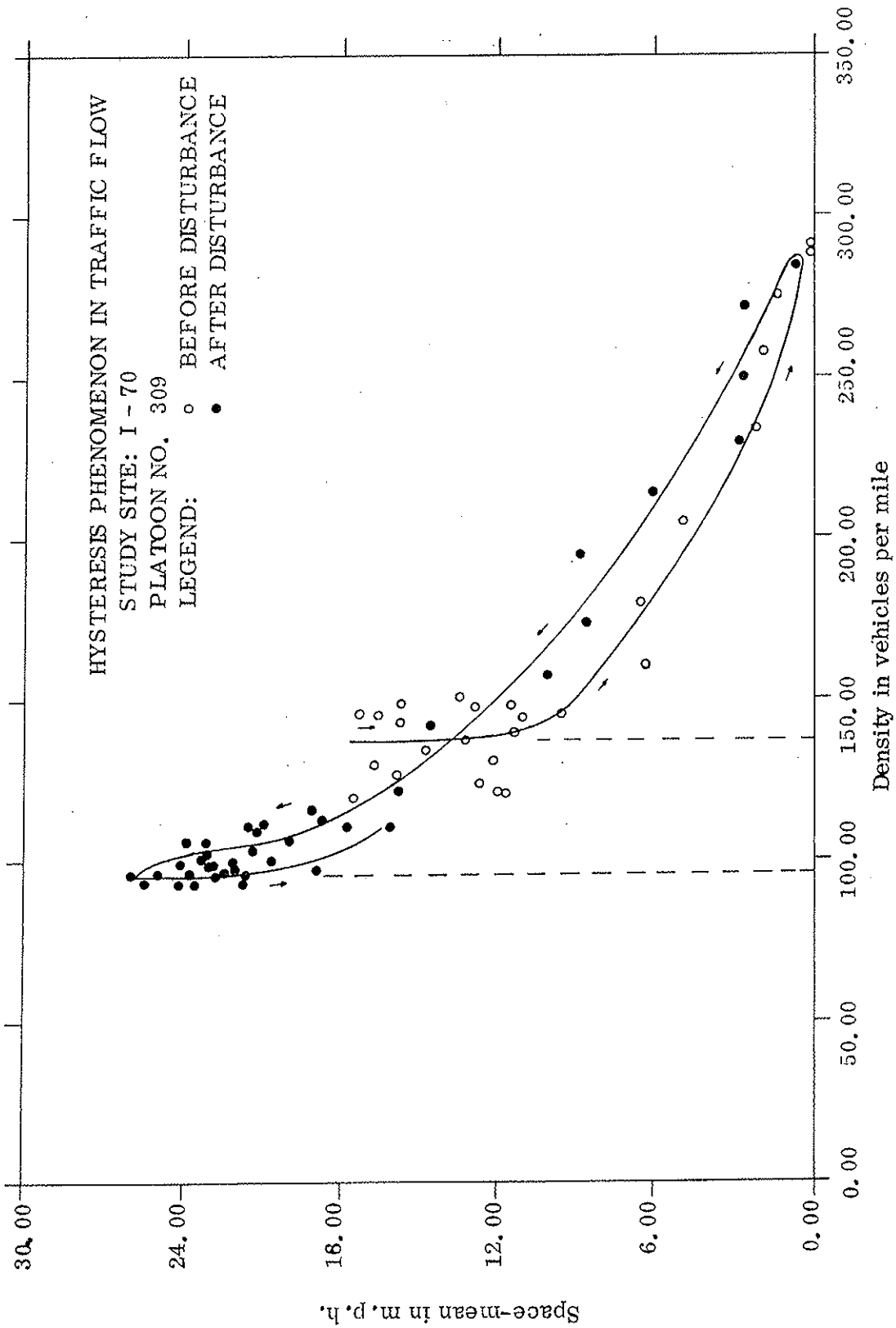


Fig. 7.35: Continuous record of the speed-density relationship of a platoon of 7 vehicles going through a kinematic disturbance.

supported by the observed speed range. The speed range for the A-loop, observed on I-71, was from zero to about 25 mph. and recovery occurred at a range of about 25 to 50 mph. Platoon 313 on I-70 reached about 25 mph. in the recovery phase but the phase of generating and entering a new disturbance starts at about 18 mph with a rather substantial reduction in speed at a constant density of about 125 v. p. m.

The volume-density relationship (Fig. 7.32) shows a pattern similar to the speed-density relationship except for the more pronounced drop off in traffic volume during the recovery phase. An attempt was made to confirm the findings of platoon No. 313 by studying other platoons. It was found that the most important difference to previous studies i. e. the reversed A-loop conditions with lower speeds in approaching the disturbance and generally higher speeds in recovering from the disturbance, held for all platoons though the difference was not as pronounced as in platoon No. 313. Platoon No. 301 and No. 309 (Figs. 7.33, 7.34, and 7.35) show similar tendencies in the drop off and recovery phase with regard to traffic densities, speed and volume. Table one lists these data for platoons No. 301, 302, 309, and 313.

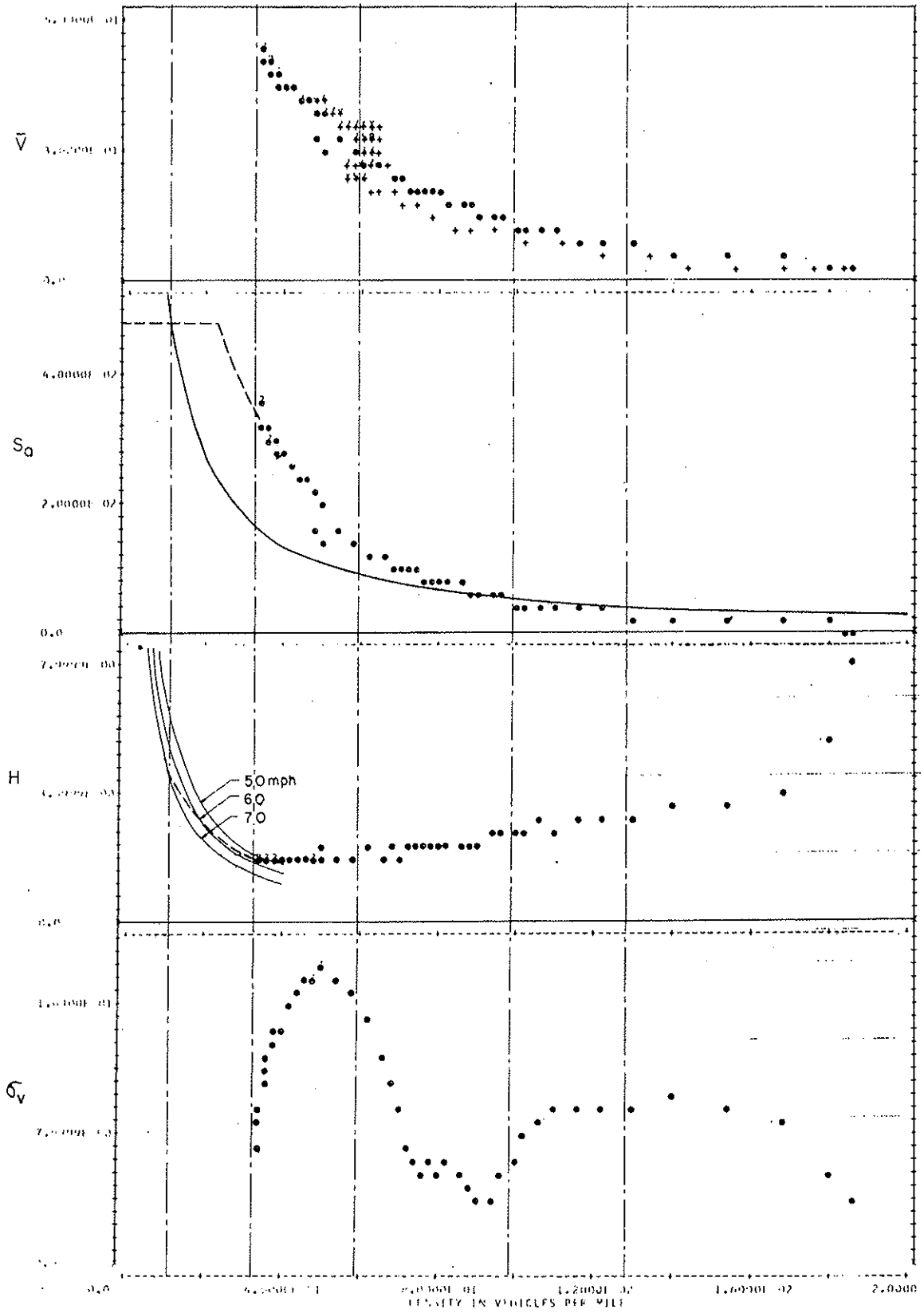


Figure 7.36 Summary of Studied Platoon Parameters and Defined Operating Regions for Platoon B

Density in phase of	Platoon No.			
	301	302	309	313
Drop-off	126 / 128	not defined	145	122 / 126
Recovery	92 / 95	75 / 76	95	77 / 80

Table 1 Densities in drop-off and recovery phases.

Some explanation can be deduced from the data obtained in the studies on I-71 (Fig. 7.36). In this study traffic density was plotted against space mean speed \bar{v} , safe spacing S_a , average headway H and the standard deviation of speed σ_v for traffic approaching a kinematic disturbance. It was found in these studies that the headway H is gradually increasing in the 100 to 160 V. p. m. density range while σ_v reaches a max. in the same region. It appears that this maximum range of the standard deviation which can be considered as the disturbance of the vehicles speed from uniform speed (acceleration noise) can also be identified as the internal energy of traffic flow or friction in traffic flow. Thus it can be expected that a high level of friction will result in a very pronounced deterioration of traffic flow, though, this was never observed in the I-71 study. The data available so far indicate that the following cycle could describe the "stop and go" operation on urban freeways. After going through the first disturbance, traffic reaches the low acceleration noise area at a density of about 70 V. p. m. (Fig. 7.37).

This condition seems to be transferred into the density range of about

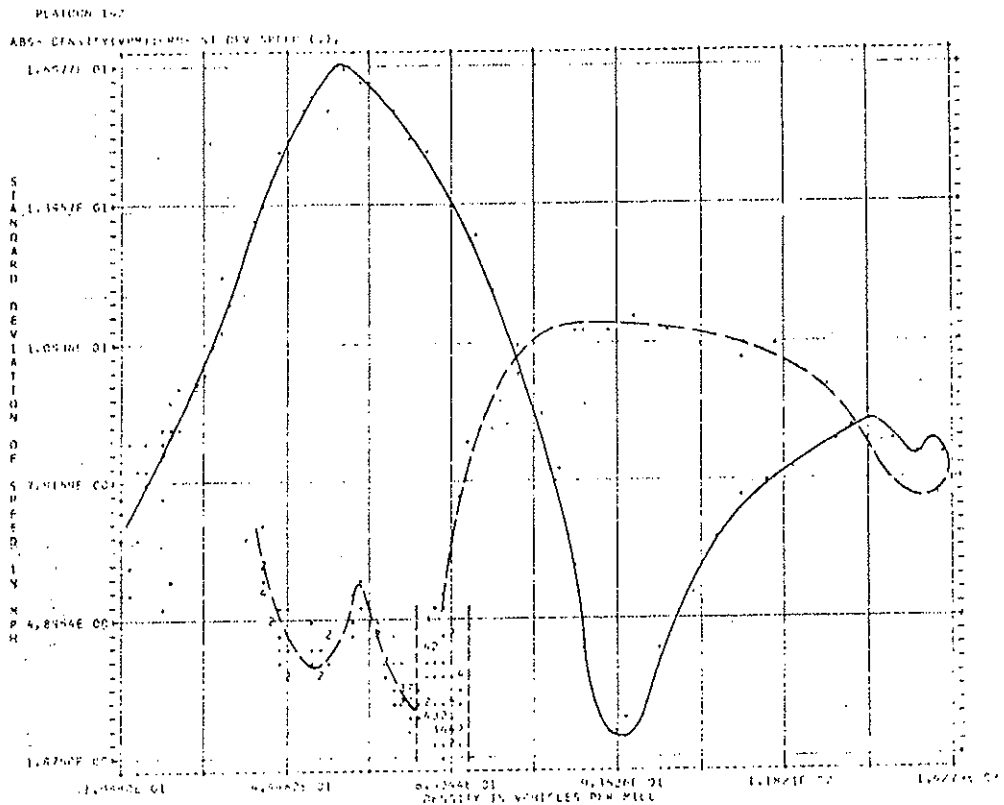


Fig. 7.37: Standard deviation of speed (acceleration noise) of a platoon of cars going through a disturbance.

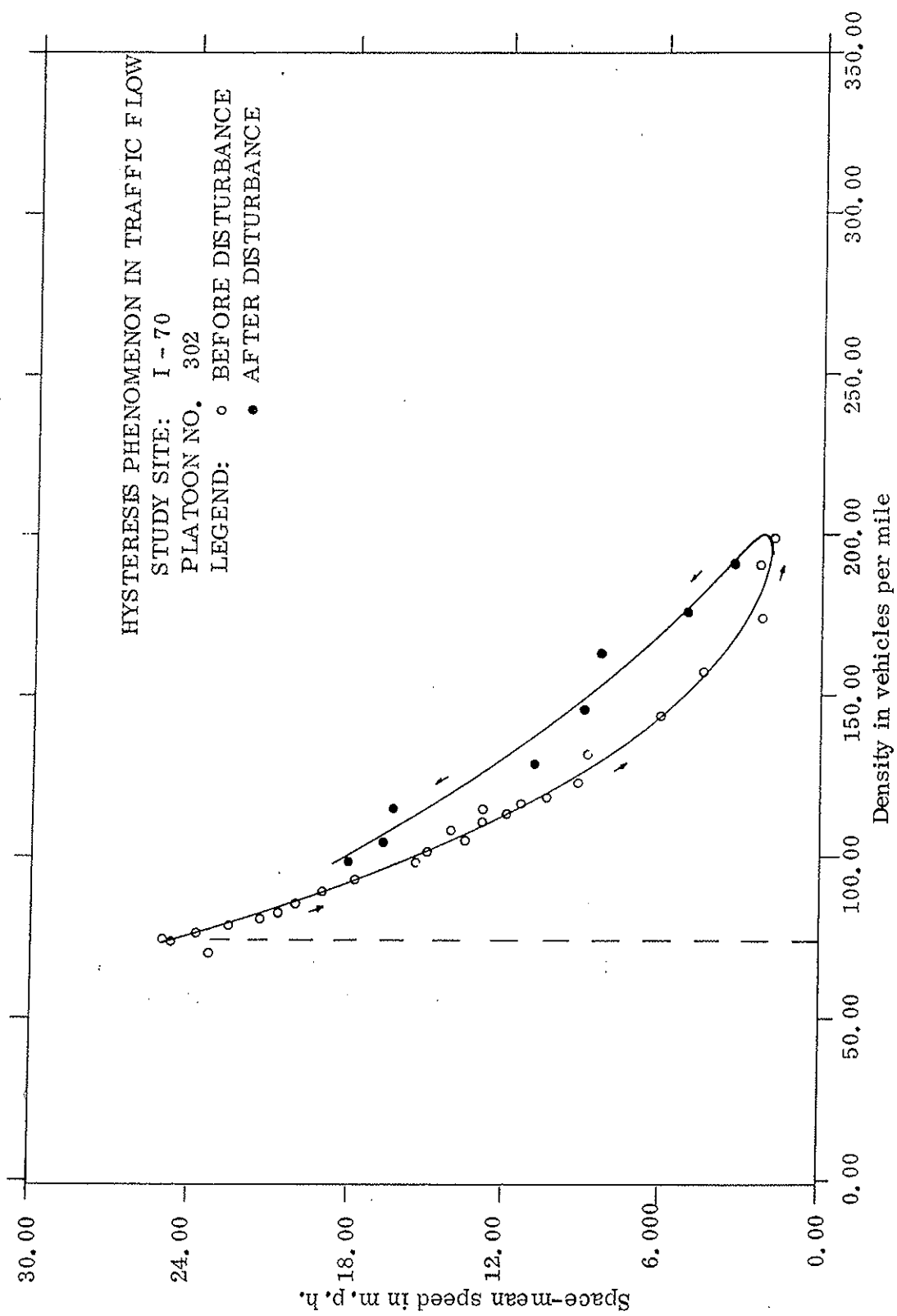


Fig. 7.38: Continuous record of the speed-density relationship of a platoon of 11 vehicles going through a kinematic disturbance.

70 to 100 V. p. m. and projects into the range of 125 V. p. m. Fig. 7.37 shows a record of the standard deviation against density for a platoon of vehicles which recovered completely from a disturbance. The cluster of data points of low σ_v 's in the 70 V. p. m density range can lead to the left - i. e. a complete recovery with increasing speed in the σ_v range of about 8 mph - or to the right and join the low σ_v range of traffic approaching a disturbance.

Not all platoons, however, did show the typical cycle as recorded in Figs. 7.31, 7.33 and 7.35. Platoon No. 302 (Fig. 7.38) shows a gradual decrease in speed over the density range of 75 to 200 V. p. m. and no specific drop off density was found. The volume-density plot (Fig. 7.39) shows a similar characteristic though there is a marked concentration of data points in the 80 V. p. m. range. The hysteresis loop is indicated but no closed A-loop is formed.

Conclusions

The data obtained by aerial surveys on I-70 have added new knowledge to the dynamic characteristics of traffic flow. The hysteresis phenomenon previously observed on I-71 has been expanded from the cycle of single disturbance to recycling of the "stop and go" operation. A-loops only have been recorded and it appears that multiple disturbances have a characteristic which shows the following differences from the single disturbance characteristic :

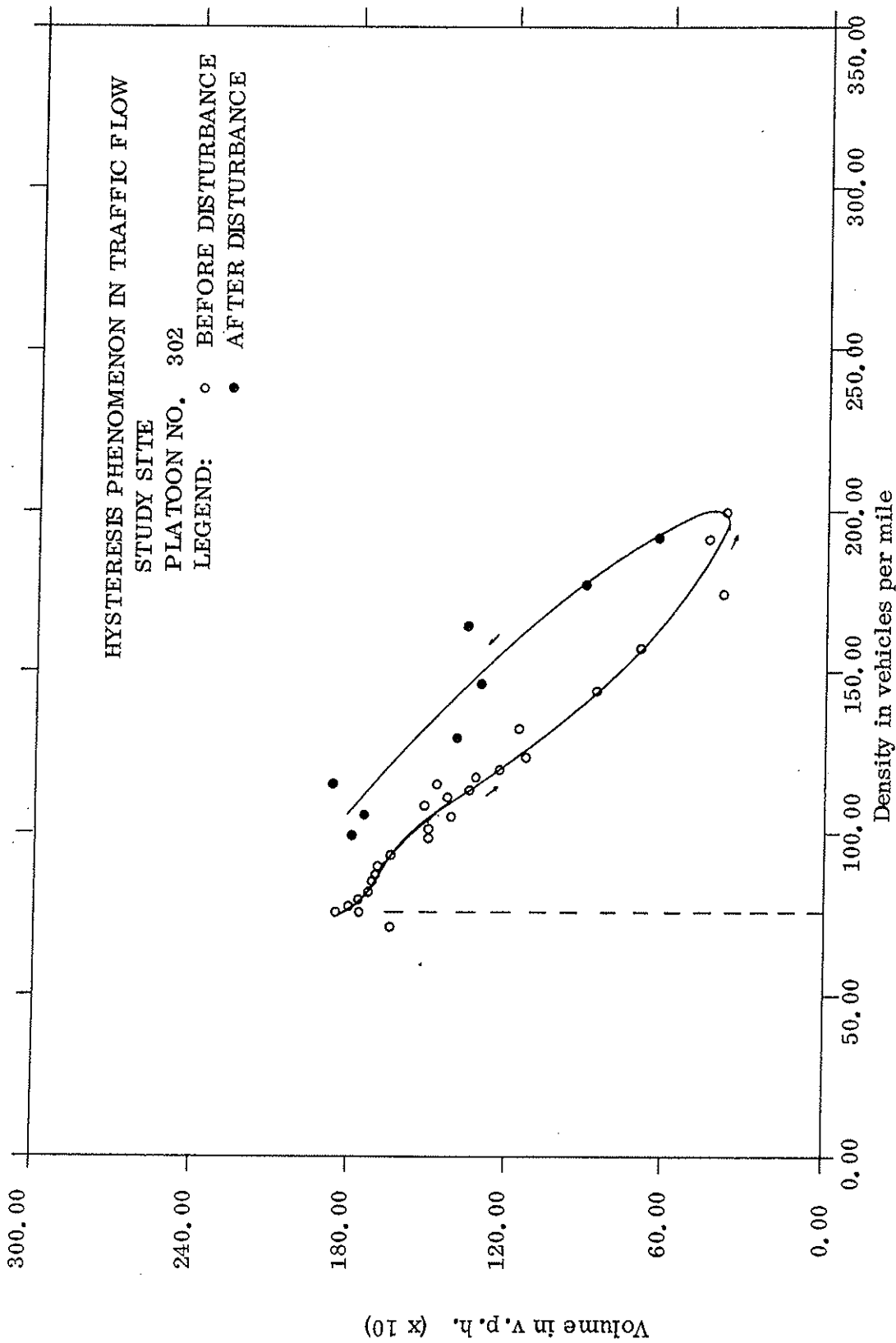


Fig. 7.39: Continuous record of the volume-density relationship of a platoon of 11 vehicles going through a kinematic disturbance.

- 1) The sequence of the A-loop is reversed with lower approach and higher recovery speeds.
- 2) Though recovery occurs in the 70 to 90 V.p.m. density range similar to the data recorded for the single disturbance, the drop off in approaching multiple disturbances occurs about 120 to 150 vehicles per mile.
- 3) Higher peak densities have been recorded for "stop and go" operating conditions.

It appears that understanding kinematic disturbances is of great importance for a successful and efficient computer control system.

Research findings indicate that traffic density together with the space mean speed at critical sections are useful and sensitive parameters to determine the operational mode for a computer based control system.

Still more data are required to develop an optimum operation model for traffic control on urban freeways.